Journal of Marine Technology and Environment

Vol.II, year 2010

ISSN 1844-6116

YEAR III, 2/2010
ISSN 1844 – 6116
JOURNAL OF MARINE TECHNOLOGY AND ENVIRONMENT

This Journal has been founded in 2008 as a biannual publication of
Constanta Maritime University/ROMANIA

TOPICS

- Marine Science and Engineering
- Marine Environmental Issues
- Marine Renewable Energy and Sustainability
- Maritime Safety
- Marine Chemistry
- Marine Corrosion and Material Science
- Ship Design, Building Technologies
- Ocean Engineering
- Advanced Technologies for MET
- Advances in numerical methods for marine engineering
- Algorithms for multidisciplinary problems in marine engineering

and other related topics

JOURNAL ADDRESS
Journal of Marine Technology and Environment
Constanta Maritime University, 104, Mircea cel Batran Street, 900663, Constanta, Romania
Tel: +40 241 664 740/ 107
Fax: +40 241 617 260
E-mail: jmte@imc.ro
http://cmu-edu.eu/jmte/

EDITURA NAUTICA
Constanta Maritime University
Constanta Maritime University, 104, Mircea Cel Batran Street, 900663, Constanta, Romania

CONTENTS

ASSESING THE CHANGE OF DRAG ACTING ON A SHIP WITH DIFFERENT DRAUGHT IN THE COURSE OF OPERATION

[1]ALEKSANDROV ZAMFIR, [2]STOYANOV RUMEN

[1]*Technical University – Varna, Bulgaria,* [2]*Nikola Vaptsarov, Bulgaria*

The purpose of this paper is to create a methodology for assessing the change of drag on a ship caused by the fouling of the hull and the increase of its roughness with different draught in the course of operation.

Keywords*:*Ship resistance, specific drag, ship's propulsion system

1. INTRODUCTION

The mode of operation of a ship's propulsion system is determined by the mechanical characteristics of the main engine, the propeller screw and the hull. A change in one of these will affect the interaction between the other two elements and bring about a new mode of operation of the system. In the course of a ship's operation, the mechanical characteristics of the screw and the hull are subject to the most intensive changes. This is due both to their fouling and the increase of the degree of their roughness. This increases the moment of resistance of the propeller screw, decreases the thrust it generates, and increases the drag on the ship [1].

The purpose of this paper is to create a methodology for assessing the change of drag on a ship caused by the fouling of the hull and the increase of its roughness with different draught in the course of operation.

2. DESCRIPTION AND ANALYSIS

To this end, we adopted the idea to measure the ship's speed while coming to an inertial stop with the main engine off, which is described with the equation

$$m\frac{dV}{dt} = -CV^2, \tag{1}$$

where

m – the ship's mass together with the added mass of water, assumed to be constant for a short period of time;

V – the ship's rate of movement on a straight course;

C – the overall specific drag acting on the ship underway;

t – time

The differential equation (1) can be expressed as follows:

$$\frac{dV}{V^2} = -k\ dt \tag{2}$$

where the designation *k,* called "coefficient of inertial stopping" [2], is introduced:

$$k = -\frac{C}{m} \tag{3}$$

After integrating equation (2) in the time interval $\Delta t = t_2 - t_1$, when the ship decelerates during inertial stopping from V_1 to V_2, the following is obtained for *k*:

$$k = \left(\frac{1}{V_1} - \frac{1}{V_2}\right)\frac{1}{\Delta t} \tag{4}$$

or:

$$k = \frac{V_2 - V_1}{V_1.V_2.\Delta t} \tag{5}$$

The expression (4) for the coefficient of inertial stopping can be represented as follows:

$$k = \frac{1}{S_1} - \frac{1}{S_2} \tag{6}$$

Therefore, the value of the coefficient *k* equals the difference from the reciprocal values of the path S_1, which the ship will travel over the time of the measurement Δt if moving at the constant rate V_1, equal to the initial one, and the path S_1, which the ship will travel over the same time Δt, if moving at the constant rate V_2, equal to the one at the end of the measurement.

Let us assume that in calm sea and absence of currents and with certain draught T_0, respectively mass m_0, the time Δt_0 is measured, over which the ship decelerates from V_1 to V_2 in inertial stopping mode. The value k_0 for the coefficient of inertial stopping in these conditions is taken as a reference:

$$k_0 = \frac{V_2 - V_1}{V_1.V_2.\Delta t_0} \tag{7}$$

In the course of operation, due to the inevitable accumulation of fouling of the hull and the increase of its roughness, with the same conditions as the reference conditions and ship's mass $m^* = m_0$, it will decelerate for a shorter time $\Delta t^* < \Delta t_0$ and

$$k^* = \frac{V_2 - V_1}{V_1 . V_2 . \Delta t^*} \tag{8}$$

Thus, collating the equations (7) and (8), the following relations are obtained:

$$K = \frac{k^*}{k_0} = \frac{\Delta t_0}{\Delta t^*} . \tag{9}$$

When the ship's mass m^* is the same as the one used when k_0 is determined, the result is:

$$\frac{C^*}{C_0} = \frac{R^*}{R_0} = K . \tag{10}$$

This means that in the new conditions of travel in result of fouling and increased roughness of the hull with the draught unchanged, the value K equals the relative change of drag when moving at the same rate of speed. Its magnitude relatively increases as much as the decrease of the relation of the time Δt against Δt_0.

When the ship's mass m^* is different from the one when the reference value k_0 of the coefficient of inertial stopping is determined, the relations (9) appear as follows:

$$\frac{C^* / m^*}{C_0 / m_0} = K \qquad C^* = K \frac{m^*}{m_0} C_0 . \tag{11}$$

The value for the overall specific drag C^* depends not only from the time of deceleration from V_1 to V_2 while the ship is coming to an inertial stop, but also from the relation of the masses m^* and m_0. To clarify the manner in which these two factors affect drag, the following situations must be analysed:

A) The ship's mass m^* is less than the reference mass m_0 used to determine the value of k_0:

$$m^* < m_0$$

With the ambient conditions and the hull state the same as the reference, there will, of course, be less drag ($C_m < C_0$). In the course of the operational life of the system, the following four combinations can possibly occur:

$$K > 1 , \quad K \frac{m^*}{m_0} > 1 \qquad \text{- Fig.1 (12.1)}$$

$$K > 1, \quad K\frac{m^*}{m_0} < 1 \qquad \text{- Fig.2 (12.2)}$$

$$K > 1, \quad K\frac{m^*}{m_0} = 1 \qquad \text{- Fig.3 (12.3)}$$

$$K \leq 1, \quad K\frac{m^*}{m_0} < 1 \qquad \text{- Fig.4 (13)}$$

In the case of (12.1), the decreased inertness leads to faster stopping, and even if there is no fouling on the hull, the recorded time is $\Delta t_m < \Delta t_0$. While a ship is being operated, this tendency intensifies, K increases and has greater effect on the value of the overall drag on the ship C^* than the decrease of the mass: $C^* > C_0$ - Fig. 1.

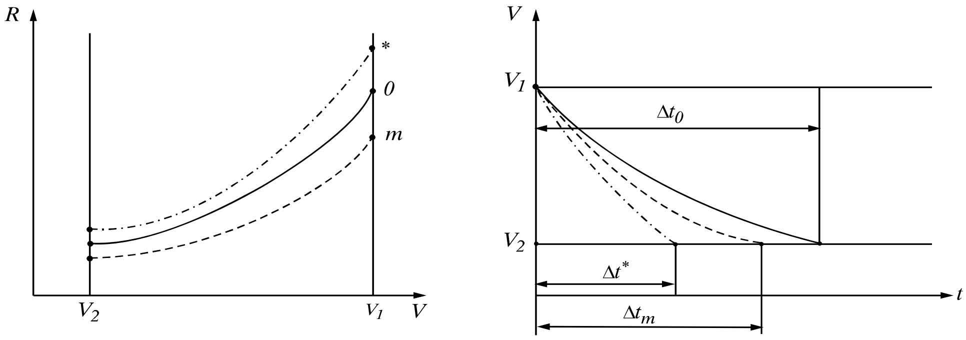

Figure 1.

Fig. 2 shows the dependencies which illustrate the inequations (12.2). There is less drag when a ship with a mass m^* is underway in the same ambient conditions and state of the hull as the reference: $C_m < C_0$. The decrease of the time $\Delta^{t^*} < \Delta t_m$ due to the increased fouling and roughness does not lead to exceeding the value of the overall specific drag C_0 as determined in the reference conditions: $C^* < C_0$.

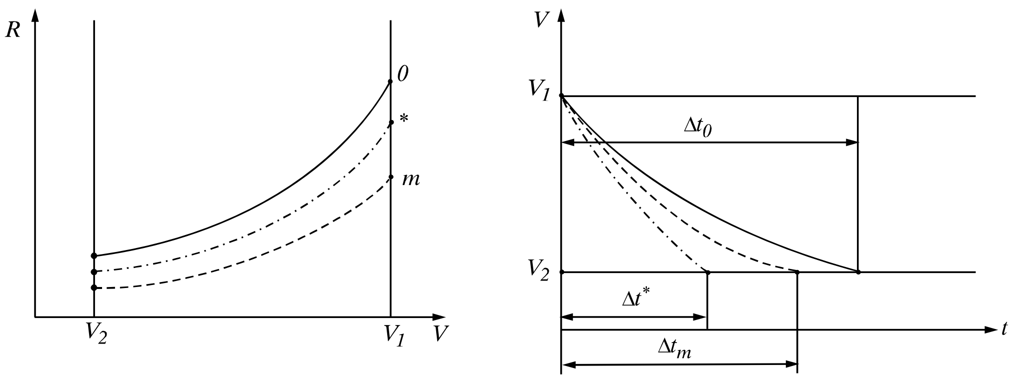

Figure 2.

A special case (12.3) is also possible when the decreased inertness and the increased drag as a result of the fouling of the hull and its increased roughness mutually compensate each other. The overall drag acting on a ship with less load but more fouling – C^*, equalises with the value determined when the ship's mass is greater and the hull is cleaner - C_0, as illustrated on Fig. 3.

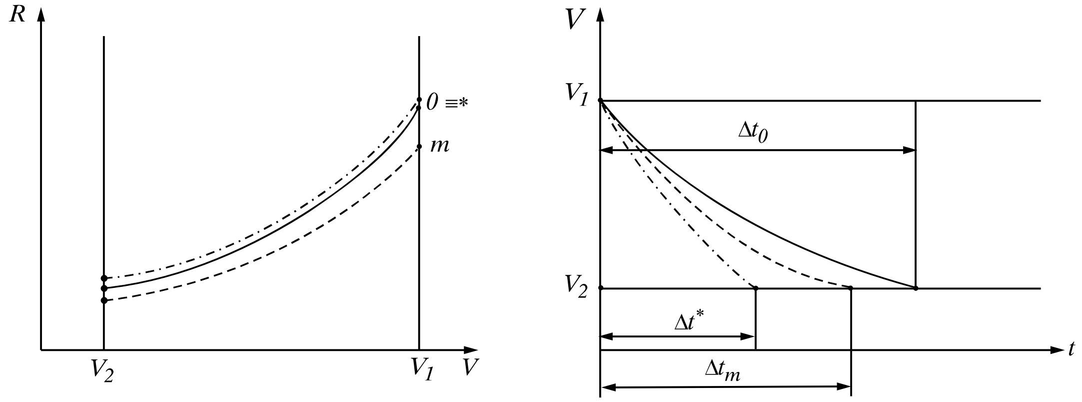

Figure 3.

Fig. 4 shows the diagrams derived from the inequations (13). Despite the decreased mass, in conditions identical to the reference conditions, there is a relatively greater decrease of drag on the ship and during inertial stopping the deceleration from V_1 to V_2 takes a longer time interval: $\Delta t_m > \Delta t_0$. The fouling of the hull and its increased roughness lead to a decrease of the time of deceleration from V_1 to V_2, but this can exceed the reference value. In result, the calculated new value of the overall specific drag C^* is less than the one determined in reference conditions: $C^* < C_0$.

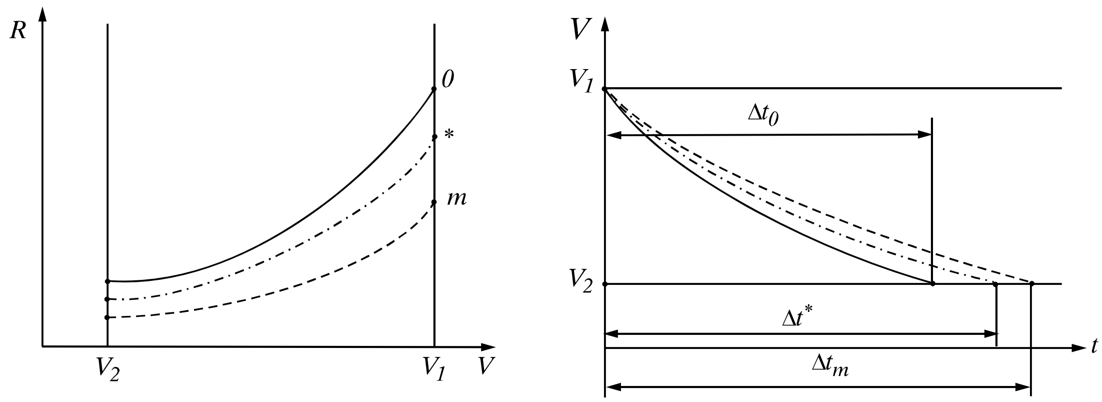

Figure 4.

Obviously, such a situation would only occur at a certain ratio between the change of drag and the change of the ship's mass with respect to the change of its draught.

B) The other alternative is that the ship's mass m^* is greater than the one the ship had when determining the reference value of the coefficient of inertial stopping k_0:

$$m^* > m_0$$

The probability for this inequation to occur is greater, because the value of k_0 may have been determined during sea trials, with the ship's draught lower than the design draught.

With this ratio of the masses, four alternatives are theoretically possible again:

$$K \geq 1, \quad K\frac{m^*}{m_0} > 1 \qquad \text{- Fig.5 (14)}$$

$$K \leq 1, \quad K\frac{m^*}{m_0} > 1 \qquad \text{- Fig.6 (15.1)}$$

$$K \leq 1, \quad K\frac{m^*}{m_0} = 1 \qquad (15.2)$$

$$K \leq 1, \quad K\frac{m^*}{m_0} < 1 \qquad (15.3)$$

Condition (14) shows that $\Delta t_0/\Delta t^* > m_0/m^*$. This means the despite the increased inertness of the ship $m^* > m_0$, with overall specific drag $C_m > C_0$, the deceleration when stopping in the same conditions as the reference increases in absolute value and the ship decelerates V_1 to V_2 over a shorter time interval $\Delta t_m < \Delta t_0$. In result of fouling and increased roughness of the hull, the drag increases with respect to the reference value: $C^* > C_0$.

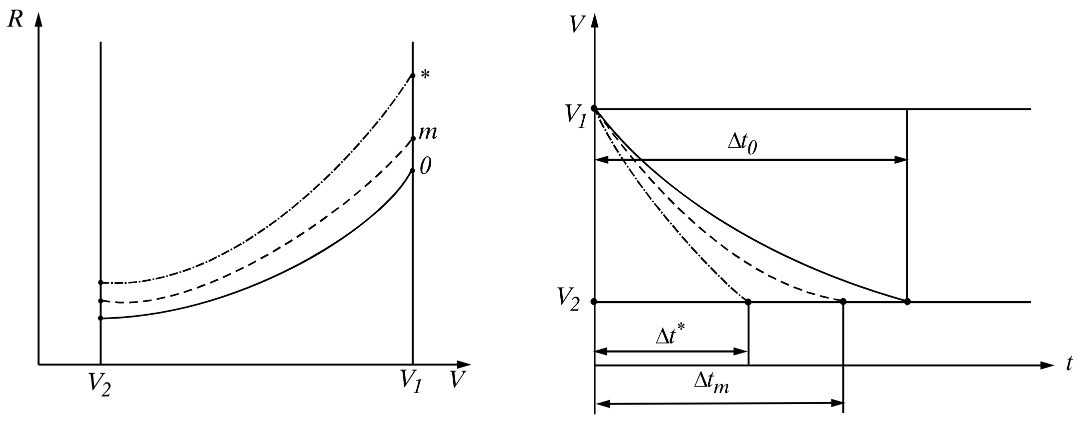

Figure 5.

The diagrams on Fig. 6 on the left show the change of drag as a function of the ship's speed, and the deceleration from V_1 to V_2 during inertial stopping for the case (15.1).

In reference conditions, despite the increased drag on the ship $C_m > C_0$, the increased inertness leads to an increase of the deceleration time from V_1 to V_2, which results in $\Delta t_m > \Delta t_0$. Due to fouling and increased roughness of the hull, the drag goes up $C^* > C_0$, which leads to shorter deceleration time in the same interval and $\Delta t^* < \Delta t_m$, but this can exceed the measured value in reference conditions: $\Delta t^* > \Delta t_0$. In the new conditions of sailing, the value for the specific drag exceeds the reference value: $C^* > C_0$.

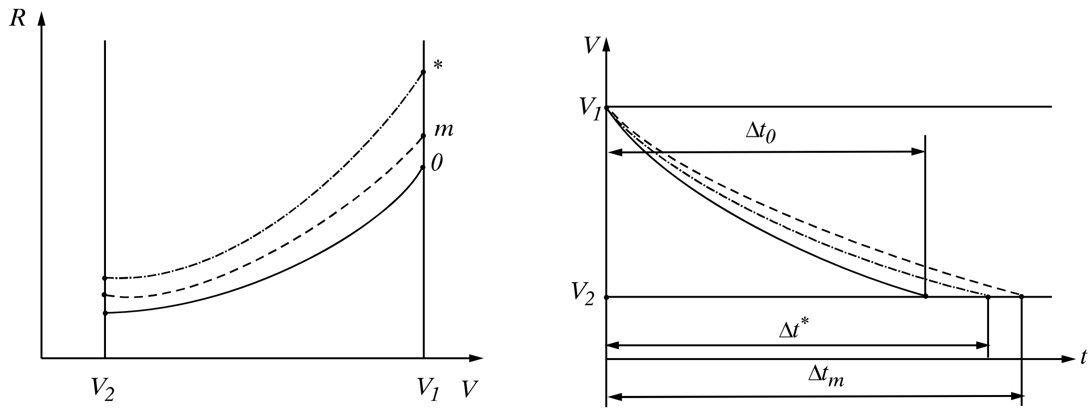

Figure 6.

Options (15.2) and (15.3) are only given *pro forma* and cannot occur in practice. For them to come into existence, the increased inertness of the ship due to the greater mass $m^* > m_0$ has to result in longer time Δt^* for deceleration from V_1 to V_2, but the value of the specific drag has to stay the same as the one at the reference trials: $C^* = C_0$ – condition (15.2) or even to go down: $C^* < C_0$ – condition (15.3).

This is in contradiction with the following premises established by practice:

- with the state of the hull being the same, there is more drag when the draught, respectively the mass, become greater.
- with the draught and the mass being the same, there is more drag at a certain speed when the fouling and the roughness of the hull become greater.

3. MAIN CONCLUSIONS AND RECOMENDATIONS

1. We expounded on the physical significance of the coefficient of inertial stopping *k,* expressed with relation (6). The values S_1 and S_2 cannot be registered experimentally, but they are easy to calculate. To this end, it is necessary to know the speeds V_1 and V_2 at the start and at the end of the time interval Δt when the ship is in inertial stopping.

2. Each of the conditions from (12.1) to (15.1) includes the ratio between the ship's mass m^* in the changed conditions of operation and the mass m_0 which the ship had when the reference value k_0 of the coefficient of inertial stopping was determined. To assess the change of drag in the course of operation, the ship's mass with respect to the draught must be known.

3. To determine the value K by means of (9), it is not necessary to use the formulae (7) and (8) to obtain respectively k_0 and k^*. If a ship decelerates from V_1 to V_{2_0} for the time Δt in reference conditions, when underway with different draught and with $m^* \neq m_0$ the speed will go down from V_1 to a different value $V_2^* \neq V_{2_0}$. This means that the coefficients of inertial stopping k_0 and k^*, calculated by means of (5), will be different. By absolute value $|k^*| > |k_0|$ when $V_2^* < V_{2_0}$, and, reversely, $|k^*| < |k_0|$ if $V_2^* > V_{2_0}$.

4. If the ship's mass m^* in the changed operational conditions is less than the reference m_0, the value of the specific drag coefficient will can be less than the value determined in the reference trials: $C^* < C_0$, despite the fouling of the hull.

3. CONCLUSIONS

The proposed methodology allows calculating the change of drag in operational conditions different from the reference conditions for the calculation of the value of the coefficient of inertial stopping k_0 and the value of the resistance R_0. Their change, resulting both from the increased fouling and roughness of the hull and the different draught and mass of the ship, is taken into account.

To assess the behaviour of the ship's propulsion system and its components, it is also necessary to know the change of the thrust generated by the propeller screw when the draught is changed and the propeller screw is fouled and becomes rougher. Furthermore, in the course of longer operation, the mechanical characteristics of the main engine are impaired, which also takes its toll on the operation of the system and needs to be analysed. When the changed mechanical characteristics of the engine, the screw and the hull are known, it is possible to forecast the change of the propulsive qualities of the ship's propulsion system.

REFERENCES

[1]. Avanzini, G., Benedetti, L., and Penna, R., - ***Experimental Evaluation of Ship Resistance for RANS Code Validation,*** ISOPE '98, Montreal, Canada, Maggio. 1998.
[2]. Stoyanov R. – ***Investigation of the ship's resistance,*** Thesis of the doctorat, Naval-Academy Varna 2010.

AN ANALYSIS OF THE POLLUTION RISK IN THE MEDITERRANEAN SPANISH COAST

[1]AMABLE V. ESPARZA LORENTE, [1]XAVIER MARTÍNEZ DE OSES F.

[1]*Universitat Politècnica de Catalunya, Spania*

Pollution risks coming from the shipping traffic is one of the real risks that Spanish coast can face. It is much closed the remember of the Fedra bulk carrier in the strait of Gibraltar, the Prestige tanker in Finisterre or the Castor near accident off the Almeria coast. The main objective of this paper is to analyse, identify and further to quantify, the areas in the Mediterranean Spanish coast, with biggest risk of suffering a hydrocarbons spill coming from the tankers maritime traffic. The study, in which this paper is based, has been considered a set of variables among which we can remark the geographic particularities, the climatic issues, the ships' age or the traffic density; that are going to feed an algorithm. This objective function will weight those different parameters in the entire coast and will identify the ones with the biggest risk probability. The results are going to put in evidence where are the most critical areas in the Spanish coast, when talking about its risk of spill.

Keywords: pollution, Mediterranean Spanish coast, risk of spill

1. INTRODUCTION

The Mediterranean Sea extends approximately on 3,800 km from East to West and 800 km from North to South, covering a surface of 2.5 millions of km2 which represents 5 times the surface of Spain. Its basin keeps a volume of 3.7 million of km3 with an average depth of 1,500 km which is clearly lower than the ocean average. The Mediterranean Sea is linked to the Atlantic Ocean through the Gibraltar Strait that is about 14 km wide and 300 metres deep. Other secondary passes from the hydrological point of view, is the connection with the Black Sea and the Indic Ocean through the Red Sea. From a general point of view we can identify two clear basins in the Mediterranean, limited by the Sicily canal and called Eastern and Western Mediterranean.

The Mediterranean basin, is identified by the limited agricultural, forest, cattle and even fishing, resources, including the energetic ones at least in the Northern coast, but with large reserves of natural gas and hydrocarbons in the Southern coast. In a parallel sense we find a population of 500 millions of persons and around 300 millions of tourists per year that are expected in this decade. Also in this coast there are the main hydrocarbons export ports, most of all in Libya, the Mediterranean country with the biggest reserves. In the European coast we must remark the port of Marseilles, as the biggest import port in terms of volume, with 65 millions of metric tones per year or Italy where there are placed the three main ports of such kind of traffic, with an added volume of 90 millions of metric tones.

The Mediterranean hydrocarbon traffic routes, from a internal point of view, are the ones from North to South and East to West, but we should add the crude oil traffic in transit that in the year 2006 sum up to 421 millions of metric tones only of crude oil, from which 72 millions where among non intra Mediterranean ports [10].

2. THE LEGAL SCENARIO

Those traffic figures, have contributed to sometimes accidents with disastrous spills. From a regulation point of view, the year 1967 was testimony of the Torrey Canyon accident that stranded in the English Channel, with a result of 120,000 tones of crude oil spilled. At that moment the international community began to be conscious of the magnitude of the possibility of accidents involving tanker ships every time bigger.

From a historical perspective, the number of accidents and the associated volume of spills, has been decreased globally from the year 1970, around the 86%, probably due to the enter in force of the MARPOL 73/78 convention [6], the OPA 90 [9] or the ISM Code [7]. Even the quantity of spills were previously directly related to the volume of crude carried, in the last years this tendency has been changed because the exchange commercial exchange of crude oil has increased but the quantity of oil spilled has proportionally decreased.

Analysing the spills in the last four decades, it is understood that most of them are produced in the routine operations of tankers, usually are port or terminals. The operational spills are reduced in volume, and 90% of them are less than 7 tones. Talking about the accidental spills, due to collisions or stranding and the 86% of them suppose spills of more than 700 tonnes. Among the most important accidents we can list apart the one of the Torrey Canyon, the MT Jakob Maersk in 1973, the MT Urquiola in 1976, the MT Amoco Cádiz in 1978, the MT Castillo de Bellver in 1983, the MT Exxon Valdez in 1989, the Aegean Sea in 1993, the MT Erika in 1999 or the MT Prestige in 2010, inter alia.

However and in a parallel way, the Mediterranean community begin to be conscious and understand the degradation situation of its own sea, the Mediterranean. In the year 1969, the CGPM [3] of the FAO [2], together with the CIECM [5], meets in a working group, elaborating in 1972 a report that is considered as the first complete study on the Mediterranean pollution. The spilled hydrocarbons at sea [1], can be split in different origins (see table 1).

Table 1: Causes of accidents involving spills up to 2004. Source own based on Cantano, A.

Causes	Average
Natural	10%
From shore	64%
Tankers operations	*7%*
Accidents	5%
Oil rigging at sea	2%
Other than tanker ships	12%

Additionally it is easy to check that the Mediterranean Sea is one of the most polluted area due to hydrocarbons spill in the world, with almost half a million of tones of hydrocarbons per year, compared with the assessed world volume of 3.2 millions of tones. But this area only represents the 1% of teh world sea water and the 30% of total transit in the world.

The Barcelona Convention in 1976, was established to protect the Mediterranean Sea against the pollution, carrying the UNEP (United Nations Environment Programme) out the tasks for its application. The convention was modified in June 1995 and changed its name, but also adopting additional protocols. In 1993, Spain ratified the International Convention on Oil Pollution Preparedness, response and Co-operation of 1990 (OPRC 90). The protocol on Preparedness, Response and Co-operation to pollution Incidents by Hazardous and Noxious Substances was apporved in 2000 (OPRC-HNS Protocol) but entered in force in June 2007. At the same time, the international regulations on pollution prevention from ships, has its stronger pillar in the MARPOL 73/78, that had its first steps on November 1973, accumulating up to 20 amendments and being its last part to be enforces the Annex VI in May 2005.

From a national perspective, we should remark the Order of 23rd of February of 2001, by means of which there was approved the National Contingency by Accidental Sea Pollution Plan, that was followed by other autonomical or regional, contingency plans in the Mediterranean litoral. From a general point of view, we can say that in the last four decades the fighting mechanisms against sea pollution, have advanced pollution, being the residues retirement still one of the most important points to be dealt. Also the detection and tracking of the spills has been aided by the new technologies as the air patrols or the satellite surveillance, together with the dispersion models, in order to get predicting the evolution of the oil slicks.

3. THE OPERATIONAL SCENARIO

The dangerous goods traffic intensity, is important mainly in certain “longitudinal paths” as the Suez – Gibraltar and Bosphorus cases and in other “latitudinal paths” as the routes between the North of Africa to the petrochemical complexes in the European coast, mainly Italian, French and spanish; ones. The traffic identification is not a problem nowadays due to the unified and electronic data transmission systems like the EDI manifests, the Toll Unified Dispatch Documento r form the ships point of view, the AIS system or the newest LRIT, [4] this last one in force from. From first of January of 2010 (and almost at) with a (its) 90% of penetration (now).

Within the Spanish waters it is possible to register the 70% of the European Mediterranean traffic, in order to reduce the risks motivated by its density, the OMI has approved different Traffic Separation Schemes (TSS). The first one in the Gibraltar strait in 1968, followed by the off Cabo Gata TSS in 1998 and further by the TSS off Cabo Palos and Cabo Nao, both in 2002. From the data of the public ports entity (Puertos del Estado), the oil refinement activity in Spanish port terminals is at their maximum levels, but the number of tanker ships calling at port, has been decreased compared with the eighties data. This is because the growing size of the ships. Additionally the coast wise traffic has decreased from the first years during the nineties due to the opening of the oilduct net from CLH company.

This tendency was changed in the last nineties due to the increase of the consumption and the saturation of the Spanish refinement capacity.

The routes followed by the ships carrying hydrocarbons, have been analysed with data from the national port authorities, in the years 2006 y 2007, being the results showed in the following table:

Table 2: Traffic volumes of oil in the Spanish waters. Source own based on Port Authorities data.

Corridor	Hydrocarbons or derivates, traffic	Rate
Axis Alboran Sea/Gibraltar strait	19.194.581	29,39%
Axis Spanish Med., Gulf of Lyon, Genoa	6.515.835	9.98%
Subtotal Axis Spanish coast	*25.710.416*	*39.37%*
Axis Arcew –Tarragona, Castellon	5.757.334	8,82%
Axis Arcew – South of Spain	433.076	0,66%
Axis Skikda	346.805	0,53%
Axis South Western Italy	755.094	1,16%
Axis East West	31.763.107	48,64%
Axis Balearic islands	534.766	0,82%
Total.	65.300.600	

4. STUDY METHODOLOGY

In order to get a risk value of the Spanish coastal areas, the study has selected a number of parametres among which we should remark the maritime traffic, the maritime climate, the coast morphology and the fleet age.

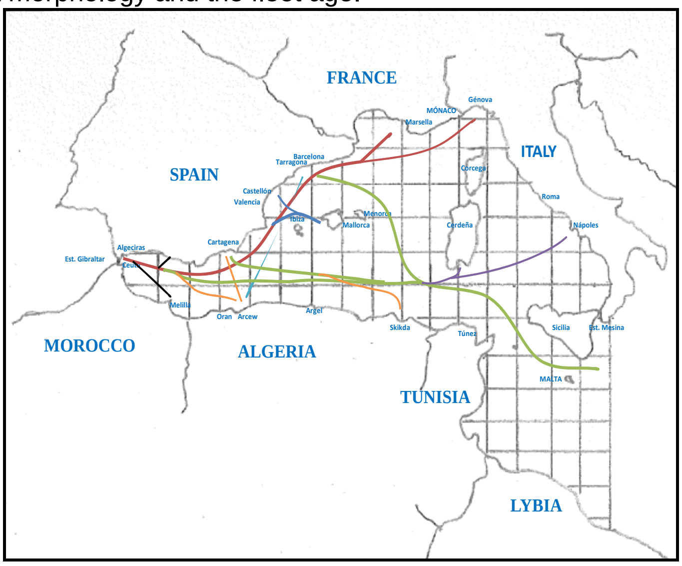

Fig. 1. Picture of the main hydrocarbons transport routes, calling at the Spanish Mediterranean ports. Source: own base don port authority data

The Mediterranean Sea and mainly the East-West axis, supports an important traffic of oil. During the year 2006, there were reported in the Mediterranean up to 4,224 shipments of tankers, carrying 421 millions of crude oil metric tones; and only 457 shipments totalized up to 72 millions of tones in transit among non Mediterranean ports [11].

The ports surrounding the Gibraltar strait, are the ones where most of the tanker ships are calling within the entire Spanish port system, reaching the 34% of the berthings followed by Tarragona and Barcelona with the 20% and 16%, respectively. Keeping in mind the Gibraltar calls, in one year the number of them will exceed the number of 4000, considering that the number of ships crossing the Gibraltar strait during the year 2007 were up to 105,954. In the year 2006, among all the ships in transit through the Gibraltar strait, the 19% were tankers, representing the 32% of the total tonnage.

In order to get a geographical distribution of the different areas in the Mediterranean, we have proceeded to divide the Mediterranean area into squares with a rate of risk from 0 to 10 depending on the volume of traffic supported.

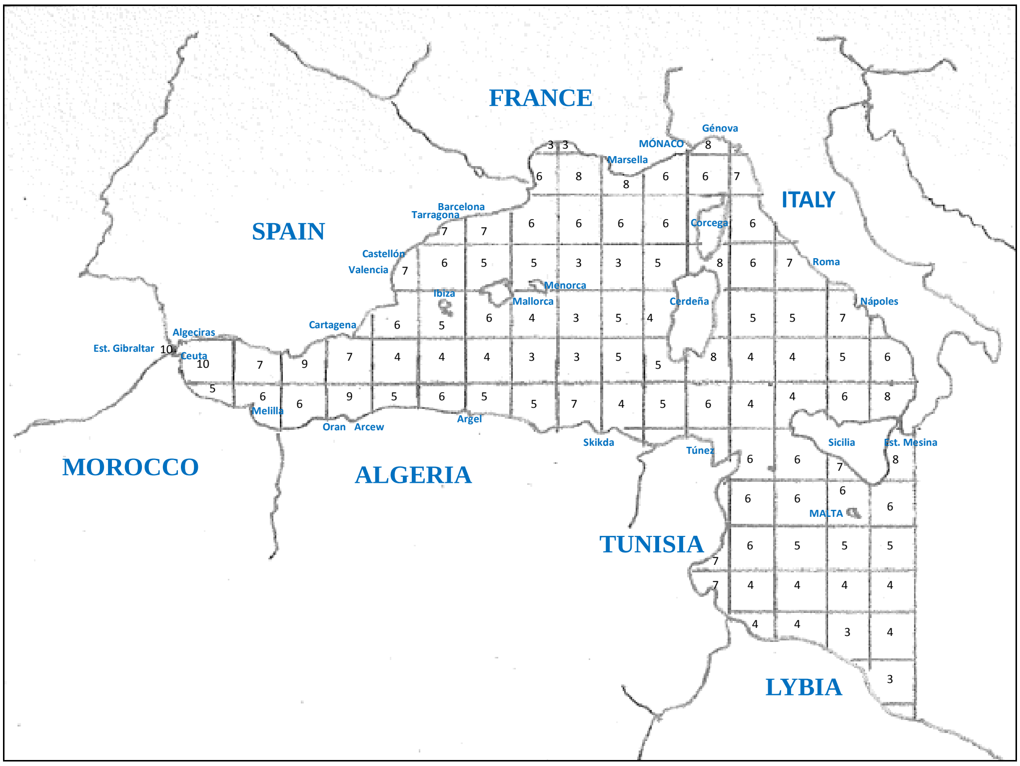

Fig. 2. Risk weight in each area limited in the Spanish Western Mediterranean

Another variable to be analysed, was the wind and wave regimes, based on the data from REMRO, XIOM and HIPOCAS project. In the most Eastern zones, the data has been acquired from “Instituto Superiore per la Protezione e la Ricerca Ambientale”, thriugh its Rete Ondametrica Nazionale - RON. In the other hand, the information related with the Sea of Lybia, was acquired from the EuroWeather service, Meteomed Mediterranean Forecast.

Based on the average significant wave height data, each one of the Squares in which the mediterranean was divided, has been scored.

The third main parametre studied, has been the Western Mediterranean morphology, through the nautical and batimetric charts, we get mainly the depth, together with other secondary data. Finally the age of the fleet was analysed, because one of the factors affecting the accidentability and probability of misfunctioning of the ships is the age; and those factors together are related with the number of sinistries. In the last decade, the age of the fleet has decreased drastically, for example in the case of tankers, those have reduced around the 32.7% with an average age of 10 years. In developped countries, tankers were younger with an average age of 7.7 years on january 2007. Around the 70% of crude that crossed the Mediterranean Sea, was carried out on board tankers younger than 10 years old nd only the 4% exceeded the 20 years old.

Another collateral factor to the age of the ship, is the registry flag. Analyzing the tanker ships flags, on a general view, the 65% of the cargo capacity of the tankers calling in the main Spanish Mediterranean ports, is from western countries and less than the 10% is under third countries flag. We should keep in mind that some of the conveninece flag fleets, are managed by western owners, being the flag only a costs or fiscal, question. The ports of Tarragona and Escombreras in Caratagena with both refineries of the Spanish company Repsol YPF, get cargo capacity from Western flags, of around 56%. Around 81% of the carried hydrocarbons are issued through tankers not directly related with oil companies nor states, due to the fact that oil companies have sold some time ago their fleets.

5. PRELIMINARY RESULTS

Once analysed the four main risk factors, we proceeded with the risk points census calculations. The weighting factor of each parametre has been obtained from questionnaires sent to different relevant stake holders in the maritime sector, getting a weighting factor as follows, 60% to traffic, 15% to waves, 10% to the morphology and 15% to the fleet age.

Applying the suggested weights in the different squared areas, the study identified among the 20 identified points, the 6 ones that has been the most risky points in the Western Mediterranean.

Table 3: Table showing the weighing of the most risky areas in the Western Mediterranean.

	Gibraltar Strait	Cabo Gata	Ceuta	Algeria Arcew	Sardinia	Marseille s
Traffic	6,00	5,40	6,00	5,40	4,80	4,80
Clima	0,75	0,90	0,60	0,45	1,05	0,90
Morphology	0,70	0,80	0,10	0,70	0,80	0,70
Fleet age	0,90	0,90	0,90	0,75	0,60	0,60
TOTAL	**8,35**	**8,00**	**7,60**	**7,30**	**7,25**	**7,00**

In order to get the wind values along all the Mediterranean field, there exists a net of deep water buoys (REDEXT net) and meteorological stations (REMPOR net); placed in fixed positions, measuring the wind intensity and direction every day, within specific time lapses (usually every hour) and on a long term basis. With this information it is possible to get instantaneous information together with long term data. In the most important points within the Spanish Western Medterranean the wind speed annual average, has been calculated taking the origin data from the mentioned web sites and from the public entity that manages the Spanish port system (Puertos del Estado).

The currents in the Mediterranean are mainly developing on the surface and caused by the wind action on a certain lapse of time. But we must remark the existence of another current based on difference of densities between the Atlantic and Mediterranean waters, that circulates in an anticlockwise sense, flowing Eastwards off the coast of North Africa from the Gibraltar Strait, up to Port Said in the Egyptian coast. At that point it turns to North off the coasts of Israel and Lebanon and further to West.

The set of the current is obtained from the Oceanographic section of Puertos del Estado and also from the Sailing Directions or Pilot Books of the Mediterranean and some other web sites like www.poseidon.hcmr.gr, www.meteofrance.com, www.hidromare.it, www.eurometeo.com y www.freemeteo.com. Classifying the wind and current data, we have applied an average movement of an oil slick that usually advances at the 3% of the surface wind speed [11]. With an approximate formula that combines the wind speed and direction effect, together with the existing current, the study obtained an average displacement speed of an oil slick as the following table shows.

Table 4: Table showing the approximate speed of movement of an oil slick in specific areas of the Western Mediterranean.

Geographical areass	Speed in km/h
Gibraltar Strait	9,307
Cabo Gata	5,225
Arcew (Algeria)	3,001
Marseilles	3,958

The estimation of speeds and directions of an oil slick, were assessed for the winter and summer times, getting different values of for example how many time the slick needs to arrive the coast.

6. CONCLUSIONS

Tanker fleet around the world has been renewed in the last years. In the OCDE countries the tankers fleet had an avergae age of 7.7 years old, being the world's average in 10 years old, slightly oler than container carriers.

New technologies on ballast management, tank cleaning, residues recovery and others have increased the operational safety and reduced the sinistrability to unbelivable levels some decades ago. As it has been showed in the table 4, the three of the main four points are placed in the South part of the peninsula, especifically in the Alboran Sea (together with the one in the North of Africa) and the fourth one in Marseilles. This last one can affect the NorthEast part of the peninsula. Among all the four points, two of them have less probability to affect the Spanish coast, even concentrating an important rate of traffic. The areas of Cape of Gata and Arzew, have less probability of produce a pollutant impact on the Spanish Coast, due to the existing sea currents.

Zones	Summer Oil slick direction	Winter Oil slick direction
Gibraltar Strait	North Coast, Strait and Coast of Malaga	Coast of Malaga
Cape of Gata	Coast of Algeria	Coast of Algeria
Arcew (Algeria)	Coast of Algeria	Coast of Algeria/Open sea
Marseilles	Marseillesa/Open sea	Catalan Coast/Open sea

In a situation of an oil spill in the area off Marseilles, could have an incidence on the Catalan coast (NE of Spain), starting on the Cape of Creus, there the continental through loses width and speeding the oil spill up, arriving to the coast of the Natural Parc of cape of Creus. It is estimated that there are up to 2 days to avoid the pollution in the Spanish coast.

The most dangerous area is the one in the Gibraltar Strait. The high density of traffic and aldo the high number of tanker ships sailing there and calling the Bay of Algeciras, supposes a considerable risk factor. In case of accident and a subsequent spill, the weather conditions would mean that the coast of Spain up to the coast of Malaga, would be affected depending on the wind intensity but with a lase rate of between 2 to 6 hours.

REFERENCES

[1]. Cantano, A. ***El convenio MARPOL 73/78. Un estudio detallado.*** MIRMAL. Issue 14, 2004. United Kingdom
[2]. Feed and Agriculture Organisation, Geneve, Switzerland
[3]. General Commission of Fishing of the Mediterranean, France
[4]. ***Guidance on the implementation of teh LRIT system.*** MSC.1/Circ.1298. International Maritime Organization, 8th December 2008. London, United Kingdom
[5]. Intergovernmental Oceanographic Commissio
[6]. ***International Convention on Maritime Pollution prevention***. International Maritime Organisation 1973/78 as amended, London, United Kingdom
[7]. ***International Safety Management Code.*** International Maritime Organization. 1996 as amended, London, United Kingdom
[8]. ***Manual on the Pollution Ocasioned by Hydrocarbons,*** Part IV Fighting against the Hydrocarbons Spills. International Maritime Organisation. London, United Kingdom
[9]. Oil Pollution Act. Department of Trade. 1990, Washington D.C., United States of America
[10]. ***Study of Maritime Traffic Flows in the Mediterranean Sea*** - Final Report – July 2008/REMPEC
[11]. ***Study of Maritime Traffic Flows in the Mediterranean Sea*** - Final Report, July 2008, REMPEC Malta.

CORROSION RESISTANCE OF THE LAYERS OBTAINED BY ELECTRICAL SPARKING WITH ALUMINIUM AND BRONZE ELECTRODE

[1]BARHALESCU MIHAELA, [1]SABAU ADRIAN

[1]*Constanta Maritime University, Constanta, Romania*

The work entitled "Corrosion resistance of the layers obtained by electrical sparking with aluminium and bronze electrodes" presents the research done by the authors in regards with obtaining some superficial metallic layers, on samples made of carbon steel OL 37 brand, with the help of some electrodes from a corrosion resistant material (CuSn10 and Al). The corrosion resistance of the obtained experimental layers was determined through gravimetrical method. The superficial layers subject to the corrosion agent (sea water) were analised through optical microscopy, using the computers QX3 Intel Play microscope.

Keywords: superficial layers, electrical discharge impulses, corrosion resistance

1. INTRODUCTION

The superficial treatment through impulse electrical discharges is a procedure through which the proprieties of the metallic materials can be improved. The process is that during the discharges (short period) an erosion of the cathode takes place and a transfer of erosion products on the treated surface takes place.

The geometric and microstructure characteristics of the superficial layers experimental obtained depend on the work parameters used in the treatment process.

The optimal values of the discharge process parameters are construed only from experimental research.

The proprieties of the superficial layers obtained through this procedure are the same as the electrodes material being used or very close to this one, the resulted proprieties though micro alloying and the diffusion of the steel probe electrodes material

2. EXPERIMETAL RESEARCH

The superficial treatment through impulse electrical discharge was made with the ELITRON 22 A equipment, where made on parallelepiped probes from steel carbon OL 37 brand. The electrodes using to electrical sparking are CuSn10 and Al.

The treatment through electrical discharges where made manually, the active electrode is under a 60^{o} angle with the treated surface.

When treatment with electrical discharges a significant importance in the formation of the superficial layer and it's qualities, has the electrode section surface, influence that will be manifested at the working regime temperature variation and at the current density which passes through the electrode.

In the experiments wasn't specified the electrode vibration amplitude value because this does not influence neither the layer thickness, or it's structure, the only importance is to be big enough to prevent the solder of the electrode with the surface which will be treated.

In table 1 are presented the recommended values for the electrode cross section in regard tot the work regime of the ELITRON – 22A equipment and the current value at every regime.

Table 1 The recommended values for the electrode cross section

Electric work regime ELITRON – 22A	1	2	3	4	5
Electrode cross section value [mm]	4	5	$4 \div 6$	$5 \div 6$	$6 \div 9$
Work current [A]	0,5	0,8	1,3	1,8	2,3

Through the corrosion research process using the gravimetrical method, the parallelepiped probes superficial treated with electrical sparking, with the surface of 0,00127512 m^2 where suspended with an synthetic line (nylon) of $\phi = 0,2\,mm$ in a plastic material tub at 4 cm above the tubes liquid level (see water), being immersed 285 days in static see water at the environments temperature.

The probes on which the superficial treatment was made through impulse electrical discharges where individually weighted on the analytic balance at different time intervals, determining the corrosion process speed:

$$v_{cor} = \frac{\Delta m}{S \cdot t} \tag{1}$$

where: v_{cor} - rate of corrosion $\left[g \cdot m^{-2} \cdot day^{-1}\right]$;

Δm - variation weight $\left[g\right]$;

S – samples surfaces in contact with see water $\left[m^{-2}\right]$;

t – time of exposure $\left[days\right]$.

The research of superficial layers processed with electrical sparking using CuSn10 and Al electrodes, immersion 285 days in sea water was realized through optical microscopy using QX3 Intel Play Computer microscope at 60:1 enlarge power.

At long immersions of the probes in sea water, the exposed surface suffers modifications in the way of puncture of the superficial layer resided and corrosion takes place in dots after the penetration of the corrosive agent.

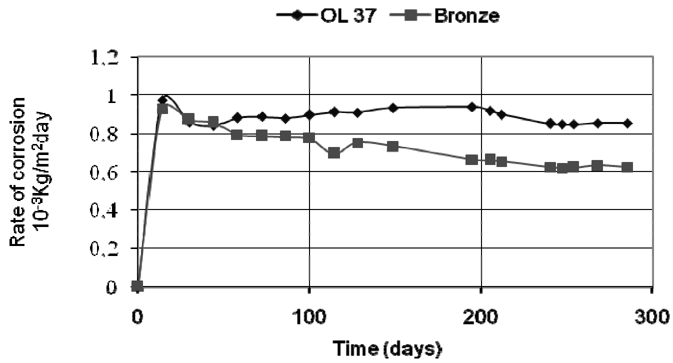

Fig. 1 Rate of corrosion

The OL 37 steel sparked with the using electrodes, is corrosion resistant, having the estimated scale of 4 (according to STAS 9684-82), the corrosion speed between 0.21 – 1.0 g/(m^2.zi) in comparison to the steel used as original probe which has the estimated scale 5, and the corrosion speed between 1.0 – 2.1 g/(m^2.zi)

On the superficial layers subjected to see water, initially you can observe a progressive increase of the corrosion speed, because of the oxygen absorption. After the effect of microorganisms, the corrosion drops to an almost stationary value. This is because of the fact that microorganisms eliminate oxygen from the surfaces, but an anaerobic corrosion still persists.

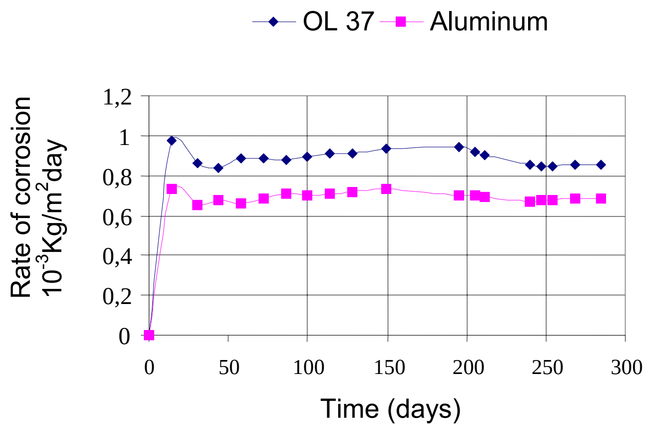

Fig. 2 Rate of corrosion

From the graph shown in Figure 3 is observed that the time interval of 149 days the most stable is OL 37 steel coated with Al electrode surface. At time t = 150 days, steel coated with Al electrode has the same stability with bronze coated steel electrode. After this time the order of corrosion resistance for both types of coverage is change, the most stable surface layer is covered with bronze electrode.

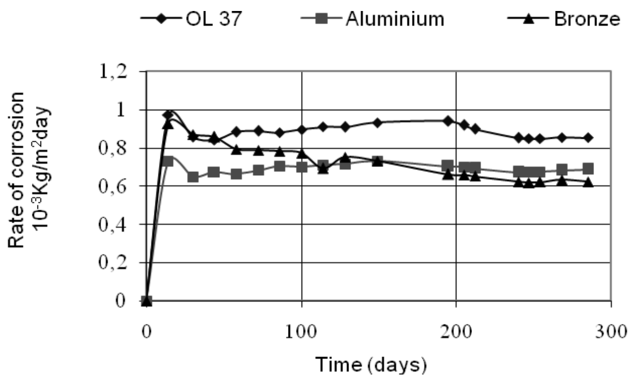

Fig. 3 Rate of corrosion

The metalographic analyses on was made on the samples surface. The sample was tacked off from the corrosive medium, washed, cleaned from all the corrosion products and dry.

The optical metalographics analyses of the original probe from OL 37 steel and sample sparked with bronze electrode are present in figure 4 and 5.

On the original probe from OL 37 steel we can observe corrosion products (iron oxides); it has brown color (figure 4,a). On the side of the sample appear the reaction products, which are blue color (figure 4,b).

Level differences on the surface could be observed as result of the cleaning the corrosion products from the sample.

When used bronze electrode to obtained a compact deposition with few corrosion product which are in brown color zones (figure 5, a).

Because the superficial layers have not a constant thickness on the surface sample, after long immersion of the probes in sea water, appear exposed zones of the corrosive agent (figure 5,b) where a micro relief has appear. Hear we can observe higher zones without corrosion and lower zones where corrosion has advanced to the basic material

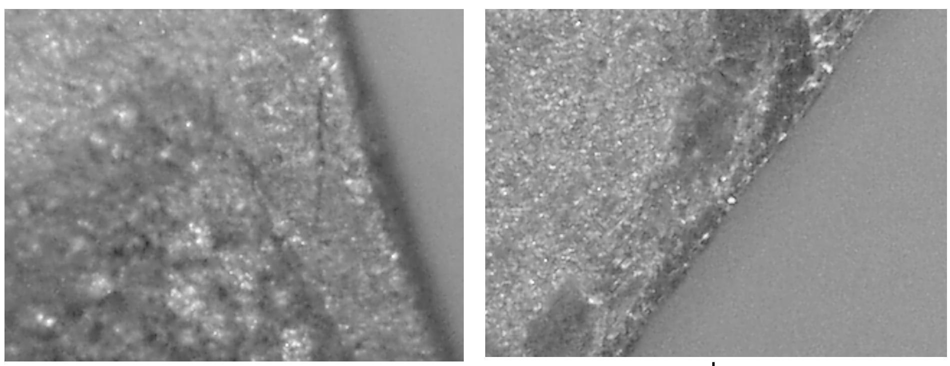

a b

Fig. 4. OL 37 sample steel - 60:1

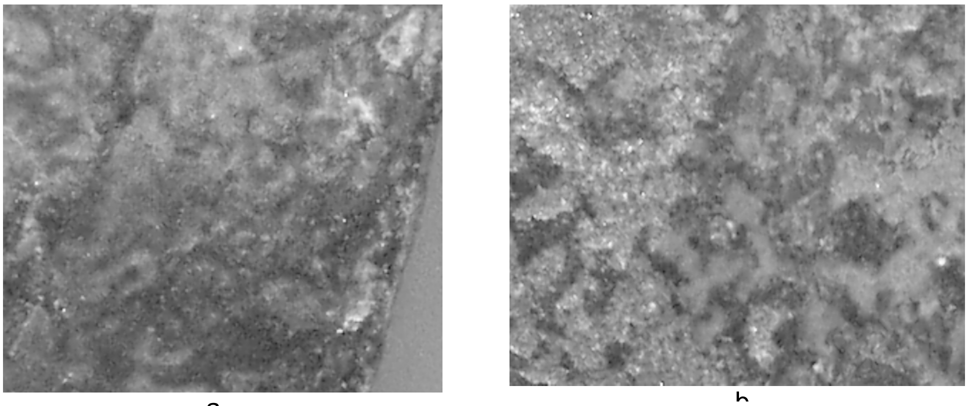

a b

Figure 5. OL 37 steel samples sparked with CuSn10 electrode – 60:1
Work regime 2 - 60:1

Samples sparkle with aluminum electrode after exposure to sea water shows a uniform deposition without consistent corrosion products (Figure 6, a), which leads to the conclusion that the aluminum oxide film formed when the water deposited layer interaction greater evidence of good protection of the exposed area to the corrosive agent.

In Figure 6 b there is a sample area of aluminum proof, which is not covered because the manual method of filing the superficial layer. Uniform deposit layer aluminum core material allowed to be exposed to corrosive agents and corrosion effect is apparent.

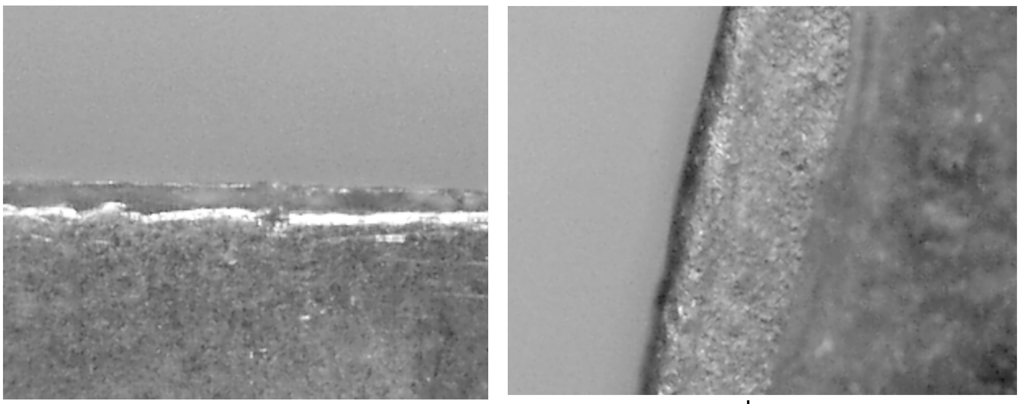

a b

Fig. 6. OL 37 steel samples sparked with Al electrode – 60:1
Work regime 2 - 60:1

3. CONCLUSIONS

From optical metallographic analysis superficial layers subjected to sea water, is observe zones where the layer is uniformly deposited did not allow corrosive agent to interact with the material basis. In these zones, did not exist effects of corrosion. Zones where defects appeared are most attacked, resulting reaction products after the corrosion.

The superficial layers laid through Aluminum and Bronze electrodes sparking proves a improved corrosion resistance to sea water compared to the base steel, specially for long term tries, when the corrosion speed is stabilizing remaining almost constant.

Throughout the interval studied, the stability is preserved, the less stable is steel coated with the CuSn10 electrode.

After the optical metallographic analysis on the superficial layers, after the contact with the corrosion agent could be observed zones where the deposed layers is uniform and the corrosion agent could not interact with the basic material, so in these zones is not any effect on the corrosion process.

REFERENCES

[1]. Barhalescu M. - ***Cercetari privind obtinerea si analiza structurala a straturilor metalice subtiri rezistente la coroziune***, Teză de doctorat, Facultatea "Stiinta si Ingineria Materialelor" Iaşi, 2007

[2]. Barhalescu M., Pascu R., Dinescu M. - ***Corrosion Protection of Metallic Surfaces by Processing with Impulse Electrical Discharges, Protective coatings and thin films 07*** of E-MRS 2007 Spring Meeting, 28 May-1 June, Strasbourg

[3]. Barankova H., Bardos L., Berg S**.** - ***Surface and Coatings Technology,*** No. 94-95, 1997

[4]. Boian R. - ***Corrosion Tests and Standard: Application and Interpretation, ASTM Publication***. 2 nd edition. 2004

[3]. Zolotih. B. N., Melider. R.R. - ***Fiziceskie osnovielektroerozionnoi***, Masinostroenie, Moskva

*** ***Ustanovska ELITRON 22***, Academia Nauk, Chisinau,1991

ORIGINAL METHOD FOR DETERMINING THE HYDRAULIC RESISTANCES IN THE PIPING INSTALLATION

BEAZIT ALI

Naval Academy “Mircea cel Batran” Constanta, Romania

Starting from the analogy for hydraulic pipes and respectively for electrical conductors in the permanent flow of the equal density fluids the relations and relevant indicators from energetically point of view can be obtained electric-dynamic.

Keywords: Equivalent hydraulic resistance, flow rate module in the effluent flows.

1. INTRODUCTION

In the case of a constant density fluid, the specific energy in a current is defined as:

$$e = z + \frac{p}{\gamma} + \frac{v^2}{2g} = e_p + e_k \text{ [m. fluid heigh],} \tag{1}$$

the first two components (the geometrical height *z* and pressure height $\frac{p}{\rho g}$) are static or potential, and $\frac{v^2}{2g}$ is kinetic.

In a section the power of the fluid current can be written as:

$$N_h = G\&e = \rho \cdot g \cdot Q \cdot e \text{ [W],} \tag{2}$$

where:

- $G\&= m\&g$ being the gravity flow rate,
- $m\& = \rho \cdot Q$ is the mass flow rate.

We can say that the variations of the potential energy of position and of kinetic energy are low (insignificant) in comparison with the variation of the potential energy of pressure. Thus, in the case of liquids and gases or vapours in industrial installations, traversed with relatively low velocities (under 50 m/s), Δp is preponderant in this case. So the following relation determines the hydraulic power:

$$N_h = \Delta p \cdot Q \text{ [W],} \tag{3}$$

Starting from this presented quantities an energetically optimisation can by made, which is detailed in this article and leads to accurate measurements that can by taken in the projected phases, so that the optimal flows of exploitation can by chosen, which have as a final effect the energy economy.

The transport of fluids under pressure for effluent movement is particularised in the article, given for example two real cases.

2. TEORETICAL CONSIDERATIONS

The following couple of dimensions are analogous: $N_h \approx N_{el}$, $\Delta p \approx U$, $Q \approx I_c$
As it follows, we can write:

$$N_h = R^* Q^2 \quad \text{[W]} \tag{4}$$

and

$$\Delta p = R^* Q \quad \text{[N/m}^2\text{]}, \tag{5}$$

where R^* is the equivalent hydraulic resistance, analogous to Joule's law:

$$N_{el} = U \cdot I_e = R \cdot I_e^2 \quad \text{[W]} \tag{6}$$

and Ohm's law:

$$U = R \cdot I_e \tag{7}$$

From here, is necessary to define a new equivalent hydraulic resistance of hydraulic conductor $R^* \approx R$ and to analyse a few energetic consequences and interpretations.
In this way, we are able to obtain:

$$R^* = \frac{k_a \cdot \dot{m}}{2A^2} \quad \text{[N}\cdot\text{s/ m}^5\text{]} \tag{8}$$

in which it was recommended an analogue dimensionless original constant /indicator

$$k_a = \frac{1}{\mu^2}, \tag{9}$$

particular to the different kinds of movements. The R^* dimensions is:

$$[R^*] = \frac{[p]}{[Q]} = \frac{N/m^2}{m^3/s} = \frac{N \cdot s}{m^5}, \tag{10}$$

The expression of equivalent hydraulic resistance (8) it's kind of surprising and inconvenient, being superior qualitative and quantitative to the physical phenomenon of flow resistance through a fluid conductor, proportional with the weight rate, having a big influence over the ideal motion.

We can emphasise the determinant factors of the hydraulic resistance by introducing the Reynolds criterion (the flow regime):

$$\mathrm{Re} = \frac{\rho \cdot v \cdot d}{\eta},$$

(11)
in which we consider:

- the circular cross-section $A = \frac{\pi d^2}{4}$,
- $v = \frac{Q}{A}$ the average speed in the cross-section,
- η dynamic viscosity coefficient of the fluid.

We will obtain a new expression:

$$R^* = \frac{2}{\pi} \cdot k_a \cdot \frac{\eta \cdot \mathrm{Re}}{d^3} = \frac{2}{\pi} \cdot \frac{\eta \cdot \mathrm{Re}}{\mu^2 d^3} \tag{12}$$

We note:

$$C_m = \frac{k_a}{2A^2} \text{ [m}^{-4}\text{]} \tag{13}$$

and we will obtain:

$$R^* = C_m \cdot \dot{m} \tag{14}$$

The impulse is the dynamic action force:

$$I = \rho \cdot Q \cdot v = \dot{m} v = A \cdot \rho \cdot v^2 = 2A \cdot p_d \text{ [N]} \tag{15}$$

caused by dynamic pressure (stagnation, impact):

$$p_d = \frac{\rho \cdot v^2}{2} \text{ [N/m}^2\text{]} \tag{16}$$

We can obtain:

$$R^* = \frac{C_i \cdot I}{Q}, \tag{17}$$

noting the proportionality coefficient (impulse constant):

$$C_i = \frac{k_a}{2A} \text{ [m}^{-2}\text{]} \tag{18}$$

The relation (17) can be understood as expressing the specific/unitary impulse deficit (for a unitary volume rate), because of the resistance at flow. The relation (17) can be written as:

$$R^* = C_i(\rho v) \tag{19}$$

In this case (ρv) is the weight speed. The relation (16) can be used as unique definition for the impulse force:

$$I = C_i^{-1} R^* Q \text{ [N]} \tag{20}$$

construed in the case of the appropriate devices/instruments/machines, which generates and/or uses fluid jets in dynamic purposes (active or reactive). There are also defined two relations of energetic transformation of the specific potential energy into specific dynamic energy (of motion), for an unitary flow rate:

$$p_d = k_e \cdot \Delta p \text{ [N/m}^2\text{]} \tag{21}$$

and

$$e_d = k_e \cdot e_p \text{ [m.fluid heigh],} \tag{22}$$

where:

$$k_e = k_e^{-1}, \tag{23}$$

where the recommend original coefficient, of proportionality k_e may be used as a sub-unitary dimensionless indicator of energetic transformation, having the meaning of a conversion efficiency considering the specific energy losses through hydraulic resistance at flow.

As it follows we will make the appropriate particularisation for some kinds of motions.

In the case of laminar effluent flows (through orifices, nozzles, short tubes of discharge) it is denoted, usually, the geometric cross-section of the orifice A_o=A, and the flow rate coefficient with μ, depending on the orifice's shape and position, the wall thickness and the fluid nature/state. The flows is determined by the level difference $z = h$ and/or by a possible overpressure (measured with the manometer) p_m, so:

$$e_p = h + \frac{p_m}{\rho g} \text{ [m fluid heigh]} \tag{24}$$

and

$$\Delta p = \rho \cdot g \cdot h + p_m \text{ [N/m}^2\text{]}, \quad (25)$$

The relation (9) and (23) give k_a and k_e respectively.

In the case of the ducts for tanks emptying or the case of the ducts for fluid flow it was defined the flow rate coefficient:

$$\mu = \frac{1}{\sqrt{\alpha + \lambda \frac{L}{d} + \sum \zeta}} = \frac{1}{\sqrt{\alpha + \lambda \frac{L_{tot}}{d}}} \quad (26)$$

where:

- *L* being the duct's geometrical length of diameter *d,*
- L_{tot} is the total length *(L* plus the equivalent sum of lengths to the local hydraulic resistances, which have the coefficients ζ),
- λ is the linear hydraulic loss coefficient, and a is the Coriolis coefficient.

The coefficient λ and a are depending on the flow regime (Reynolds criterion) and on the relative roughness of the inner wall.

The expression (9) and (23) give the indicators k_a and k_e*,* respectively.

In the case of using, for designing, the flow rate modulus it results:

$$k_a = \frac{2gL}{C^2 R_h}, \quad (27)$$

or

$$k_a = \lambda \frac{L}{D} = \lambda \frac{L}{4R_h} \quad (28)$$

R_h being the hydraulic radius (for non-circular cross-sections), *D = d,* and *C* is the constant from the Chèzy velocity relation.

In the case of the ducts in the parallel lines are used analogies with Kirchhoff s laws. The algebraic sum of the rates/currents in anode is zero.

$$\sum_{i=1}^{n} Q_i = 0 \quad (29)$$

and the pressure difference between nodes

$$\Delta p_j = (\lambda_j \cdot \frac{L_j}{D_j} + \sum \zeta_j) \cdot \frac{8\rho}{\pi^2 D_j^4} Q_j^4 \quad (30)$$

is the same on all lines of the system.

The energetic optimisation presented by the present article can be obtained by proper measures, from the design stage, but also later interferes of exploitation. We want to minimise hydraulic resistance R* by:

- minimisation of the weight rate *m&* (generally, this is imposed);
- increasing the flow cross-section *A*; it appears at the 2nd power at the denominator

from the right member of the relation (8), so in the case of the circular pipes the diameter D appears at 4th power, the influence being very big.

We want also to minimise the coefficient k_a*,* and to make $k_e \approx 1$, so to maximise the flow rate coefficient μ, $\mu \to 1$. This one appears at the 2nd power at the denominator of the relation (9), being sub-unitary, so the influence is important.

In the case of relation (24) we want to minimise the dimensionless expression $\lambda L / D + \sum \zeta$ (so $\lambda \to \min, L \to \min, \sum \zeta \to \min$), which will also produce the increasing of the diameter *D*.

Related with the Coriolis coefficient, α a is 2 in laminar flow and α is 1,03...1,01 in turbulent flow. So, is preferred to obtain the smooth turbulent movement, which approaches α to the unitary value, and a is minimum (calculable with Blasius formula).

The present study may simplify the solver of two categories of problems: of exploitation and design.

Concerning the exploitation problems the system is given and the determination of the flow rate is requested:

$$Q = \frac{\Delta p}{R*} \quad [\mathrm{m}^3/\mathrm{s}] \tag{31}$$

The most important factors and the accurate measurements can be distinguished through the *R** (expressions) relations.

Concerning the design, the Q flow rate is frequently imposed and a combined optimisation can be achieved($k_e \to \min, k_e \to 1$). The calculus can be iterative.

3. PRACTICAL APPLICATIONS

It can be seen through two applications, one for effluent movements and another for the transport through a pipe.

The case of a circular aperture made in a thin wall of an reservoir is considered, the flow coefficient being μ=0.64, so $k_e = \mu^2 = 0{,}41$, which represents a small transformation value (the utilisation of potential energy). A cylindrical Borda nozzle is attached to this aperture with μ= 0.82 so $k_e = \mu^2 = 0{,}675$, that conduces to a decrease of the hydraulic resistance and an increase of the energy valorisation with 64%.

If a convergent typical profiled nozzle is used for e.g. after two circular arcs, with μ=0.95; so $k_e = \mu^2 = 0{,}69$ a remarkable progress is obtained (a loss to the potential energy transformation in kinetic energy is only 10%).

To show the case of a water pipe design with the length *L* = 120m, is necessary to transport a volume flow rate *Q* = 0.01 m^3/s.

Initially a diameter *D* = 60 mm and a top with ζ_R = 5 (in fully open position), It can be determined:

v = 3.54 m/s,
Re =3,2 $\cdot 10^5$ (rugged turbulent movement),
λ = 0.02,
*R** =1,0610^8 Ns/m^5 (very big),
μ =0.147,
k_e = 2,17$\cdot 10^{-2}$ (small),
p_d = 2,3$\cdot 10^4$ Pa,
Δp = 2.81 bar.

The flow is assured with a series centrifugal pumps, but the energetically loss is big.

In a second variant a pipe with a diameter *D* = 80 mm and a top with ζ_R = 5 is proposed. It is recalculated:

v = 2m/s,

Re = $1,6 \cdot 10^5$ (rugged turbulent),
λ = 0.02,
R* = $7,2 \cdot 10^6$ Ns/m^5 (very much low),
μ = 0,166, k_e = $2,78 \cdot 10^{-2}$,
$p_d = 2 \cdot 10^3$ Pa
Δp =0.693 bar.

The flow can be assured with a normal (series) water centrifugal pump, with a training power of app. 1kW, at a pump efficiency of 0,72.

The energetically loss can be reduced through the use of a plastic pipe; in this case the flow movement becomes smooth turbulent.

So, by diminish the linear loss coefficient λ = 0,0158, we can obtain a pressure loss Δp = 0.57 bar, which leads to a decrease of used power with 13%.

4. CONCLUSIONS

The paper presents a simple method for obtaining a quickly practical design. This way conduces to an important energy economy and material consumption respectively minimal investments.

REFERENCES

[1]. Ali B. - ***Calculation of the load losses in the marine piping installation*** , Buletinul celei de-a XXXIII-a Sesiune de Comunicari Stiintifice Internationale a Agentei de Cercetare pentru Tehnica si Tehnologii Militare , vol II, pp. 230 – 235, Bucuresti, 2002

[2]. Nicolae F., Ali B. – ***Procese termice si hidraulice în masinile si instalatiile navale si portuare. Aplicatii***, Editura Academiei Navale "Mircea cel Batran ", pp.171 - 195, Constanta, 2002, ISBN 973–97913 - 5-2

[3]. Benche V., Ungureanu V.B. - ***Contributions to the generalisation of the economical calculus for pressurised fluid pipes***. Ovidius University Annals of Constructions, vol. I, No. 3, pp. 229 - 232, Constanta, 2002

[4]. Popa I., Ali B.,**- *Calculul şi proiectarea instalațiilor navale cu tubulaturi***, Buletinul Simpozionului Stiintific international "Universitaria ROPET 2003", pp.137 - 140 , Petrosani, 2003

[5]. Ali B., LIGIA - ADRIANA Sporit L.A., Ali L. **- *Examples regarding the estimation of hydraulic loss in naval installation with tubes*,** *The* Knowledge Based Organization International Conference KBO 2009, „Nicolae Balcescu Land Forces Academy", *pp. 32 - 36,* Sibiu, 26-28 noiembrie 2009, ISSN 1843-6722

AN EXPERIMENTAL METHOD OF CONTROL OF THE PROCESS OF DRYING OF SHIP HIGH-VOLTAGE INDUCTION MOTORS BY PROGRAMMABLE LOGIC CONTROLLER

[1]BOHOS APRAHAMIAN, [2]BORISLAV DIMITROV

[1]Nikola Vaptsarov Naval Academy, Varna,Bulgaria, [2]Technical University, Varna, Bulgaria

The high-voltage induction motors are widely used in ship electric propulsion drives, like AZIPOD and in ship bow thrusters.
The stability of insulation resistance of the electrical machines is closely connected to the methods of control of the process of drying during the periods of operation and repair.
We propose an experimental method that enables to control the process of drying of ship high-voltage electrical machines by programmable logic controller.

Keywords: drying of electrical machines, insulation resistance, process control with PLC

1. INTRODUCTION

The insulation of the electrical machines can be moistured from the environmental conditions during transportation, storage, installation or operation. This requires systematic checking of the insulation resistance and taking necessary measures in deterioration of the moisture.

It was found that the critical value of the constant absolute humidity, which changes the electrical properties of insulating materials is not less than 15 g/m^3. Of all the climatic factors affecting the electrical insulation, the impact of high humidity (tropical climate) is the most severe and most often causes malfunction of electrical products and burn them. It is known that abrupt changes in temperature cause condensation on electrical equipment that in the presence of salts and contaminants can cause deterioration of the electrical properties of the materials. In the manufacture of ship's electrical equipment the nominal calculated environment temperatures for open decks are accepted from +45°C to -30°C. Air humidity is sufficiently high (93±2) % at a temperature (25±3) °C. Under the influence of moisture may occur changes in the electrical, physical, mechanical and chemical properties of insulating materials. The water has a rather low electric resistance and connect to salts forming electrolytes and becoming not only a conductor of electric current, but initiator of electrochemical reactions that accelerate the destruction of the insulation. Thus, the temperature and the humidity are factors that trigger the accelerated aging and destruction of insulation and are the reasons for failure of responsible devices [8].

Passing current through windings is one of the most effective means of drying motors. These internal heating methods apply heat at the winding conductors where it is most effective in driving out the moisture. However, care must be used not to apply too much heat by this method as vapor pressure can be built up within the damp insulation which may rupture it.

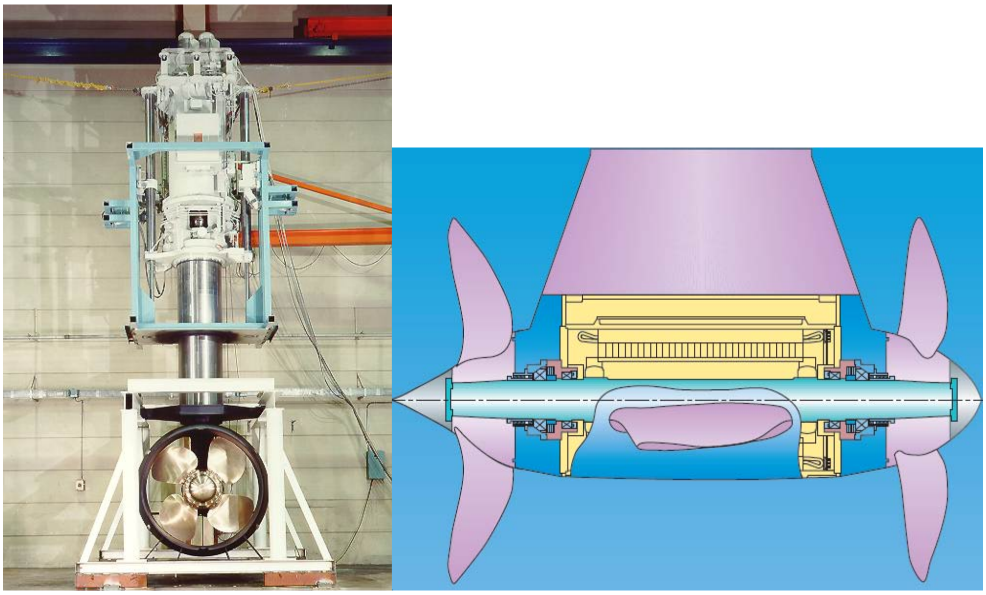

Figure 1: A LOHER Bow Thruster Drive for shuttle tanker, output power up to 2200 kW, voltage up to 11kV [1] and Siemens Schottel Propulsion (SSP) Drive System with high-voltage permanently excited synchronous motor [2].

This danger can be avoided by starting with a low value of current and increasing it gradually until a maximum temperature of 85 °C is observable on the surface of the coils. The motor must be sufficiently open so that moisture can easily escape outside the enclosing frame. A forced-air draft by electric fan or blower also reduces the time needed for dryout, which may require hours or days. The current should be reduced or cut off intermittently, if necessary, to prevent excessive temperature so that no scorching could occur.

The progress of dryout should be watched by taking insulation resistance readings using a low-voltage instrument to avoid puncturing the wet insulation. If previous measurements of the dry insulation resistance are available, they will afford a "benchmark" of the normal insulation to show by comparison when dryout has been completed. This often shortens considerably the drying time and helps to prevent false interpretation of the dryout curves when these curves tend to level off at values below normal due to entrapped moisture or local wet spots. Any sudden downward drop in the resistance readings not accounted for by a rise in temperature indicates that trapped moisture is still present and dryout should continue. Each motor will have its own final top reading and Fig. 2 illustrates how the resistances should be plotted against time [3].

The proposed system is designed for drying of high-voltage asynchronous and synchronous electrical machines. It is applicable to work with ship motors with nominal voltage up to Un = 15 kV, widely used in ship electric propulsion drives, like AZIPOD and in ship bow thrusters – Fig.1.

The main objective of the process is ensuring acceptable insulation resistance between the three phases [6], [7]. The applied method of drying is through a high power electric three-phase voltage Uz = 380V. Moreover, the removal of moisture is carried out by heating the stator coil by the flowing current.

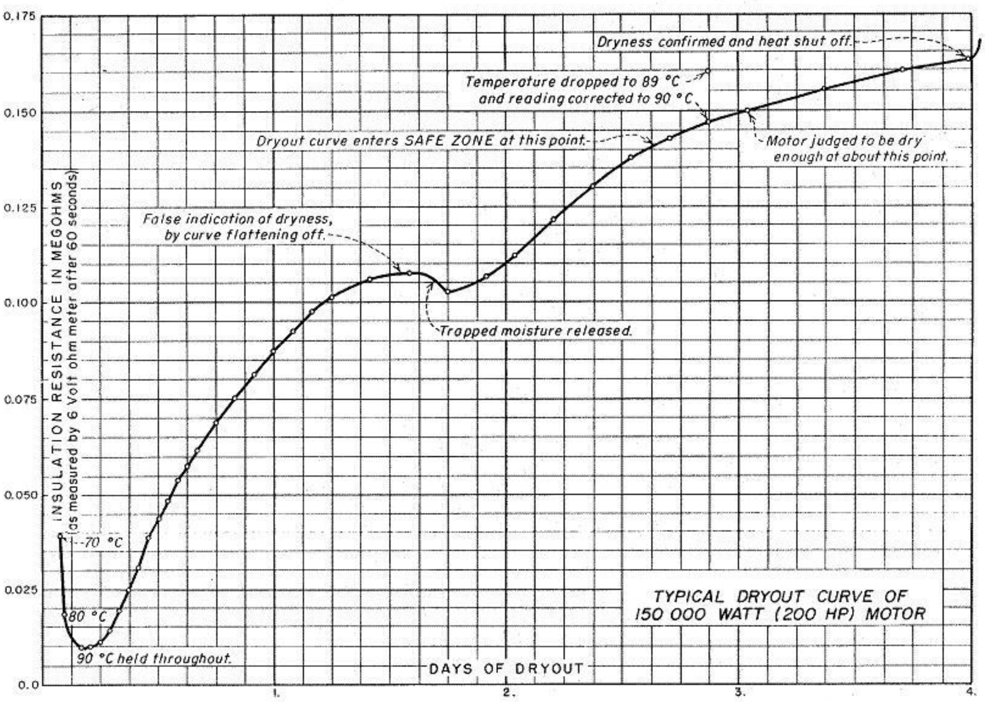

***Figure* 2: A typical dryout curve of 150 kW electric motor [3].**

The article proposes a drying system, allowing control by programmable logic controller (PLC). Following functions are provided:

- Automatic control of the drying process carried out through the implementation of the PLC software. This lapses the need of human involvement. Practically, the control of insulation in the drying process is carried out in the recommended interval of 1-2 hours, which in standard conditions is imposed by the measurement operator.
- Suspension of the drying process after reaching the nominal parameters of insulation. In terms of energy efficiency, this system reduces the possibility of excess consumption of electricity.
- Option to record measured values and determining the absorption coefficient used for analysis of the drying process, respectively assess the state of the motor.
- The proposed system is built on a programmable controller of the company Moeller [4], Easy Series 700, 800, MFD [5]. Practically, the development of the device can be performed with the use of any PLC, providing the necessary functions. Therefore, the article examines the general algorithm of the sequence of compiling and execution of the program.

2. THE ROOT OF THE PROPOSED METHOD

We propose an experimental method that enables to control the process of drying of ship high-voltage electrical machines, widely used in ship electric propulsion drives, like AZIPOD and in ship bow thrusters.

Drying of the motor is taken when a low insulation resistance is registered. The determination of the required insulation resistance Ri of high-voltage electric machines can be made trough equation:

$$R_i \geq \frac{k_p U_n}{1000 + 0{,}01.S_n},$$

where **U_n ,V** is the rated voltage of the electric machine, **S_n , kW or kVA** is the rated output power and **k_p –** correction factor, considering the dependence of insulation resistance on its temperature.

The main elements of the proposed system for drying of high-voltage electric motors are shown in Fig. 3.

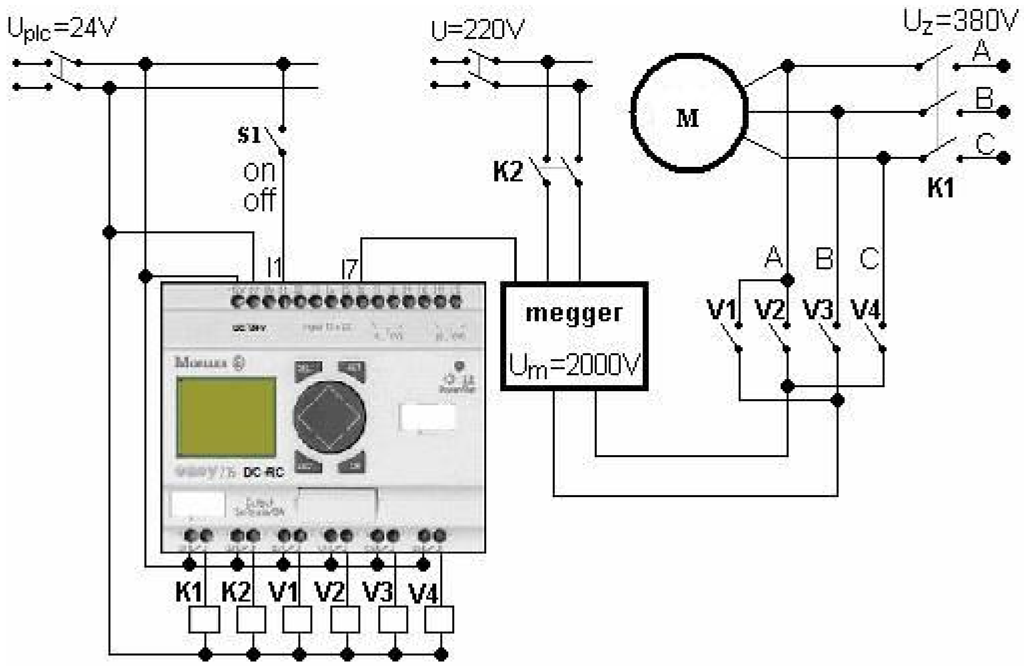

Figure 3: Wiring diagram of a PLC controlled system for drying of high-voltage induction motors.

The main elements of the proposed system are:

- **PLC.** The choice of the programmable device is connected to the proper determination of the functions needed for the control of the drying process. In our case, the main functional blocks are: A - timers, B - analog comparator, C - counter.
- **Megger (Megohmmeter).** Megger voltage is determined by the requirements of the controlled object. The measurement of the insulation resistance is carried out with Um = 2kV. The megger - PLC connection is through an analog signal into tared linear scales in the range of 0 -10V, depending of the amount of the leakage current in the motor's insulation.

- **High voltage switches.** Block V1-V4 (Fig. 3) consists of four contactors, operated by the controller through which the terminals of the megger switch on to the three phases of the motor. Their parameters must be consistent with the output voltage Um.

The algorithm of the work requires the following sequence:

1. Initial insulation resistance measurement. The megger is controlled from the PLC through the contactor K2, connected to output Q2. In the process of measuring the contactor K1 (output Q1), supplying the voltage U_Z to the motor, is off. By the switches V1-V4, the resistance of the insulation between the three phases is consistently measured. According to that shown in Fig. 3, the sequence of switching is: insulation resistance between phases A and B - V1, V2; phases A and C - V1, V3; phases B and C - V2, V3. For V1-V4 are used the controller outputs Q3-Q6.
2. After completing the test, the contactor K2 is excluded, which excludes the megger. Typically, in the process of measuring of the insulation resistance of high-voltage electrical machines certain electrical charge is accumulated. Normally, its dilution is made by connecting the phases to ground, but the absence of such in a vessel requires certain particularities. After completing the test, it is possible to realize the following option in the program of the PLC: the four contactors V1-V4 switch on, which short-connect the three phases of the motor. Time needed in this scheme must comply with specific machines. The process of dilution will be hampered by the lack of land to which connect the phases of the engine. It should be borne in mind that it is necessary to protect the power supply line by the surge caused by the charge into the engine at the moment of re-submission of the drying voltage Uz.
3. The controller accounts the measured values of the insulation resistance between the three phases. In case of poor insulation resistance the contactor K1 is turned on for submitting the voltage Uz to the electric motor. The parameters of this apparatus must comply with specific motor and the current flowing through his windings during the drying. If it is provided that the rotor shoud be stationary, a three-phase rectifier (Larionov circuit) and constant power supply must be used.
4. After a certain time, set by the timer setting in the controller, the insulation resistance measurement is repeated.
5. The process ends when acceptable insulation resistance between the phases is registered. A signal for completion of the drying process is done by the controller.

The functional blocks of the built experimental model of the PLC controlled drying system, are shown in Fig. 4. Their setup and use, regardless of the selected controller type, requires the implementation of functions used to manage the system and the process of drying.

Fig.4 A - timer. It is necessary to use three timers T01, T02 and T03 for time recording: T01 - between two consecutive measurements (e.g. 30 minutes), T02 – by the beginning of the running measurement up to 15s and T03 – by the beginning of the running measurement up to 30s. The coefficient of absorption is determined by the last two timers.

Fig.4 B - comparator. Compares the measured analog value coming from the megger with a constant value. By the result the state of the insulation is determined and the comparator decide after starting of K1 or termination of the drying.

Fig.4 C - counter. The use of multiple counting units allows the realization of some additional options. By counting the cycles of drying can be estimated the running time. In some cases, it stipulates that the drying process continue for some time after reaching the allowable insulation resistance, as a normative calls that may be 1-2 hours. Implementation can be done with a timer set at the required time without interrupting the process or by counting the necessary cycles of drying by control measurements.

The used PLC have sufficient resources for implementation of additional features: temperature control of the motor, indication of information on the display and more.

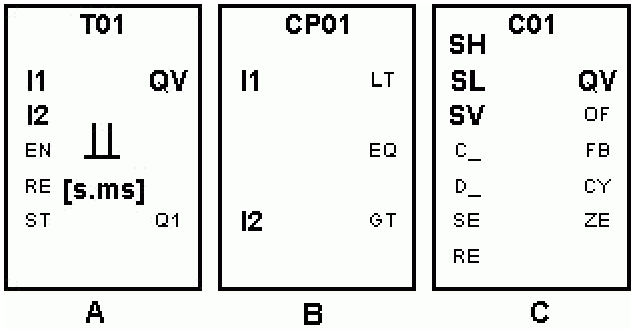

Figure 4: Functional blocks of the PLC family Moeller Easy 822 DC-TC: A - timer; B - comparator; C – counter.

3. EXPERIMENTAL RESULTS

Basically, the proposed system for drying of electric machines with PLC control is applicable to high-voltage machines regardless of their type - synchronous or asynchronous. Experimental studies were conducted with four high-voltage induction motors with a nominal voltage **Un = 6kV**, 50Hz. Technical parameters are shown in more detail in Table 1.

Table 1: Rated technical parameters of the motors, used in the experiments.

№	P,kW	M, kg	J, kg.m²	n, min^{-1}	η, %	cos φ	I_n, A	Mn, N.m	Ms/ Mn	Is/ In	Mm/ Mn
1	500	1980	13,0	1485	94,6	0,87	58,5	3180	1,0	7,0	1,6
2	630	3835	57,7	740	94,5	0,81	79	8020	1,0	6,0	1,6
3	800	3200	28,1	1485	95,2	0,87	93	5080	1,0	7,0	2,0
4	1000	3565	33,0	1485	95,5	0,87	116	6360	0,8	7,0	1,6

The drying time depends on many parameters: degree of hydration - respectively the primary insulation resistance, type of insulation used, ambient temperature, voltage of drying, the riched temperature of the coil caused by the ongoing current and others. Should be expected that the process will have a different scope and duration. Experimental results are shown in Fig. 5 and Fig. 6, respectively, beginning - the first 3hours and end (about 10 - 13 hours) after reaching the allowable insulation resistance. The charts reflect the drying process of four different machines, operating in similar conditions. Measured unacceptably low insulation resistance is the result of condensed moisture in the stator coil after prolonged stay of the engines turned off. Before starting the drying process the functionality of the terminal box is proved and the power cord is disconnected. After reaching the limit value, the process of drying is terminated from the PLC.

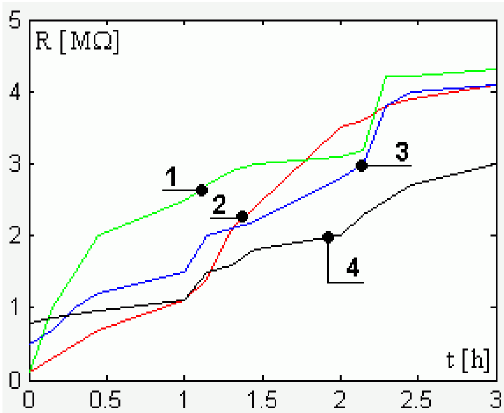

Figure 5: Insulation resistance (R) as a function of time (t) at the beginning of the drying process of the four electric motors.

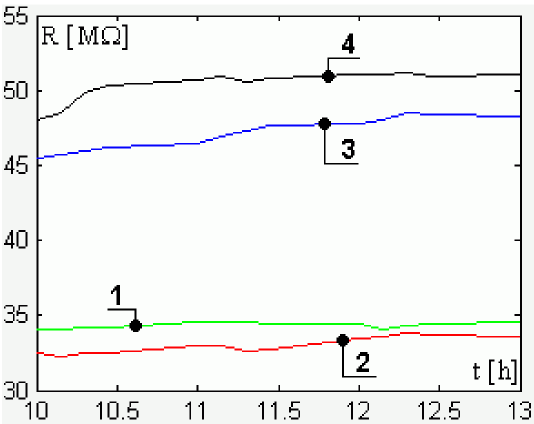

Figure 6: Insulation resistance (R) as a function of time (t) at the end of the drying process of the same four electric motors.

Additional experiments were conducted with other types of electrical machines (rated voltage **Un = 15kV**), operating under different conditions. The results are shown in Fig. 7. Whereby different type of graphs were obtained.

4. CONCLUSIONS

The main conclusions of our work are:

- The PLC system allows automatic control of drying and according to timer settings provide cyclical measure of insulation. This frees up staff from routine monitoring of the process.

- The system provides timely suspension of drying, after reaching the introduced in the program limits. Thus, in terms of energy efficiency, is ensuring lower cost of electricity for drying, i.e. the process does not continue unnecessarily long.

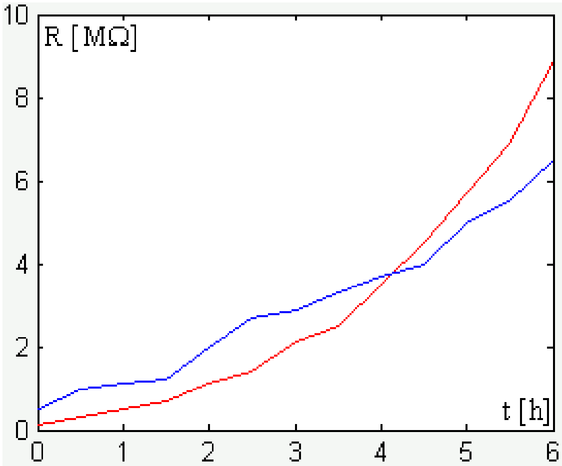

Figure 7: Insulation resistance (R) as a function of time (t) at the beginning of the drying process of two electric motors with 15kV rated voltage.

- Advanced programmable devices allow routine recording of values, connection to a computer, etc. The data obtained is suitable for analyzing the overall condition of the motor.
- Although the proposed model is used to Moeller Easy PLC family, the proposed system can be built with any programmable apparatus having the necessary functions. Thus, the proposed hardware allow the construction of relatively inexpensive and reliable system.
- The experiments show that the drying process of high-voltage machines, with low three phase voltage may occur in different ways. Those graphs (Figs.5-7) have a different character, which is due to many factors, but this feature does not affect significantly to the performance of the proposed system.

REFERENCES

[1]. http://www.offshore-technology.com/contractors/hydraulics/loher
[2]. The SSP Propulsor, An Ingenious Podded Drive System, Consortium SSP, Siemens AG & Schottel GmbH, brochure, 2006
[3]. Facilities Instructions, Standarts and Techniques, Keeping Motor Windings Dry, Volume 3-4, Facilities Engineering Branch Denver Office, Denver, Colorado, USA, September 2000.
[4]. http://www.moeller.net
[5]. Display, Operate, Switch, Control, Regulate and Communicate, Moeller GmbH, brochure, 2004
[6]. Lloyds Register, Rules and Regulations for the Classification of Ships, Electrical Engineering, Part 6, Chapter 2, July 2004
[7]. Russian Register, Rules for the Classification and Construction of Ships (in Russian), vol.2, 2003
[8]. Vlasov A.B., Issledovanie izolyatsii sudovih elektricheskih machin v protsesse eksploatatsii i sudoremonta (in Russian), MGTU Journal, Volume 11, № 3, 2008, p.475-482.

RELEVANCE OF THE PLANCOAST "STATE OF ART OF COASTAL AND MARITIME PLANNING IN THE ADRIATIC REGION" FOR ROMANIA

[1]COMAN CLAUDIA, [2]LUCIUS IRENE, [1]NICOLAEV SIMION, [1]ALEXANDROV LAURA, [3]SUNDRI MIRELA IULIANA, [4]DUMITRU VALENTINA, [1]SPANU ALINA, [1]MATEESCU RAZVAN, [1]IORDACHE GABRIEL

[1]National Institute for Marine Research and Development "Grigore Antipa", Constanta, [2]Coastal & Marine Union EUCC, Berlin, Germania, [3]Constanta Maritime University, Constanta, Romania, [4]National Institute for Research and Development in Urban and Spatial Planning – Urbanproiect, Bucuresti, Romania

The new issue Integrated Maritime Spatial Planning (IMSP) supported by the European Union since the 2007 Blue Book on Maritime Policy combines principles of the Integrated Coastal Zone Management (ICZM) with needs for sustainable development, elaborating different tools and procedures for spatial planning on both coastal and marine sides. As "The Romanian Emergency Ordinance on ICZM No. 202/2002" puts Romania ahead of Baltic and Adriatic countries in terms of a legal framework for integrated planning of the terrestrial coastal zone. The Romanian Coast is under the pressure from increasing population density, urbanization, marine transport, coastal erosion, pollution. Tourism industry and unplanned urbanization have had negative effects by depreciation of the natural landscape, water quality, sandy dunes, vegetation and marine ecosystem. This paper aim is to show how could be open and develop in Romania the field of IMSP: developing, introducing and implementing the new field of spatial planning in maritime areas (sea use planning) in the coastal zone in a coherent manner; strengthening the implementation of the ICZM in Romanian coastal zone demonstrating the benefits of spatial planning to ICZM by a selected number of pilot projects; introduction international comparable GIS databases facilitating the spatial planning process according to ICZM principle.

Keywords*:* Integrated Maritime Spatial Planning, Integrated Coastal Zone Management

1. INTRODUCTION

The report "State of art of coastal and maritime planning in the Adriatic region" published in October 2007 was subcontracted by the Regional Activity Center of Priority Actions Programme (PAP/RAC) Croatia in the framework of the INTERREG IIIB CADSES PlanCoast project. It is comparing and assessing the current legal framework and practice of spatial planning and other management approaches in the Adriatic Sea region based on experience in the Italy (Emilia-Romagna region), Slovenia, Croatia, Bosnia & Herzegovina, Montenegro and Albania (BaltCoast, 2005; Gee et al., 2006; PlanCoast, 2007; Schultz-Zehden et al., 2007, 2008). Particular focus was put on the off-shore areas and the new emerging instrument of integrated maritime spatial planning, which is promoted by the EU through its Future Maritime Policy (UNESCO visions for a sea change, 2006; Commission of European Communities, 2007) (Fig.1÷4).

As "The Romanian Emergency Ordinance on ICZM No. 202/2002" (Guvernul Romaniei, 2006) puts Romania ahead of Adriatic countries in terms of a legal framework for integrated planning of the terrestrial coastal zone, many ICZM issues of the Adriatic discussed in the "State of the art" are of less relevance to Romania and therefore not mentioned in this document. The Adriatic coast also differs in some geological features (e.g. rocky vs sandy coasts). Its climate, use, pressures, and political systems nevertheless provide many parallels to the features of the Romanian coast. This document aims at highlighting these parallels as well as good practice examples in order to provide orientation and inspiration for Romanian authorities dealing with coastal and marine planning and management.

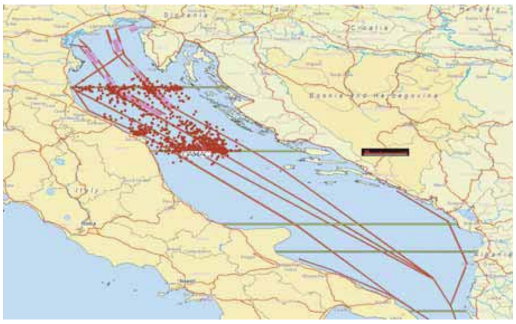

1. Shipping intensity in the Northern Adriatic in 2005

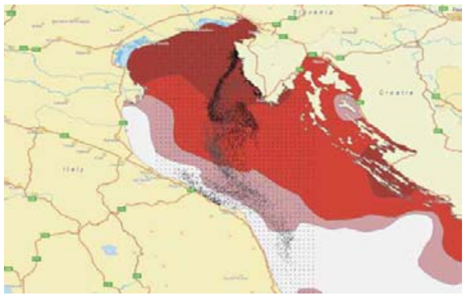

2. Oil spill risks related to fishery on North Adriatic

3. Planned Adriatic motorway on the sea along the ecological protection zones

4. Reference area

Fig. 1÷4 Adriatic Sea and Black Sea reference areas
(after Schultz-Zehden, 2008, modified)

2. INTEGRATED MARINE SPATIAL PLANNING

Integrated Marine Spatial Planning is officially supported by the European Union since the 2007 Blue Book on Future Maritime Policy. It combines the tools and procedures of terrestrial spatial planning with the principles of Integrated Coastal Zone Management (ICZM). Through its combination of ecosystem approach, involvement of all stakeholders and application of area-wide GIS data, the integrated approach is not only applicable in the coastal areas, but a perfect tool for maritime planning too. Moreover, strong economical, social and environmental land-sea interactions are indisputable. That is why, in the new definition of Integrated Maritime Spatial Planning on-shore coastal stripe and off-shore areas reaching as far as the EEZ and beyond, are equally represented. Marine Spatial Planning is currently acknowledged and recommended management approach in the EU. Nevertheless there is still a lack of experience, instruments, tools and capacities available to the policy makers and practitioners to implement these recommendations. **Similar in Romania**, the field of MSP is very new. It must be involved in the whole plan for terrestrial planning in Romania, developed by the Ministry of Regional Development, Public works and Houses in a perspective of the next years till 2030 (Fig.5).

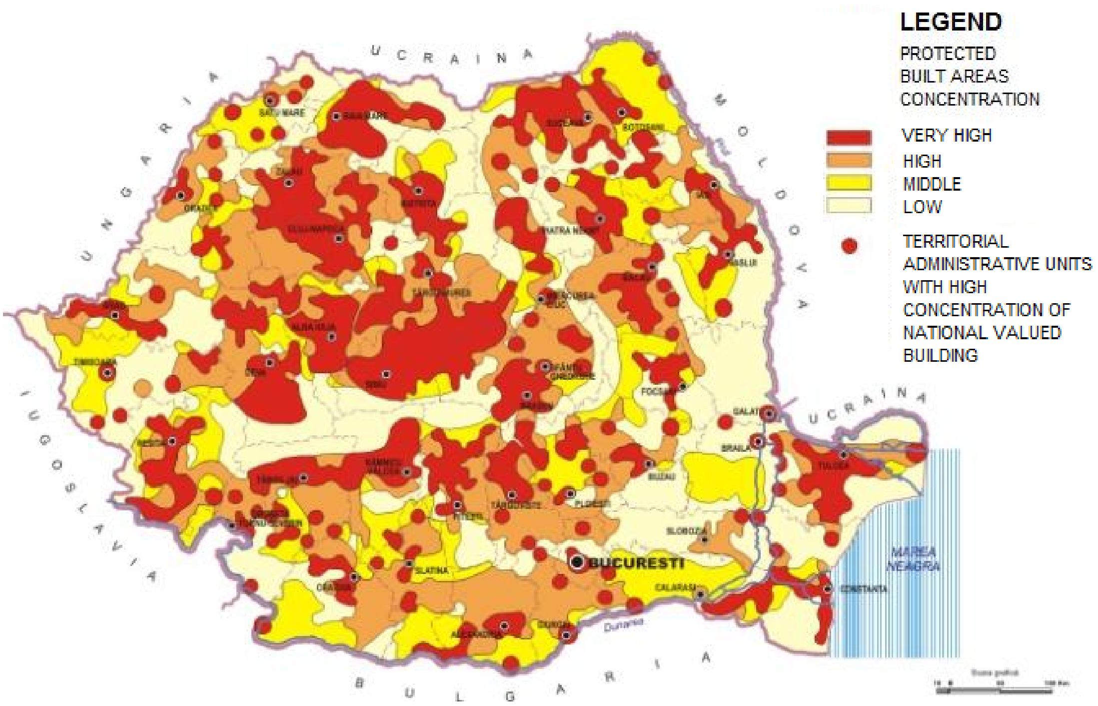

Fig.5. Romanian Terrestrial Plan. Protected Built Areas
(after Urbanproiect, 2007)

Adriatic countries examined in this report have only started to develop a regulatory framework for maritime spatial planning. Despite the acknowledged growing crowdedness of off-shore areas, no urgent problems are reported from a purely national perspective that could be triggering the obligatory maritime spatial planning in Adriatic countries. and aquaculture which collides with the sustainable vision of the region as a naturally intact tourist destination. However, from transnational perspective, it can be seen that it is only a matter of time that space conflicts in the Adriatic Sea will escalate to the point when major conflicts are inevitable. In particular it is the economic development through energy extraction, commercial sea traffic

In none of the Adriatic countries there is a necessary legal and regulatory frame to allow for maritime spatial planning nor are the relevant institutions yet entitled with maritime spatial planning procedures. The same situation is at the Black Sea coast and in Romania. But MSP is an important tool of ICZM and sustainable development. So, it could be developed under The Romanian Emergency Ordinance on ICZM No. 202/2002 (Fig.nr.6). A new legal basis is therefore required that gives equal weight to all land uses and development interests including agriculture water management, environmental management, nature protection and tourism etc. Moreover, to allow for improvement of Maritime Spatial Planning, the said regulatory frame has to include also provisions for the MSP instruments, legislation, institutional setup, technical framework and procedures, also in Romania.

As there is no legal basis for maritime planning (except Slovenia and Montenegro- but even there it is not practiced yet) there is no clear responsibility attached to one institution. As a result, common responsibility means in practice: no one feels responsible. It would be desirable to have these functions integrated in one authority in order to ease the reconciliation of different interests or to have coordinative institutions or platforms where different parties can come together. The experience of Montenegrin Coastal Enterprise ‘Morsko Dobro’ shows that this is the right way forward. At the same time it has to be stressed once more that there is no need to create new institutions, since there is in almost every country an agency which could take a lead for implementation of ICZM, it only has to be aided with additional funds and resources. Slovenia is the only country in region, which introduced legally the possibility of maritime spatial planning and could therefore serve as a model for Romania.

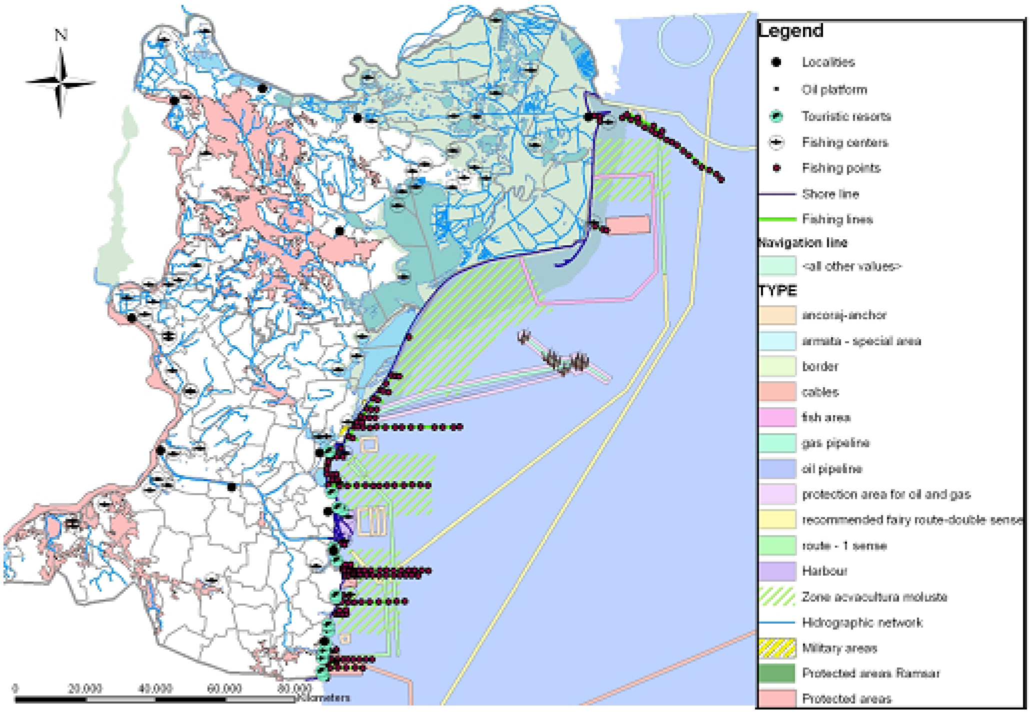

Fig.6. Integrated map of Maritime Uses and Activities

3. TOURISM

While in the past, degradation of the coast was caused by land reclamation, agriculture, mining and industrial pollution, the present threats come from urbanization, intensive resource exploitation and tourism. Local landowners are attracted by high land prices to convert their land from low intensity use into land for building. Local governments usually see this as an important source for increasing their tax base through land and property tax and so they support these negative developments. Such extreme form of tourism development not only puts severe burdens on the existing infrastructure, especially roads as well as water and sewage networks, but more significantly deteriorates the landscape and natural qualities of the coastal regions. Paradoxally, the unique potential of these areas for individual and more sustainable tourism is thus being drastically reduce

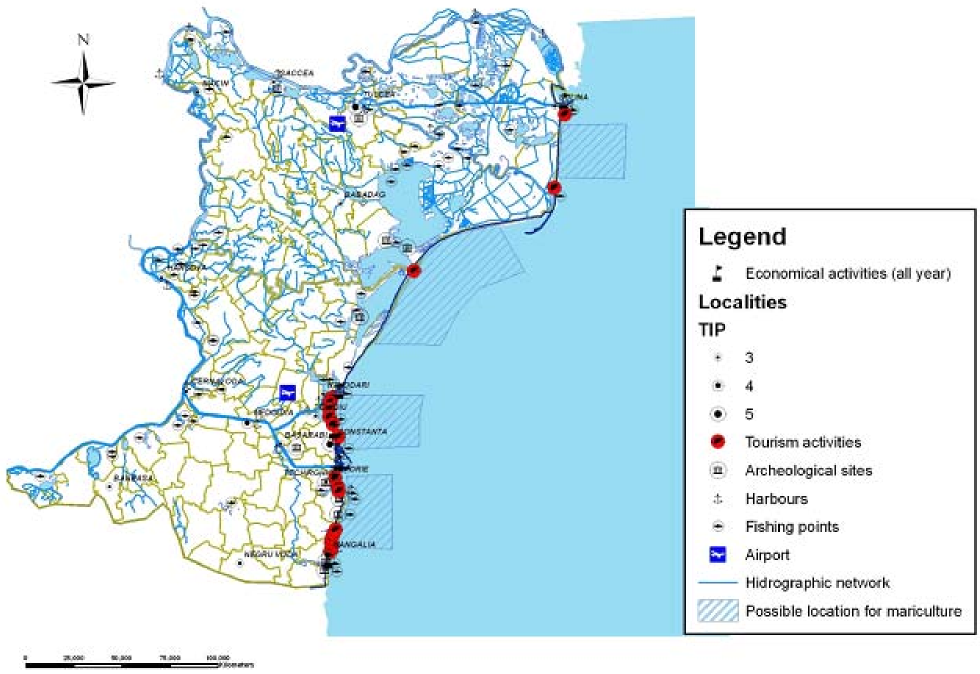

Fig. 7. The Romanian coastal zone main activities: tourism resorts, harbours, aquaculture

Perceiving tourism as the main driving force of the coastal economy does not mean reducing other economic sectors of importance and attention, or making a separate 'integrated tourism development plan' but rather privileging it as an ordering power of all others, because tourism will naturally thrive only if the sea is clean and fish, mobility on the coast works well, coastal agriculture is quality-based and environmentally efficient.

An important and growing branch of tourism in the Adriatic is the nautical tourism. In some areas, e.g. in Montenegro the demand for yacht mooring is much bigger than supply. On the other hand there is a growing demand for building new public bathing spots for tourists. Overall, the private versus public space arrangement on the limited ground is one of the major problems on the Adriatic coast. With a well known international significance the Romanian's coastal tourism has been a very developed sector of economy reaching during summer the environmental stress and demography. The natural potential must be supported by a good administration and management which is in present under new plans and prognosis, grace of political interest for future development (Fig.7).

4. SHIPPING

Shipping traffic in the Adriatic Sea, both private and commercial is becoming increasingly dense. Moreover, new transit ports are expected to gain significance in the south of the eastern Adriatic coast. Trends in the development of international shipping activities will lead to an increased density of traffic (also due to projects such as "Motorways on the Sea", (Fig.3), and the volume of transport of oil and other harmful substances, including liquefied natural gas (LNG). Maritime transport, especially the petroleum transport, is an additional source of marine pollution due to possible accidents and to improper disposal of ballast and bilge waters and solid wastes (Fig.2). A spill could have disastrous effects on the vulnerable nature and natural resources of the Adriatic Sea, as well as on its important uses such as for tourism and local fisheries. This is why the consideration of navigable waterways in the Adriatic and their control is becoming very important. In Romania the oil exploiting platforms and transport ways are well known. Shipping routes must avoid them and all fishing kinds of tools and installation. The MSP has mainly this aim: to permit avoid conflicts between different maritime activities and uses (Fig. 8).

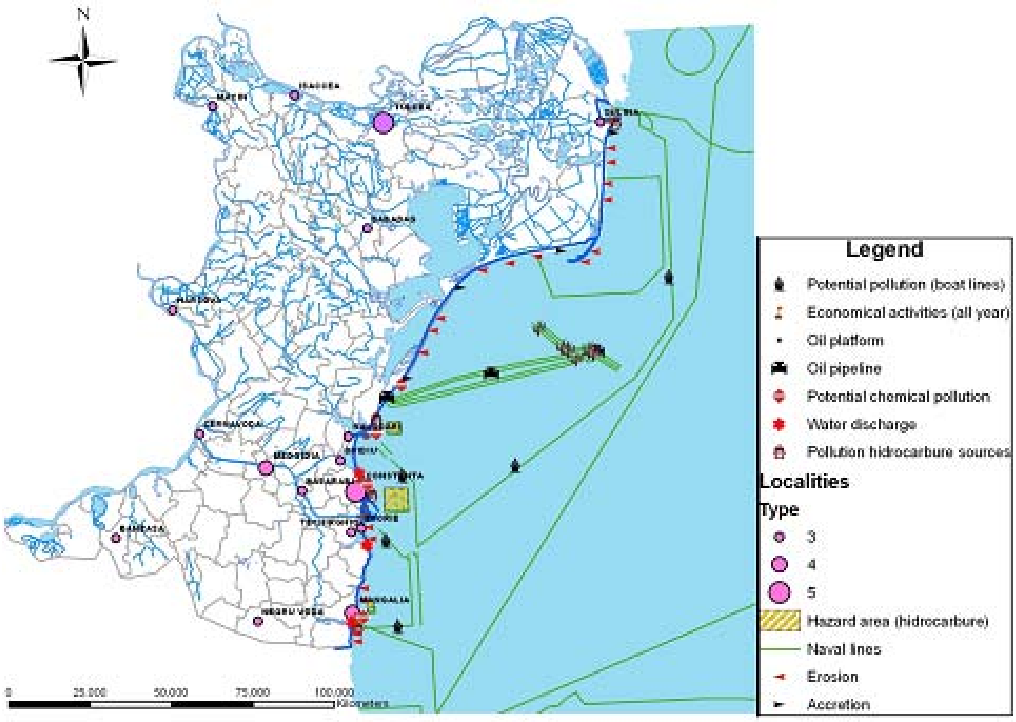

Fig. 8 The Romanian maritime activities: shipping, oil transport, potential chemical pollution and risks

5. FISHERIES

Fishery has been traditionally an important sector in the Adriatic countries; however, along with the shrinking of fishing resources as a result of over-fishing and unfavourable ecological conditions, it is constantly dropping its share in the national economies. The new trend can be observed to aquaculture, especially in Croatia and Slovenia, which however is not entirely free of environmental and spatial constrains.

Fish protection zones should become another integral part of maritime spatial planning, also in the Black Sea Region. Situations like the current one in Croatia should be avoided, where the Zone of Ecological Protection and Fisheries was proclaimed but its restrictions are applied only to Croatian and other non-EU countries' ships, not to EU ships. Such implementation of PEFZ regulation is perceived as unfair among Croatian fishermen and - above that - a highly ineffective one.

Romanians are traditionally high fish consumers, based mainly on the freshwater species. Maritime fishing and fisheries are less developed, but the national fleet had a spread network on the Earth's marine and oceans zone (Fig. 9). In present this important sector of the economy must be developed based on new European rules and regulations regarding both the state and private sector. NIMRD "Grigore Antipa" Constanta is the only one performing research in this aim in spite on lack of funds for industrial field. New European programs and funds must be accessed to support fishing and fisheries activities.

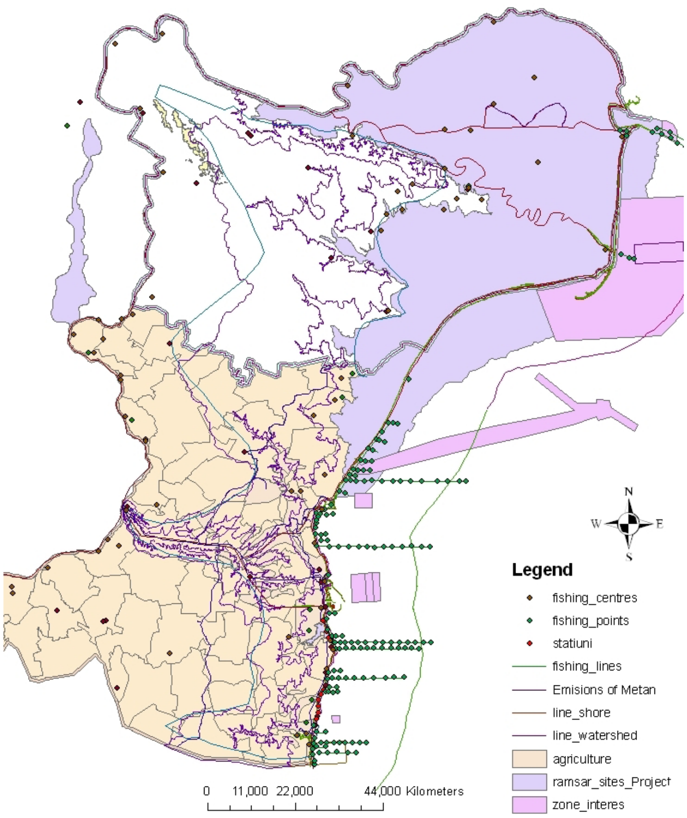

Fig. 9. Romanian fishing points; Aquaculture

6. BIODIVERSITY

Protected areas management planning presents a huge potential for spatial planning, especially offshore, in absence of other planning instruments like statutory Maritime Spatial Planning. However, at the moment major reported gap are the management plans of protected areas. If existing at all, they are too restrictive and not operational enough to keep up with the rapidly developing economy. On the contrary, good management plans should, beside the obvious restrictions, show the possible links and synergies between protection and economical development, health and cultural values. Such approach to management planning is recommended already for NATURA 2000 areas and Water Framework Directive water basin plans.

At present, most protected sea areas are directly managed by the communes in charge for the territory where the areas are. However, apart from the sheer designation of protection areas there is little activity in carrying out of their protection measures. There is a large network of existing, mostly terrestrial protection areas in the Adriatic region, and there can be a lively activity observed in the designation of new protected areas on the sea. Speaking of the latter ones, enforcement seems to be a wide spread problem.

Marine Protection Areas are an emerging field of marine space-use in the Adriatic. Around 50.

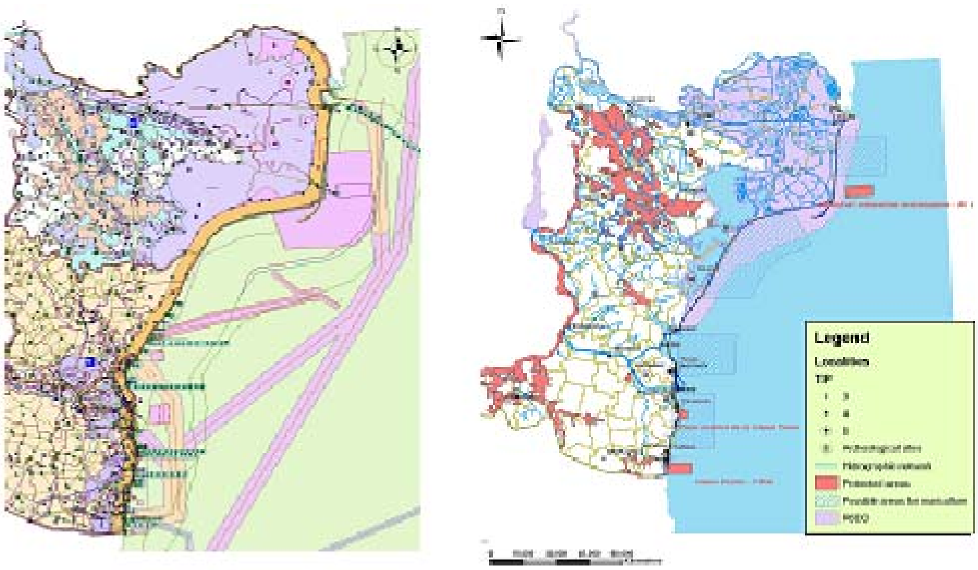

a) Functional areas b) Protected areas

Fig. 10 (a, b). Romanian coastal functional integrating terrestrial and maritime protected areas

MPA's are designated at the moment in Italian, Slovenian and Croatian waters. Some of them underlay the regulatory framework of NATURA 2000 EU directive, some are national parks on water according to national law (e.G. the Croatian Maly Losnij dophine reserve).

Marine protection areas play a key role in the Italian marine planning activity. At present, there are in 24 marine protected areas totally protecting about 184.000 hectares of sea and about 580 kilometers of coast. Protected sea area management is entrusted to public bodies, scientific institutions or recognized environmental associations also cooperating with one another.

If an MPA cannot be adequately marked on maps and on the sea by buoys, trespassing can occur and protection goals will not be kept.

Biodiversity is not one subject within the ICZM – on the contrary, biodiversity and landscape protection should be the central theme of all policies: either tourism, fishery, infrastructure planning etc. Maritime Spatial Planning, but also the impact assessment tools such as EIA and SEA are perfect 'Trojan horses' for this purpose.

In Romania are identified coastal habitats and also are nominated the most important protected areas marine protected areas not only coastal terrestrial ones (Fig.10). The new research related these zones permit a future sustainable development of the coastal area. NIMRD "Grigore Antipa has the custody of the Vama Veche – 2 May Marine Protected Area, elaborating the Management Plan for it. This marine protected area has a transbondary significance having in Bulgaria the same MPA as shore continuity.

7. HORIZONTAL CO-ORDINATION AND LAND-SEA INTEGRATION

A specific type of horizontal integration is the land-sea-integration, as these two kinds of space are traditionally divided by a transparent 'administrative wall'. On the land side of the coast, sectoral integration is in some cases (Italy, Croatia, Slovenia) guaranteed through the statutory spatial planning system (see above). On the sea however, there are no comparable coordination instruments.

Slovenia is the only one of the examined countries, where attempts at integration of activities and legislation between land and sea are made. An interesting example of horizontal harmonisation between land and sea sectors can be observed in Slovenia on the basis of EU Water Framework Directive. In case of the Detailed Water Management Plan coordination with spatial planning and sectoral plans is ensured because every spatial plan must obtain the Minister's consent that it is in compliance with water management plans and the Water Act provisions which regulate the interventions into aquatic, coastal and other areas. Moreover, the participation of public and stakeholders is ensured through the Water Council (representative body which consists of the representatives of local communities, the holders of water rights and non-governmental organizations). The Water Council monitors the implementation of the national water management programme, participates in the preparation, monitoring and implementation of water management plans.

Romania is the only Black Sea country and one of the few world-wide, which has a special legal and institutional framework for ICZM. In 2004, following the recommendation of the Romanian ICZM strategy the National Committee of the Coastal Zone (NCCZ) was founded under the responsibility of the Romanian Ministry of Environment and Sustainable Development. The Technical Secretariat of NCCZ is based at the National Institute for Marine Research and Development "Grigore Antipa" in Constanta and operates via its 6 thematic working groups: WG 1: delineation of the coastal zone, urbanism and spatial planning; WG 2: coast protection; WG 3: technical and legal assistance; WG 4: ICZM policies, strategies and action plans; WG 5: monitoring and surveillance; WG 6: information and communication.

8. CONCLUSIONS

The main conclusion of the PlanCoast project wich translated for the first time the Adriatic basin experience in Maritime Spatial Planning to the Black Sea, including Romania proved that the success of IMSP depends on co-operation across sectors and spatial scales.

REFERENCES

[1]. BALTCOAST: ***BaltCoast Project Recommendations*** (short version), 2005. Available online at http://www.plancoast.eu

[2]. Commission of European Communities 2007: ***An integrated maritime policy for the European Union.*** Brussels, SEC(2007) 1278. Online at http://ec.europa.eu/maritimeaffairs/.

[3]. Gee, K. et al.: ***Integrated Coastal Zone Management (ICZM): Strategies for coastal and marine spatial planning – the role of spatial planning and ICZM in the sustainable development of***

coasts and seas. Federal Ministry of Transport, Building and Urban Affairs (BMVBS) and Federal Office for Building and Spatial Planning (BBR). Final Report, Berlin, 2006. Downloadon http://www.bbr.bund.de/cln_005/nn_62854/EN/ResearchProgrammes/GeneralDepartmentalResearch/SpatialPlaning/ICZM/05_Publikation.html

[4]. Guvernul României - ***Ordonanță de Urgență nr. 202 din 18 decembrie 2002privind gospodărirea integrată a zonei costiere,*** Bucureşti, 2002.

[5]. PlanCoast: ***Climate change and growing sea use pressures: solutions offered by Maritime Spatial Planning.*** Documentation of the 4th PlanCoast conference held in Berlin on 21 November 2007. Online at http://www.plancoast.eu

[6]. Schultz-Zehden, A. et al.: ***The Role of Spatial Planning in ICZM. Findings and Recommendations from the Interreg III B BaltCoast Project*** -Executive Summary, 2007. Online at http://www.sustainable-projects.eu

[7]. Schultz-Zehden A, Gee K., Scibior K. – ***Plan Coast. Adriatic/Baltic/Black Sea. Handbook on Integrated Maritime Spatial Planning,*** Imprint s.Pro, Berlin, 2008. Available online at www.plancoast.eu; www.plancoast.ro.

[8]. UNESCO VISIONS FOR A SEA CHANGE. ***Report of the First International Workshop on Marine Spatial Planning. Intergovernmental Oceanographic Commission and the Man and the Biosphere Programme,*** UNESCO Headquarters, Paris, France, 8-10 November 2006. See also http://ioc3.unesco.org/marinesp/files/FinalConclusionsNextSteps_041206.pdf.

[9]. Urbanproiect. National Institute for Research and Development on Urban and Spatial Planning. ***Plan Coast /Adriatic/Baltic/Black Sea/. Categories of Development Plans.*** 2007, 2nd Plan Coast meeting 31st May to 2nd June, Constanta, Romania. Available online at www.plancoast.eu/files/constanta/presentations.

CALCULATION OF THE INDUCED CURRENT IN A TEST COIL BY A HIGH POWER ELECTROMAGNETIC PULSE

[1]DATCU I., [1]BACIU A., [1]SOTIR A., [1]SAMOILESCU GHEORGHE

[1]*Naval Academy "Mircea cel Batran", Constanta, Romania*

This work deals with an issue of great importance, related to the possible destructive effects of a high power electromagnetic pulse – as the lightning pulse – upon electronic equipments in its area of influence. Lightning pulse characteristics are presented for type 2 / 50, one of the most common, where the number 2 mean length of the front and number 50 - the average duration of current pulse, in microseconds. It is calculated, based on specific linear antenna's relationships, electromagnetic field components caused by the lightning current pulse, both in the close area - the field of induction, and in the far area - the radiation field. Based on these is calculated the induced power density and its corresponding energy in a test coil, located at 100 m from the point of lightning strike, and are compared the values obtained with maximum allowed energy levels of different components and electronic devices; the comparative analysis serves to draw useful conclusions about the need of using anti-disturbance protection for these equipments.

Keywords*:* high power electromagnetic pulse, near field, far field, test coil, induced electric power

1. INTRODUCTION

A high power electromagnetic pulse can be produced by an atmospheric discharge (lightning) on the ground, and also - by an electromagnetic pulse weapon. In these conditions has been estimated that the natural discharge of atmospheric electricity, as linear lightning – the most common, can be a good reference to develop a theoretical model for determining the induced current in a test coil. This model can be used to verify the behavior of electronic equipment like the command and control system, computers, modems, receivers and radio transmitters, radars, but also of the human body against the effects of this destructive phenomenon.

2. THE ELECTRICAL FORMING CONDITIONS OF THE STORM DISCHARGE PULSE

According to [2], the linear lighting is the most common source of HPEP (high power electromagnetic pulse). The cause for this phenomenon is the storm cloud, which accumulates inside a large amount of contrary signs electric charges, with a volume distribution (the cloud polarization). The phenomenon is explained by condensation of water vapors, the electrifying by polarization of those as a positive and negative ions form and the separation of electrically charged water droplets from the cloud under the action of intense air flow, mainly the upward ones.

The gradual accumulation of electric charges with opposite polarity in higher areas (75-85%-positive) and lower (75-85%-negative), is developing inside the cloud an electric field whose intensity is increasing to the critical value for air (about 30 to 45 kV / cm).

At this point starts lightning, a variant of electrical discharge in gas with a very long bow, from a few hundred meters, to several kilometers. The lighting atmospheric discharge starts with a dominant stage and ends with reverse discharge, which is in fact the main discharge, whose duration is about 20-150 μs.

In Figure 2.1 is shown a typical discharge form as a linear lightning, on the ground.

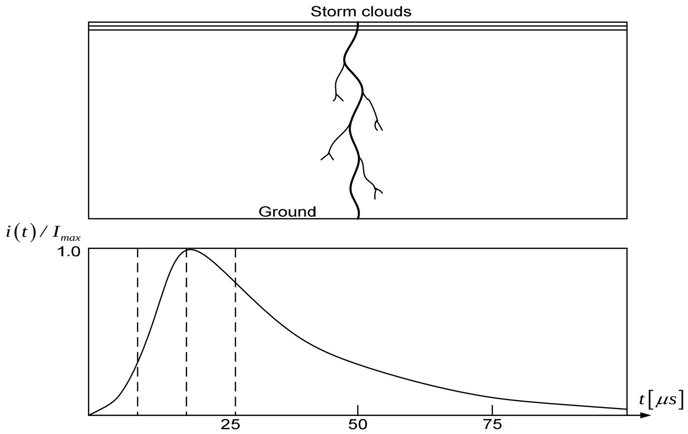

Fig.2.1. The typical discharge form as a linear lightning

3. CHARACTERIZATION OF THE CURRENT PULSE PRODUCED BY LIGHTNING

The main features of the current pulse produced by a linear lightning are shown in Figure 3.1. The current time variation curve has two parts: a slope with the current rapid growth from zero to maximum, followed by another, which decreases slightly more slowly to zero.

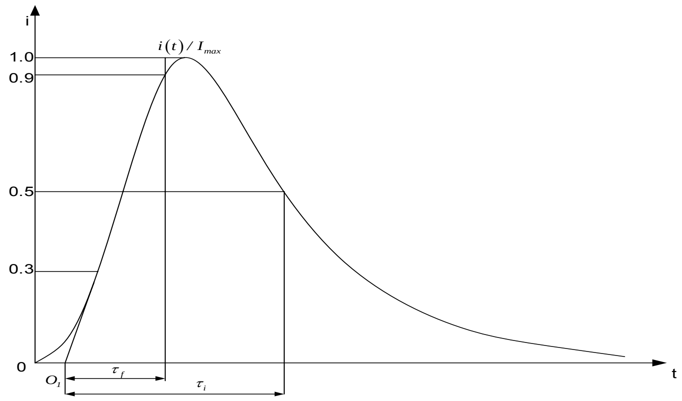

Fig.3.1. Diagram "Amplitude-duration" of a lightning current impulse

To simplify the mathematical model of the curve front it will be determined the points O1 and O2 of the pulse, obtained by intersection of straight lines passing through the curve, that corresponds to the values 0.3 Imax and 0.9 Imax, and intersect the abscissa. In the graphic it was recorded: τ_i - pulse front duration; τ_f - pulse duration at half amplitude. One of the main parameters that characterize this type of pulse is the ratio τ_f / τ_i, where τ_i and τ_f are defining time constants of the double exponential type mathematical expression of the analyzed pulse. During the development of such a pulse other factors occur such as soil resistivity, which directly influence the current amplitude.

The research on storm discharges shows that when lightning strikes the earth, the two parameters, τ_i and τ_f take the values contained within 1-15 μs, and 10-100 μs.

It was found that lightning current amplitude ranges as follows: a. in soils with high resistivity that are bad conductors (ρ_p = 600-1000 Ωm), $I_{max} \cong$15 kA; b. in soils with low resistivity that are good conductors (ρ_p= 10-100 Ωm), $I_{max} \cong$150 kA.

In the presented simulation model they considered as statistical average values of a storm discharge:

- current amplitude (peak value) - three variants [A] 10.000; 15.000; 20.000
- pulse front duration [μs] 2
- pulse duration at half amplitude [μs] 50
- total pulse duration [μs] 100-150

The current pulse frequency spectrum corresponds to the range 300 Hz - 20 kHz, at the average pulse duration of 50μs. Taking into consideration the pulse front corresponding harmonics then the upper frequency range can reach tens of MHz. We specify that the highest values of amplitudes in the radiation spectrum of lightning correspond to frequencies between 300 - 20,000 Hz. In the presented simulation program was considered an average frequency of 0.5 MHz, corresponding to the analyzed lightning impulse front duration (2μs).

The lightning current analytical expression form is [3]:

$$i(t) = k \cdot I_0 \cdot \left(e^{-a_1 t} - e^{-a_2 t}\right) = I_m \left(e^{-a_1 t} - e^{-a_2 t}\right) \tag{3.1}$$

where:

I_0 – pulse amplitude value (peak value), in [A];

a_1,a_2 – parameters for approximating the pulse shape;

k – standardization factor determined by the condition of equalizing the current amplitude with 1;

I_m – the pulse amplitude (standardized).

Standards factor k is the expression:

$$k = \frac{1}{\left(\frac{a_1}{a_2}^{a_1 / a_2 - a_1} - \frac{a_1}{a_2}^{a_2 / a_2 - a_1} \right)} \tag{3.2}$$

determined by the condition of current standardization.

If the pulse type is (2/50)* can be defined the following parameters:

k= 1.037; a_1 = 0.0138·10^6 (s^{-1}); a_2=1.6248·10^6 (s^{-1}).

Usually relations linking the parameters a_1, a_2 of durations τ_i and τ_f are of the form [5]:

$$a_1 = 0.7/\tau_i\ ;\ a_2 = 3.25/\tau_f\ ,\ with\ \ a_2 >> a_1 . \tag{3.3}$$

4. THE PULSE ELECTROMAGNETIC INFLUENCE IN THE NEAR FIELD ZONE AND FAR FIELD ZONE

The current pulse of the typical weather discharge, linear lightning type, can disrupt nearby various electronic equipment or even the ones at a greater distance, both through the near and the far (radiation) electromagnetic fields it produces, leading to erroneous operation, damage or even destroy these equipments.

Criterion-out of the area of action of the two types of field is, according to Electromagnetic Compatibility standards, following [1], [4], [5]:

a) for the near field: $r << \lambda / 2\pi$;

b) for the far field: $r >> \lambda / 2\pi$,

where "λ" is the wavelength of the electromagnetic field components produced by the pulse and "r" - geometric mean distance between the perturbed equipment and the field source. It was considered that the field wave, the magnetic component - in our case, has the same frequency as the current pulse.

Taking into account only the frequency of 500 kHz, corresponding to the pulse front duration, we obtain:

$$\lambda = c \cdot T = \frac{c}{f} = \frac{3 \cdot 10^8}{500 \cdot 10^3} = 600(m) \tag{4.1}$$

It follows that $\lambda : 2\pi \cong 100m$ and therefore the two field areas can be separate as:

a) near field is found at: $r \ll 100m$ of the lightning strike;

b) far field can be found at: $r \gg 100m$ of it.

At the distance of approximately 100 m are virtually found both, near and far fields

5. THE ENERGETICALLY APPROACH OF THE PROCESS

To assess which types of receptors (appliances, devices, equipment and electronic systems) are the victims of a lightning impulse, it must be known the power density, respectively – the energy that is released from such a pulse.

Knowing the energy levels that may affect, damage, or even destroy the electronic components, according to Table 5.1.[4], also the energy emitted by the pulse, we can identify the sensitive receptors to be taken out of service by inducing in the electronic circuits electric high values voltages and currents.

* τ_f =2 (the pulse front duration); τ_i=50 (the pulse duration at half amplitude)

Table 5.1. Susceptibility to disturbance energy (joules) of electrical and electronic receivers

Power gen., mod., transf.	10^{4}	10^{5}
Relays, measurement instruments, power transf.	10^{-3}	10^{0}
Electronic tubes	10^{-3}	10^{1}
Measurement resist., winding resist.	10^{-3}	10^{2}
Metal film resist.	10^{-4}	10^{-2}
Capacitors	10^{-4}	10^{-3}
Wound inductors for filters	10^{-2}	10^{-1}
Transistors	10^{-7}	10^{0}
Signal diodes, switching diodes	10^{-6}	10^{-2}
Integrated circuits	10^{-7}	10^{-3}
Diodes for microwave	10^{-10}	10^{-4}
Computers sensitive components	10^{-7}	10^{-3}
Electric detonators	10^{-5}	10^{-3}

10^{-10} 10^{-9} 10^{-8} 10^{-7} 10^{-6} 10^{-5} 10^{-4} 10^{-3} 10^{-2} 10^{-1} 10^{0} 10^{1} 10^{2} 10^{3} 10^{4} 10^{5} J

The dangerous induction effect is considered being generated by the electromagnetic field produced by lightning. This field is produced by the main current pulse and also by the spectral components of the current pulse front, components that can reach very high frequencies, considering its steep slope.

In case of a plane wave emitted by lightning pulse, with $\overline{\mathrm{E}}$ and $\overline{\mathrm{H}}$ vectors perpendicular to each other and in phase in any perpendicular plane to the direction of propagation, the average density of power flow of such wave is given by:

$$w_m = \frac{E_{\max}^2}{2z_0} = \frac{H_{\max}^2 \cdot z_0}{2} \left(W/m^2 \right) \qquad (5.1)$$

where: E_{max} and H_{max} are the amplitudes of electric respectively – magnetic fields intensities, both produced by the pulse, and $z_0 = 120\pi$ - wave impedance of free space.

It is considered that the incident electromagnetic wave is linearly polarized.

If it placed in an test area a corresponding frequency receiving antenna, with effective area S_{ef}, the total energy discharged into the load of the antenna, in terms of adaptation, during one second, is calculated from the relationship:

$$W = S_{ef} \cdot w_m \ (J) \tag{5.2}$$

where w_m is the density of energy produced by the antenna in load, in the same period of time. If upon the receiving antenna simultaneously acts several sources, the energy discharged into the antenna load is totalized. Calculating this value and comparing it with the energy levels maximum allowed by the components and devices, given in table 5.1, can be obtained valuable information on the need to protect them from such a pulse.

6. DETERMINATION OF LIGHTNING FIELD EFFECTS

To exemplify those shown before, it were determined the possible effects of lightning electromagnetic field, namely - the calculation of induced electric power, and also of the current density induced in a circular copper coil, based on a calculation and simulation program developed in MAPLE. Were used the following data:

- The location and test coil parameters: $a = 0,05(m)$ – the coil radius; r = 0,001 (m) – coil conductor radius; R = 100(m) - distance from the source to the test coil circumference (it is considered that the effect of electrical discharge on the coil occurs when it reaches 1 m from the soil); $\sigma_{Cu} = 58 \cdot 10^6 (S/m)$; $\theta = 89^\circ$ (angle between R and the discharge vertical);
- Pulse and pulse electromagnetic wave parameters:
  - current, amplitude and frequency: 10.000; 15.000; 20.000 (A); f = 500 (KHz); $\lambda = \frac{c}{f} = 600(m)$;
  - length of the atmospheric discharge l = 1000 (m);
- Electromagnetic parameters of the environment : $\mu_0 = 4\pi \cdot 10^{-7} (H/m)$; $\varepsilon_0 = \frac{1}{4\pi \cdot 9 \cdot 10^9} (F/m)$; $z_0 = 120\pi\,(\Omega)$ (free space impedance).

The components of the electromagnetic wave produced by lightning, considering it as a linear antenna, for the near and far field, are [1], [2]:

$$\underline{E}_\theta = z_0 \cdot \frac{l\hat{I}\lambda \sin\theta}{j8\pi^2 R^3}\left[1 + j\frac{2\pi}{\lambda}R + j\left(\frac{2\pi}{\lambda}R\right)^2\right] \cdot e^{-j\frac{2\pi}{\lambda}R} \tag{6.1}$$

$$\underline{H}_\varphi = \frac{l\hat{I}\sin\theta}{4\pi R^2}\left[1 + j\frac{2\pi}{\lambda}R\right] \cdot e^{-j\frac{2\pi}{\lambda}R} \tag{6.2}$$

where:

$z_0 = \sqrt{\mu_0 / \varepsilon_0} = 120\pi = 377(\Omega)$ - wave impedance in free space;

$\beta_0 = \frac{2\pi}{\lambda} = \frac{2\pi}{vT} = \frac{2\pi f}{v} = \frac{\omega}{v} = \omega\sqrt{\varepsilon_0 \mu_0}$ - wave phase constant;

$v \cong c = \frac{1}{\sqrt{\varepsilon_0 \mu_0}}$ - wave propagation speed in free space (theoretically equal to the speed of light).

In these relations the terms of the near field decrease generally with the square distance and the terms of the far field - with the distance to the source.

The magnetic induction for near field is:

$$B_a = \mu_0 H_{\varphi_a} \quad (6.3)$$

and the electric power induced in the test coil by the near field, considering the sinusoidal field, is [1], [4]:

$$E_a = \frac{a}{2} \cdot \omega \cdot B_a (V/m) \quad (6.4$$

As a result, the induced current density in the test coil by the near field becomes:

$$J_a = \sigma \cdot E_a = \sigma \frac{a}{2} \cdot \omega \cdot B_a \left(A/m^2 \right) \quad (6.5)$$

Similarly can be calculate the induced electric field and the induced current density by the far field components of the electromagnetic wave generated by the pulse.

Field components values of the induced current densities into the coil and of the corresponding electromagnetic energies to these fields are presented in Tables 6.1. and 6.2. They are calculated with the mentioned program for three values of the peak current: 5kA, 10kA, 15kA.

Table 6.1.

Peak current $\hat{I}(A)$	Near field			
	$E_{\theta_a}\ (V/m)$	$H_{\varphi_a}\ (A/m)$	$J_{H_a}\ (A/mm^2)$	Released instantaneous energy - W (J) (t=1s)
10000	2.074067012	0.003978873576	0.02277654674	0.00298415518
15000	3.111100518	0.005968310364	0.03416482011	0.00671434916
20000	4.148134025	0.007957747152	0.04555309348	0.01193662073

Table 6.2.

Peak current $\hat{I}(A)$	Far field			
	$E_{\theta_d}\ (V/m)$	$H_{\varphi_d}\ (A/m)$	$J_{H_d}\ (A/mm^2)$	Released instantaneous energy - W (J) (t=1s)
10000	150.0000000	0.004166666667	0.02385154397	0.003272492346
15000	225.0000000	0.006250000000	0.03577731596	0.007363107783
20000	300.0000000	0.008333333335	0.04770308799	0.01308996940

7. CONCLUSIONS

It can be seen, from the data obtained, that the current densities induced in the test coil by the atmospheric pulse, as well as the corresponding energies, exceed the permissible values for electronic components (e.g. - integrated circuits), which leads to the conclusion that in case of both near and far field exists the real risk of taking them out when it used the electronic devices. Therefore it must be taken appropriate protective measures (e.g. shielding, avoiding parasitic circuit loops, filtering etc.) to provide a normal function and a reliability of these.

REFERENCES

[1]. IANOZ, M., (1992) ***Compatibilité Electromagnetique***, handbook, Politechnical University of Lausanne, Elvetia. Bucharest, AGIR Conference

[2]. Iosif, F.D., Moşoiu, I.T., (2007) ***Protectia mijloacelor radioelectronice (MRE) la perturbatii electromagnetice de mare putere (PEMP).*** Constanta, Editura ANMB

[3]. MOCANU, C.I., (1981) ***Teoria campului electromagnetic***. Bucuresti, Editura Didactica si Pedagogică

[4]. SCHWAB, A. J., (1996) ***Electromagnetic Compatibility.*** Bucuresti, Editura Tehnica

[5]. SOTIR, A., (2005) ***Disturbing Electromagnetic Interferences. Theoretical Bases.*** Bucharest: Military Printing House

THE DETERMINATION OF THE MOMENTS OF INERTIA AND FRICTION – TORQUE DEPENDENCE

[1]DELIU FLORENTIU, [1]SARBU SORIN

[1]Naval Academy "Mircea cel Batran", Constanta, Romania

In applications that require precise and rapid adjustment is very important to know the value of moment of inertia and friction torque dependence.
Current industrial applications can be classified into two categories:
1) moment of inertia is constant during the adjustment to all operating modes;
2) moment of inertia can vary with values between a minimum J_{min} and maximum value Jmax, specific value of each operating mode (eg elevators carrying a variable number of people).

Keywords: Moment of inertia, electromagnetic torque, friction torque, angular velocity

1. ESTIMATION OF THE MOMENT OF INERTIA

For J = constant:

Determination of J requires the measurement of shaft torque, relatively simple since placing a torque transducer to the MA shaft is relatively simple.

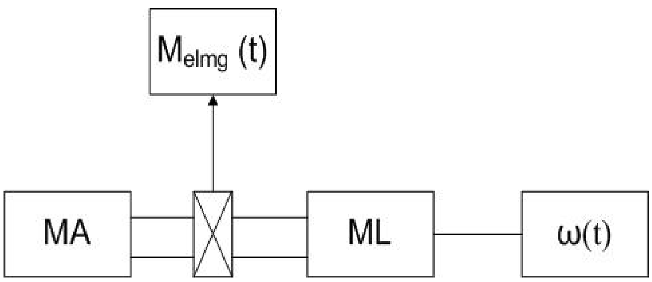

Fig.1. Evolution over time of the electromagnetic torque.

It presents three cases:
a) Operation at two velocities
b) Launch Method
c) Measurement of the electric energy at startup

Operation at two velocities. From the movement equation we obtain:

$$J\frac{d\omega}{dt} = M_{elmg}(t) - M_{rez} \quad (1)$$

and J resulting from integration:

$$J=\frac{\int_{t_1}^{t_2}(\mathrm{M_{elmg}}-\mathrm{M_{rez}})dt}{\omega_2-\omega_1} \tag{2}$$

where:

ω_1 - rotor angular velocity at the beginning of the process

ω_2 - rotor angular velocity at the end of the process

Integration of torque function: $M_{elmg}(t)$ can be done ,in principle, with the same equipment the torque was registered with over time , as it is presented below:

$$\mathrm{I_1}=\int_{t_1}^{t_2}(\mathrm{M_{elmg}})dt \tag{3}$$

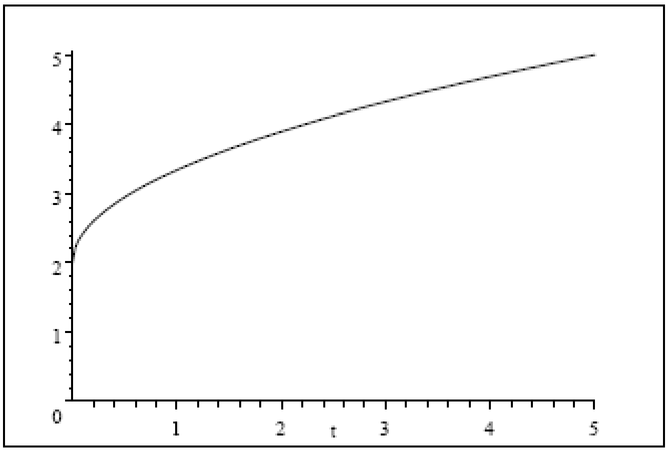

Fig.2. Torque registration $M_{elmg}(t)$

$$\int_0^5 \mathrm{M_{elmg}}(t)dt=20 \tag{4}$$

It is numerically evaluated with the same tool that was used for registering the $M_{elmg}(t)$ function and h = 20[Nms] was obtained as result.

To obtain the resistant torque integral:

$$\mathrm{I_2}=\int_{t_1}^{t_2}(\mathrm{M_{rez}})dt \tag{5}$$

the resistant torque registration with a second transducer mounted in the working area is necessary.

Without this transducer a linear variation can be estimated between :

$M_{res}(t_1)=M_{elmg}(t_1)=2$[Nm] and $M_{res}(t_2)=M_{elmg}(t_2)=5.896$[Nm]

and thus I_2 is:

$$I_2 = \int_{t_1}^{t_2} (\mathrm{M}_{\mathrm{rez}})dt = \int_0^5 (\mathrm{M}_{\mathrm{rez}})dt = 19,34\left[Nms\right] \tag{6}$$

With this results the moment of inertia is obtained as:

$$J = \frac{\int_{t_1}^{t_2} (\mathrm{M}_{\mathrm{elmg}} - \mathrm{M}_{\mathrm{rez}})dt}{\omega_2 - \omega_1} = \frac{I_1 - I_2}{\omega_2 - \omega_1} = \frac{20 - 19,34}{250 - 200} = 0,0052\left[Kg \cdot m^2\right] \tag{7}$$

The launch method at

$$t = 0,\ \omega = \omega_0\ ,\ M_{elmg}(t) = 0 \tag{8}$$

MA disconnects from the network and the equation of motion becomes

$$J\frac{d\omega}{dt} = -M_{friction}(\omega(t)) \tag{9}$$

Through integration we obtain:

$$J\int_{\omega_0}^{0} d\omega = -\int_{0}^{t_{stop}} M_{friction}(\omega(t))dt \tag{10}$$

Friction torque $M_{friction}(\omega(t))$ velocity dependency it is known from operating at zero resistance torque at various velocities when:

$$M_{elmg} = M_{friction} \tag{11}$$

The electromagnetic torque estimation *M_{elmg}* (at different velocities) it is done through a torque transducer or through calculation:

$$M_{elmg}(t) = p(I_q I_{dr} - I_d I_{qr}) \tag{12}$$

At angular velocities between $0 \div \omega_0$.

In the analyzed case friction torque depends on ω as it is presented in the figure below:

$$M_{friction}(\omega) = 0,1 + 2,1\left(\frac{\omega}{314}\right)^2 \tag{13}$$

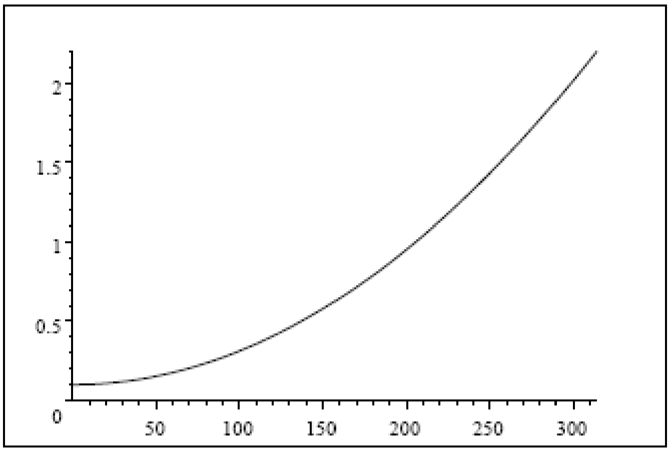

Fig.3.Torque dependency on friction $M_{friction}(\omega)$

The decrease of rotor angular velociti $\omega(t)$ over time is given in figure 4.
$T_{stop} = 6$ [s]

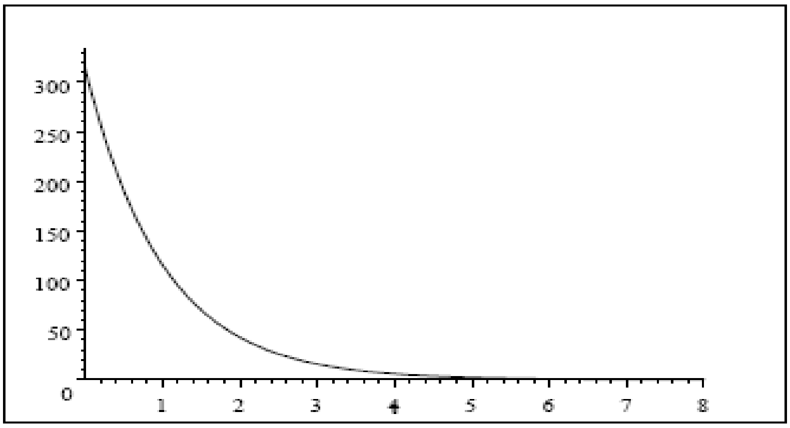

Fig.4. The decrease of ω over time

From the two functions:

$$M_{friction}(\omega) \tag{14}$$

$$f_2 = \omega(t) \tag{15}$$

we obtain the function:

$$f_1(t) = M_{friction}(\omega(t)) = M_{friction}(t) \tag{16}$$

friction torque variation over time from $\omega = \omega_0$ to $\omega = 0$ (stop):

$$M_{friction}(\varpi(t)) \tag{17}$$

$$\int_0^6 M_{friction}(t)dt=1.65 \tag{18}$$

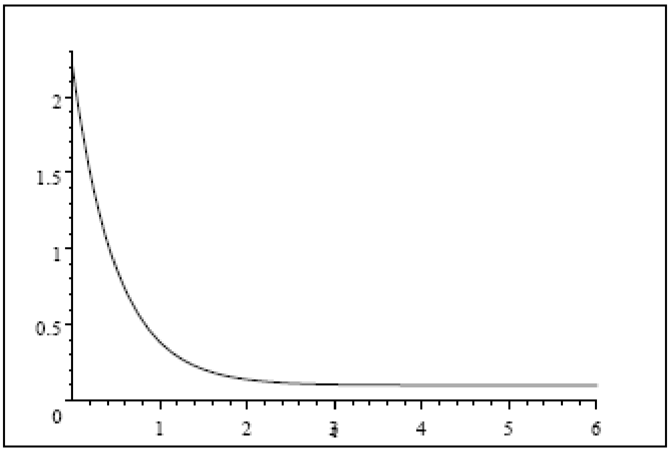

Fig.5. Friction torque variation over time.

Integrating the movement equation:

$$J\frac{d\omega}{dt} = -M_{friction}(t) \tag{19}$$

results

$$J\omega_0 = \int_0^{t_{stop}} M_{friction}(t)dt = \int_0^{t_{stop}} f\,dt \tag{20}$$

or

$$J \cdot 314 = \int_0^6 M_{friction}(t)dt=1.65 \tag{21}$$

from where

$$J = \frac{1.65}{314} = 0.\ 00525\ [Kg \cdot m^2] \tag{22}$$

Determining the momentum of inertia J with the launch method ,means knowing:
-function $\varpi(t)$-angular velocity registration over time until stoped;
-function $M_{friction}(\varpi)$ –torque dependency on ϖ friction
The method has a higher precision degree than the classic one for wich J is calculated through the origin tangent to the $\varpi(t)$ curve.

2. MEASUREMENT OF THE ELECTRIC ENERGY AT STARTUP

The following presents the determination of J from the electric energy measured at startup.

In the startup process the electric energy measured with the electric meter is:

$$E = \frac{1}{2} J\omega_0^2 + E_{caloric} = \frac{1}{2}J\omega_0^2 + \frac{1}{2}J\omega_0^2 = J\ \omega_0^2 \tag{23}$$

because $E_{caloric}$ is the heat energy, the electric heating effect is located,mainly in the MA rotor:

$$p_2 = s \cdot P = s \cdot \omega_0 \cdot M_{elmg} \tag{24}$$

and so

$$E_{caloric} = \int_0^{t_0} p_2 dt = \int_0^{t_0} s \cdot P_{elmg} dt = \int_0^{t_0} s \cdot \omega_0 \cdot M_{elmg} dt \tag{25}$$

using the equation of movement

$$J\frac{d\omega}{dt} = M_{elmg} \tag{26}$$

we obtain

$$\begin{aligned} E_{caloric} &= \int_0^{t_0} s \cdot \omega_0 \cdot M_{elmg} dt = \int_0^{t_0} s \cdot \omega_0 \cdot J\frac{d\omega}{dt} dt = \omega_0 \cdot J \int_0^{\omega_0} s \cdot d\omega = \\ &= \omega_0 \cdot J \int_0^{\omega_0} \frac{\omega_0 - \omega}{\omega_0} \cdot d\omega = \frac{1}{2} J\omega_0^2 \end{aligned} \tag{27}$$

The determination with the measurement of the electric energy at startup method ,of the inertia momentum J,means knowing just two variables:

ω_0 –rotoric angular velocity
E –electric energy at startup

3. TORQUE DEPENDENCY ON VELOCITY FRICTION

Torque dependency on velocity friction is very important in applications wich require fast and precise velocity adjustments.

The determination of friction torque at different operating velocities is not a difficult problem, when you havel an inverter that can give variable frequency (and voltage) and the electromagnetic torque value through the calculation of the function:

$$f(\omega) = M_{elmg}(\omega) = pM(I_q I_{dr} - I_d I_{qr}) \tag{28}$$

If you have a torque transducer then the electromagnetic torque can be determined by experiment (figure 6)

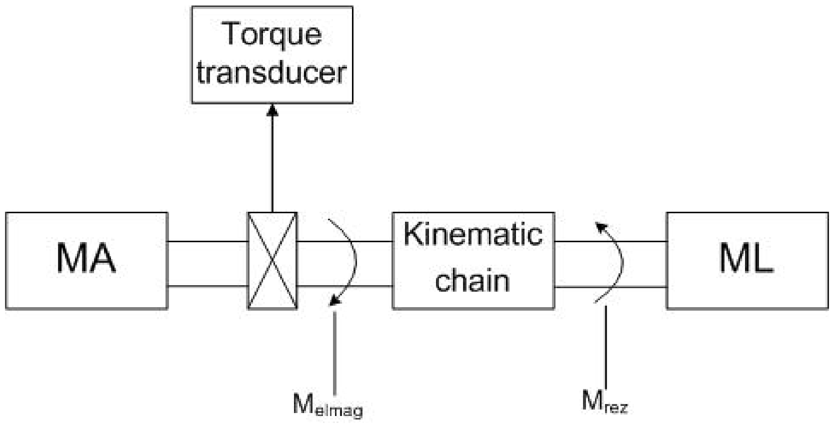

Fig.6. Experimental determination of the electromagnetic torque.

In steady regime friction torque $M_{friction}$ can be calculated through the decrease of the two torques:

$$M_{friction} = M_{elmg} - M_{res} \tag{29}$$

Operating în gol of the machine ($M_{res} = 0$), the electromagnetic torque becomes equal with the friction torque:

$$M_{friction} = M_{elmg} \tag{30}$$

Therefore, doing more test at different speeds (and various angular mechanical ϖ velocities) function $M_{friction}(\varpi)$ is obtained:

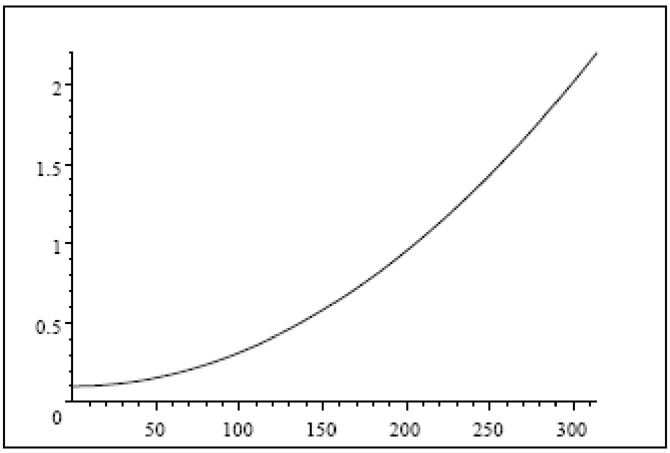

Fig.7. Torque $M_{friction}$ dependency on ϖ

At null velocity n = 0 (ω = 0), friction torque is called static friction torque and depends ,mainly, on the oil viscosity from the kinematic chain. The mean friction torque $M_{average}$ (average friction torque) has a special significance ,in that the energy balance:

$$\frac{J\omega_0^2}{2} = M_{average} \cdot \beta \tag{31}$$

$$f(\omega) = M_{elmg}(\omega) = pM(I_q I_{dr} - I_d I_{qr}) \tag{32}$$

where:

$\frac{J\omega_0^2}{2}$ – system kinetic energy with the momentum of inertia J at rotoric angular velocity ω_0

$M_{average} \cdot \beta$ – average torque mechanical work $\left(\beta = \int \omega(t)dt\right)$ the momentum of inertia can be determined:

$$J = \frac{2 \cdot M_{average} \cdot \beta}{\omega_0^2} \tag{33}$$

T_{stop} = 6 [s]

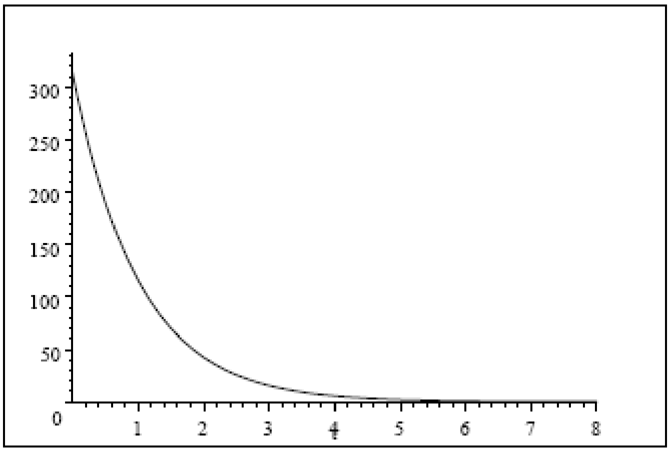

Fig .8 Rotoric angular velocity over time

β angle can be obtained through the velocity registration (ω) over time la at a free launch (figure 8) and is equal with $S = \beta = \int_0^{t_{stop}} \omega(t)dt = 313,22[rad]$

The staded above is demonstrated in the example below. The friction torque dependent on ω in the form:

$$M_{friction} = 0,1 + 2,1\left(\frac{\omega}{314}\right)^2 \tag{34}$$

and looking like in figure 9.

$M_{friction}(\omega)$

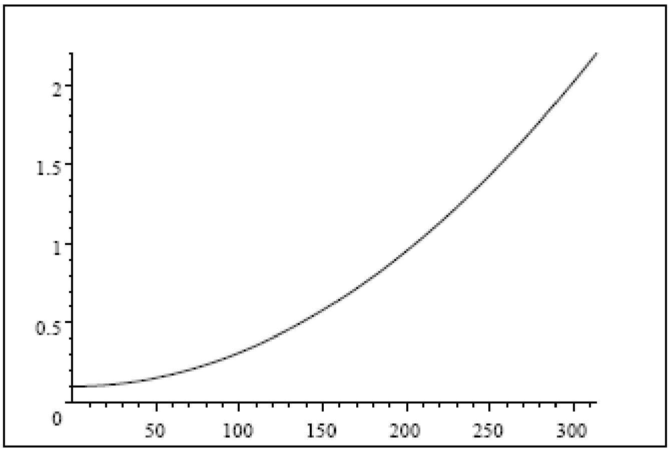

Fig.9. Variation of the friction torque with ω

The average value of the friction torque $M_{average}$ is obtained from:

$$M_{average} \cdot \omega_0 = \int_0^{\omega_0} M_{friction} d\omega \tag{35}$$

or

$$\mathrm{M}_{\mathrm{average}} \cdot 314 = \int_0^{314} \left(0{,}1 + 2{,}1 \left(\frac{\omega}{314} \right)^2 \right) \mathrm{dt} \quad = 251{,}2 \tag{36}$$

from where

$$\mathrm{M}_{\mathrm{average}} = \frac{351{,}2}{314} = 0{,}8 [Nm] \tag{37}$$

same values can be calculated from the momentum of inertia J:

$$\mathrm{J}_1 = \frac{2 \cdot \mathrm{M}_{\mathrm{average}} \cdot \beta}{\omega_0^2} = \frac{2 \cdot 0{,}8 \cdot 313{,}22}{314^2} = 0{,}0051 \left[kg \cdot m^2 \right] \tag{38}$$

Previous value, calculated with the launch method was:

$$\mathrm{J}_2 = 0{,}00525 \left[kg \cdot m^2 \right] \tag{39}$$

The difference between J1 and J_2 is very small :

$$\Delta\mathrm{J} = 0{,}00007 \left[kg \cdot m^2 \right] \qquad \text{meaning } 1{,}3\% \tag{40}$$

From the above we can notice the great importance of knowing the ω friction torque variation and with this the determination, relativly, very small of the momentum of inertia J.

The method says:

- knowing the function ω(t) and
- the function $M_{friction}$(ω

REFERENCES

[1]. Andreescu D. ***Estimated in control systems of electrical*** **drives**, Ed. Politehnica Timişoara.
[2]. Babescu M., Păunescu D., ***Electrical Machines - mathematical analysis of the transitional arrangements,*** Ed. Polithenica, Timişoara, 2001
[3]. Boldea I., Nasar S.A., **„*Vector Control of AC Drives*”**, CRC Press, Florida, 1992
[4]. Jiao S., Hunter G., Ramsden V., Patterson D.—“***Control system design for a 20 KW wind turbine generator with a boost converter and battery bank load”,*** in Proc. IEEE PESC, Vancouver, BC, Canada, Jun. 2001, pp. 2203-2206
[5]. Kana C. L., Thamodharan M., Wolf A.—“***System management of a wind energy converter***”, IEEE Trans. Power Electron., vol. 16, no. 3, pp. 375-381,May 2001
[6]. Karlsson P.—“***DC distributed power systems-Analysis, design and control for a renewable energy system”*****,** Ph. D. dissertation, Lund Univ., Lund, Sweden,2002
[7]. Lane N., Boesch D. F.—***Vision 2033, part 6: Energy, the environment, and global change***. The American Association of the Advancement of Science [Online].2004
[8]. Park. ***J.K Control of state-constrained linear dynamical systems: Antireset windup approach***, IEEE Proc. Control Theory Appl. Vol.147, No.2 February 2000

WAVE CLIMATE

DUMITRESCU GABRIELA SIMONA

"Mihai Eminescu" National College, Constanta, Romania

A ship or any ocean vehicle or structure is exposed to the marine environment. Enviromental forces at sea come from wind, seaway, current, tidal waves, and waves from earthquakes (tsunamis). Generally, seaway is generated by the wind at the sea surface. Information on wind-generated wavTes has been based on: visual observation; instrumental buoy measurements; remote sensing from satellites; calculation with spectral models using barometric fields and wind field analysis.It underestimates the recurrence of heavy storms. Buoy measurement data are smaller in volume and limited to a small number of years. The storm class depends on the shape of the wind force versus time. The wave class depends on the shape of the seaway spectrum versus frequency. Storm class I is generating waves during limited time. Storm class II is generating a fully developed sea. Storm classes III,IV,V: combinations of class I and II.

***Keywords**:* marine, climate, storm, environment, wave

1. THE SHIP IN THE MARINE ENVIRONMENT

A ship or any ocean vehicle or structure is exposed to the marine environment. It is a complicated and often hostile environment. Environmental forces at sea come from wind, seaway, current, tidal waves, and waves from earthquakes (tsunamis). From the practical point of view, the seafarer has to cope with wind and seaway. Generally, seaway is generated by the wind at the sea surface.

The occurrence and magnitude of wind and seaway depend on the sea area and on the time of the year. Wind and seaway vary randomly and can be described by statistical methods based on probability theory. In detail, we look at the rate of occurrence, the magnitude, and the time variations of wind and seaway.

It is convenient to make a distinction between long-term (in terms of days up to years) and short-term time (in terms of hours) variations of the seaway. While the long-term approach allows for the rate of occurrence and the severity of the seaway, the short-term time variations are important for the dynamic ship response in a particular seaway of constant energy. Seaway is represented by gravity waves of the water at the sea surface. The exciting wave forces vary in time. The ship responds to the oscillating external forces as a dynamic system.

Wind and the wave data have been assembled by observation, by measurement, and by mathematical description. Goals of the near future are, for example, to apply the non-linear pattern of extreme irregular seas in ship operation, and to have sea on-line data on the bridge.

2. WAVE CLIMATE

Information on wind-generated wavTes has been based on:
Visual observation
Instrumental buoy measurements
Remote sensing from satellites
Calculation with spectral models using barometric fields and wind field analysis.

Although observation has the lowest quality of data, it has the largest statistical data available. It underestimates the recurrence of heavy storms. Buoy measurement data are smaller in volume and limited to a small number of years. Satellites and calculation models will give better information in the near future.

We can speak of a ‘wave climate’ to include the whole wave states at sea. Storms and waves can be classified into typical structures. Boukhanovsky et al.(2000) proposed to apply five storm classes and four wave classes. The storm class depends on the shape of the wind force versus time. The wave class depends on the shape of the seaway spectrum versus frequency.

Storm class I is generating waves during limited time.
Storm class II is generating a fully developed sea.
Storm class III, IV, V: combinations of class I and II.

The storm class is characterized by storm duration, time of growth and time of decay. Figure 1 shows the dimensionless wind force versus time. Table 2.1 gives the frequency of occurrence of the storm shapes and the mean shapes of duration (from measurements in the Black Sea, Boukhanovsky et al.(2000)). While I is triangular, II is more trapezoidal in shape. Storm class III is similar to IV, but the peaks exchanges (not drawn).

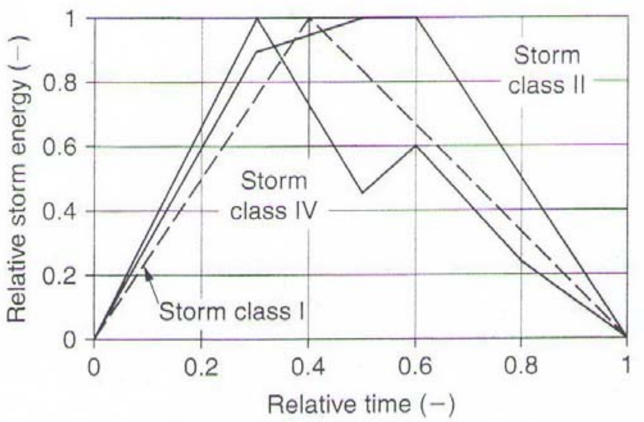

Fig. 1. Storm shapes classes I, II and IV

Storm class I, with 50% occurrence in the Black Sea, has the largest percentage of the five storm classes, see Table 2.1. Wave class II (wind waves) shows for all classes of wind and storm the largest percentage.

Table 2.1: Percentage of storm and wave classes in the Black Sea

***Storm** class*	*I*	*II*	*III*	*IV*	*V*
Occurrence	**50%**	15%	6%	19%	10%
Wave class	Occurrence (%) of wave class related with storm class				
I (swell)	41	33	31	33	24
II (wind waves)	**46**	**54**	**53**	**55**	**61**
III complex	9	9	13	8	11
IV complex	4	4	3	4	4

The sea surface $\zeta(x, y, t)$ is stochastic in the time and space domain. Directional seaway spectra, $S_{\zeta\zeta}$, constitute 'wave weather'. $S_{\zeta\zeta}(\omega, \mu)$ varies in space (x, y) and in time t. It is non-stationary and not homogenous. Seaway spectra are classified according to:

- S swell WW wind waves CS complex sea.

Wind waves and swells are discriminated into four classes with typical spectral shapes according to Table 2.1 see Figure 2. It must be kept in mind, that all spectra are average estimates of statistical data, so on-line spectra can show large scatter.

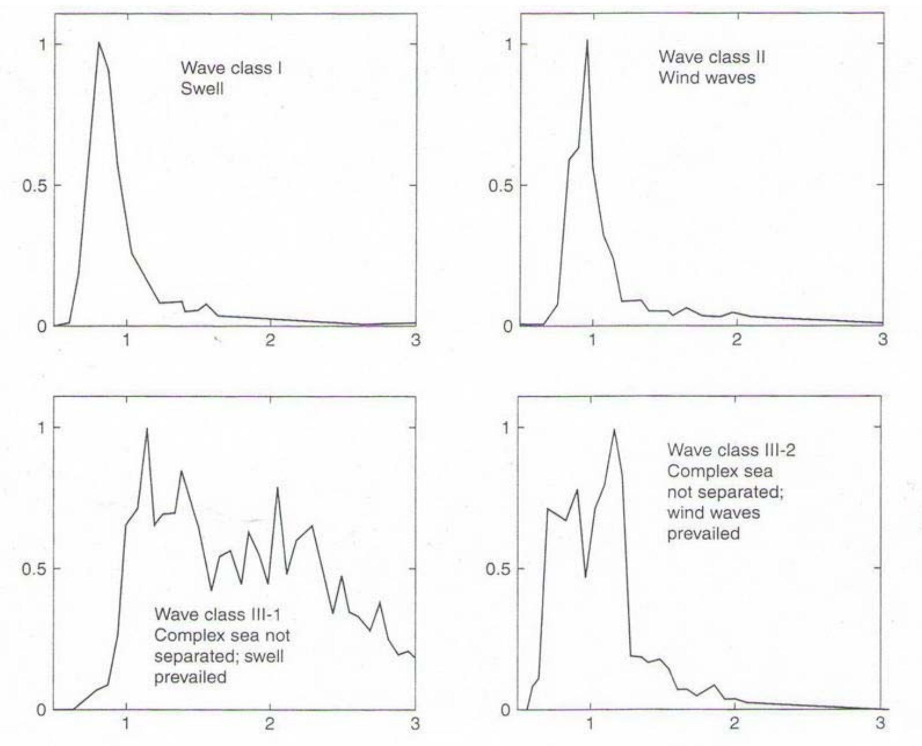

Fig. 2 a. Wave class I, II, III - 1, III – 2

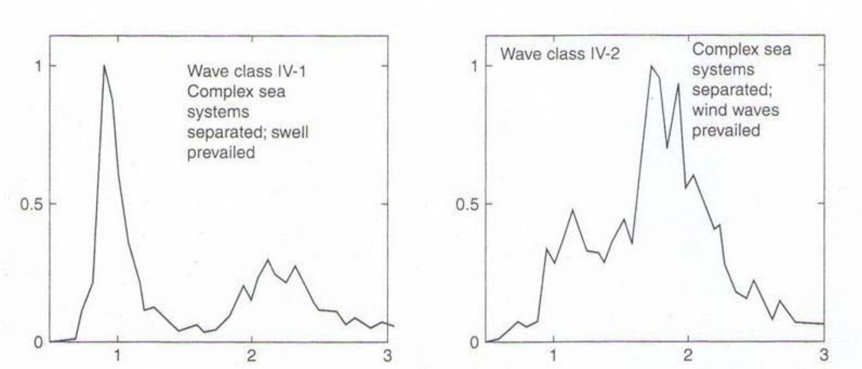

Fig. 2 b. Wave class IV - 1, IV – 2

Wind and wave climates allow analyzing operational conditions at sea in more detail. Satellites will give direct data on the wave climate distribution, and can even detect rare but feared freak waves. So we can expect to get more direct seaway information on the bridge in the near future. The Atlas of the Oceans by J.T. Holland and I.R. Young (1966) gives information on global meteorology and the GEOSAT satellite mission.

3. CONCLUSIONS

The occurrence and magnitude of wind and seaway depend on the sea area and on the time of the year. Wind and seaway vary randomly and can be described by statistical methods based on probability theory. In detail, we look at the rate of occurrence, the magnitude, and the time variations of wind and seaway.

Wind and the wave data have been assembled by observation, by measurement, and by mathematical description. Goals of the near future are, for example, to apply the non-linear pattern of extreme irregular seas in ship operation, and to have sea on-line data on the bridge.

Wind and wave climates allow analyzing operational conditions at sea in more detail. Satellites will give direct data on the wave climate distribution, and can even detect rare but feared freak waves. So we can expect to get more direct seaway information on the bridge in the near future. The Atlas of the Oceans by J.T. Holland and I.R. Young (1966) gives information on global meteorology and the GEOSAT satellite mission.

REFERENCES

1]. Boukhanovschy, A.V., Degtyarev, A.B., Lopatoukhin, L.J. and Rozhknov,Y.V. – ***Stable states of wave climate: Applications for risk estimation',*** Proc. of STAB'2000, Vol. 2, Launceston, Tasmania, pp.831-846, 2000.

[2]. Holland J.T. and Young I.R. – ***The Atlas of the Oceans,*** pp.120- 130, 1996.

[3]. ***The Maritime Engineering Reference Book,*** A Guide to Ship Design, Construction and Operation, pp.3, 18-20, USA, 2008.

DEVELOPMENT OF A SIMULATION ENVIRONMENT FOR TRAINING AND RESEARCH IN MARITIME SAFETY AND SECURITY

[1]FELSENSTEIN CHRISTOPH, [1]BENEDICT KNUD
[2]BALDAUF MICHAEL

[1]Hochschule Wismar, ISSIMS Warnemünde, Germania,
[2]World Maritime University Malmö, Suedia

Currently, one major priority in passenger shipping is to train ship's officers and crew with sufficient skills and appropriate procedures to provide adequate protection and ensure the safety of all passengers and crew especially on ferries and cruise ships. For this purpose it is essential to establish a permanent process of change and development with regard to new precautionary measures against terrorism both in ports and onboard vessels in accordance with existing regulations. Training human mentality and motivation is vital to create a permanent underlying security culture. Simulators have proved beneficial for ship operation training in real time. Modern maritime training institutions all over the world increase the complexity of simulations by connecting full mission ship handling, ship engine and Vessel Traffic Services (VTS) simulators. There is ongoing research and development to also provide and integrate specific simulation facilities for maritime safety and security issues. For these purposes a new type of simulator is under development for integrated training and research of the specific aspects of maritime safety and security. A so called Safety and Security trainer (SST) simulation system, designed for two- and three-dimensional visualisation, is developed. It contains the 3D visual model of a real ferry. This visual model implemented into the SST is interfaced to an integrated decision support system to assist trainees to cope with safety and security challenges during manoeuvres of the vessel in a full-mission simulation environment. The system is designed to allow for more detailed evaluation of the effectiveness of safety and security plans under varying conditions and during different courses of events by different series of simulation runs. This paper will introduce the basic concept of the safety and security training simulator and describe the work entailed for its integration into the complex environment of full mission ship-handling- and ship-engine-simulators. Selected results of a case study dealing with first basic implementation of training scenarios will be demonstrated.

***Keywords**:* Integrated full-mission Simulation, Maritime Safety, Security, System Modelling

1. SIMULATION FOR MARITIME SAFETY AND SECURITY INTRODUCTION AND BACKGROUND

Piracy and Terrorism is threatening the maritime industry for decades. The quality of piracy nowadays cannot be compared with piracy during the last centuries. The criminal economic based piracy attacks recently are even correlated to the terrorism scene and corresponding in financial interests.

That is why sufficient skills and knowledge about methods and procedures to provide protection and to ensure the safety of life of passengers and crew is a major demand to all ship officers and crew members especially of ferries and cruise ships. The best way to achieve knowledge and to gain corresponding skills are education and training including exercises on special designed simulators representing the real complex conditions on board of such vessels.

The increased power of modern simulation technologies have proved beneficial for ship handling training in real time e.g. especially on high sophisticated integrated bridges systems throughout the last decades. However, mainly due to the complexity and the great variety of processes, simulation for maritime safety and security issues is one of the most challenging tasks. Especially in emergency situations the officer of the watch (OOW) and the bridge team has not only to handle the emergency of e.g. a fire onboard or an explosion in engine room, itself but also to ensure safe navigation. Safety science is addressing this by discussing and studying the problems using the approach and principles of socio-technical systems (see e.g. [1] and [5]).

Rules, Regulations as well as guidelines basing on formal risk analysis and safety assessments (see [6], [7]) are set into force in order to avoid errors and to overcome identified shortcomings and lacks of observed behaviours and existing procedures. High sophisticated technical (information and decision support) systems are developed and installed to assist the human operator in his risk management tasks. Such assistance systems are usually tested against technical parameters but should also be tested with respect to the impact regarding the interaction with and the actions of the operators. Finally, in order to estimate and assess the efficiency of certain courses of actions and the usability and practicability of established procedures and guidelines they need to be tested before their introduction into practice by full-mission test scenarios either in real or in a simulated environment. The different categories of situations and scenarios are visualized in Figure 1 below. This figure is inspired by Hollnagel, who had adapted and further developed an idea of Westrum [1] to explain the classification of possible situations regarding the evaluation of changes in the (maritime) socio-technical system.

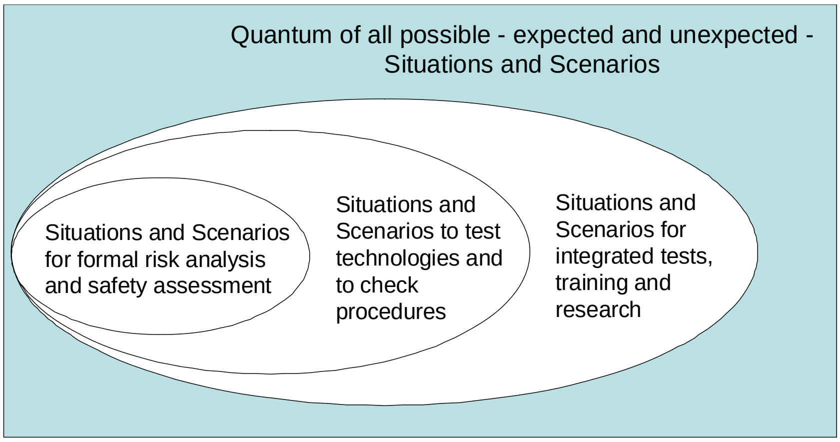

Fig. 1. Framework, structure and content of research work to enhance passengers' safety on RoRo-Passenger ferries

Under the aketched aspects of socio-technical systems, it becomes apparent that only integrated simulation is adequate for purposes of training and research subjects related to operational management and handling of maritime safety and security.

On the basis of the mentioned facts a new type of simulator is under development for training and research of specific aspects of Maritime Safety and Security. Wismar University in cooperation with World Maritime University has been involved in the conceptual design and development of this new simulation system made by Rheinmetall Defence Electronics (Bremen) and is already to be successfully introduced into the maritime education and training for both student lectures and further training for shipping manpower.

Within the frame of investigations into potential improvements of maritime safety and security, the use of simulation facilities is under observance. In addition to the existing simulators, the full mission Ship Handling Simulator (SHS), Ship Engine Simulator (SES) and Traffic Simulator (VTS), a new type of simulator called the Safety and Security Trainer (SST) is available for training specific aspects of maritime safety and security. The complex simulation platform with four full mission simulators enables the trainee to simulate the entire maritime sub-system "ship" and offers challenges to officers and crew on board the vessels.

2. ENHANCEMENT OF PASSENGERS' SAFETY ON RoRo-FERRIES

By recognizing the necessity and demands of the aforementioned factual information a strategic project for research and technological development was designed and planned. The main focus of the work is set on safety and security of ferry passengers. The investigations and the related development were founded on in-deep risk analysis and the derived work plan especially takes into account the aspects of:

- check-in procedures to increase the safety level for entrances to ferry ships and ports
- preventive measures on board (constructive and administrative)
- Sea side protection of ships in ports as well as in open sea when sailing
- investigations into potential improvement of measures in case of crises
- The analysis and investigations are dealing with subjects as:
- use and optimisation of monitoring and detection systems
- aspects of potential integration of decision support systems on board ships
- identification of potential for optimisation of processes and measures/procedures including the integration of new innovative technologies and
- consideration and application of rules and regulations according to national and international law.

With reference to risk based scenarios in ports and on board RoRo-Passenger ferries the following fields of investigations are defined:

- Process Analysis from the entrance of the port, including booking and check in procedures, towards to the vessel and access of embarkation
- Process Analysis on board the vessel from embarkation/departure until arrival/disembarkation
- Analysis of the ISPS Code and measures for the full integrated application on board
- Measurements for improved processes on board and access to the vessels and developing new security technologies and procedures
- Developing a support decision system for emergency measures on board the vessel in case of safety and/or security casualties

The aims and the principle structure of the research and development work are given in the following figure.

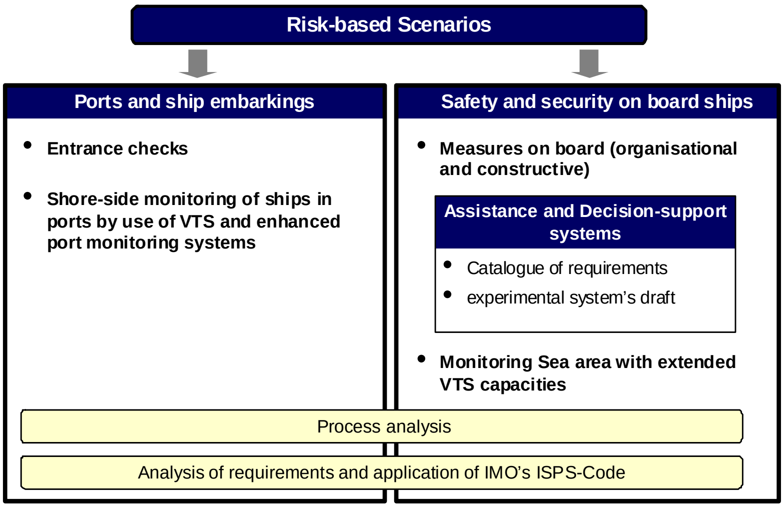

Fig. 2. Framework, structure and content of research work to enhance passengers' safety on RoRo-Passenger ferries

The fundamental legal framework and basis for the research work is given by the ISPS-Code. The Diplomatic Conference on Maritime Security in London in December 2002 adopted new provisions in the International Convention for the Safety of Life at Sea, 1974 and the International Code for the Security of Ships and of Port Facilities - ISPS Code, which entered into force 01st July 2004. The Code is in two parts, Part A which is mandatory and Part B which is recommendatory. The minimum requirements for ships respectively ports are ship (as well as port facility) security assessment, ship (and port facility) security plans in ports and on board the vessels and certain appropriate security equipment.

Apart from existing regulations it is very important to recognize the permanent process of changing and further developing precautions and measures against terrorism in ports and onboard the vessel. Human mental attitude and motivation are important and on the premises to create a security culture. Basing on this the so called ACCEPT-principle was created and is to be introduced into safety and security training courses. It consists of the following listed elements:

ACCEPT security:

- Apply risk management
- Contemporary security knowledge
- Create security culture
- Enhance policies and procedures
- Protective measure
- Training commitment

In order to realize and apply each the component of the developed concept it was found that high sophisticated integrated simulation-based technologies are urgently needed. Simulations for safety and security purposes need to reflect the complexity of the complete nautical and technical ship operation in case of any emergency. However, until today the technical solutions for research and training are very limited especially in respect to this specific context.

3. INTEGRATION OF NEW MODULES FOR SAFETY AND SECURITY INTO AN EXISTING FULL-MISSION SIMULATION ENVIRONMENT

According to its unique complexity of the connected different types of maritime simulators the Maritime Simulation Centre Warnemünde (MSCW) is one of the most modern simulation centres worldwide. It comprises the full mission Ship Handling Simulator (SHS), Ship Engine Simulator (SES) and Traffic Simulator (VTS) as well as the new type of simulator called the Safety and Security Trainer (SST). The complex simulation platform with four full mission simulators enables the trainee to simulate the entire system ship and offers challenges to officers and crew on board the vessels.

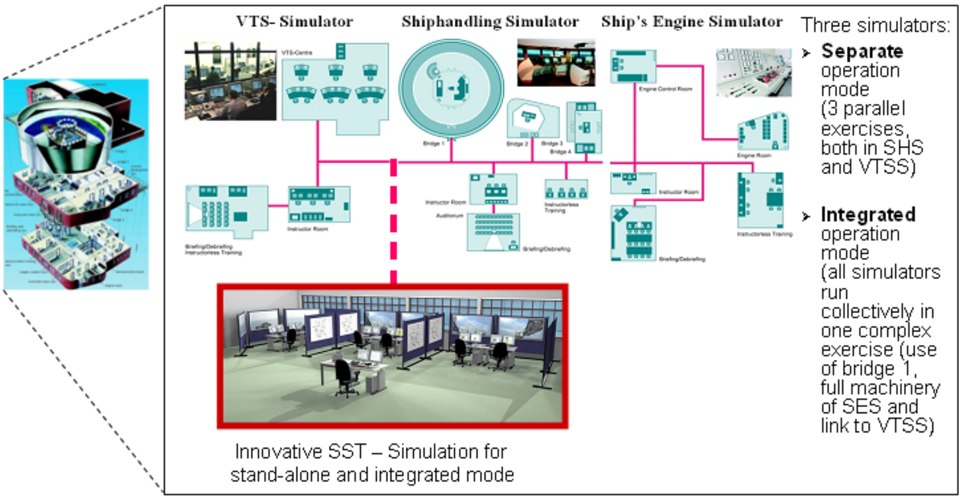

Fig. 3. Sample case of a full-mission maritime simulation environment (Maritime Simulation Centre Warnemünde (MSCW) – building and structure)

The simulator arrangement comprises already

- a Ship Handling Simulator SHS with four Full Mission bridges and 8 Part Task Bridges,
- a Ship Engine Simulator SES with 12 Part Task stations and
- a Vessel Traffic Services Simulator VTSS with 9 operator consoles

The new simulation system, implemented as Safety and Security Training environment (SST), is developed and designed in close cooperation with a system developer and manufacturer, who provides the basic technological platform and implements functionalities and components that are further developed by the Institute of Ship Technology, Simulation and Maritime Systems at Hochschule Wismar, Department of Maritime Studies. The safety and security simulation environment was originally the experimental basis version with two-dimensional (2D) presentation and is now being developed into a high sophisticated simulator with integrated three-dimensional (3D) visual components. The simulator can specifically be used for stand alone and moreover for integrated training with the SHS. Together with the full set up of training material including all ships safety plans it was introduced as the first unique comprehensive Training and Education Concept "mars²" for Maritime Safety and Security including an innovative Simulation System. Beside the use for training the simulation system will be installed and used also for specific simulation based studies into potential enhancements of existing safety and security procedures.

4. CONCEPTUAL DESIGN OF INTEGRATED SAFETY AND SECURITY SIMULATIONS FOR TRAINING AND RESEARCH

The situation in the shipping world with regard to emergency preparedness is affected in general by the following elements:

- Abilities and Experiences in case of „disturbed" operation of systems are reduced or simply not existing
- Multilingual Crews cause specific problems in case of Emergency Situation
- Reduction of Crew Members causes lack of available Personnel
- Complexity of Emergency Equipment is permanently increasing, but Training in Emergency Handling is not following this Development
- New Management Systems and regulations of the IMO (ISM/ISPS) are demanding new methods and technology for emergency training

Development of simulation based training courses in safety and security for different level of competency, for ratings on basic level, for officers and Master on management level has to comply with IMO standards and can be structured as given in the figure below.

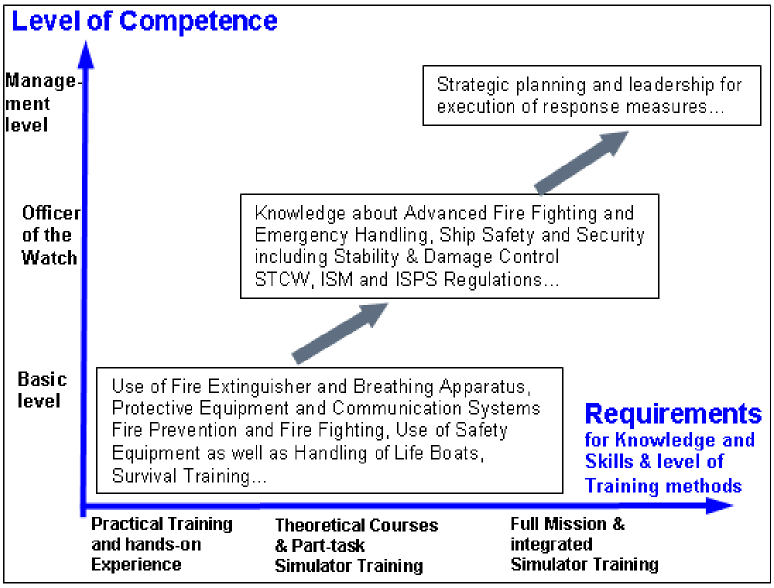

Fig. 4. Level of competence and required safety and security training

The design of the workplace concept of the Safety- and Security Trainer module was created for up to 10 stations are being installed in the MSCW. The experimental installations consist of eight training stations (one directly integrated on the simulation bridge 1 and linked to the SHS) and two instructor consoles. Each station consists of two monitors. One screen is used as Situation Monitor and the other is named Action Monitor. The workplace concept provides full equipment for comprehensive safety and security training (Figure 5).

Fig. 5. One Instructor and several stations for training with the SST simulator

The Monitors provides, inter alia, a bird's eye view of one deck inside the simulated ship. It is mainly shown on the situation monitor. A person simulating a member of the crew can be moved through the rooms in the deck. Positioning the figure on specific IMO symbols the related safety equipment is indicated as generic panel on the action Monitor. All interaction done at such panels is done at the action monitor. If the „Strategic Figure" is not located on symbols representing safety equipment, the action monitor shows the ship safety plan of the appropriate deck.

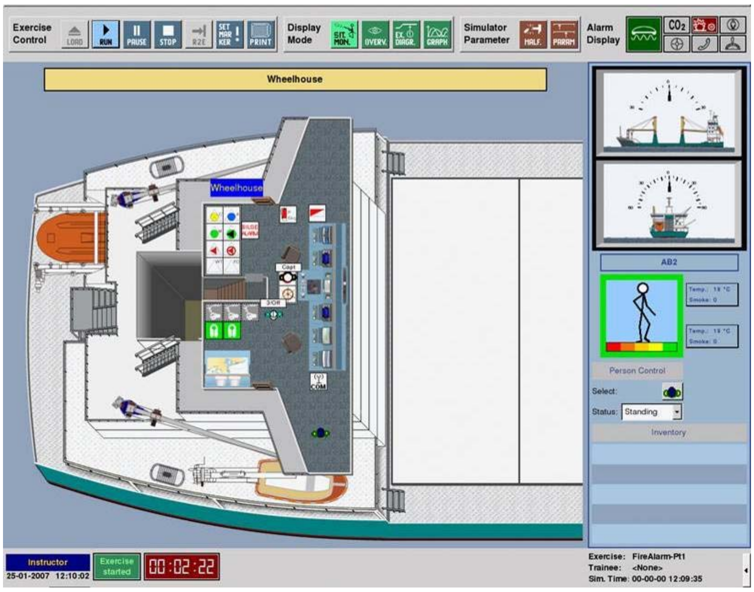

Fig. 6. Sample of a Display on the Situation Monitor

In Figure 6 the main desktop displays an overview about one deck. The menu bar provides access to other windows. It is possible to create new exercises and store replays. Also malfunctions, fire, water inrush and criteria for the incorporated assessment can be set. The actual ship status as indicated by draught, trim and list angle is shown. The name of selected person, health index and moving type (standing, kneeing and lying) is shown in the status display window, also the kind of protective clothes worn by the figure. A single mouse click selects a person, e.g. Captain, which than can be moved normally or quickly to any other position and to the IMO symbols, in which case the action monitor will show the related operable switch gear or the emergency equipment according to the Ship Safety Plan.

5. DEVELOPMENT AND INTEGRATION OF MARITIME SAFETY MODULES

Most of the actions performed by the trainees with the safety equipment are performed at the action monitor. A fire model optimised visually and given noticeable effects for human beings is incorporated into the mars simulator. A modern fire alarm management system with smoke detectors and manual calling points is built into the ship. Rooms with easily flammable materials are protected by fire resistant A60 walls and doors. The fire model including smoke visualisation and the fire fighting system and equipment such as fire extinguishers, water hoses and hydrants, breathing apparatus, CO2 systems and foam, enables the trainee to simulate a realistic fire fighting arrangement on board and interact with supporting teams and the management team on bridge and engine room. During the simulation the strategic figure's health condition is monitored in relation to oxygen, smoke, temperature and other health influencing parameters and the measurements are monitored in diagrams (Figure 7).

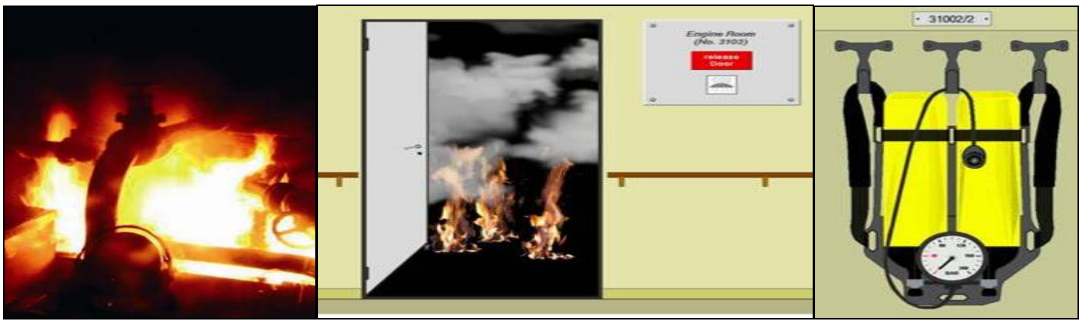

Fig. 7. Fire Model on board as well as 2D-presentation and Breathing Apparatus in the simulator monitor

One further feature of the mars simulation system is a model calculating water inrush and its influence to the stability of the ship. A ballast system is implemented and can be used during simulation of an emergency case to stabilize the ship. The trim and stability calculator is used to predict the consequences of a water inrush and show the stability, bending moments and share forces. Water tight doors are built into the modelled vessel. The ballast and stability measuring system is implemented in the simulator, which will enable the trainee for countermeasures.

6. IMPLEMENTATION OF INNOVATIVE 3D-VISUAL MODELS

One of the most challenging innovations for integrated maritime simulations is the 3D-designed RoPax ferry "Mecklenburg-Vorpommern" and its integration into the SST. As a first application the ship plans were realised in 3D using Studio Max © version for test trails of the sophisticated 3D-visualisation of the vessel. All decks of the RoPax ferry are meanwhile implemented in the 3D-version and integrated together with the dynamic safety equipment into the games engine by the simulator manufacturer. Functional tests of the developed system are in progress and running successfully. Figure 8 depicts the ships plan of the decks 5 and7 of the RoPax ferry whereas the Figures 9 and 10 are giving examples of the implemented 3D visualisation of selected deck areas and public areas of the ferry generated from the 2D model.

Fig. 8. Ships plan Deck 5/7 of RoPax ferry – Scandlines (VESPER)

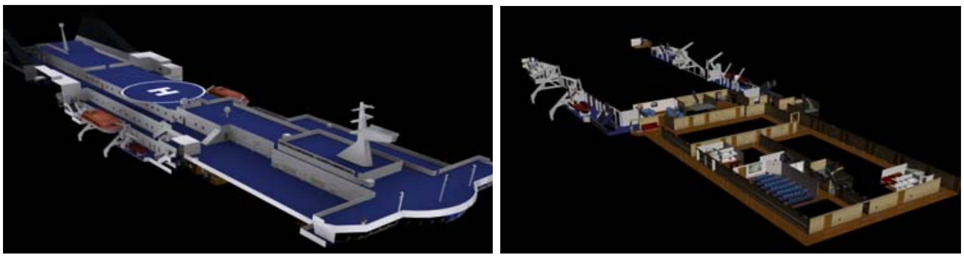

Fig. 9. Deck 6-9 in 3D RoPax Ferry (left) and Deck 6 in 3D RoPax Ferry (right)

Fig. 10. Three-dimensional Simulation environment of Cinema room (left) and Public area on the simulated RoRo-Pax Ferry

7. GENERIC APPROACH FOR COMBINED TRAINING AND RESEARCH SCENARIOS CONNECTING SHIPHANDLING - AND SAFETY AND SECURITY - SIMULATION

The level of complexity of simulation at the MSCW has entered a new generation. Until now the training at the full mission ship handling simulator, the ship engine simulator as well as the ashore based vessel traffic simulator (VTSS) embraced a network targeting ship handling and nautical and technical management on board. All systems can be combined for complex on board training and with the VTS including a ship monitoring system from ashore [2]. The innovation and integration of the safety and security trainer, until now considered as a useful but separate tool for training in safety and security matters, will enable the trainee to confront the entire system ship with complex scenarios and in addition to being faced with navigational and technical issues, forced to "dive inside the vessel". Now the target is to combine all simulation systems to reflect the issues which determine the reality on and around the ship. A new quality of scenarios can and has to be generated in future for comprehensive and adequate training for ship officers. Taking into consideration the research and first developments of former projects (see [3] and [4]) by using the results of developed areas, models and drafted scenarios, the approach to a complex scenario is possible.

Parallel to the technical development of the simulation environment the design and development of scenarios had begun. This process follows the fundamental principles of building a simulation model. In order to implement a suitable model for integrated safety and security simulations, instead of the real processes, general steps are necessary and are depicted in the following figure.

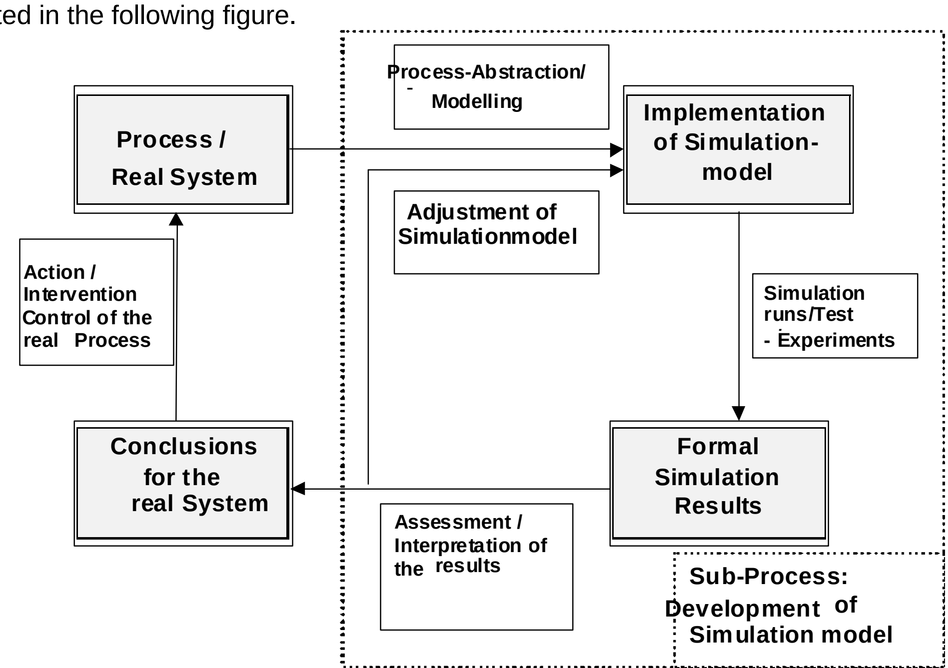

Fig. 11. General Simulation Process with Adjustment of Model and Application of Results

The simulation model comprising the potential Adjustment of Model with respect to its structure or parameters, drawing conclusions for the real process, e.g. to set control parameters or as one example for the Application of Results.

This global plan of developing a simulation model can be applied for the explanation of using simulation for the purposes of safety and security training and research. Education & Training is one of the fields of application, apart from other application for the use of simulators in addition to other areas.

The integration of the new simulation environment will provide the following benefits:

- Support development of and sustain student‘s mental model
- Improve students knowledge on processes /systems
- Gain experience and skills
- Create expertise and assess competency

For the development and implementation of integrated training scenarios the general scheme starting with the selection of performance standards and competencies for simulator training from STCW 95 rerquirements, followed by the definition of simulator training objectives and the corresponding design of the scenarios and the definition of assessment parameters and criterias. Assessment criteria for the field of safety and security training are not yet available as commonly proved standard. Therefore more detailed scientific investigations are needed and even for this task the integrated simulation environment will be of valueable support.

In principle the developed complex simulation environment also allows for its application in Design & Development processes for e.g. the validation of new constructionsor procedures. Another important application especially for safety and security issues is its use for Process-Management & Control tasks. In this way on the one hand simulation-based monitoring and control can be realised. On the other hand even decision support and predictions can be generated to ensure a certain level of safety where the risk is in the ALARP range (risk is as low as reasonable practicable).

8. SUMMARY AND CONCLUSION

In the frame of investigations into potential enhancements of maritime safety and security the use of simulation facilities were investigated. The Safety and Security Trainer, which can be used in the same scenario optional in 2D- and 3D-version, is a new simulation system developed by Rheinmetall Defence Electronics Bremen in corporation with the Maritime Simulation Centre Warnemünde at Wismar University, Department of Maritime Studies in Rostock-Warnemünde and assistance of World Maritime University Malmoe (Sweden).

The realized simulation system can be used as a standalone version for up to sixteen training stations and would be extendable according to the product system for training of entire ship’s crew. The SST is designed for potential integration into the existing simulators of the MSCW for training comprehensive scenarios in combination with the SHS, SES und VTS. The complex simulation platform with four full mission simulators enables the trainees to simulate the entire system ship and challenges to officers and crew.

On the other hand this new and enhanced simulation facility allow for in deep studies of the effects of the safety plans and to evaluate in more detail its effectiveness under different conditions and different courses of events by series of simulation runs.

ACKNOWLEDGEMENTS

The investigations and developments described here are mainly performed in a project for research and technical development funded by the German Ministry of Education and Research Berlin and surveyed by VDI Technology Centre Düsseldorf.

During the project also cooperation were established with World Maritime University. This cooperation covers e.g. aspects of international harmonisation of training requirements and standards.

The authors would like to thank Rheinmetall Defence GmbH as well as the cruiser company AIDA Cruises Ltd and the ferry companies TT-Line and Scandlines for their grateful assistance and cooperation to develop this new approach for integrated combined safety and security training scenarios.

REFERENCES

[1]. Adamski, A. J.; Westrum, R.: Requisite Imagination: ***The Fine Art of Anticipating What Might Go Wrong*.** In E. Hollnagel (Ed.), *Handbook of cognitive task design* (pp. 193–220). Mahwah, NJ: Lawrence Erlbaum Associates. 2003

[2]. Benedict, K.: ***Integrated Operation of Bridge-, Engine Room- and VTS-Simulators in the Maritime Simulation Centre Warnemuende*.** Conference on Simulation CAORF / JSACC 2000, New York, 3-7 July 2000, Proceedings Vol. 1.

[3]. Benedict, K., Böcker, T., Förster, W., Felsenstein, C. et al: ***Development of a technique for simulation of averting dangers*** (in German). Final Report "Integriertes Security System des InnoRegio-Verbundprojektes Maritime Allianz Ostsee". Fkz.: 03i0733B, Warnemünde, March 2006

[4]. Benedict, K.; Felsenstein, C.; Baldauf, M.: ***Integrated Training Concept including Manoeuvring simulation for Crews of Ship New buildings*** (in German) InnoRegio-Verbundprojektes "Ausbildung und Qualifikation für den Betrieb maritimer Systeme", Warnemünde, May 2004

[5]. Hollnagel, E*.:* ***The ETTO Principle: Efficiency-Thoroughness Trade-OFF – Why Things that go right go sometimes wrong****,* Ashgate 2009

[6]. IMO*.:* ***International management Code for the safe operation of ships and for pollution prevention (International Safety Management (ISM) Code)****.* Assembly Resolution A.741(18) adopted on 4 November 1993.

[7]. IMO***.: Guidelines for Formal safety Assessment (FSA) for use in the IMO rule-making process*.** MSC/Circ.1023, MEPC/Circ.392, 5 April 2002.

[8]. Meyer, V.; Benedict, K***.: Maritime safety and security environment mars - a unique way to make Ship operation safer.*** Paper at IMSF Conference 2007, August 20 – 24 2007 Busan / Korea

[9]. Oesterle, A. (2007): ***The new Simulator Safety and Security Trainer mars² and its use training*** *(*in German), in F. Ziemer (ed.): Moderne Konzepte in Schiffsführung und Schifffahrt. Schriftenreihe des Schiffahrtsinstituts Warnemünde: 2007,pp 105 – 118

[10]. Reason, J.T*.:* ***Managing the risks of organizational accidents****.* Aldershot, Ashgate, 1997

[11]. Sauer, T.: ***Contribution to Improvement of Safety & Security Trainer by user friendly Modelling of ships using Cruise Liner AIDAdiva.*** Diploma Thesis (in German), Dept. of Maritime Studies of Hochschule Wismar, June 2008

[12]. Valentin, T.; Steijaert, S.; Bijlsma, R. and Silva: ***Approach for Modelling of Large Maritime Infrastructure Systems,*** in Kuhl, Steiger, Armstrong and Joines (Eds.): Proceedings of the 2005 Winter Simulation Conference. Piscataway, New Jersey: Institute of Electrical and Electronics Engineers, Inc. pp 1577-1585

FUEL CELLS TECHNOLOGY IN MARINE AND NAVAL MEDIA

[1]LEO TERESA J., [2]GONZALEZ OSCAR, [2]GOMEZ-BEY ANA, [2]CADARSO LUIS, [2]NAVARRO EMILIO

[1]*Escuela Técnica Superior de Ingenieros Navales, Universidad Politécnica de Madrid, Spania,* [2]*Escuela Técnica Superior de Ingenieros Aeronáuticos, Universidad Politécnica de Madrid, Spania*

In this work, the possibility of implementing fuel cell technology in marine and naval media is considered. The potential application fields are revised and the main projects in each area that, at present, are being developed are discussed. Some already operative commercial applications such as submarines and small scale power generation are described. The main constraints from the environmental and technical points of view are analysed in order to elucidate the viability of future developments.

Keywords*:* fuel cells, marine applications, naval applications, environmental constraints

1. INTRODUCTION

Fuel cells are electrochemical devices that directly produce electricity from chemical energy of a fuel (Barbir 2005, Hoogers 2003). The fuel cell operating principle was discovered by Sir William Grove in 1839, although it seems that a Swiss scientist Christian F. Shoenbein independently discovered the very same effect at about the same time.

Inside the fuel cell an oxygen reaction reduction occurs between hydrogen and oxygen giving rise to water and heat. The electrons released in the reaction are driven by an external circuit producing electricity. Then, fuel cells are in some aspects similar to batteries. They have an electrolyte, a cathode and a anode, and generate direct current electricity through electrochemical reactions. However, unlike batteries, fuel cells require a constant supply of fuel and oxidant. Typically hydrogen is used as fuel. Pure hydrogen, present in a mixture of gases or directly hydrocarbons such as methane or natural gas for example, could be used. Oxidant is pure oxygen or air.

Only if a fuel cell works with pure hydrogen as a fuel, water and heat are the unique products. That means they are cleaner than conventional generators, in which, for example, carbon dioxide is always an exhaust gas. Moreover, a typical conventional generator efficiency is about 15-20%, whereas the efficiency of a fuel cell is about 30-40%, or even more than 70% when cogeneration is used. This higher efficiency is due to energy conversion, contrary to that occurs in conventional generators, is done in a single step without burning neither involving any moving parts. Therefore fuel cells can be more efficient, quieter, with less maintenance and more durability.

It is known that the global energy availability and sustainable development is a big challenge and big efforts have to be undertaken in all energy consumption sectors and this technology, characterised by particularly high electrical efficiencies and low emissions, would help to reduce carbon dioxide emissions.

Normally fuel cells produce low voltages and they must be assembled into a fuel cell stack to reach the power required in usual applications. Then, fuel cells are by their nature, modular devices and their power can go from microwatts to megawatts, which makes them useful in a variety of applications: automotive, marine, naval, space or stationary electricity generation have already been dated but also portable applications are possible.

A fuel cell stack is constituted by:

- *Bipolar plates*: they are electrical conductive parts which put in contact the anode of one cell with the cathode of the next cell. The first cell and the last one have end plates instead bipolar plates, and they are in contact with the current collectors. They are usually made of stainless steel or graphite.
- *Mass flow channels*: they are ducts inside which fuel and oxidizer flow. Their walls are the bipolar plates.
- *Gas diffusions layers*: are porous media situated between the bipolar plate and the catalyst layer.
- *Catalyst layers*: they are the zones where the electrochemical reactions take place.
- *Electrolyte*: it is a substance which carries electrically charged particles from one electrode to the other of the same cell.
- Another parts of a fuel cell are seals, current collectors or some interconectors.

In the case of a single fuel cell, the most common constituents, shown in Fig. 1, are almost the same of a fuel cell stack.

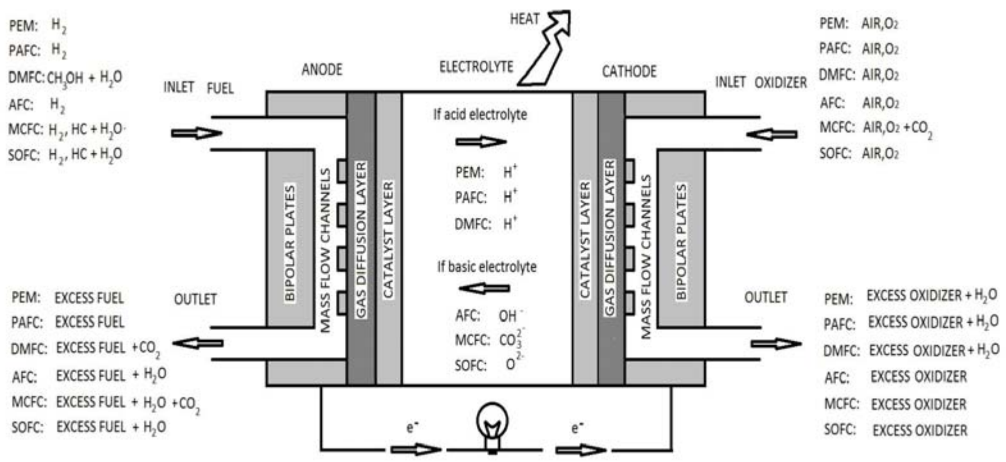

Fig. 1. Schematic representation of a single fuel cell with indication of its main components. The flows corresponding to the different fuel cell types attending to the electrolyte used are represented

There are several types of fuel cells, as it is presented next, but in a general way they can be divided into two general groups, those having an acid electrolyte and those having an alkaline one. If the electrolyte has acid behaviour, the protons travel across of it, and if not, there are the negative ions which cross the electrolyte.

The processes taking place inside a fuel cell with acid electrolyte begin with hydrogen flowing through the anode channels, as well as oxygen through the cathode channels; the flows are addressed to the gas diffusion layers. When they reach the catalyst layers, electrochemical reactions, including all the intermediary steps, happen. Then, proton transport through proton-conductive electrolyte occurs from the anode to the cathode. Meanwhile electrons are driven through electrically conductive cell components to the external circuit and return to the fuel by the cathode side, where react with oxygen and protons to produce water and heat.

So, the electrochemical reactions in a hydrogen fuel cell happen simultaneously on both sides of the electrolyte, the anode and the cathode. The basic fuel cell reactions are:

At the anode: $H_2 = 2H^+ + 2e^-$

At the cathode: $1/2\ O_2 + 2H^+ + 2e^- = H_2O$

Overall: $H_2 + 1/2\ O_2 = H_2O$

The most usual classification of fuel cells is made attending to the type of electrolyte they use. These types are summarized in Fig. 1 and described below:

- *Alkaline fuel cells* (AFC) use KOH as the electrolyte. Operation temperatures go from less than 120ºC to 250°C. They have been used in the space program (Apollo and Space Shuttle) since the 1960s.
- *Polymer electrolyte membrane or proton exchange membrane fuel cells* (PEM), use a thin proton conductive polymer membrane as the electrolyte, typically a perfluorosulfonated acid polymer with operating temperatures between 60 and 80°C, or an acid doped polybenzimidazole for temperatures above 120ºC (HTPEM). PEM fuel cells are a promise for automotive applications, but can also be used for small-scale distributed stationary power generation, and for portable power applications. There is a type of PEM directly fed with methanol which is called direct methanol fuel cell (DMFC).
- *Phosphoric acid fuel cells* (PAFC) use concentrated phosphoric acid as electrolyte. Usually a SiC matrix is used to retain the acid. Operating temperatures are between 150 and 220°C. Hundreds of 200 kW PAFC units have been installed all over the world for stationary electricity generation.
- *Molten carbonate fuel cells* (MCFC) have the electrolyte composed by a combination of alkali (Li, Na, K) carbonates in a ceramic matrix. Operating temperatures lie between 600 and 700°C where the carbonates form molten salt with high conductivity. These fuel cells are suitable for stationary power generation applications.
- *Solid oxide fuel cells* (SOFC) use a solid electrolyte, usually Y203-stabilized ZrOi (YSZ). The operating temperatures are the higest of all the fuel cells, from 800 to 1000°C. These fuel cells are also for stationary power generation applications, although smaller units are being developed for auxiliary power and portable power units.

There is also a hybrid between fuel cell and battery known as *semi-fuel cell* because one of the electrodes, the anode, is solid, made of aluminium (Al), and no feeding is neccessary, whereas hydrogen peroxide (HP) is continuously added to maintain the oxidant concentration in the alkaline electrolyte (Hasvold, 1999). Reaction equations are as follows :

At the anode: $Al + 4OH^- = Al(OH)_4^- + 3e^-$

At the cathode: $H_2O_2 + 2e^- = 2OH^-$

Overall: $2Al + 3H_2O_2 + 2OH^- = 2\ Al(OH)_4^- + 6e^-$

2. THE FUEL CELLS IN THE FRAME OF ENVIRONMENTAL CONSTRAINTS

Europe's energy supply is today characterized by structural weaknesses and geopolitical, social and environmental shortcomings, particularly as regards security of supply and climate change. Energy is a major determinant of economic growth and these deficiencies can have a direct impact on EU growth, stability and the well being of Europe's citizens. Energy supply security, mitigating climate change and economic competitiveness are therefore main drivers for energy research, within the context of sustainable development (Project Synopsis, 2004).

Broadly, sustainability encompasses meeting the needs of the present without compromising the needs of the future. Fuel cells can make a major contribution to environmental and economic sustainability in the following ways:

- Being zero emissions (apart from water) if pure hydrogen is used.
- Being zero emissions on a life cycle basis.
- Reducing point of use emissions, including CO_2, NO_x, SO_x and particulate matter for a range of carbon based fuels.
- Reducing noise and ambient air pollution.
- Increasing the efficiency of electricity and heat generation.
- Contributing to economic growth and wealth creation.
- Contributing to job creation.

EU funded research in the area of fuel cell systems is aimed at reducing the cost and improving the performance, durability and safety of fuel cell systems for stationary and transport applications, to enable them to compete with conventional combustion technologies. This will include materials and process development, optimization and simplification of fuel cell components and sub-systems as well as modelling, testing and characterization. The long-term goal is to achieve commercial viability for many applications by 2020 (Project Synopsis, 2004).

As said in the previous section, fuel cells are intrinsically clean and very efficient (up to double the efficiency of internal combustion engines) and capable of converting hydrogen and other fuels to electricity, heat and power. They can also be sited close to the point of end-use, allowing exploitation of the heat generated in the process (Hoogers, 2003).

The next twenty years will be critical, both for climate change and for security of supply. In this period, irreversible and catastrophic damage may be done to the climate. Over this period also, the costs of dependence on very few large producers of energy might also become painfully apparent. Europe can meet these challenges only through the application of technology and the adoption of difficult changes to social values and behavior.

3. PRESENT AND FUTURE OF FUEL CELLS

At present costs, large-scale use of fuel cells is not competitive. Difficult, but achievable advances could change this. The fuel cell is not a comprehensively disruptive technology; it can be seen as a replacement for conventional power trains, generators or batteries.

One of the characteristics of fuel cell systems is that their efficiency is nearly unaffected by size. This means that small, relatively high efficient power plants can be developed, thus avoiding the higher cost exposure associated with large plant development. As a result, initial stationary plant development has been focused on several hundred kW to low MW capacity plants. Smaller plants (several hundred kW to 1 or 2 MW) can be sited at the user's facility and are suited for cogeneration operation, that is, the plants produce electricity and thermal energy (combined heat and power CHP). Larger, dispersed plants (1 to 10 MW) are likely to be used for dispersed electric-only use. The plants are fueled primarily with natural gas. Once these plants are commercialized and price improvements materialize, fuel cells will be considered for large base-load plants because of their high efficiency.

Since the late 1980s, there has been a strong push to develop fuel cells for use in light-duty and heavy-duty vehicle propulsion. A major drive for this development is the need for clean, efficient cars, trucks, and buses that can operate on conventional fuels (gasoline, diesel), as well as renewable and alternative fuels (hydrogen, methanol, ethanol, natural gas, and other hydrocarbons). With hydrogen as the on-board fuel, such vehicles would be zero emission vehicles. With on-board fuels other than hydrogen, the fuel cell systems would use an appropriate fuel processor to convert the fuel to hydrogen, yielding vehicle power trains with very low emissions and high efficiencies. Further, such vehicles offer the advantages of electric drive and low maintenance because of the few critical moving parts.

It is estimated that in about 30 years, the fleets of developed countries (currently over 750 million units, including cars, buses and trucks) will have more vehicles with an electric motor powered by fuel cells than powered by internal combustion engines (Project Synopsis, 2004).

However, currently the main problem in driving this technology in the transport sector is the high cost of manufacturing, fuel quality and size of the unit. The research in this area seems to have opted to use methanol as a fuel source and use oxygen from the air. This could eliminate the fuel reforming process.

Because of the modular nature of fuel cells, they are attractive for use in small portable units; the continued development of fuel cells has contributed to the development of many mobile electronic devices. The miniaturization of fuel cells offers serious advantages over conventional batteries, such as increased operating time, reduced weight and ease of reloading.

When portable fuel cell systems are discussed in public, what often springs to mind first are applications where fuel cells compete with batteries. Well-known examples are cellular phones, laptop computers, camcorders, and similar electronic devices. For these applications, the following parameters to be given on the batteries will be necessary to consider:

- Low temperature operation.
- Availability of fuel.
- Quick Activation.

Whether these applications will be successful or not depends on several considerations, including if:

- Fuel cell systems can win the race against advanced battery technology such as lithium ion secondary batteries.
- They can be made small enough to fit inside portable electronic devices.
- The price is attractive enough.
- The fueling problem can be solved.

The fueling problem means that replacement fuel cartridges or similar devices must be readily available and must be more convenient to handle than, say, a second battery pack for a laptop computer. Also, the overall fueling process must have clear advantages over recharging from a power socket, which is now readily available almost everywhere.

Another consideration is safety. It may be doubted that airlines will allow such cartridges or tanks to be taken on-board, particularly where flammable liquids are involved.

It is expected that military applications represent a significant market for fuel cell technology. The efficiency, versatility, extended running time and quiet operation make fuel cells a system tailored to the needs of the military. Fuel cells could provide power generation solution valid for portable military equipment land or sea (U.S. Congress, 1986).

The miniature fuel cells could offer great advantages over conventional solid bulky batteries and also eliminate the problem of recharging.

In the same vein, the efficiency of fuel cells for transportation would be reduced dramatically the need of fuel needed for the maneuvers. The vehicles would be able to travel long distances or work in remote areas for longer and the number of support vehicles, personnel and equipment needed in the combat zone could be reduced. Since 1980 the U.S. Navy has used fuel cells in vessels for the study of deep sea and unmanned submarines (Hirschenhofer, 1998).

In space applications, the combination of light weight, the supply of electricity and heat without significant noise and vibration, and with the added benefit of drinking water production, gave the fuel cell with considerable advantages over other alternative energy sources.

4. MARINE AND NAVAL APPLICATIONS OF FUEL CELLS

Due to their efficiency and environmental advantages seen before, fuel cells are suitable as marine or naval propulsion systems. Nowadays, several countries and companies are involved in development projects consisting in the installation of fuel cells in different types of vessels. All of them are secondary propulsion systems, so the challenge is to achieve a fully electric powered ship using fuel cell technology. This is considered to be achievable in 10 years time. However, there are some challenges to overcome. Moreover, there are already operative some commercial applications (submarines and small scale power generation).

The current framework regarding marine environmental issues helps the implementation of fuel cell technology on ships. Air pollutant emissions from ship engines are covered by Annex VI of the Marine Pollution Convention, MARPOL 73/78, of the International Maritime Organization (Adamson, 2005). The revised Annex VI enters into force on 1st July 2010. According to this new regulation, some regions are imposing Sulphur Emission Control Areas (SECAs), and in the Baltic and North Sea NO_x free zones have been introduced. As well, the United States are looking to reduce pollution within 200 NM of its coastline. Therefore the trend will be the imposition of taxes and penalties.

***Fig. 2. Hydra boat on the Rhine river in Germany* (*http://hydrogencommerce.com*)**

On the other hand, the fossil fuels decline which implies higher and unforeseeable prices, and geopolitical dependency, among other problems, is another potential ally for the fuel cell technology. To comply with these regulations new energy sources must be developed. The current lead technology in the search of substitute energy sources is the LNG (liquefied natural gas) burnt in thermal engines, being the fuel cells experimental at this stage.

As the fuel cell technology is new, there is a lack of regulations and standards regarding marine applications. The future IGF code (International Code of Safety for Gas-fuelled Engine Installations in Ships) will not cover the fuel cell systems. Bureau Veritas is developing guidelines for the design, manufacture, performance and maintenance of marine fuel cell systems (De Jong, 2009).

Some of the fuel cell advantages are very useful for marine applications (Georgescu, 2006). Apart from low vibration, noise and emissions, it is remarkable the high efficiency (up to 50%), the fact that a fuel cell system has fewer moving parts than a conventional engine, and also the different types of fuels which can be used. Some of these characteristics make the fuel cell technology more comfortable for the crew. If it is not possible to use hydrogen directly, the alternative is to obtain it through a reforming system from other fuels such methanol, ethanol, natural gas, or even diesel, which has been tested by the US Coast Guard, using NATO F-76 diesel fuel, worldwide available. Besides, fuel cells have a high operational flexibility, being capable, for example, of varying a 10% of the output power in only one second. Finally, the high temperature fuel cells (SOFC, MCFC) allow the combined production of heat and electricity (CHP).

Nevertheless, there are disadvantages in the use of fuel cells on ships. The main are: high cost, low power density, long endurance under marine conditions not proven, safety issues (hydrogen flammability and high pressures; methanol toxicity), and low availability of hydrogen as a fuel (Ingeniería Naval, 2009). Most of them have real possibilities of being mitigated. The first three disadvantages are expected to be solved with the current experimental projects. They are due to the lack of maturity of the fuel cell technology: few manufacturers, little production, and the lack of regulations and hydrogen infrastructure. Current projects running experimental fuel cell systems on ships are helping to grow up the marine fuel cell systems, improving the reliability under the hard marine conditions, and helping to reduce the costs, which are between 3,000 €/kW and 5,000 €/kW due the expensive materials used in the catalysts and electrolytes. It is an unknown if a fuel cell can maintain at sea the same operational life that can reach onshore. The high capital cost of the fuel cell is already compensated by the lower fuel consumption and the saving in environmental taxes.

The hydrogen has a low energy density that implies the need of storing the hydrogen at high pressures. This fact, together with its flammability, results in specific safety issues on a ship, such as ventilation, additional safety and fire detection devices and fire fighting procedures.

High temperature fuel cells, SOFC and MCFC have their main applications in offshore ships, while low temperature (PEM, AFC) are more suitable for boats and submarines. The reason is the great size of high temperature fuel cells and the time required (few days) to reach the maximum temperature (and maximum power) and to cool down the system. As a result of the analysis of the different experimental projects that are currently in development, or have been launched in recent years, the fuel cell marine applications could be divided into the following groups:

- *Propulsion system for ships*. The current developments are focused on coastal and onshore ships, suporting conventional engines. The intention is to achieve a fully fuel cell powered, offshore ship in ten years time. The high temperature fuel cells, such as SOFC or MCFC are very suitable for this application allowing, as well, a combined production of heat and electricity (CHP).
- *Auxiliary Power Units* (*APUs*). Using a reforming system or not, fuel cells could be an environmental and cost effective option to substitute the conventional APUs in the future. MCFC, SOFC and PEM fuel cells have been used in several projects.
- *Main propulsion system for boats and small vessels*. There are already some developments running, particularly in Germany, Fig. 2. The low temperature PEM fuel cells are very suitable for this application, although AFC systems have been also used. There are some hybrid systems, which combine fuel cells and batteries, and some of them even have rechargeable devices based on solar cells.
- *Small scale power generation*. There is already a DMFC (Direct Methanol Fuel Cell) commercial system for sailing yachts, but these devices could use hydrogen in the future as PEM fuel cells.
- *Submarines*. Military research is also leading the fuel cell technology. The evidence is the great development concerning AIP (Air-independent Propulsion), used as a support system in some non-nuclear submarines to avoid operating without the need to access atmospheric oxygen. This capability increases the autonomy and, together with the silent operation of the fuel cell, improves the tactical features of the submarine (Brey, 2005). Several German submarines are already in service with different fleets, using a PEM based AIP, and there are more projects to come soon (Jane's, 2007-08).
- *Unmanned Underwater Vehicles* (*UUVs*). There are commercial systems based on low temperature Aluminum Oxygen fuel cells with applications in oil and gas exploration, fisheries and military applications, like mine reconnaissance.

Some examples of real projects, both civil and military, are detailed in the following paragraphs.

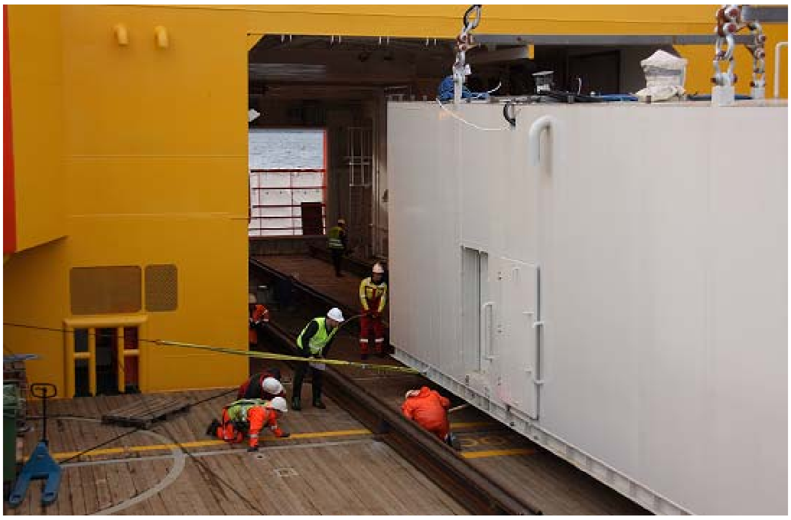

***Fig. 3. Viking Lady fuel cell lifted on board* (*http://vikinglady.no*)**

The Viking Lady, within the FellowSHIP project, operative since December 2009, is probably the most important project involving fuel cell propulsion in large ships (The Naval Architect, January 2010). It is a working ship supplying oil platforms in the North Sea, with a hybrid fuel cell/LNG system which provides electrical power and heat for the crew

accommodation block. Fuel cell technology of this power size, 320 kW MCFC, Fig. 3, has never been installed before in merchant vessels and the highly innovative project is unique on a world scale. FellowSHIP is being project managed by Det Norske Veritas (DNV), and has been designed and integrated by Finnish manufacturer Wärtsilä. Other partners are Eidesvik and the Norwegian Research Council. Operators say that fuel costs are 3,500 €/day less, apart from saving in NO_x taxes, while the capital costs are only 10% higher. The system has met efficiency and environmental goals, and is being very useful to develop the new regulations in marine fuel cells. The next step is to produce a 1 MW fuel cell reducing the size, to make it commercially viable. On the other hand, the U.S. Navy has been investigating since nineties the use of fuel cells for ship-board power with hydrogen sourced from diesel fuel (Allen, 1998).

Wärtsilä, within the Methapu project, is also developing an Auxiliary Power Unit (APU) (The Naval Architect, February 2010). It is a SOFC 20 kW. The project is funded by the European Union with €1 million. The aim is to validate the use of methanol as a fuel in cargo ships. Other partners are Wallenius Marine, Lloyd's Register, The University of Genoa and DNV.

Regarding small boat projects, Alsterwasser is a boat which sails on Alster Lake (Hamburg) with a main propulsion system consisting of a battery and hybrid system (2x50 kW PEM), with hydrogen storage (Ingeniería Naval, 2009). In addition, Bureau Veritas is working on a Dutch project, HHHT (Hydrogen Hybrid Harbor Tug), with hybrid diesel/hydrogen (2x100 kW PEM), so that it is expected a 70% higher efficiency and substantial reduction in emissions. On the other hand, Hydra is the first fuel cell boat in Germany (5 kW AFC), certified to carry 22 passengers on the Rhine in Bonn.

With regard to the small scale power generation, the German company SFC has developed a commercial methanol fuel cell for sailboats, to provide electrical current to appliances on board, running with fuel cartridges. The charging capacity ranges vary from 600 to 2,160 watt hours per day. The French company Max Power has developed similar products.

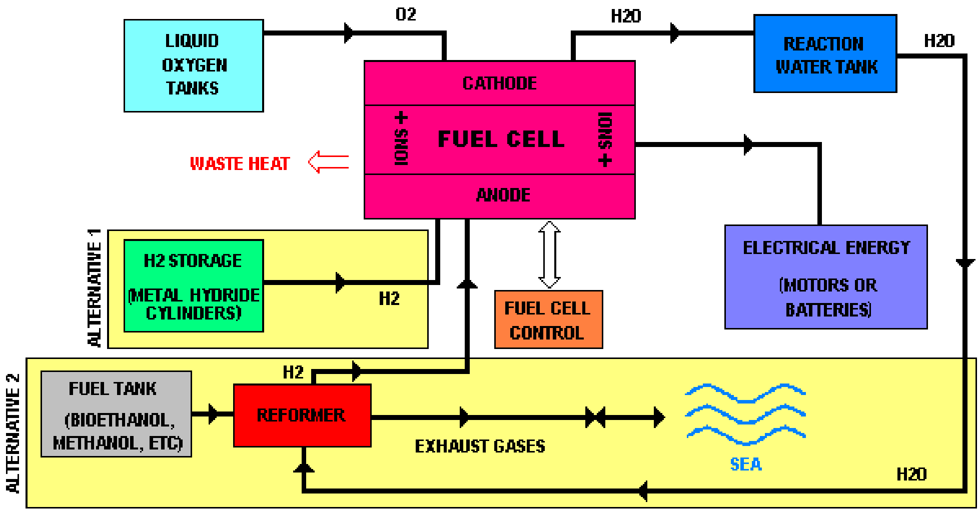

Fig. 4. Two typical alternatives for an AIP system using fuel cells

The German shipyard HDW has developed with its partner Siemens an AIP system based on a PEM fuel cell, which is in service with the models U212 (Germany and Italy) and U214 (Greece and South Korea), (Weaver, 2003 and Hammerschmidt, 2006). The rated power is 2x120 kW for the second generation. The fuel is hydrogen stored in cylinders and the main propulsion system consists of conventional diesel engines. As well, the Spanish shipyard Navantia, together with UTC and Abengoa, is currently building a series of four submarines for the Spanish Navy. They will include an AIP based on a PEM fuel cell, and using bioethanol as fuel. A special processor will transform the bioethanol in hydrogen with a high level of purity. The main propulsion system consists of conventional diesel engines. The AIP is used in low power maneuvers. Two possible alternatives for an AIP system are shown in Fig. 4.

Finally, there are some examples of Unmanned Underwater Vehicles (UUVs), particularly based on Aluminum Oxygen fuel cells. The Norwegian Defence Research Establishment (FFI) started in 1995 the Hugin Project in cooperation with Norwegian industry. The Hugin II has been in routine use by the Norwegian Underwater Intervention AS (NUI), which has operated the UUV for high-precision seabed mapping down to a water depth of 600 m (Hasvold, 1999 and Hasvold,2006). Today there is a complete Hugin family built by Kongsberg, Fig. 5. The American Manufacturer C&C Technologies produced the first commercially operated UUV for oil and gas exploration. The payload consists of several sensors (camera, sonar, data link, etc). An UUV powered by a 4 kW PEM fuel cell system was completed by the Japan Agency for Marine-Earth Science and Technology (Tsukioka, 2005). The fuel cell system generates electric power for the control electronics and propulsion system.

Fig. 5. Hugin 4500 UUV ready to operate **(*www.km.kongsberg.com*)**

To achieve all the aims of these projects there is a necessity, in the long term, of a hydrogen-based economy. Perhaps the first country in reaching this status will be Iceland, where the government is intending to substitute fossil fuels by hydrogen produced from thermal energy, available in Iceland at low cost, with a six-phase plan (Hordeski, 2009). Iceland may start with methanol powered PEM vehicles and vessels. The fishery fleet is a major fossil fuel consumer in that country and it is proposed to substitute diesel engines for fishing vessel power supply with fuel cell technology. These measures are widely supported by the population. Phase 4 will demonstrate PEM fuel cell boats. Phase 5 will replace the entire fishing fleet with fuel cell powered boats and in the next phase, Iceland will sell hydrogen to Europe and elsewhere. The last phase is expected to be finished by 2030-2040.

5. CONCLUSIONS

From the developments in course and taking into account the commercialized products of fuel cells in marine and naval applications, it can be concluded that this is a promising technology in this area.

Although durability tests must be checked, experimental projects show that fuel cells give rise to low emissions in the marine medium. The apparent problem of costs will probably disappear due to that high oil costs are foreseen and also due to the savings obtained from emissions reduction.

In addition, although volume reduction of fuel cell systems must be achieved, the weight does not seem to represent a big problem in marine systems, and to centralize hydrogen suppliers in harbours seems to be feasible.

REFERENCES

[1]. Adamson K. – ***Fuel cells and marine applications,*** Fuel Cell Today 2005
[2]. Allen S., Ashey E., Gore D., Woerner J. et al. – ***Marine applications of fuel cells,*** Naval Engineers Journal , pp.93-106, January 1998
[3]. Barbir F. – ***PEM Fuel Cells Theory and Practice,*** Elsevier Academic Press, 2005, ISBN 0-12 078142-5

[4]. Brey J. ***Sistemas de Propulsión Anaerobios basados en Pilas de Combustible,*** Seminario sobre tecnologías de conversión de potencia para el sector de las Energías Renovables. Sevilla, 12 de Mayo de 2005
[5]. De Jong, G. ***Guidelines for the safe application of fuel cell systems on ships***, in Annual Marine Propulsion Conference, 2009
[6]. Georgescu C., Mamut, E. – ***A study concerning the possibilities for using fuel cell systems for maritime propulsion,*** Romanian Journal of Physics., Vol. 51, Nos. 1–2, P. 49–56, Bucharest, 2006
[7]. Hammerschmidt A. E. — ***Fuel cell propulsion of submarines,*** Paper presented at Advanced Naval Propulsion Symposium 2006, October 30-31, Arlington, VA, USA
[8]. Hasvold Ø., Johansen K. H., Mollestad O., Forseth S. et al. – ***The alkaline aluminium/hydrogen peroxide power source in the Hugin II unmanned underwater vehicle,*** Journal of Power Sources, 80, pp.254-260, 1999
[9]. Hasvold Ø., Størkersen N. J., Forseth S., Lian T. – ***Power sources for autonomous underwater vehicles,*** Journal of Power Sources, 162, pp.935-942, 2006
[10]. Hirschenhofer J.H., Stauffer D.B., Engleman R.R. and Klett M.G. – ***Fuel Cell Handbook***, U.S. Department of Energy, Office of Fossil Energy, Federal Energy Technology Center, November 1998
[11]. Hoogers G. - ***Fuel Cell Technology Handbook***, CRC Press LLC, 2003, ISBN 0-8493-0877-1
[12]. Hordeski, Michael Frank ***- Hydrogen & Fuel Cells. Advances in Transportation and Power,*** The Fairmont Press, 2009, ISBN 0-88173-561-2
[13]. Jane's Fighting Ships. Edition 2007-2008. ISBN: 978-0-7106-2799-5. Coulsdon: Jane's Information Group
[14]. ***Las células de combustible como opción para la propulsión,*** Ingeniería Naval, Octubre 2009, pp.59-60
[15]. Project Synopsis, Sixth Framework Programme, ***European Hydrogen and Fuel Cell Projects***, European Comission, Directorate-General for Research, Directorate J – Energy, Unit J2 – Energy production and distribution systems, 2004, ISBN 92-894-8003-3
[16]. Tsukioka S. – ***The PEM fuel cell system for autonomous underwater vehicles,*** Marine Technology Society Journal, Volume 39, Number 3, Fall 2005 , pp. 56-64(9)
[17]. U.S. Congress, Office of Technology Assessment, ***Marine Applications for Fuel Cell Technology—A Technical Memorandum****,* OTA-TM-O-37 (Washington, DC: U.S. Government Printing Office, February 1986)
[18]. ***Viking Lady steals the limelight,*** The Naval Architect, January 2010, pp.54-56
[19]. ***Wärtsilä and partners develop methanol fuel cell,*** The Naval Architect, February 2010, pp.58
[20]. Weaver G., Barrett S. – ***Marine applications of fuel cell technology,*** Fuel Cells Bulletin, January 2003, pp. 56-64

ADVANCED ANALYSIS TOOLS OF ENERGY CONVERSION SYSTEMS

[1]MEMET FEIZA, [1]STAN LIVIU

[1]*Constanta Maritime University, Constanta, Romania*

In accordance with increased global demand for a clean and efficient sea transport, the marine energy sector became lately very sensitive to this subject.
Energy conversion systems on board the ships should produce energy – intensive products at sea. In order to analyse and after that to improve such systems, are presented important tools at the hand of marine energy specialists: exergoeconomic analysis and exergoenvironmental analysis. By using the both methods is possible to reduce costs in energy conversion systems and to assess environmental impacts, in order to optimise energy conversion systems from economic and ecological point of view.

Keywords: energy conversion systems, cost, environment

1. INTRODUCTION

Our society and most the academicians are interested in the relation established between our environment and the human activity. It is very important to study the way in which we live and the environment has the capacity to receive and assimilate the waste produced by mankind. The assessment of the environmental impact related to the actions of our civilization involves technical, economic and social studies.

The exergoeconomic (thermoeconomic) analysis was introduced in order to support a thermal and economical analysis for thermal systems. This analysis consider the quality of energy (exergy) by allocating production costs to different products produced during a process. It is possible an optimisation of the entire studied system, not only of the specific variables of each subsystem.

This analysis was revealed using the Second Law of Thermodynamics combined with exergetic analysis (Tsatsaronis, 1985). It is allowed a better measurement of the lost energy quantity in relation to the amount of supplied energy under the form of energy resource. Also, it is offered a more accurate possibility of evaluation of the quality or loss on thermodynamic basis.

So, the objectives of an exergoeconomic analysis are:

I) to evaluate separately the costs of each product generated by a system able to deliver more than one product;

II) to understand the cost formation process and the flow of costs in the system;

III) to optimize specific variables in a single component (to optimize the entire system).

Energy conversion systems should be improved in order to reduce their environmental impact. Exergoenvironmental analysis is a new tool, which combined with the exergoeconomic analysis lead to the identification of the parts of a system that ask economic and ecological optimization, due to the fact that environmental impacts of each component of conversion systems should be correlated with energy and material streams. Figure 1 decipts the relation between different types of advanced thermodynamic analysis.

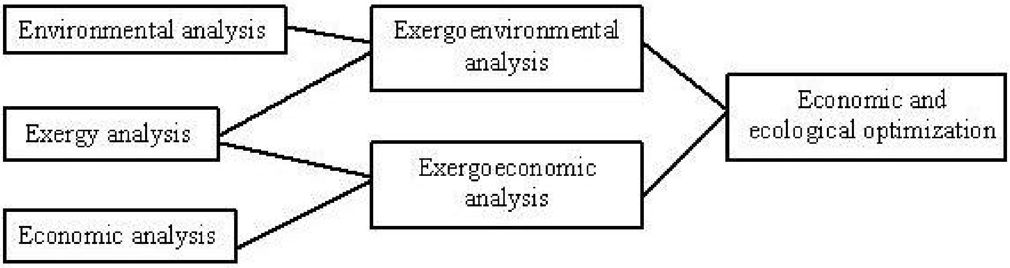

Fig. 1. Types of analysis involved in optimization of energy conversion systems.

2. EXERGY AND EXERGY ANALYSIS

Exergy is defined as being the maximum amount of shaft work obtained from a stream of matter, heat or work as it comes to equilibrium with a refernce environment.

The exergy is conserved for reversible processes of the system and the environment, while exergy is destroyed during irreversible processes. Exergy analysis related to power plants reveals thermodynamic imperfections known as exergy destructions, which are wasted work or wasted potential for work production. Similar to energy, exergy also can be transferred or transported across the boundary of a system. For every kind of energy transfer/transport exists a corresponding exergy transfer/transport. Exergy analysis considers thermodynamic values of heat and work. The exergy transfer related to the shaft work is equal to the shaft work. The exergy transfer related to the heat transfer is based on the temperature at which it occurs in relation to the temperature of the environment.

Its general equation is written as:

$$Ex = (H - H_0) - T_0(S - S_0) \tag{1}$$

In order to apply the exergy analysis in a process, is used the block method, where the block is the process, the equipment or a combination of these (see Figure 2).

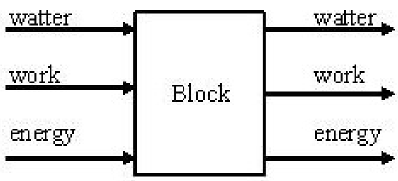

Fig. 2. Representation of a block.

Exergy analysis offers a more accurate view on the real efficiency of a process. More specific, exergy analysis allows the identification the parts of a plant were efficiency improvements are asked. This is why exergy analysis is superior to the energy analysis. Table 1 shows the exergy content of some forms of energy.

Table 1: Clasification of different forms of energy

Form of energy	Quality of energy	Exergy content (%)
Potential energy Kinetic energy Electrical energy	EXTRA SUPERIOR	100 100 100
Nuclear energy Sunlight Chemical energy Hot stream	SUPERIOR	~100 95 95 60
Waste heat	INFERIOR	5

On a thermodynamic basis, the exergetic efficiency (ε) offers a real measure of the performance of an energy conversion system. The exergy rate balance, given belows, implies the resource (*F*), the product (*P*), the destruction (*D*) and the loss (*L*):

$$\varepsilon = 1 - \left\{ \left(\dot{E}x_s + \dot{E}x_L \right) / \dot{E}x_F \right\} \tag{2}$$

$$\dot{E}x_F = \dot{E}x_P + \dot{E}x_D + \dot{E}x_L \tag{3}$$

Exergy is destroyed because of the irreversibilities happen within the control volume, while exergy is lost from the control volume via stray heat transfer material stream vented to the surroundings, etc.

The already mentioned exergetic efficiency indicates the percentage of the fuel exergy supplied to a control volume to be found in the product exergy. The missing percentages from 100% to the value of exergetic efficiency means fuel exergy wasted in the control volume, under the form of exergy destruction and exergy loss.

3. EXERGY COST

At the entrance of a real process the exergy is always higher because of destructions and losses taking place. That is why the exergetic cost of the product will always be higher than the resource. Is defined the unitary exergetic cost (*k*) as the relation between the exergetic cost flow (*Ex**, in kW) and the exergy flow (*Ex*, in kW):

$$k = \frac{Ex^*}{Ex} = 1 + \frac{Loss + Destruction}{Product} \tag{4}$$

The following five propositions were enunciated in order to estimate exergetic costs of the flows related to equipments (Moreira, 2007)

P_1 – the exergetic cost is a conservative property:

$$\sum Ex_{in}^{*} - \sum Ex_{out}^{*} = 0 \tag{5}$$

P_2 (the resource rule) – the exit unitary exergetic cost related to a general system is equal with the inlet one (see Figure 3):

$$k_1 = k_2 \Leftrightarrow \frac{Ex_1^*}{Ex_1} = \frac{Ex_2^*}{Ex_2} \tag{6}$$

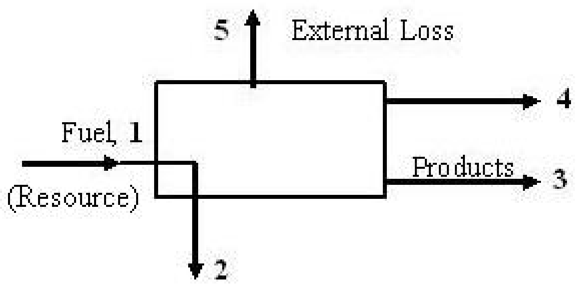

Fig. 3. A general system.

P_3 (the product rule) – the unitary exergetic cost is the same for each product of a general system:

$$k_3 = k_4 \Leftrightarrow \frac{Ex_3^*}{Ex_3} = \frac{Ex_4^*}{Ex_4} \tag{7}$$

P_4 – for no value of the externall loss, the unitary exergetic loss is zero:

$$k_5 = 0 \Leftrightarrow \frac{Ex_5^*}{Ex_5} = 0 \tag{8}$$

P_5 – in the absence of external value, for the system inlet, the exergetic cost flow is the same with exergy flow:

$$Ex_1^* = Ex_1 \tag{9}$$

4. EXERGOENVIRONMENTAL ANALYSIS

This type of analysis is usualy developed on the following levels:
- exergy analysis of the energy conversion process;
- assessment of environmental impacts using LCA (Life Cycle Assessment), an analysis dealing with all the effects on the environment of a product during its life, “from cradle to the grave” (from the production to the consumption and recycling, taking into consideration even the transport process);
- endowment of environmental impacts to exergy streams in the process;
- calculation of exergoenvironmental variables and development of exergoenvironmental evaluation.

It is defined the specific environmental impact rate of each material and energy stream (b_j), as being the ratio between the environmental impact rate ($\dot{B}_j$) and the exergy rate ($\dot{Ex}_j$) of the j th stream:

$$b_j = \frac{\dot{B}_j}{\dot{Ex}_j} \tag{10}$$

The environmental impact balance for a system with *k* elements is written as:

$$\sum \dot{B}_{j,k,in} + \dot{Y}_k = \sum \dot{B}_{j,k,out} \tag{11}$$

It is stated that together with an exergy flow through the considered system, there is also a flow of environmental impacts.

In the last equation, the term $\dot{Y}_k$ means the facility related environmental impact rate, which given by environmental impacts related to activities like construction ($\dot{Y}_k^{CT}$), operation and maintenance ($\dot{Y}_k^{O+M}$) and disposal ($\dot{Y}_k^{Di}$):

$$\dot{Y}_k = \dot{Y}_k^{CT} + \dot{Y}_k^{O+M} + \dot{Y}_k^{Di} \tag{12}$$

If the exergy analysis gives the possibility to evaluate the exergy destruction rate in the k-th component of a system, the exergoenvironmental analysis permits the assessment of the environmental impact rate, $\dot{B}_{D,k}$, related to this kind of exergy rate, with the help of the specific environmental impact of the exergetic fuel of the k-th component, $b_{F,k}$:

$$\dot{B}_{D,k} = b_{F,k} \cdot \dot{Ex}_{D,k} \tag{13}$$

The relative difference between the specific environmental impact of the exergetic product, respectively fuel, indicates the potential of diminishing the environmental impact related to that component:

$$r_{b,k} = \frac{b_{P,k} - b_{F,k}}{b_{F,k}} \tag{14}$$

The exergoenvironmental factor is useful for the comparison of pollution sources in a component:

$$f_{b,k} = \frac{\dot{Y}_k}{\dot{Y}_k + \dot{B}_{D,k}} \tag{15}$$

5. CONCLUSIONS

The development of maritime transport is related to the increasing energy demand, mainly fossil fuels.

Marine conversion systems should reduce their environmental impact and energy delivery costs when using fossil fuels on board the ships.

The right assessment of energy conversion systems implies exergoeconomic analysis and exergoenvironmental analysis, both methods being developed on the fact that in energy conversion systems, just the exergy is the realistic basis when evaluating environmental impacts and costs related to energy carriers and to the inefficiencies within the system.

REFERENCES

[1]. Lattouf R., de Oliveira Jr.S. – ***Exergy analysis of environmental impact mitigation processes,*** Proc of ECOS 2003, pp.397-404, Copenhagen, Denmark, 2003.

[2]. Meyer L. et al. – ***Formation of environmental impacts in energy conversion processes revealed by a novel exergoenvironmental analysis,*** Proc of ASME IMECE 2007, IMECE 2007-42210, Seattle, USA, 2007.

[3]. Moreira H.L. – ***Exergoeconomic comparison between spark ignition engine and compression ignition engine with renewable fuels,*** Proc. of ECOS 2007, pp.139-146, Padova, Italy, 2007.

[4]. Najafzadeh K. – ***Exergy analysis, an effective approach for selection of sustainable technology and optimization of available systems – Three case studies in Iran cement industry,*** Proc. of ECOS 2008, pp.939-948, Cracow, Poland, 2008.

[5]. Tsatsaronis G., Winhold M. – ***Exergoeconomic analysis and evaluation of energy conversion plants.1. A new general methodology,*** Energy, Vol. 10, pp.69-80, 1985.

BACKGROUND SUBTRACTION METHODS FOR MOTION DETECTION IN VIDEO SURVEILLANCE SYSTEMS

[1]NIKOLOV BORIS, [2]KOSTOV NIKOLAY, [2]VELIKOV NIKOLAY

[1]Nikola Vaptsarov Naval Academy, Varna, Bulgaria, [2]Technical University, Varna, Bulgaria

A main activity of many computer vision systems is foreground object detection. Motion is used in a video sequences to identify target objects. Many background subtraction methods have been proposed to identify motion that belongs to a moving object. Each has advantages and disadvantages when it is applied in different conditions.
An overview of five background subtraction methods is proposed in this paper. The selected methods described and compared are: temporal averaging, frame differencing, Kernel Density Estimate, $\Sigma-\Delta$, and mixture of Gaussians. One of the features that was found, was that the more complex methods, such as Kernel Density Estimate and mixture of Gaussians achieve high precision and recall when applied to practice. A lower precision and recall were the results of the more basic methods. However the more basic methods are cheaper in computational cost

***Keywords**:*surveillance systems, substraction methodts, computer

1. INTRODUCTION

The most important part in video surveillance systems is the computer vision, where is necessary to identify foreground target objects in a scene. Precise identification of these objects can allow further processing, for example object identification and tracking. Often, motion is used as a cue to find the pixels which are part of the foreground objects in the current frame of a video sequence. The moving obgects must be segmented under changing lighting and environmental conditions.

A common method for identifying motion is background subtraction, which includes creating a background model to represent the scene with no moving objects in the foreground. Then, each image in the sequence is compared with the estimated background model. The values of the pixels in the current image that differs from the estimated background are classified as foreground. Areas of foreground pixels can then be grouped to represent the moving objects in the scene.

Many problems must be solved by background subtraction method. It must be accounted that the noise from the image sensor may result in a change in pixel colour between the estimated background model and the current image background. Another challenge in outdoor scenes that may affect the accuracy of the foreground segmentation is the camera jitter, caused by moving the camera by the wind. The accuracy of the method must remain over long time, and to adjust automatically to changing scene conditions. This is critical in open air surveillance, which is long running and includes fast changes of the lighting caused by varying clouds, and also rain, and varying objects densities, which range from empty congestion in the scene. If a background motion does not constitute a foreground target, the moving object must be discarded, for example tree branches blowing in the wind. All these restrictions must be realized in real time with low requirements of memory and processing power, because further processing power may be needed for knowledge extraction and tracking.

Greyscale video footage which consist only information for luminance, is often used for background subtraction. In *Robust techniques for background subtraction in urban traffic video*-[1] is given survey of techniques using luminance information. If we use all the information available in colour video footage the results can be more accurate. The progress in available processor power and memory made this reality. The similar methods, such as shadow suppression, which will not be examined in this study, are more effective when using colour information. In *Shadow detection algorithms for traffic flow analysis*-[2] are shown two shadow suppression methods for traffic scenes.

2. BACKGROUND SUBTRACTION METHODS

For identifying foreground objects in a video sequence, motion is usually a reliable cue, and is very appropriate for object tracking applications, where movement is used to find the trajectory of each object. For each pixel location it is expected that the colour that appears most often at that location over time will be the background colour. If there are any colour changes caused by foreground disturbances at that location they are expected to be transient and are not classified as a foreground. Only present object moves across that location are classified as a foreground. So, the quantity that indicates that a foreground object has moved across a current pixel is the deviation from the usual value of the pixel. Foreground objects are extracted from the consecutive images of a video sequence and the pixel value at location x, y in the image at time t is stored in register for $I_{t(x,y)}$. The goal of the process of the foreground extraction is to create a foreground mask, M_t , which includes the locations of all foreground pixels in each image, I_t. This mask is created by comparing B_t which is the estimated background model at each time step, with I_t, which is the value of the current pixel at each image, and regions where they differ are stored in the mask. To keep the background model current with changes in the true scene background it is updated in period of time.

The process of identifying the foreground in a video sequence has to face many challenges that are nonobvious to humans. There are many common real world scenarios that must be taken into consideration when evaluating the performance of a background subtraction method. For example periodic motion, sudden lighting changes, foreground objects that remain motionless for long periods of time and objects with a similar colour to the background.

2.1. TEMPORAL AVERAGING

The background subtraction method using temporal averaging, shown in *A real-time system for monitoring of cyclists and pedestrians*-[8], maintains an estimate of the scene background, B_t, accepted as a threshold for each pixel, proposed in *A new motion detection algorithm based on sigma-delta background estimation*-[3]. This variance is updated puting a recursively updated average of a history of pixel values for all pixel locations. The difference, D_t , which classify each pixel is:

$$D_t = \left| B_t - I_t \right| \tag{1}$$

where B_t is the background, and I_t is the current frame.

The foreground mask $M_t\left(x, y\right)$ is given by:

$$M_t\left(x, y\right) = \begin{cases} 0, \ D_t\left(x, y\right) \le T \\ 1, \ D_t\left(x, y\right) > T \end{cases} \tag{2}$$

where *T* is threshold.

At each time step the background model, B_t, is updated by:

$$B_{t+1} = \alpha I_t + \left(1 - \alpha\right) B_t \tag{3}$$

where α is a learning rate and is used for applying the adaptive mean

For each frame the estimated background moves a small value toward the current image's pixel values. So if there are any changes which remain constant over a period of time, the method will estimate these conditions as a background. Because of that the estimated background is adaptive to changes in lighting and changes in the true background of the scene.

2.2. FRAME DIFFERENCING

The most computationally efficient foreground extraction method presented in this paper is the frame differencing method. The detection of the foreground is implemented by comparing consecutive images in a video sequence and identifying regions where they differ. The algorithm is simple and is done by creating an absolute image difference value, D_t, which is given by:

$$D_t = \left| I_{t-1} - I_t \right| \tag{4}$$

where I_t is the current frame and I_{t-1} is the previous frame.

The foreground mask is:

$$M_t\left(x, y\right) = \begin{cases} 0, \ D_t\left(x, y\right) \le T \\ 1, \ D_t\left(x, y\right) > T \end{cases} \tag{5}$$

Where *T* is a threshold and represents the change required to classify a pixel as foreground. It can be considered that for the frame differencing method, the background model, B_t, is actually the frame I_{t-1}. The computationall price of his method is inexpensive and the method does not maintain an precise calculation of the background, and only can identify objects that are in continuous motion.

2.3. KERNEL DENSITY ESTIMATE

As it is proposed in *Background and foreground modeling using nonparametric kernel density estimation for visual surveillance*-[1], The Kernel Density Estimate (KDE) method is a nonparametric method which estimates the true distribution of colours for a pixel over a given history. The benefit of this method is that the repeating backgrounds can be recognized. The classification of each pixel is given by calculating whether it has a high probability of being described by this distribution.

The probability that a current pixel, X_t , will have a certain colour value at time t is:

$$P\left(X_t\right)=\frac{1}{N}\sum_{i=1}^{N}K_\alpha\left(X_t-X_i\right), \tag{6}$$

where N is number of the past frames which history is $\left\{X_1,...,X_t\right\}=\left\{I_t\left(x,y\right):t-N\le i\le t\right\}$,

K_α is the kernel estimator function with bandwidth α , and is chosen to be a Gaussian function. X_i is the value of each pixel of the multitude of N .

The foreground mask is given by

$$M_t\left(x,y\right)=\begin{cases}0, & P\left(I_t\left(x,y\right)\right)\ge T\\ 1, & P\left(I_t\left(x,y\right)\right)<T\end{cases} \tag{7}$$

where $P\left(I_t\left(x,y\right)\right)$ is the probability for each pixel value and T is global threshold. The pixel is classified as foreground if the probability, $P\left(I_t\left(x,y\right)\right)$, is below the global threshold, T .

To keep the the computational cost realizable, The Kernel Density Estimate method uses only a relatively short history, allowing quick adaptation to changes but not precise for a long term of history.

2.4. $\Sigma-\Delta$ BACKGROUND MODELLING

To make a background-foreground classification decision, the $\Sigma-\Delta$ (Sigma Delta) background modelling method uses an approximation of the median and $\Sigma-\Delta$ variance, as it is proposed in *A new motion detection algorithm based on sigma-delta background estimation*-[3]. The method is called $\Sigma-\Delta$, because the similarity to analog to digital conversion of a time varying signal using $\Sigma-\Delta$ modulation as it is interpreted in [3].

A current pixel is classified as foreground if the pixel value is greater or less than that of the estimated background by more than the per-pixel $\Sigma-\Delta$ variance. The $\Sigma-\Delta$ variance is different to the standard mathematical definition of variance. As it is defined in [3] it is a measure of the variation of the colours of each pixel over time. Depending on the difference between the current pixel value and the background, the $\Sigma-\Delta$ mean and $\Sigma-\Delta$ variance are updated at each time step by incrementing or decrementing them by one.

The current background is given by:

$$B_{t+1}(x,y)=\begin{cases} B_t(x,y)-1, & D_t(x,y)<0 \\ B_t, & D_t(x,y)=0 \\ B_t(x,y)+1, & D_t(x,y)>0 \end{cases} \tag{8}$$

where D_t is the difference, which is:

$$D_t = B_t - I_t\ , \tag{9}$$

If this background update rule is applied, B_t becomes an approximation of the median of the video sequence, as it is shown in *Segmentation and tracking of piglets in images*-[11]. As it is presented in [3], to adapt for different conditions at different areas in the image, a perpixel $\Sigma-\Delta$ variance, $V_{t(x,y)}$, is used as a threshold for each pixel. To update this variance $V_{t(x,y)}$ we implement the equation:

$$V_{t+1}(x,y)=\begin{cases} V_t(x,y)-1, & C.\left|D_t(x,y)\right|<V_t(x,y) \\ V_t(x,y), & \left|D_t(x,y)\right|=0 \\ V_t(x,y)+1, & C.\left|D_t(x,y)\right|>V_t(x,y) \end{cases} \tag{10}$$

where, *C* is a user set parameter that determines how large the difference must be, before the variance is updated. Therefore, this is a comparison between the current variance, $V_{t(x,y)}$, with the multiple, *C* , of the difference between the current and estimated pixel value, and incrementing or decrementing the current variance by one. The foreground mask is given by:

$$M_t(x,y)=\begin{cases} 0, & \left|D_t(x,y)\right|\le V_t(x,y) \\ 1, & \left|D_t(x,y)\right|>V_t(x,y) \end{cases} \tag{11}$$

The temporal variation of colour for each pixel location in the scene is represented by the $\Sigma-\Delta$ variance. High $\Sigma-\Delta$ variance is typical for pixels of repeating backgrounds, for example, leaves waving by the wind and wavy surface of a river or sea which is included in the real background of the scene. And because of this, those pixels would not be classified as foreground for small changes of their values.

2.5. MIXTURE OF GAUSSIANS

To describe each pixel in the scene the mixture of Gaussians method, proposed in *Adaptive background mixture models for real-time tracking*-[5] uses multiple Gaussian distributions, permitting each separate cluster of colours to be represented by a distribution with its associated variance, weight and mean.

As previously described in this section the background modelling methods, use only one colour to represent the background at each pixel location. But if there is more complex sequence with repeating backgrounds this is not suitable. For example, a tree branch waving back and forth in the wind, a wavy streaming water in an outdoor scene or a flickering monitor in an indoor scene will be wrong classified as foreground. That is the reason why the mixture of Gaussians method use the information of all colours.

Distributions with a low weight, or a high variance are assumed to result from the movement of foreground objects, while distributions with the highest weight and lowest variance are assumed to describe the background colour.

As it is described in [5], the probability of observing the current pixel value *x* at time *t* at a particular pixel location is given by:

$$P\left(x\right)=\sum_{i=1}^{K}\omega_{i,t}\eta(x;\mu_{i,t},\Sigma_{i,t}) \tag{12}$$

where $\omega_{i,t}$ is the weight of the i^{th} Gaussian at time *t*, *K* is the number of Gaussians distributions representing each pixel, η is the Gaussian probability density function with parameters: *x* is the current pixel, $\mu_{i,t}$ is the mean of the i^{th} distribution at time *t*, and $\Sigma_{i,t}$ is the covariance of the i^{th} distribution at time *t*. It is computationally expensive to implement the covariance matrix for precise calculation and because of that it is assumed that the red, green and blue channels of x are independent and have the same variances.

The Gaussian probability density function η is given by:

$$\eta\left(x;\mu,\Sigma\right)=\frac{1}{\left(2\pi\right)^{\frac{n}{2}}\left|\Sigma\right|^{\frac{1}{2}}}e^{-\frac{1}{2}\left(x-\mu\right)^{T}\Sigma^{-1}\left(x-\mu\right)}, \tag{13}$$

A particular value *x* being observed at a pixel location has high probability if it is close to the mean of a highly weighted Gaussian distribution with a low variance. So, this is the Gaussian distributions that best describe each pixel. To update each distribution we use an adaptive learning rate described in *Effective gaussian mixture learning for video background subtraction*-[6]. This learning rate depends on the strength of the match between the current pixel value and the i^{th} distribution, q_i.

The weight of the i^{th} Gaussian at time *t* is given by:

$$\omega_{i,t}=\left(1-\alpha\right)\omega_{i,t-1}+\alpha q_i, \tag{14}$$

where α is the learning rate and q_i is the i^{th} distribution

In case there is no match it is created a new Gaussian distribution with a mean equal to the current pixel value, a low weight and a high variance. So, this new distribution replaces the distribution with the lowest weight and highest variance. It is assumed that the background is represented by Gaussian distributions with the highest weight and lowest variance. To estimate the background, the distributions are first sorted in order of decreasing ω/σ. The pixels that belong to the background are the first *C* distributions and *C* is given by:

$$C=\arg\min_{c}\left(\sum_{k=1}^{c}\omega_k>T\right). \tag{15}$$

If the value of the threshold *T* is high, it is more likely that multiple Gaussian distributions will be used to represent the background. That makes possible describing the repeating backgrounds. If the first *C* Gaussian distributions represent the background and the current pixel does not match one of them it is classified as foreground. This method can separate repeated motion as foreground by explicitly representing multiple detached background colours per pixel. This allows fast reaction in situation where a foreground object is moved into the background and moves to the horizon.

If the value of the threshold *T* is high, it is more likely that multiple Gaussian distributions will be used to represent the background. That makes possible describing the repeating backgrounds. If the first *C* Gaussian distributions represent the background and the current pixel does not match one of them it is classified as foreground. This method can separate repeated motion as foreground by explicitly representing multiple detached background colours per pixel. This allows fast reaction in situation where a foreground object is moved into the background and moves to the horizon.

3. DISCUSSION

The classification of the results of each background subtraction method is separated in four groups. The decision depends on that if each pixel belongs to the real background or foreground and if it is correctly recognized. The four groups are: true positive for a correctly recognized foreground pixel, false positive for a background pixel that was incorrectly classified as foreground, true negative for a correctly recognized background pixel, and false negative for a foreground pixel that was incorrectly classified as background.

The precision and recall are estimated after every pixel had been classified into one of the four groups. If the most of the pixels recognized as foreground are correctly classified that indicates high precision of the method. If the method classified most of the foreground pixels in the ground truth as foreground, the recall is high.
The precision and recall are given by:

$$precision = \frac{T_p}{T_p + F_p}, \tag{16}$$

$$recall = \frac{T_p}{T_p + F_n}, \tag{17}$$

where T_p is true positives pixels, F_p is false positive pixels and F_n is false negative pixels.

The precision and recall are used to estimate the advantages and disadvantages of each method when it is applied to the real sequence. There is an overview, below that analyze the properties of each of the proposed methods in this paper. The results are based on the references listed in the end of this work.

3.1. TEMPORAL AVERAGING

The main advantage of this method is that it stores an estimated background image. It correctly handles large inter frame target displacements, homogeneous regions and low frame rates. A disadvantage of this method is that for every pixel in the image is used only a single, global threshold. This may not be suitable for scenes in which different areas include objects with different properties. For example, in different regions of a single scene may exist different lighting levels. The single mean value is not able to describe more than one expected background colour, so the repeating backgrounds are also incorrectly recognized. Because of that the repeating backgrounds are constantly classified as foreground.

In traffic scenes where the lighting is stable and the background is static, this method works well. But the more sophisticated methods perform better results in more complex scenes.

3.2. FRAME DIFFERENCING

The simplest method presented in this paper is the frame differencing method. It is the most computationally efficient method, requiring minimum memory than the other methods. When it is applied to more complex and overcast scenes the quality of the results decreases sharply. The fact that no historical estimated background is stored and used in the background-foreground decision is the main reason that frame differencing is ineffective as a robust background subtraction method for object segmentation. The information that can be used to detect moving objects in the current image is only the previous frame. Because of that there is a list of problems: if in only two consecutive frames the foreground object remains stationary, it will be incorrectly classified as background; the surrounding area of an object with a homogeneous colour will be wrong classified as background. Also, if there are repeating backgrounds the result will be false positive pixels when there are background changes.

If there is a need only of rough motion detection algorithm without need of precise foreground object segmentation, the frame differencing method can be useful to get the approximate area where a continuous motion is.

3.3. KERNEL DENSITY ESTIMATE

This method stores the history of the values of each pixel and use it to estimate a non-parametric distribution. Because of storing a history of each pixel there are multiple results: the true distribution of this history can be calculated and that allows correct classification of repeating backgrounds; by reason of the memory and computational power required for processing the history of every pixel, only a short history can be stored for each pixel. As a result of that the kernel density estimate method is able to adapt quickly to new background conditions, for example caused by fast changes in lighting. If the objects move relatively freely, it is not a problem that no long term information is stored, because fast moving objects don not require long history. The kernel density estimate method has relatively few parameters than other sophisticated methods, for example, the mixture of Gaussians method, and than makes the method easy to apply in different conditions.

3.4. $\Sigma - \Delta$

The key feature of the $\Sigma - \Delta$ method is that there is a non-linear response to the difference between the estimated background and current pixel value. This saves the estimated background from corrupting when there are transient changes and allows it to learn a change in the true background quickly. Therefore, the method is ideal for situations where the scene is filled of constantly moving objectst. But there are disadvantages of this method and one of them is that when an object is less transient, when the object remains in the same position for a relatively long time, it will be estimated as a background relatively quickly.

Also, the $\Sigma - \Delta$ method uses an adaptive variance measure that increases the foreground threshold if there are fast changes in pixel colour between successive frames.

Low $\Sigma-\Delta$ variance and low perpixel threshold are representative for pixels belonging to area on the image where are not passing objects for a period of time. This threshold will prevent camera noise, and the pixels of the area where motion is frequently, will be sensitive to the colour changes caused by a object. The pixels with high $\Sigma-\Delta$ variance and a low sensitivity to changes in colour will be caused by a continuously waving tree or other repeating background, and those pixels will be classified as background. There is no require for large amount of memory or computational power to maintain the $\Sigma-\Delta$ method.

When the sequence includes scenes with heavy traffic this method may give an incorrect background-foreground decision. There is a conflict between what forms background and what forms foreground in a scene. The waving tree and heavy traffic shows similar pixel behaviour – frequently changing colours at a single pixel location, but we expect that the one situation will be treated as background and the other as foreground. This continuous colour changes between successive frames would result in a high $\Sigma-\Delta$ variance at the heavy traffic pixels and before a pixel will be classified as foreground, large changes would have to occur. Therefore, some moving object pixels will be incorrectly classified as background.

3.5. MIXTURE OF GAUSSIANS

The most sophisticated method proposed in this paper is the mixture of Gaussians. It has high precision and recall, although it is more complex to implement and configure and it has relatively long running time. The fact that this method stores multiple distributions is an advantage, making it able to describe repeating backgrounds very correctly. In contrast to the other methods proposed in this paper, slow moving or stationary foreground objects could not corrupt the expected background so easy. At every time step new distribution is created when the new observed pixel does not match previous Gaussian distribution. If this pixel belongs to a foreground object which then moves away, the mean and variance of the previous distribution, which represented the true background, would not have been changed and will replace the new distribution.

To achieve an optimal result using the mixture of Gaussians method there are many parameters to be set for different video situations and this is disadvantage of this method. The parameters that has to be set are: learning rate, number of Gaussian distributions, background-foreground threshold, distance from the mean of a each Gaussian and initial variance. It is computationally expensive and requires relatively large amount of memory to store, update and sort multiple Gaussian distributions.

The mixture of Gaussians is useful when there is enough computational power and memory and this method allows correct estimation of scene which contain heavy traffic of moving objects and repeating backgrounds.

4. CONCLUSIONS

The most suitable background subtraction method is determined of the computational power available, the expected properties of the scene and the requirements of the consumer of the background-foreground classification. The methods such as $\Sigma-\Delta$ and temporal averaging has lower computational cost and that makes them suitable for applications where processing power is limited or needed for further analysis and tracking. If there are large moving object and there is no repeating background, these more basic methods can correctly separate the scene. The use of the more sophisticated methods is not necessary when the consumer of the background-foreground classification does not require perfect pixel classification. However if there is a need of precise foreground-background decision and there is enough available computational power and memory, more accurate methods such as mixture of Gaussians are preferable.

REFERENCES

[1]. Ahmed Elgammal, Ramani Duraiswami, David Harwood, Larry S. Davis, R. Duraiswami, and D. Harwood - ***Background and foreground modeling using nonparametric kernel density estimation for visual surveillance*** - In Proceedings of the IEEE, VOL. 90, No. 7, July 2002 Pages 1151–1163, 2002.

[2]. Andrea Prati, Ivana Mikic, Costantino Grana, and Mohan M. Trivedi - ***Shadow detection algorithms for traffic flow analysis: a comparative study*** - In Proceedings of IEEE Intelligent Transportation Systems Conference, pages 340–345, Aug 2001.

[3]. Antoine Manzanera and Julien C. Richefeu - ***A new motion detection algorithm based on sigma-delta background estimation*** - Pattern Recognition Letters In Advances in Visual information Processing, Vol.28 No.3 Pages: 320–328, 1 Feb 2007.

[4]. Cheung Sen-Ching and Chandrika Kamath - ***Robust techniques for background subtraction in urban traffic video,***. Proceedings of Electronic Imaging: Visual Communications and Image Processing 2004 (Part One), January 20-22 2004, San Jose, California. Bellingham WA:SPIE, 5308, Pages: 881–892.

[5]. C. Stauffer and W. E. L. Grimson - ***Adaptive background mixture models for real-time tracking***. - In Proceedings of IEEE Computer Society Conference on Computer Vision and Pattern Recognition, Vol 2, page 252, 1999.

[6]. Dar S. Lee. - ***Effective gaussian mixture learning for video background subtraction***.
IEEE Transactions on Pattern Analysis and Machine Intelligence, Vol. 27 Issue 5 Pages: 827–832, 2005.

[7]. Fabian Campbell-West and Paul Miller - ***Evaluation of a robust least squares motion detection algorithm for projective sensor motions parallel to a plane*** - Proceedings of SPIE Opto-Ireland Image and Vision Conf., Soc. Photo-Optical Instrumentation Engineers, 2005, Pages. 225–236

[8]. Janne Heikkilä and Olli Silvén - ***A real-time system for monitoring of cyclists and pedestrians*** - Image and Vision Computing, Vol. 22, Issue 7, Visual Surveillance 1 July 2004 Pages: 563–570

[9] Lionel Lacassagne, Antoine Manzanera, Julien Denoulet, Alain Me´rigot. - ***High performance motion detection: some trends toward new embedded architectures for vision systems***. - In Proceeding of Journal of Real-Time Image Processing, Vol. 4, No. 2 ,June 2009, Pages 127-146

[10]. M. Vargas, S. L. Toral, F. Barrero, J.M. Milla - ***An Enhanced Background Estimation Algorithm for Vehicle Detection in Urban Traffic Video*** - Proceedings of the 11th International IEEE Conference on Intelligent Transportation Systems Beijing, China, October 12-15, 2008, Pages
784 – 790.

[11]. N.J.B. McFarlane and C.P. Schofield - ***Segmentation and tracking of piglets in images***. Machine Vision and Applications, Vol.8, No.3 Pages:187–193, May 1995.

[12]. Nan Lu, Jihong Wang, Q.H. Wu and Li Yang - ***An Improved Motion Detection Method for Real-Time Surveillance*** - Proceedings of International Journal of Computer Science, IAENG, 35:1, IJCS_35_1_16, January 2008

[13]. Nan Lu, Jihong Wang, Li Yang, Henry Wu - ***Motion Detection Based On Accumulative Optical Flow and Double Background Filtering.*** In Proceedings of the World Congress on Engineering 2007, Vol. 1 WCE 2007, July 2 - 4, 2007, London, U.K.

[14]. P. Kaew Tra Kul Pong and R. Bowden - ***An improved adaptive background mixture model for real-time tracking with shadow detection*** - In Proceedings of Second European Workshop on Advanced Video Based Surveillance Systems (AVBS '01), Kingston, UK, September 2001.

[15]. Rita Cucchiara, Andrea Prati, Roberto Vezzani - ***Real-time motion segmentation from moving cameras*** - In Proceedings of Real-Time Imaging Vol. 10, No.3 Pages: 127–143, June 2004.

RECOVERY OF LOW-TEMPERATURE WASTE HEAT AND LNG COLD ENERGY

[1] NOVAC IORDAN, [2]OLTEANU VASILE

[1]*Constanta Maritime University, Constanta, Romania,* [2]*NYK Shipmanagenent, Constanta Romania*

This paper has proposed a combined power system, in which low-temperature waste heat can be efficiently recovered and cold energy of liquefied natural gas (LNG) can be fully utilized as well. The generation of electric power using the Organic Rankine Cycle appears the most practical. It is found that less energy in the low-temperature waste heat can be converted to the power by organic Rankine cycle because boiling essentially take place at constant pressure and temperature in the evaporator.

Keywords: Cold energy, Organic Rankine Cycle

1. INTRODUCTION

LNG (Liquefied natural gas) is produced by cooling, pressurizing and liquefying crude natural gas from which impurities have been removed, at a very low temperature of -160 °C, causing it to contract to 1/600th of its volume at room temperature and making sufficiently compact for swift transport in specially insulated tankers. Producing one ton of LNG consumes about 850 kWh of electric energy.

When this gas is then warmed to an ambient temperature of 20°C, the temperature differential yields cryogenic energy of 919 kj/kg (219.5 cal kg). This cryogenic energy can be utilized for various purposes including cryogenic energy power generation, air separation, the production of liquefied carbonic acid and dry ice, cold storage warehouses, and for the reliquefaction of LNG boil off gas (BOG), and these all comprise LNG cryogenic energy applications.

Since LNG terminals at the receiving points are nearly always located near water to accommodate ocean-going tankers, sea water is usually available to provide the necessary heat of vaporization. It has long been recognized that the refrigeration potential of such vast quantities of LNG is considerable, and it has been a real challenge to attempt to economically use the cold energy that is available.

Recently however, the refrigeration potential of LNG has received increasing attention. The large-scale user of liquefied natural gas (LNG) faces a great challenge in seeking to use its cold potential. The Japanese have taken the lead and through their technology and longstanding operational experience they have gained expertise in the use of this intense cold. They have applied the LNG cold in the following areas:

1. the separation of air, which may operate at about -195° C;
2. the production of liquid carbon dioxide and dry ice, at -79° C;
3. in cold warehouses, at about -29° C;
4. production of electric energy by means of a cryogenic Rankine Cycle.

In Japan, cryogenic energy power generation systems were initiated at LNG landing bases from around 1980, and have been subsequently been installed at a total of 15 bases (three of these systems are no longer operating). The initial output was on the order of 1,000 kW, but this scale has now been expanded to 8,800 kW.

2. DESIGN OF RANKINE CYCLES FOR POWER GENERATION FROM EVAPORATING LNG

The generation of electrical power has been one of the more frequently investigated uses of the cold energy potential of LNG. Same idea shows the recovery of power during the vaporization of LNG by a single expansion of a condensable circulating refrigerant, such as propane or ethane, and suggests the use of sea water to provide an ambient heat source. The potential problems that can occur from the use of sea water in a confined area from the standpoint of "cold water pollution". Some idea is proposes to use a circulating freon stream which can be expanded to drive a turbine, to create mechanical energy and ultimately generate electricity. The idea specifically discloses the use of LNG to condense nitrogen, which is subsequently expanded to create power after being pumped to high pressure and vaporized by condensing freon which is used as the working fluid in a main power plant.

Few of the existing systems designed to utilize the available LNG refrigeration appear to have true commercial potential. Low temperature uses of LNG are often at inconvenient levels or not well matched to utilize the cold potential without any limitation upon LNG's primary role, which is to supply natural gas to a distribution network at a variety of pressures and appropriate temperatures. Therefore, although these various systems may have certain advantages in particular situations, the electrical power-generating industry and the natural gas pipeline industry have continued to search for more efficient and economical systems.

The two methods being used for cryogenic energy power generation are the direct expansion method and the Rankine cycle method, and there are also combined systems that use both methods. Under the direct expansion method, the LNG is heated and vaporized using seawater, used to turn an expansion turbine, and then shipped as natural gas (NG). In contrast, the Rankine cycle method uses a coolant. The coolant is liquefied via heat exchange with the LNG, and its pressure is increased.Then, through heat exchange with seawater the coolant becomes a high-pressure gas, which is used to turn a turbine. Under this method, the LNG is shipped as natural gas (NG) after it has been heated from the heat exchange with the coolant. Combined systems use the direct expansion method for heat exchange with the coolant, and then utilize a Rankine cycle.

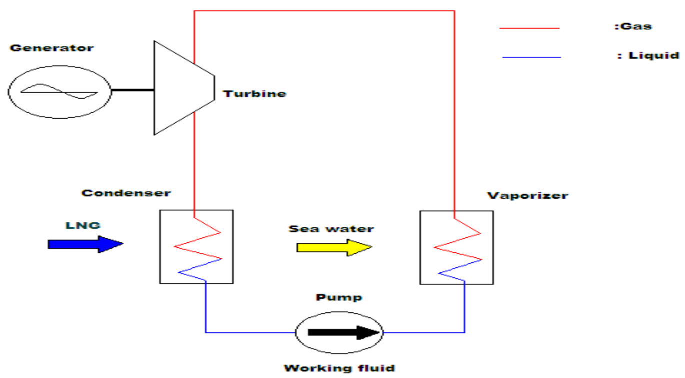

Figure 1 Cryogenic power generation facility

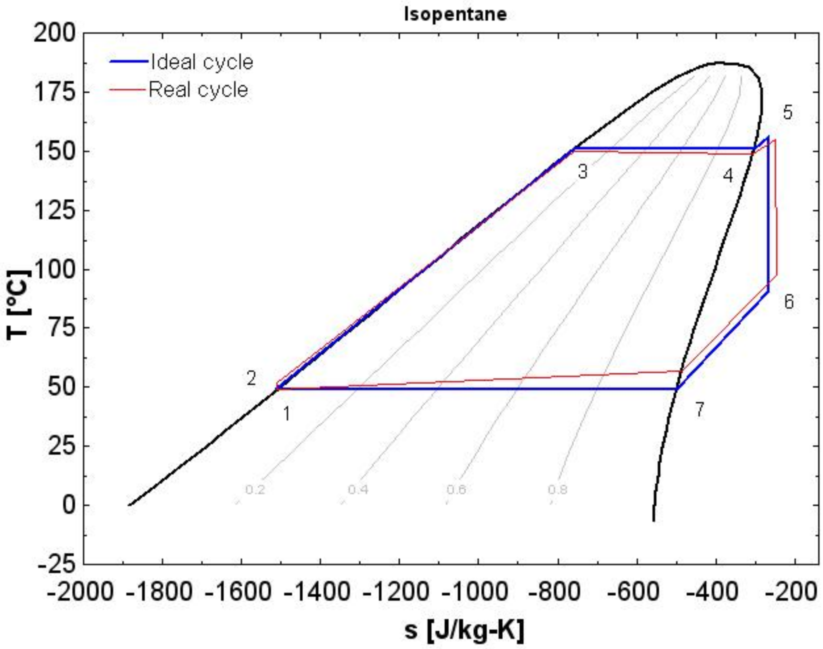

Figure 2 Gas expansion Rankine cycle

Of the different ways of using the cold available from the large scale evaporation of LNG the generation of electric power, using the organic Rankine Cycle, appears the most practical. Many such plants have so far been installed in Japan.

2.1. VAPORIZATION OF LNG

Natural gas, depending on its composition is liquefied under atmospheric conditions at -162 ˚C. Its density increases ~600 times which permits the transportation of huge quantities of gas in special methane tankers. Upon arrival this LNG is stored in insulated tanks and has to be revaporized before it can be delivered to the grid. This phase change necessitates the addition of heat, the amount depending on the revaporization pressure, the composition of the LNG and final temperature wanted.

There are many ways to heat the LNG as: submerged burners (SMV)and sea water vaporizers, open rack type (ORV). In these cases no effective use of the LNG cold is made. The SMV necessitates the burning of a certain percentage of imported energy, whereas the ORV needs a huge quantity of sea water.

This Paper deals with the transformation of this cold potential into mechanical and/or electrical energy by means of an organic Rankine Cycle (ERV or Energy Recuperation Vaporizer). Special attention is thereby given to the selection of a working fluid adapted to a given configuration of a Rankine Cycle.

2.2. CRYOGENIC RANKINE CYCLE

It is possible to take heat from the sea water (hot source at ambient temperature) to evaporate a working fluid which is then expanded in a turbine and condensed to liquid in the condenser against the LNG (cold source at cryogenic temperature), which is evaporated. A pump returns the liquid to the evaporator.

This method of LNG vaporization with simultaneous production of electric energy was used first time in Japan. They started experimenting in 1979 and have since then installed a generating capacity of 46 MW using the cold potential of 1.055 t LNG h" '. By 1985 there were 14 installations in Japan which generate power from LNG. The working fluids include propane, mixed refrigerants, R13BI, R22 and R23. The majority use single stage expansion, although one installation at Tobata employs double expansion. They vary in power output from 150 to >4000kW and the ratio kW output tonne LNG varies from 25 to 63. Some plants use axial flow turbines, others radial ones.

A new system was developed, called Kalina Cycle. The so called Kalina cycle using ammonia /water mixtures has been developed to attain higher thermal efficiency than Rankine Cycle. The variable boiling point nature of this binary fluid at a specific pressure enables more heat to be extracted. We intend to discus about Kalina cycle in separate article.

2.3. SIMULATION OF THERMODYNAMIC PROCESS

The thermodynamic transformations of the working fluid can all be expressed by a set of linear equations linking the different variables. For this the different points in the circuit have been numbered in a logical order as shown in Figure 3.

As is known all thermodynamic values for pure substances can be defined when two variables for each point, pressure and temperature, are known.

The following equations can be written:

$$\text{evaporation: } (H_1 - H_2)D_h = (H_3 - H_6)D_s \quad (1)$$

$$\text{condenser: } (H_4 - H_5)D_s = (H_8 - H_7)D_c \quad (2)$$

$$\text{turbine: } (H_3 - H_4) = (H_3 - H_{4is})\,\eta_T \quad (3)$$

$$\text{pump: } (H_6 - H_5) = (H_{6is} - H_5)\,\eta_P \quad (4)$$

Since the number of variables outnumbers the quantity of equations a few variables can be given a set value. Experience has shown which should be selected.

- H_1 and H_7 are given.
- $(H_1 - H_3)$ is known when we decide on $\Delta T_h = (T_1 - T_3)$ and
- similarly $(H_5 - H_7)$ is known when $\Delta T_c = (T_1 - T_3)$ is selected.

The existing mathematical model was elaborated to calculate more complex configurations such as:

1. 8-points cycle,
2. 10-points cycle with fraction x and economizer,
3. 10-points cycle with a three stream-condenser,
4. the double expansion, configurations 1 and 2,
5. the expansion of two different fluids in a thermodynamic coupled cycle.

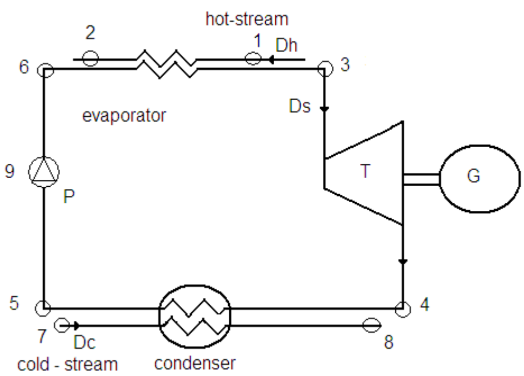

Figure 3. 8-points cycle

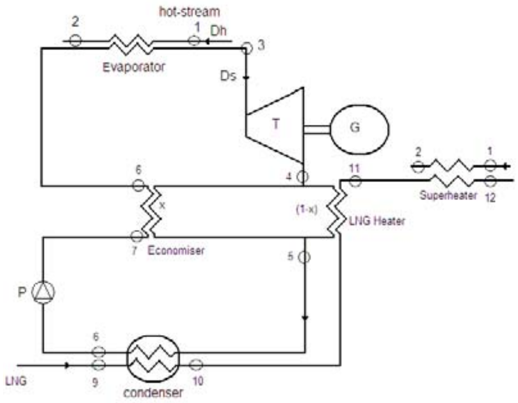

Figure 4 Cycle 10 points with economizer

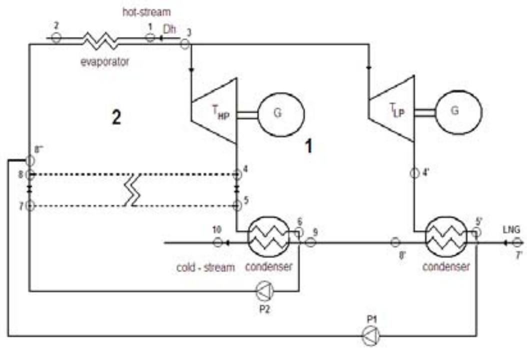

Figure 5 Double expansion

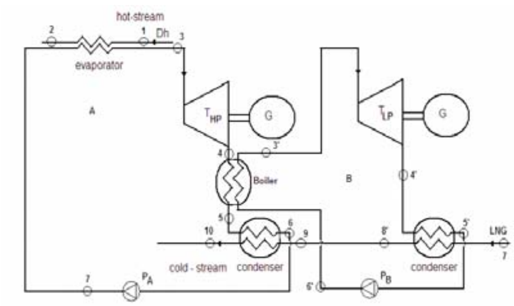

Figure 6 Thermodynamic coupled

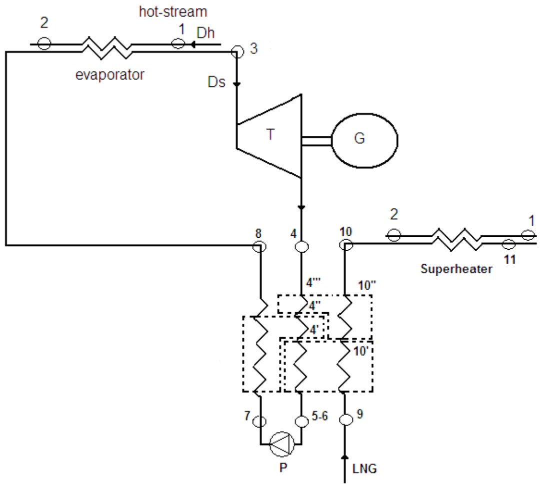

Figure 7 Cycle 10 points, with 3 streams condenser

This mathematical model has an easy access to a databank containing the thermodynamic properties of the hydrocarbons, certain gases and refrigerants. It permits the calculation of mixtures of hydrocarbons with nitrogen and certain binary mixtures of refrigerants. The model was transformed into an interactive and self-adapting and controlling system permitting an optimization study in a dynamic way.

2.4. SELECTION CRITERIA FOR WORKING FLUIDS IN ORGANIC CYCLES

The selection of a working fluid depends on the needs and wants expressed when the options for the ERV were outlined, i.e. maximization of energy output or minimization of capital outlay, or any other option. Other considerations such as the physical, chemical and thermodynamic properties of the fluid should be regarded as well as its economic availability.

In the Table 1 below are listed some properties which should be considered.

Table 1: Property to be considered when selecting working fluids for organic cycles

Physical	Chemical	Thermodynamic
Critical point	Chemical stability	Heat transfer coefficient for Condensation and boiling
Solidification point	No-toxic	
Molecular weight	No-flammable	Thermal conductibility
Specific volume	Non-corrosive	Latent heat
	Non-carcinogenic	Wet, dry or neutral expantion
	Material compatability	Sonic velocity

The selection of the working fluid is of key importance in low temperature Rankine Cycles. Because of the low temperature, heat transfer inefficiencies are highly prejudicial. These inefficiencies depend very strongly on the thermodynamic characteristics of the fluid and on the operating conditions.

In order to recover low-grade heat, the fluid generally has a lower boiling temperature than water. Refrigerants and hydrocarbons are the two commonly used components.

Optimal characteristics of the working fluid :

- Isentropic saturation vapor curve :

Since the purpose of the ORC focuses on the recovery of low grade heat power, a superheated approach like the traditional Rankine cycle is not appropriate. Therefore, a small superheating at the exhaust of the evaporator will always be preferred, which disadvantages "wet" fluids (that are in two-phase state at the end of the expansion). In the case of dry fluids, a regenerator should be used.

- Low freezing point, high stability temperature :

Unlike water, organic fluids usually suffer chemical deteriorations and decomposition at high temperatures. The maximum hot source temperature is thus limited by the chemical stability of the working fluid. The freezing point should be lower than the lowest temperature in the cycle.

- High heat of vaporisation and density :

A fluid with a high latent heat and density will absorb more energy from the source in the evaporator and thus reduce the required flow rate, the size of the facility, and the pump consumption.

- Low environmental impact

The main parameters taken into account are the Ozone depletion potential (ODP) and the global warming potential (GWP).

- Safety

The fluid should be non-corrosive, non-flammable, and non-toxic. The ASHRAE safety classification of refrigerants can be used as an indicator of the fluid dangerousness level.

- Good availability and low cost
- Acceptable pressures

Example of working fluid:
a) Hydrocarbons: ethylene, ethane, propane, propylene.
b) Refrigerants: R13, R13B1, R14, R22, R23.
c) MFR (multicomponent fluid): eprobuni, etaproba, etaprobu, frigova, gulf,valk1, valk2.
d) Two fluid for Parallel rankine cycles: propane-ethylene, propane-ethane, propane-R13, R12-R13.

2.5 CONFIGURATION OF THE RANKINE CYCLE

There are many other ways to improve the performance of the Rankine Cycle and to augment the recovery of the liquefaction energy of the LNG. Our research was focused on finding ways to increase the massflow of the working fluid by using part of its energy released in the condenser to heat another useful massflow (economizer, thermodynamic coupled cycles) or to use the full expansion ratio of the working fluid (multiple expansion). Our findings are briefly discussed.

Double expansion

As shown previously in this Paper the expansion ratio is sometimes limited by the vapour quality at the turbine outlet. For these working fluids the cycle output can still be augmented by having recourse to multiple expansions with an equal number of condensers in which the LNG is heated. Our studies have shown that the LNG should at first drain the heating capacity of the low pressure condenser so that the total capacity of the LP (low pressure) turbine is fully used. Of course the added output by each additional stage will have to be weighed against the added investment cost. This method also allows the LNG to be heated to the outlet temperature of the HP (high pressure) turbine, diminishing at the same time the size of the LNG superheater which follows the ERV to bring the gas to the desired temperature before delivery to the grid. Through a multiplication of the expansion steps it becomes possible to obtain an expansion course that follows step by step the heating curve of the LNG.

Thermodynamic coupled Rankine Cycle

Another method to increase the output is to couple two Rankine Cycles, each using a different working fluid specially selected for the given temperature differences. In such a cycle the massflow in cycle A is augmented by the heat duty required in the boiler to heat fluid B, increasing thereby the total output of the cycle as compared to the above mentioned double expansion. However such a boiler increases the total exchange surface needed and hence the total investment. There is no limit to the inventiveness as we can couple a single expansion to a double expansion, and so on.

Use of a MFR (multicomponent fluid for Rankine Cycle)

For a single component fluid the phase change occurs along an isobar which is also isothermal. Hence, it becomes impossible for a cycle working with such a fluid under the conditions outlined previously to augment the massflow of the fluid by installing an economizer. By replacing a single component fluid by a MFR it is possible to increase the massflow enormously and to use an economizer. Figure 8 indicates the changes that occur when replacing a single component fluid by a MFR in a 10-points cycle. As can be seen, the heat available in the condenser to heat the LNG is reduced by the quantity absorbed in the economizer, (H8 - H7) = x(H4 – H5), see Figure 8.

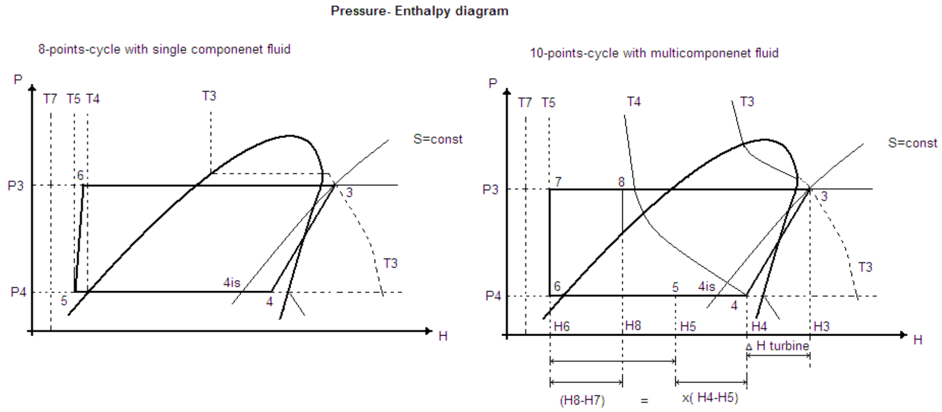

Figure 8 Changes occurring when replacing a single component fluid by a multicomponent fluid in a 10-points cycles

In Figure 7 the thermodynamic cycle called a 3 stream condenser' shows the working principle. The condensing fluid heats the LNG and the pressurized working fluid at the same time. For a given quantity of LNG a greater massflow of working fluid is needed. By selecting an appropriate composition of MFR it becomes possible to obtain a condensing curve of the MFR parallel to the LNG heating curve at a defined temperature difference. Needless to say, this solution multiplies the required heat exchange surface. Its economical application is restricted by the limits imposed in the construction of plate-fin heat exchangers. An MFR with a high temperature difference between the bubble and the dew point is not suitable for a multiple expansion cycle.

3. CONCLUSIONS

This studies show that the output almost doubles when replacing the seawater by waste heat at 50 C.These figures show:
1. the extreme importance of the temperature of the hot source:
2. that no single working fluid optimizes all cycles under all circumstances;
that the lower the vaporization pressure of the working fluid, the more sensitive the cycle
3. output is to a temperature change of the hot source;
4. the final determination of a working fluid depends on the options taken for the recovery of the energy Considering the environment and security regulations.

REFERENCES

[1]. Maertens, J. - ***Design of Rankine Cycles for Power Generation from Evaporating LNG,*** Rev. Int. Froid, 9: 137-143 (1986).
[2]. Masaki Sugiyama - Director and Production Department Manager, Tokyo Gas Co., Ltd., ***The Utilization of LNG Cryogenic Energy***.
[3]. McGuire and White - ***Liquefied Gas Handling Principles on ships and in terminals (SIGTTO)***, Published by Witherby & Company Limited 32-36 Aylesbury Street, London EC1R OET.

THE EXPLOITATION OF MARINE CURRENT´S ENERGY ON THE STRAIT OF GIBRALTAR

[1]NUÑEZ - RIVAS LUIS R., [2]ROJAS EVA M. NOVOA

[1]*Technical University of Madrid, Spania,* [2]*Foundation Technological Centre SOERMAR, Spania*

The two great currents of water going along The Strait of Gibraltar give rise to an interchange of large masses of water between the Mediterranean Sea and the Atlantic Ocean. They flow one over the other in opposite directions and both are very important renewable sources of energy that at present time are not in use at all. This work begins with a description of the way in which the energetic potential of both currents can be estimated, afterwards a study on the possibilities of getting a partial use of this potential is done, without navigation´s restrictions and also looking for the protection of the marine environment. Indeed, the work shows how to use the energy source with several types of submerged turbines that are being developed nowadays, the analysis about where the devices must be placed is done and which are the rates of electrical energy that will be get. Finally, the paper is concluded giving an exposition of the basic parameters for the design procedure of one submerged electrical generation park located in the zone. How the devices must be arranged into the current is indicated and the forecast of the energy production of the park is done

Keywords: Marine renewable energy sources, Exploitation of marine currents energy

1. INTRODUCTION

Gibraltar´s strait (Fig. 1) is the natural way to join Mediterranean Sea and Atlantic Ocean, it´s limited by a section between the Cape of Trafalgar on Europe and the Cape of Esparter on Africa at west and by the section between Punta Europe and Punta Cires at east. It has a variable width with one maximum of 44 km in the strait´s narrows between Tarifa and Punta Cires. The strait´s axis goes in east-west direction along 60 km over 36º N parallel. The bathymetric profile is irregular with overage depth of 550 m in the main channel and zones where 90 m are only and another with maximum depth of 960 m.

On this strait the interchange of large masses of water between Atlantic Ocean and Mediterranean Sea happens, having its origin in two main motives one is the different density between Atlantic waters, cooler and less salty and the Mediterranean ones, hotter and with more quantity of salt obviously more dense and the other is a different level of waters in both sides of the strait. Both effects generate a double internal gradient of pressure in opposite directions that is translated in two great currents, one over the other. One is a superficial current of Atlantic waters towards Mediterranean Sea and another by the bottom level in counter side into Atlantic Ocean.

Both currents have an important energetic potential and the analysis about a solution by partial profit of it using systems and technology that in present time are is the objective of this paper.

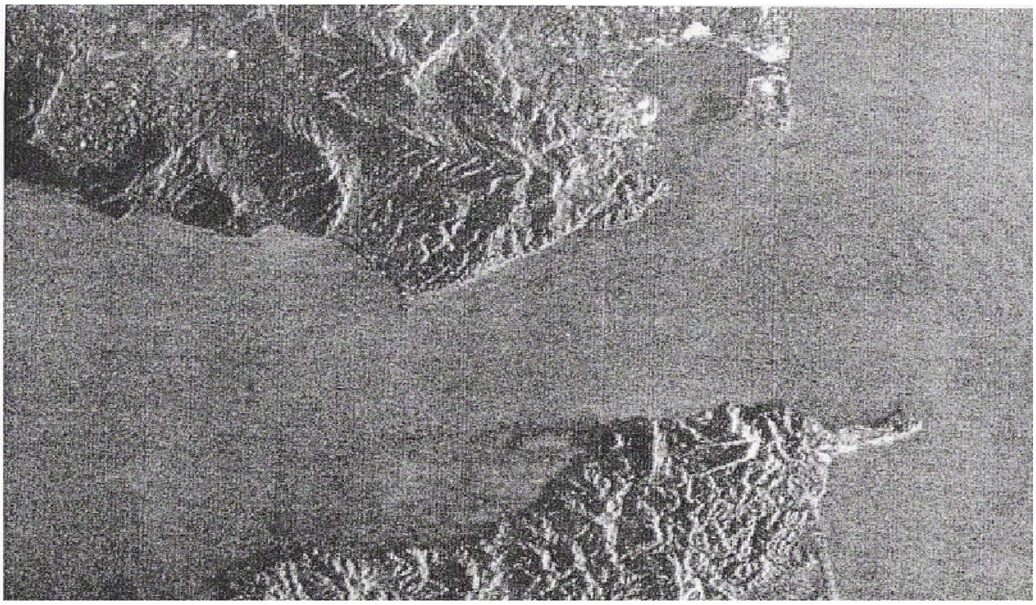

Fig.1 The Strait of Gibraltar

2. OCEANOGRAPHIC ANALYSIS

The energetic resource is making up by a double current that has its origin in the Strait by several superposing effects that are: Different density between both masses of water, the different level between the Ocean and the Sea, the tides that are generating in the Atlantic side of the strait and go into Mediterranean Sea and the currents originated by local winds.

The study and modelling of these currents obtaining the estimate of their flows rate, mean velocity and also the importance of the energy that are in the semidiurnal tide and in the sub inertial flow too, had been done by several authors as Bryden, Lacombe&Richz Luis del Cañizo and others.

From the conclusions of these studies is possible to say the following statements:

- The great part of the energy come from the tides flows
- The superficial currents are more intense than deep ones because of the strong intensity of the winds with low stability
- The current that goes out of Mediterranean Sea, has its flow concentrated in the middle part of the sea bed and erode the west wall of the Strait bottom. This current has “cuasi” constant flow and must run by a very narrow channel on the sea bed
- The current´s velocities are over 0.5 m/s (1 knot) and have ways along the Strait´s axis
- The greater rate of superficial current´s velocity is getting on the minimum width strait´s zone (Tarifa-Punta Cires Meridian)

The most important part of the energy associated to these masses of water in movement is given by semidiurnal tide flow component, getting its high intensity on the main threshold of the Strait (Punta Paloma-Punta Malabata, Meridian) because this place is the smaller section strait's zone which is about 3.6 * 10^6 m^2.

The principal part of the energy associated to the tide is into the upper Atlantic waters current and it is going along a hypothetic channel surrounding by the sea surface and one level that is situated over 100 m depth. This place in the threshold zone gets a section about 1.8*10^6 m^2. Another big part of the energy is associated to the low waters current that is going along a channel worked in the sea bed, this low flow has a transversal section on the threshold over 1.95*10^6 m^2.

3. WAY OF DEVELOPMENT

Nowadays, there are only one useful technology named Marine Currents Technology and with that it will be possible to have a significant partial exploitation of the current´s energy in the Strait without limitations for shipping and also without damages aver the marine environment and of course with a large economic profitability in a next future.

The basic principle of Marine Currents Technology is the conversion into electrical energy of the kinetic energy that these masses of water in movement have as wind turbine does with the wind flow.

The energetic potential that a caudal of Q kg/s of marine water has when the flow is crossing along a transversal section of A m^2 with an average velocity of V m/s, is given by:

$$E_c = 0.5*Q*V^2 \qquad (1)$$

But obviously not all this potential is useful and it is necessary to put a coefficient of exploitation C_p that means the rate of useful energy that the device in use gets. On this way the useful energetic potential of that caudal is given by:

$$E_{cu} = C_p*0.5*Q*V^2 \qquad (2)$$

Nowadays all the developments of submerged turbines need be placed them into the stream of water at one of the following ways:

- Mounted over a structure that lays on the sea bed with their foundations into it
- Mounted being suspended of a structure that are afloat

Thinking to exploit only the energy of the upper current it is better to choose a device from the first of these two groups and also its necessary to say that all of those turbines need a current with a mean maximum velocity over 2 m/s (4 knots) to be cost effective.

And now is necessary to choose the geographical point in the Strait where the devices for the electrical generation will be installed, the site needs the following requirements:

- Maximum current´s speed over 2.0 m/s
- No more than 80 m deeper and sea bed with smooth level to anchor the equipments foundations easy
- Relative nearness to the coastline and in this way have an easy land electrical network connections
- Far enough from, fishing waters, shipping channels or military zones

In Gibraltar´s strait there are several locations with these characteristic and some of them in the narrow zone of the Strait where the greater speeds of the currents are, one of them is situated on 6º W 33´ Tarifa-Punta Cires Meridian, it´s over 2000 m away from the Spanish coast and where there is 80 m depth and sandy sea bed. Here the upper current gets high velocities and its direction goes in a parallel way to the coastline. With the results of experimental research works that where doing in the zone is possible get an average velocity of the upper current more high than 2.0 m/s.

4. ENERGETIC ANALYSIS

At present time there are a wide variety of designs and configurations of marine currents turbines, but a large part of them are in experimental design level or building a research prototype. There are only one systems that have one industrial prototype installed into the sea, this is the “Sea Gen” developed by Marine Current Turbines LTD and the Sea Gen machine is 1.2 MW with twin turbines and it was installed in the Strangford Narrows (UK) in 2008. “Sea Gen” has a twin two-blade rotor machine and the two rotors are mounted on wing-like extensions either side of a tubular steel monopole some 3 m in diameter and the complete wing with the two power units in it can be raised above the sea surface to permit safe and reliable maintenance. The rotors have 26 m diameter and are pitch regulated turning through 180º at the change of the flow direction. A view of the machine is in Fig 2 and with this device is possible to get a C_p coefficient on 0.45 (Data from Marine Current Turbines), the rotors turns slowly no more than 30 rpm and does not offer any serious problems to fish or marine mammals, because all marine creatures that swim into strong currents of water have excellent agility and the ability to successfully avoid collisions with statics or slow moving underwater structures. The “Sea Gen” needs a special installation using jack up vessel or similar and at nowadays there are very few vessel with these characteristics and their use is very expensive.

Fig. 2. The Sea Gen prototype

Choosing this device to build the exploitation farm on the Strait on the location that shortly before it was described and in the supposing that it will possible raising 80 m depth if the monopile could have a jacket structure at the base and over 40 m large so it could be installed by a very large crane mounted over a big barge.

The array of the farm with twenty machines (forty twin blade turbines) need that the foundations of the devices have a distance between them over 400 m in the direction of the flow and 300 m in the transversal one , that display use a surface on the sea bed over 187 hectares and the twenty devices are connected between them forming one electrical net by power wires that are laying into the sea bed, the electrical energy will be transported to the onshore and connected to the electrical transport network.

The useful energetic potential that the farm has with forty turbines mounted over twenty piles, one of them with 16 m rotor diameter and supposing a water density of 1012 kg/m^3 and a mean velocity of the current over 2.0 m/s, is given by the following equation:

$$E_{cu} = 0.5*N*\pi*\rho*C_p *D^2/4 *V^3 \tag{3}$$

and the result is shown in Table 1.

Table 1: Potential of the Farm

D (m)	V (m/s)	ρ (kg/m^3)	C_p	N	E_{cu} MW
16	2.0	1012	0.45	40	14.65

If during a year has an operational period of 12.4 hours a day (half cycle of the tide), the energy that is possible gets will be:

$$\text{Energy/year} = 14.65 \text{ MW}*4526 \text{ hours/year} = 66{,}303.9 \text{ MWh} \tag{4}$$

Obviously the last result shows clearly that it is possible to set up electrical generation farms from marine current energy at the Strait and with cost effectiveness but it will be necessary develop a new generation of turbines if the wish to get a more large exploitation of the currents in the Strait is had.

This new concept today under development, that will be submerged into waters with more depth and also will be emerged to the surface only with hydrodynamics forces can be anchoring by one mooring system at any water depth and will have one turbine with a two or three blades rotor and twenty meters of diameter or more.

One of these new devices is the Spanish project GESMEY, Fig 3, which has a three fixed pitch blades rotor assembled in a central pod that has the power take off components and the ancillary systems. All it is supported by a structure with Y shape that is formed by three columns that have one torpedo at the each one end.

The generator can be submerged or be emerged by itself and when it is floating put the rotor at open air for periodic maintenance and when it will be done itself go into the sea getting the work depth only taking the exact quantity of water ballast into the tanks without the necessity of a lit vessel and also can be towed to the shore by a tug vessel which it will be necessary.

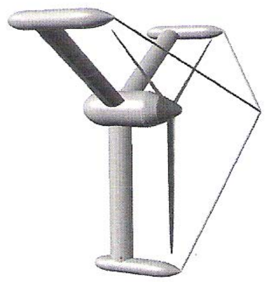

Fig. 3: The generator GESMEY

5. CONCLUSIONS

- Gibraltar´s Strait is a renewable energy source on a very large scale that at present time is not use at all.
- Now with the marine currents technologies that at present time are, it´s possible the exploitation of the currents that on the Strait are, only in several places that have no more than 80 m depth and mean velocity of the water over 2,0 m/s.
- In a very next future and with the new technologies that now are planning and developing will be possible to get very cost effective farms that will be exploit the currents in the Strait in many places without the restrictions of 80 m depth.
- There are many zones in Gibraltar´s Strait near the coast of Spain or Morocco, when the installations of these power generations farms has technical and economic high interest.
- The development of new generators that are based on ship´s propulsion system POD type will be getting a better exploitation of the Strait energetic resource.

It is sure that in next year's will see the first project with this marine currents technology to exploit a part of this natural energetic resource.

REFERENCES

[1]. Bedar R. (2008) - ***Technology Characterization Ocean Wave and Tidal Energy***, GlobalMarine Energy Conference, New York (USA)

[2]. Bahaj A.S., Myers C. (2004) - ***Analytical estimates of the energy yield potential from the Alderney Race (Channel Islands) using marine current energy converters,*** pp 1931-1943 Renewable Energy Vol 29 Elseiver (UK)

[3]. Fraenkel P.L. (2006) - ***Marine Current Turbines: pioneering the development ofmarine kinetic energy converters,*** pp 159-169 Proc. IMechE Vol 221 Part A J. Power and Energy (UK)

[4]. Juanes Gonzalez J.M. (2008) - ***El potencial energético de las corrientes marinas en el estrecho de Gibraltar"*** Tesis Doctoral Universidad Politécnica de Madrid (UPM) (Spain)

[5]. López Piñeiro A., Nuñez Rivas L.R., Juanes Gonzalez J.M. (2008) -***Tecnologías para el aprovechamiento de las corrientes marinas,*** Proceedings 47º Congreso de Ingeniería Naval e Industria Marítima, Palma de Mallorca (Spain)

[6]. López Piñeiro A. (2009) - ***Nuevos generadores para el aprovechamiento de las corrientes marinas,*** pp 12-15 Revista UPM Madrid (Spain)

[7]. López Piñeiro A. (2007) - ***Sistema sumergible para el aprovechamiento energético de las corrientes marinas, Patente*** P200700985/4 BOPI 16/07/08 (Spain)

[8]. Nuñez Rivas L.R., Herreros Sierra M.A. (2006) - ***Gibraltar´s Strait a marine renewable energy source,*** Proceedings World Maritime Technology Conference WMTC 2006 London (UK)

[9]. Nuñez Rivas L.R. (2009) - ***Las energías renovables marinas***, pp 7-12 Tecnologías para el aprovechamiento de la energía de las olas y de las corrientes marinas ISBN-978-84-612-9269-1 Fundación INNOVAMAR Madrid (Spain)

[10]. Savage A. et al. (2007) - ***Tidal Technologies Overview***, Sustainable Developments Commission ENTEC UK Limited, Bristol (UK)

COMPARATIVE ANALYSIS BETWEEN HYDROELECTRIC DEVELOPMENTS AND TIDAL STREAM DEVELOPMENTS

[1]NUÑEZ-RIVAS LUIS R., [1]AMABLE LOPEZ-PIÑEIRO, [1]LEO TERESA J., [2]MORAN JOSE L.

[1]*Universidad Politécnica de Madrid, Spania,* [2]*Siemens S.A., Spania*

The Hydroelectric Developments (HD) technology is very well known due to the fact that it has been studied during the last 120 years. To generate electricity from the water in the rivers or dams, different technologies have been developed but at the end only four of them are used: Pelton, Francis, Kaplan and Bulb turbines. Those technologies have had a large development although, at present, scientists and engineers are working hard to increase their efficiency above 95% in some cases. On the other hand, the Tidal Stream Developments (TSD) technology is at the beginning of its life and the existing developments are mainly used as a test to improve the technology than to generate and sell electricity. Nowadays a number of different technologies are being studied because practically each manufacturer has developed its own solution. The objective of this paper is to show analogies and differences between Hydroelectric Developments and Tidal Stream Developments as technologies suitable to generate electric power from the marine currents energy.

Keywords*:* Marine renewable energy sources, Exploitation of marine currents energy, Hydraulic Developments technology*.*

1. INTRODUCTION

The Hydroelectric Development (HD) technology is very well known due the fact that it has been studied during last 120 years. The first Hydroelectric Power Plant (HPP) was constructed in 1882 in Appleton, Fox river, EEUU; it was a small HPP with a head of only 3 m and an output of 25 kW. The first big Hydroelectric Power Plant (HPP) was built in Niagara with a head of 54 m and 10 groups with a total output of 36,700.00 MW. Although during this period different technologies to generate electricity have been developed, at the end only four of them are being used: Pelton, Francis, Kaplan and Bulb turbines. Those technologies are very well known although, nowadays, engineers are working hard to increase their efficiency above 95% in some cases.

On the other hand, the Tidal Stream Developments (TSD) technology is at the beginning of its life and the existing developments are mainly used as a test to learn more and improve the technology than to generate and sell electricity (Bedar, 2008). At present, there are more than sixty devices into the Tidal Stream generation technology and the majority of the concepts use a horizontal axis rotational method of generation. There is no evidence that the industry is converging towards a single configuration and there is only one device, The Marine Current Turbine’s Sea Gen with 1.2 MW generation power, located into the sea at the Strangford Narrows (UK), connected to the electrical grid.

The objective of this work is to show analogies and differences between HD and TSD technologies as a possible application to the conception and development of electrical power generation from marine currents energy, giving an overview to the steps and requirements that the development of a power plant must have.

2. GLOBAL STUDY OF A PROJECT OF A NEW POWER PLANT FOR THE EXPLOITATION OF A RENEWABLE ENERGY SOURCE

To carry out a Hydroelectric or a Tidal Stream Plant Project (López Piñeiro, 2008), the following issues must be taken into account:

- Location
- Technology used (type and size of the turbines)
- Potential Power
- Geotechnical, Geological and Seismic studies
- Topographical or Bathymetric studies
- Hydrological or Oceanographic studies
- Environmental impact study
- Energy generated, plant factor
- Transmission line and connection to the electrical grid
- Selling the energy generated

A comparative description of each part of the global study is done in the following sections.

3. LOCATION

Once an ideal place to develop a Hydroelectric power plant is chosen, logistics is very important in order to check its feasibility. A study must be performed to find out the type and quality of roads to reach the power plant and the water intake, the amount of new roads to be made, the capacity of the bridges according to the size and weight of the components to be transported, the distance from the nearest place where the turbines, transformers and other equipment can arrive from the manufacturer via ship, train, lorry or plane. For the construction and operation of the Hydroelectric Power Plant it can be also important the time needed to arrive at the site from the nearest airport by car, in some places of South America it can take up to 12 hours, and the distance to the nearest village in which people can live. Besides, it is very important to define the weather conditions of the locations because in several places it is not possible to arrive to the site during three or four months per year due to the snow (the Alps and other mountains). In some other cases, it is not possible to work during the construction period more than 200 days per year due to the rain (Chiloé Island, Chile).

In the case of a Tidal Stream power plant the first step will be the selection of a location offshore, but not very far from the shore, where the stream has a good mean velocity, the depth is not very large and the sea bed is plane enough (Bahaj, 2004). A detailed study of the weather conditions in the area is required to find out the theoretical number of days suitable for the assembly in site during the construction period and for the maintenance operations. In this case the logistics study is especially important, so it is necessary to define the port from which all equipments will be transported to the site and from which the maintenance and operation will be coordinated and, sometimes, when the nearest port is not big enough, different ports will be needed.

4. TECHNOLOGY USED (TYPE AND SIZE OF THE TURBINES)

For Hydroelectric Developments (HD), as said before, there are four main technologies used in the construction of a hydroelectric power plant, i. e., Pelton, Francis, Kaplan and Bulb turbines. Usually, the most appropriate technology to be used in each case is clear. Nevertheless there are always some conditions in which two of them can be used and technical and economical analyses must be made. The technology selection depends mainly on the volume flow rate (m^3/s) and the head (m) of the exploitation. Sometimes other parameters, such as the specific speed, the capacity for maintaining a high efficiency with several volume flow rate or head values during a period, can be of great influence.

As an example, a way to choose the most suitable technology as a function of the volume flow rate and the head of the exploitation site is shown in Fig.1

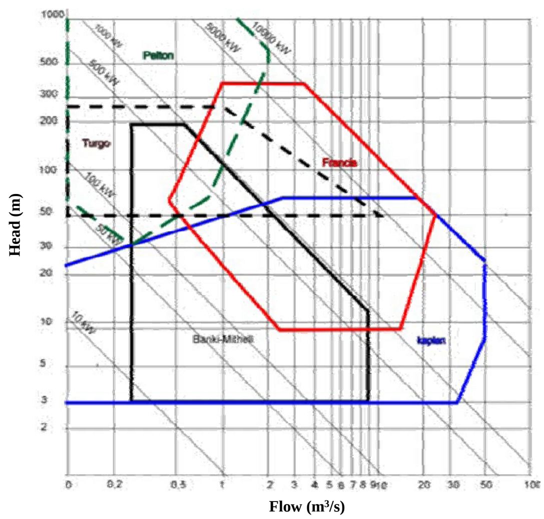

Fig. 1 Turbine selection as a function of volume flow rate and net head

In the case of Tidal Stream Developments (TSD) the situation is completely different (Savage, 2007), as many designers and developers are pursuing a wide variety of configurations. This is because this technology is at the beginning of its life and developments are used more as a test to learn and improve the technology than to generate and sell electricity. The future progresses will define the surviving ones. Surely, in the next future there will be a technology adapted to each development characteristics but, at present, there are over sixty devices into the first generation of this technology. Although the majority of the concepts use a horizontal axis rotational method of generation there are others with a vertical axis configuration (Ponte di Archimede International, 2010). In both cases there are devices with or without a duct to accelerate the flow or, in some cases, multiple open rotors with horizontal axis to maximise the installed generating capacity on each foundation of the machine. Some of them are fixed to the sea bed and some others are floating devices anchored to it; in some cases it is necessary to dive to do the maintenance and some others have solutions to get out the turbine from the water to do this task.

There is only one device, shown in Fig.2, the Marine Current Turbine's Sea Gen with 1.2 MW generation power, that it is located into the sea and connected to the electrical grid (Fraenkel, 2006).

Fig. 2 The Sea Gen prototype

The other technologic concepts are at different stages of development but not on industrial exploitation and all of them, Marine Current's sea Gen included, are not capable to exploit the currents that are more than 40 meters depth.

The most important parameters required to define the technology to be selected are the water speed, the depth of the selected site, the quality of the sea bed, the distance to the shore, the weather conditions in the surface, the maximum size of waves and also the environmental requirements.

Without trying to write an exhaustive listing, some of the companies that are working with Tidal Stream Developments at present are Marine Current turbines Ltd. (Marine Current Turbines, 2010), Blue Energy (Blue Energy, 2010), Verdant Power (Verdant Power, 2010), Hydro Venturi (Hydro Venturi, 2010), Open Hydro (OpenHydro, 2010), Lunar Energy (Lunar Energy, 2010), Hammerfest Strom, Tidal generation Ltd., etc. Their different prototypes can be seen in their web pages.

In the next future a second generation of devices for harnessing marine currents energy with a best performance will be ready. One of these is the Submarine Electrical Generator with Y shape framework (GESMEY), shown in Fig. 3. It has been developed in collaboration between a research team from the E.T.S. Ingenieros Navales of the Universidad Politécnica de Madrid (UPM), Spain, and the Foundation Technological Centre SOERMAR, Spain. The project is supported by funds from the Ministry of Industry, Tourism and Commerce of the Spanish Administration.

The Generator GESMEY (López Piñeiro, 2007, 2009) can work into deep waters getting the right depth by itself by only using hydrodynamic forces that allow it to go to the surface or to dive without any other help. GESMEY has not fixed foundations on the sea bed and it is placed in an intermediate level between the surface and the sea bed through a simple and cheap anchor system that only needs ropes and buoys. Besides, the entire device (generator and anchor system) will be able to be removed without any damage to the marine environment and to reach currents below 50 meters depth.

5. POTENTIAL POWER

The gross power that can be obtained in **Hydroelectric Developments** is related to the available water volume flow rate Q and to the head H. To calculate the power P and the energy generated E during a given period of time t the following equations apply:

$$P = \rho \cdot g \cdot Q \cdot H \tag{1}$$

$$E = \rho \cdot g \cdot Q \cdot H \cdot t \tag{2}$$

where ρ is the density and H stands for the head.

The maximum power that can be obtained is:

$$P_{\max} = \eta_T \cdot \eta_G \cdot \rho \cdot g \cdot H_N \tag{3}$$

being H_N the net head, η_T the hydraulic efficiency (around 92%, in some cases is possible to reach 95%) and η_G the generator efficiency (around 96%).

Therefore the net energy generated results:

$$E_{net} = \eta_T \cdot \eta_G \cdot \rho \cdot g \cdot \sum_i \left(Q_i \cdot H_{N_i} \cdot t_i \right) \tag{4}$$

As shown by equation (3), the maximum power is proportional to the volume flow rate and to the head.

The gross power that can be obtained in **Tidal Stream Developments** (Nuñez Rivas, 2009) is related to the velocity of water V and to the diameter of the rotor. The power and the energy generated during a given period of time can be obtained through the following equations:

$$\begin{aligned} P &= \frac{1}{2} \rho \cdot Q \cdot V^2 \\ &= \frac{1}{2} \rho \cdot A \cdot V^3 \end{aligned} \tag{5}$$

$$E = \frac{1}{2} \rho \cdot A \cdot V^3 \cdot t \tag{6}$$

where A stands for the rotor cross sectional area.

The maximum power to be obtained in this case is:

$$P_{\max} = \frac{1}{2} Cp \cdot \rho \cdot A \cdot V^3 \tag{7}$$

being Cp a coefficient power whose value can reach 0.44 (Fraenkel, 2006).

The net energy generated is:

$$E = \frac{1}{2} Cp \cdot \rho \cdot A \cdot \sum \left(V_i^3 \cdot t_i \right) \tag{8}$$

As can be seen, the maximum power is proportional to the area and to the cubic value of the velocity.

In a Hydroelectric Development small variations of the volume flow rate or the head will lead to small variations of the power and generated energy but in a Tidal Stream Development a small variations in the velocity of water will give rise to significant power and generated energy variations.

Fig. 3 The generator GESMEY

6. GEOTECHNICAL, GEOLOGICAL AND SEISMIC STUDIES

Civil works in Hydrodyelectric Developments are often important, usually taking more than 60% of the total investment. Although it depends on the case, the following structures must be constructed: water intake and barrage, dam, tunnels, channels, power house, roads, etc. To assure the viability of the construction, geotechnical and geological studies must be accomplished because different problems such as unstable slopes, slide prone geological formation, faults and liquefaction prone soils, etc. can occur. It is necessary to evaluate the soil suitability for foundations, as well as the mechanical and physical characteristics of rocks for underground works.

In the pre-feasibility study geologic maps must be analyzed and in the feasibility phase more detailed studies such as refraction seismic techniques and electrical profile exploration must be performed. Before starting to build the plant, a core recovery for soil samples and permeability test can be required in some zones.

In some locations, seismic assessments must be also accomplished in order to design the structures and foundations accordingly to the maximum earthquakes and accelerations expected in the area.

Although in a Tidal Stream Development civil works are not so important, due to the high efforts involved and the hostile environment, a geological, geotechnical and seismic study should be accomplished. The requirements will vary depending on the selected technology but a firm ground must be selected to anchor or to arrange the foundation of the device in use.

7. TOPOGRAPHICAL OR BATHYMETRIC STUDY

A topographical study in Hydroelectric Developments is necessary. This way, it is possible to define the head or dam capacity and the exact locations of all the infrastructure of a hydroelectric plant such as barrage, conducts, power house and others. Also, a topographical study must be made to project the new roads required to transport all the devices and components of the future plant.

In a Tidal Stream Development it is necessary to know exactly the profile of the sea bed area where the devices and other components will be located and this is the reason why a bathymetric study must be done.

8. HYDROLOGICAL OR OCEANOGRAPHIC, STUDY

Obviously one of the most important aspects to know is the hydrological behaviour of the river or damp, because it will define the expected energy production during the life of the project and consequently the expected revenues during the commercial exploitation.

Similarly, an oceanographic study of the marine zone where the marine current energy exploitation plant will be located is required. This is the only way to know the exact profile of velocities and therefore to evaluate the expected energy production.

9. ENVIRONMENTAL IMPACT STUDY

Civil works in Hydroelectric Developments have an important environmental impact because a number of structures such as barrages, tunnels, channels, roads and others facilities must be constructed. Obviously, it is essential to know the impact of those new constructions on the valley basin, the flora, the fauna and the human activities. Also, it is necessary to analyze the impact in the river conditions of the usage of the water and the reduction of natural water flow in some areas of the river. The environmental impact study will be always a must in order to get the necessary authorizations.

In the case of Tidal Stream Development, although there is almost no experience, it can be said that the environmental impact of the devices will be very low. Nevertheless, an environmental study of the impact of the devices on several marine elements or activities as the field of vision, noise, shipping, military use, fishing, tidal fluxes, salinity, water temperature must be made. Also, the impact of transport, construction and assembling, operation, maintenance and removing of the devices on the marine fauna and flora and especially on the marine mammals must be studied.

10. ENERGY GENERATED, PLAN FACTOR

In Section 5, the equations governing the energy generated by a hydro electrical development or also by a tidal stream one are given. Detailed analyses including hourly, daily, monthly and yearly production must be made.

In order to evaluate the plant, it is defined the Plant Factor, that is the relation between the average energy generated during a given period and the time in service during the same period.

11. TRANSMISION LINE AND CONNECTION TO THE ELECTRICAL GRID

In a Hydroelectric Development the transmission line and the connection to the electrical grid are the same that for other conventional power plants as combined cycle, thermal or nuclear ones.

This is not valid in the case of a Tidal Stream Development because an especial wire must be used to construct the submerged grid. This type of wire allows transporting the energy as a high voltage direct current (HVDC) from the location to the sea shore. Onshore there will be an electrical substation from where it will be connected to the main electrical grid of the country as conventional plants.

12. SELLING THE ENERGY GENERATED

Nowadays the electricity generated by a Hydroelectric Power Plant is sold, depending on the country, through a Power Purchase Agreement (PPA), feed-in tariff or selling to the pool.

As the technology in use is mature, normally the need of support is small and the selling price is close to the one received by non renewable energies.

This is not valid for Tidal Stream Developments, as the technology is at the beginning of its life. In order to make the project financially feasible, it will be necessary to sell the electrical energy with a special fare enough to allow the share holders to make the large investments required. In the future, when the technology is mature enough, the Tidal Stream Power Plants will be a feasible and economic reality as the Hydroelectrical Power Plants are now.

13. CONCLUSIONS

- The Hydroelectric Developments have a mature technology and now they are a very important source into the electrical generation's mix in many countries.
- The electricity that now is generated by Hydroelectric plants, depending on the country and the size, needs only a reduced economical support and it is generally sold in the electric market at pool price.
- The Tidal Stream technology is at the beginning of its life and it is not possible to get a commercial use of it.
- It is sure that in the next years the first project with this marine currents technology to exploit a part of this natural energetic resource will be seen.
- When the first farm to exploit this renewable energetic source will be constructed, the electricity generated will need a special fare to recover the large investments that now the share holders of the companies and the governments of the countries need to made.

REFERENCES

[1]. Bedar R. (2008) - ***Technology Characterization Ocean Wave and Tidal Energy***, Global Marine Energy Conference, New York (USA).
[2]. Bahaj A.S., Myers C. (2004) - ***Analytical estimates of the energy yield potential from the Alderney Race (Channel Islands) using marine current energy converters***, pp 1931-1943 Renewable Energy Vol 29 Elseiver (UK).
[3]. Blue Energy, (2010), www.bluenergy.com
[4]. Fraenkel P.L. (2006) - ***Marine Current Turbines: pioneering the development of marine kinetic energy converters***, pp 159-169. Proc. IMechE Vol 221 Part A J. Power and Energy (UK).
[5]. Hydro Venturi, (2010), www.hydroventuri.com
[6]. López Piñeiro A., Nuñez Rivas L.R., Juanes Gonzalez J.M. (2008) - ***Tecnologías para el aprovechamiento de las corrientes marinas***, Proceedings 47º Congreso de Ingeniería Naval e Industria Marítima, Palma de Mallorca (Spain)
[7]. López Piñeiro A. (2009) - ***Nuevos generadores para el aprovechamiento de las corrientes marinas,*** pp 12-15 Revista UPM Madrid (Spain)
[8]. López Piñeiro A. (2007) - ***Sistema sumergible para el aprovechamiento energético de las corrientes marinas***, Patente P200700985/4 BOPI 16/07/08 (Spain)
[9]. Lunar Energy, (2010), www.lunarenergy.co.uk
[10]. Marine Current Turbines, (2010), www.marineturbines.com
[11]. Nuñez Rivas L.R. (2009) - ***Las energías renovables marinas,*** pp 7-12 Tecnologías para el aprovechamiento de la energía de las olas y de las corrientes marinas, ISBN-978-84-612-9269-1 Fundación INNOVAMAR Madrid (Spain)
[12]. OpenHydro, (2010), www.openhydro.com
[13]. Ponte di Archimede International, (2010), www.pontediarchimede.it
[14]. Savage A. et al. (2007) - ***Tidal Technologies Overview***, Sustainable Developments Commission ENTEC UK Limited, Bristol (UK)
[15]. Verdant Power, (2010), www.verdantpower.com

EXERGETIC STUDY OF NAVAL TECHNICAL WATER GENERATOR

OMOCEA ION

Constanta Maritime University, Constanta, Romania

This paper presents the usual methods of sea water distillation at under-atmospheric pressure using the heat from the main engine cooling water system. In the first case, pre-heated condensation sea water is introduced in the technical water generator. In the second case, the sea water supply is not pre-heated.

***Keywords**:* exergy, desalination, technical water, exergetic analysis.

1. INTRODUCTION

Water needs on board is covered by the distiller or by boarding from the shore.

Flow of energy recovered from cooling water is determined by the needs of water and is made in the naval technical water generator.

We will study two cases:

- in the first case, condensation sea water, preheated is introduced in the technical water generator;
- in the second case, the sea water supply is not preheated.

The pitch of recovery in these plants is about 0.35 of cilyder cooling water energy.

All ships used technical water generator which works by vacuum (90% to 95%). The vacuum is created by an ejector.In this case the vaporization temperature is around 45 degrees Celsius.

2. ANALYSIS OF DESALINISATION SYSTEM WITH PREHEATING WATER SUPPLY

2.1.Presentation of the distillation plant

In this installation the supply water is preheated in condenser.

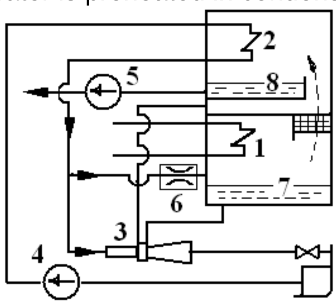

Figure 1. Distillation plant with preheating

1. evaporation system
2. condensing system
3. ejector
4. supplay pump for condensation system
5. condensate pump
6. adjustment valve
7. brine
8. condensed (distilled water)

2.2. EFFICIENCY AND LOSSES

Thermal parameters for calculation are in Table 1.

Table 1. Calculation of parameters

No.	Agent Type	Mass $\dot{m}$ $\left[\frac{Kg}{s}\right]$	Temperature t $\left[{}^{0}C\right]$	Exergetic Flow E $\left[kW\right]$
1	Cooling water input	8.8	75	375
2	Cooling water outlet	8.8	58	301
3	Sea water for cooling	12.5	34	23

Thermal efficiency η_t considering that the useful heat energy of vaporization of seawater.

$$\eta_t = \frac{\dot{m}_{tw}\lambda}{\dot{H}_1 - \dot{H}_2} = \frac{0.1 \cdot 2408}{8.8(314-242)} = 0.38 \tag{1}$$

Where:

$\dot{m}_{tw}$ -mass flow of technical water

λ -latent heat of vaporization of seawater

$\dot{H}_1$ -enthalpy flow for cooling water at 75 degrees

$\dot{H}_2$ -enthalpy flow for cooling water at 58 degrees

Utility system is generating of technical water. Exergetic flow for this water is insignificant. For this reason the exergetic efficiency for technical water is unsuitable.

We can make an exergetic characterization of the system in terms of loss of evacuation.

Exergetic relative losses for water discharged into the environment are:

$$\overline{\pi}_{outlet} = \frac{\dot{E}_{sc}}{\dot{E}_{ci} - \dot{E}_{co}} = \frac{23}{74} = 0.31 \tag{2}$$

Where:

$\dot{E}_{sc}$ -exergetic flow of sea water for cooling

$\dot{E}_{ci}$ -exergetic flow for cooling water input

$\dot{E}_{co}$ -exergetic flow for cooling water output

3. ANALYSIS OF DESALINATION SYSTEM WITHOUT PREHEATED WATER SUPPLY

3.1. PRESENTATION OF THE DISTILLATION PLANT

In this installation the supply water is not preheated in condenser.

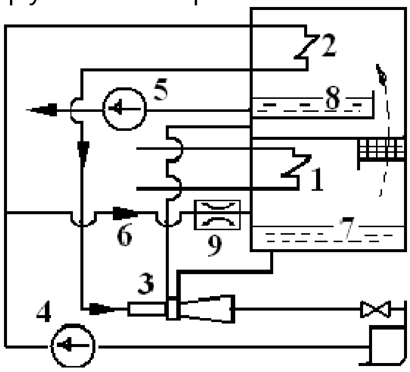

Figure 2. Distillation plant without preheating

1. evaporation system
2. condensing system
3. ejector
4. supplay pump for condensation system
5. condensate pump
6. sea water supply
7. brine
8. condensed (distilled water)
9. adjustment valve

3.2. EFFICIENCY AND LOSSES

Thermal parameters for calculation are in table 2.

Table 2. Calculation of parameters

No.	Agent Type	Mass $\dot{m}\left[\frac{Kg}{s}\right]$	Temperature t $\left[{}^{0}C\right]$	Exergetic Flow E $[kW]$
1	Cooling water input	8.8	75	463
2	Cooling water outlet	8.8	54	343
3	Sea water after ejector	12.3	36	51
4	Sea water for cooling	12.3	33.5	19

Thermal efficiency η_t considering that the useful heat energy of vaporization of seawater.

$$\eta_t = \frac{\dot{m}_{tw}\lambda}{\dot{H}_1 - \dot{H}_2 + \dot{H}_3 - \dot{H}_4} = \frac{0.1 \cdot 2408}{8.8(314-225)+12.3(151-125)} = 0.21 \qquad (3)$$

Where:

$\dot{m}_{tw}$ -mass flow of technical water

λ -latent heat of vaporization of seawater

$\dot{H}_1$ -enthalpy flow for cooling water at 75 degrees

$\dot{H}_2$ -enthalpy flow for cooling water at 54 degrees

$\dot{H}_3$ -enthalpy flow for sea water after ejector at 34.5 degrees

$\dot{H}_4$ -enthalpy flow for sea water at 30 degrees

Exergetic relative losses for water discharged into the environment are:

$$\overline{\pi}_{outlet} = \frac{\dot{E}_{sc}}{\dot{E}_{ci} - \dot{E}_{co}} = \frac{51}{120} = 0.42 \qquad (4)$$

Where:

$\dot{E}_{sc}$ -exergetic flow of sea water for cooling

$\dot{E}_{ci}$ -exergetic flow for cooling water input

$\dot{E}_{co}$ -exergetic flow for cooling water output

4. CONCLUSIONS

Analysis of two methods of desalination were discussed in this paper. These methods are with pre-heated and without pre-heated sea water supply.It was shown the superiority of the first method.

In the first case thermal efficiency is higher than the second case, respectively 38% versus 21% .

Also, in the first case the exergetic losses are lower comparing with the second case: 31% versus 42%.

REFERENCES

[1]. *** ***Documentația motoarelor Sulzer***

[2]. *** ***Documentația motoarelor M.A.N.***

[3]. Nerescu, I., Radcenco, V., - ***Analiza exergetica a proceselor termice***, Editura Tehnica, Bucuresti, 1970

[4]. Omocea I. – ***Procese in motorul cu aprindere prin comprimare, tratate cu ajutorul termodinamicii ireversibile*** - Ed. Paideia, Bucuresti, 2003

[5]. Panait T. – ***Cercetari privind recuperarea enrgiei termice din apa de racire a motoarelor termice navale*** - Teza de doctorat, Galati, 1993.

[6]. Porneala S., Beju, C., ***Reducerea pierderilor exergetice prin utilizarea regeneratorului de caldura intre solutii la instalatia frigorifica cu absorbtie***, Revista de Termotehnica, anul V, nr. 1/2001

A WAY FOR INVESTIGATION OF ELECTROMAGNETIC TRANSITIONAL DYNAMIC PROCESSES IN SHIP ELECTRICAL POWER SYSTEM

[1]PETKOV PETKO, [1]NEDEV MARIN

[1]*Nikola Vaptsarov Naval Academy, Varna, Bulgaria*

There is an untraditional way, connected with analysis and estimation of electromagnetic transitional dynamic processes in ship electrical power system. The way is based on image space vector theory and gives an opportunity to solve complicated electromagnetic problems and problems, connected with education. Including of such way in investigation the problems in "Ship Electrical Power Supply" is much more clear and easier. The analysis and estimating of complicated transitional and dynamic processes in ship electrical power systems becomes easier and clear, especially with tendency of widely speeded and used power electronics units in ship electrical equipment.

Keywords: synchronous generators, semiconductor converters, quality of electrical power, electromagnetic compatibility, image space vector, dynamic transitional processes.

1. INTRODUCTION

A tendency of widely using of power electronic controlled electrical drives and electrical power converters as a part of ship electrical power system and equipment take a place new engineering problems, connected to electromagnetic compatibility between electrical power sources and electrical consumers. Those problems become more and more complicated when the generators and the consumers powered by electronic nonlinear power converters have the same, equivalent power. None linear consumers disturb the normal work of all ship electrical power system: sources, bars, all other linear consumers, converters, automation systems EST.

When the generator with limited power sources nonlinear consumer with huge power the quality of electrical power goes low and electromagnetic compatibility depends on multi factors and equations. The most important characteristic in such cases is Total Harmonic Distortion that means instead of firs main harmonic there is a place of high harmonics. The curve deviation of the voltage is widely depending on converter load and automation system.

The analysis and estimation of the electromagnetic processes by using classical methods gives serious problems in investigation and research work. The main used method of Park is not clear enough. It needs special resources too. The electrical dynamic processes in the ship electrical power system are endless. Starting/stopping of any consumer starts dynamic processes with different complicity.

2. THE SOLLUTION

In this paper is used the image space vector, permitting the complex analysis and estimating of dynamic processes in ship electrical power plant. Complicated dynamic processes with different souses and consumers, but with equivalent electrical power could be analyzed more easily. Special attention we paid on cases connected with linear sources and nonlinear consumers. For example synchronous generators and power electrical drives, driven by three faze power electronic converters as thyrystor inverters, synchroconverters, cicloconverters and so.

In case of normal work of synchronous generator and three faze controlled thyristor bridge rectifier as a part of power nonlinear consumer we could use classic mathematical models [3], described processes in all possible variants of changed load. Traditionally processes are described by using of computers and simulating methods without physical clarity. There is no clear common view of analytic solution.

Here we are represented a method of image space vector and reswitching functions for synchronous generator and three faze bridge rectifier in vector type.

The model of synchronous generator is described in "dg_o" rectangular coordinate system vector, rotated with synchronous speed. The model of rectifier is described in static/unmoved coordinate system "$\alpha\beta_o$". Connected both math models together describes by system (1):

$$\left\| \begin{aligned} & -\overline{U}_{dg} = \frac{d}{dt}\overline{\psi}_{dg} + j\overline{\psi}_{dg} + r\overline{I}_{dg} \\ & \overline{U}_f = \frac{d}{dt}\overline{\psi}_{fdg} + rf\overline{I}_f \\ & \overline{\psi}_{dg} = X\overline{I}_{dg} + Xm\overline{I}_f \\ & \overline{\psi}_{fdg} = Xm\overline{I}_{dg} + X_f\overline{I}_f \\ & \overline{I}_{\alpha\beta} = \overline{И}.I_d \\ & \overline{I}_{\alpha\beta} = \overline{I}_{dg}.e^{jt} \\ & U_{\alpha\beta} = U_{dg}.e^{jt} \end{aligned} \right. \qquad (1)$$

Where: - $\overline{U}_{\alpha\beta}$, $\overline{U}_{dg}$, $\overline{U}f$ are the voltage image vectors of synchronous generator and exiting voltage in "$\alpha\beta_o$" and "dg_o" coordinate systems;

- $\overline{\psi}_{dg}, \overline{\psi}_{fdg}$ are image vectors of magnetic forces of generator stator and rotor;
- $\overline{I}_{\alpha\beta}, \overline{I}_{dg}, \overline{I}f$ are image vectors stator current in "$\alpha\beta_o$" и "dg_o" coordinate system, and exiting current of generator;
- rx, rf, xf, xm are active and reactive resistances of stator and rotor wounds, inductive resistance;
- $\overline{И}$ commutating image vector;
- I_d Direct current, sourced by rectifier.

All the values in system of differential equations (1) are in relative value.

After using the Laplace transformations for solving, system (1) becomes algebraic. For stator voltage and exiting voltage is founded:

$$\left\| \begin{aligned} &\overline{U}_{dg}(p) = \left[r + (j+p)X\right].\overline{I}_{dg}(p) + Xm(j+p)\overline{If}\;(p) \\ &\frac{\overline{U}f}{p} = Xm.p.\overline{I}_{dg}(p) + (rf + p.Xf\;).\overline{I}f(p) \end{aligned} \right. \tag{2}$$

After replacing the current from (2) for stator voltage of synchronous generator could be founded:

$$-\overline{U}_{dg}(p) = \left[(r+jX) + pX^{I} - \frac{Xm^2}{Xf^2}.rf(1-jT)\left(1-\frac{1}{1+pT}\right).\overline{I}_{dg}(p) + \frac{Xm}{Xf}\left(1-\frac{1-jT}{1+pT}\right).\overline{U}f\;(p)\right] \tag{3}$$

The voltage depends on exiting voltage and load current only. The dependence is very clear and very easy to use.

Where: $X^{I} = X - \frac{Xm^{2}}{Xf}$

$T = \frac{Xf}{rf}$

Following the back Laplace transformation of (3) for synchronous generator voltage could be written:

$$-\overline{U}_{dg}(t) = (r+jX)\overline{I}_{dg}(t) + X^{I}\frac{d}{dt}\overline{I}_{dg}(t) - \frac{Xm^2}{Xf^2}.rf.(1-jT).\left(1-\frac{e}{T}\right).\overline{I}_{dg}(t) + \frac{Xm}{Xf}\left(1-\frac{1-jT}{T}.e^{-Tt}\right).\overline{U}f(t) \tag{4}$$

In case of kvass stable state/mode of synchronous generator, going trough “$\alpha\beta_o$” coordinate system equation (4) riches the following description:

$$-\overline{U}_{\alpha\beta}(t) = (r + jX^{I})\overline{I}_{\alpha\beta}(t) + X^{I}\frac{d}{dt}\overline{I}_{\alpha\beta}(t) + \frac{Xm}{Xf}.\overline{U}f(t)e^{jt} \tag{5}$$

Or

$$\overline{U}_{\alpha\beta}(t) = -\frac{Xm}{Xf}\overline{U}_{f}(t).e^{jt} - (r + jX^{I})\overline{I}_{\alpha\beta}(t) - X^{I}\frac{d}{dt}\overline{I}_{\alpha\beta}(t) \tag{6}$$

The stator wound alternative current of the synchronous generator depends on only direct rectifier current [1].

$$\overline{I}_{\alpha\beta} = \overline{И}.Id$$

In such case the equation (6) gives the full analytic dependence in common view. The common solution give access rights to found synchronous generator voltage, loaded by rectifier, calculating the engine parameters, load current of converter and depth of its control.

If the parameters of synchronous generator in relative numbers are: $r = 0{,}02, x = 1{,}60/, xf = 1{,}63/, xm = 1{,}50$, the parameters of comparative transformer are: $x_T = 0{,}035/, r_T = 0{,}003$, rectifier current is I_d = 1,0 if the fire angle of thyristors control is α = 0°,30° or 60° are drown followed of image current and voltage vectors, showed on Fig. 1a, b and c.

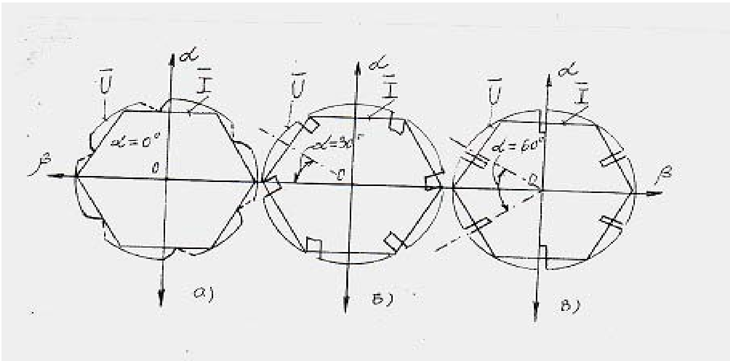

Fig.1. Voltage and current root graphs

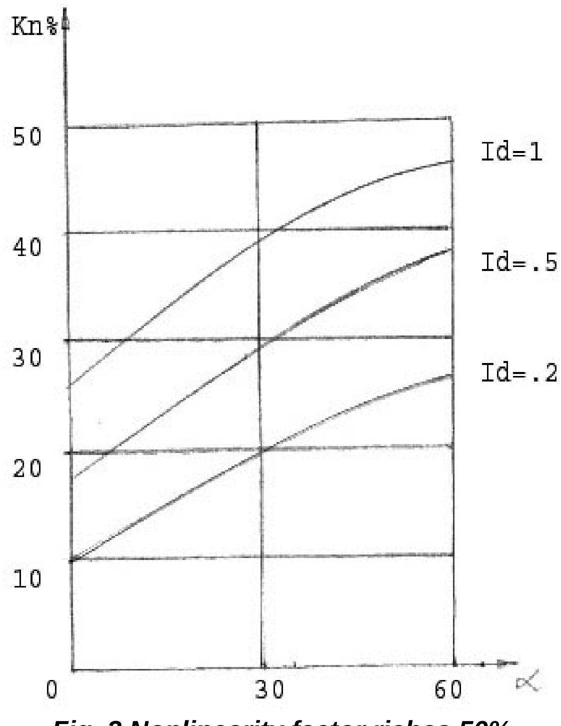

Fig. 2 Nonlinearity factor riches 50%

After geometric dividing root graphs of the voltage in the vertical and horizontal projection in coordinate system it could be calculate the faze voltages from image space vector. Following Fourier analysis of faze voltages it could calculate generated voltage harmonics, total harmonic distortion nonsynusoidality factor K_n.

For this example are calculated K_n in function of load and fire angle of controlled converter and are drown on Fig. 2.

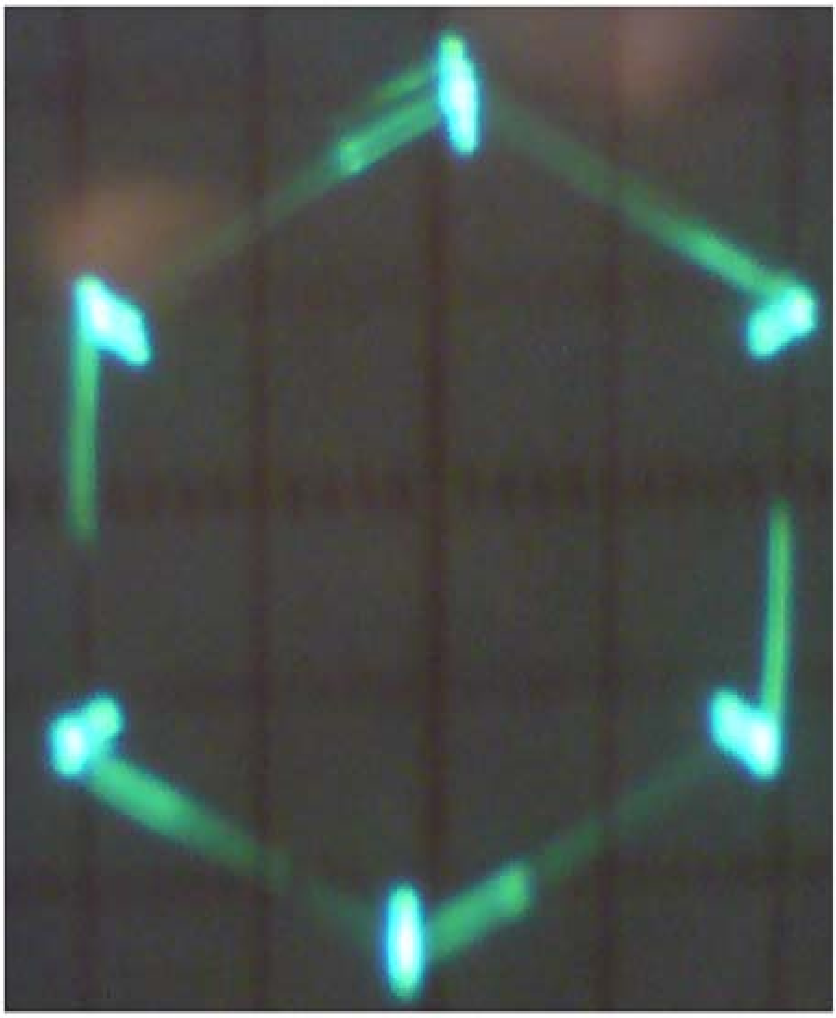

Fig. 3 View of the image space vector from oscilloscope.

3. CONCLUSIONS AND RECOMMENDATIONS

Full analytic solution of produced math model, described parallel work of synchronous generator and three faze bridge power rectifier as a consumer gives an opportunity for analysis and estimating of electromagnetic compatibility bethwin synchronous generator with limited generating power and power nonlinear load – three phase bridge rectifier. The formulated in the paper common dependence for generating voltage and none synusoidallity factor are very clear.

The common way used image space vector gives a good opportunity to solve complicated electromagnetic compatibility problems in ship electrical power supply and working ship electrical equipment.

The representative in the paper common way is very clear and exact precisely.

The way could be used in every variant of common work between synchronous generators and every nonlinear electrical load with a commensurable power.

The more clear way to investigate and study of complicated electromagnetic processes in ship electrical power plant gives the good opportunities to improve education of students too.

REFERENCES

[
1]. Chvanov V.A. – ***Dinamika avtonomnih inxertorov s prjamoj komutaciej,*** Energia, 1978

[2]. Fatec ***- Inverter application course***

[3]. Petkov P.D., Chakarov S. J. – ***Analiz na electromagnitnite procesy v avtonomna system a generator- ventilen izpravitel s impulsna korekcia na napregenieto***, Nauchna sesia TU – Varna, 1981

[4]. Sindurev V.M. – ***Algoritmizacia uproschenih energeticheskih system,*** Electrichestvo 1976.

LEISURE TIME AND ITS IMPORTANCE TO MARITIME SAFETY

RODRÍGUEZ-MARTOS RICARDO

Universitat Politecnica de Catalunya, Spania

Often when we speak about safety on board ships we consider technical aspects and if we take in account human factor then we think about stress, working hours, drougs, etc. Leisure will be not seriously consider as something related with safety. This paper tries to introduce the concern about the importance of leisure time for a proper psychological condition of a seafarer for his own safety and the safety of the ship.

Keywords: leisure time, free time, safety, job satisfaction, crews, rest, stress, human factor

1. CONCEPT OF LEISURE TIME

Leisure or free time is a period of time spent out of work and essential domestic activity. Leisure is free activity in which men look at the value of reality, and without any utilitarian quest, without having to submit themselves to the rules of useful effort. It is also the period of recreational and discretionary time before or after compulsory activities such as eating and sleeping, going to work or running a business, etc. Leisure is not just having rest, but enjoyment and opening out to everything. Leisure (otium) is the opposite of 'necotium' (utilitarian dealing with things).

In short, leisure is contemplative and enriching possession of reality. The distinction between leisure and compulsory activities is loosely applied, i.e. people sometimes do work-oriented tasks for pleasure as well as for long-term utility.

2. INCIDENCE OF LEISURE IN WORK

Contemporary definitions of career (McDaniels, 1984; Super, 1984) and career counselling have emphasized the importance of nonwork variables, such as leisure and other life roles

Additionally, leisure was found to contribute to aspects of psychological health by providing a means to cope with work stress (Trenberth & Dewe, 2002). In a study investigating the relationship of both work and leisure to a comprehensive measure of psychological health, Pearson (1998) found that although job satisfaction was the stronger predictor of psychological health, "the combination of job satisfaction and leisure satisfaction was a stronger predictor of psychological health than job satisfaction alone". In conjunction with other research, Pearson's (1998) study provided strong evidence for the need-satisfying potential of work and leisure and the subsequent justification for including work and leisure in career counselling.

A number of theories provide explanations for the potential impact of multiple roles. Super's (1980, 1990) life span, life space view of career development posited that multiple roles can have a positive impact on happiness and life satisfaction by providing more outlets for one's interests, abilities, values, and self-concept.

3. LEISURE TIME ON BOARD VESSELS

In 2001 the Turku Regional Institute of Occupational Health, Finland carried out a survey on seafarers' free time activities on board ship and on shore. The questionnaire was answered by 245 seafarers (22 of them were women) from a total of 34 ships. Reading was the most popular way of spending free time while on board ship, followed by watching television or listening to the radio and chatting with friends and sleeping/keeping to oneself was in third position.

About one in four put physical exercise and sauna baths among the three most common ways of spending free time. The most common ways of spending free time on shore were meeting friends and acquaintances and watching TV or listening to the radio. In third place were "other ways of spending leisure time", most of which included being out of door, hunting, going to the summer cottage and gardening.

Physical exercise activity was greater on shore than on board ship. The respondents were grouped into four categories: A) reader/student/hobbyist: B) sociable: C) exercise enthusiast D) TV watcher/radio listener Group A considered the ship's atmosphere and the spirit of solidarity on board better than the others. Group B had more often a good friend on board ship and less often suffered from anxiety or depression. Group C more often considered their health and working capacity good. Group D had no positive differences over the other groups. More attention should be paid to developing the ways in which free time is spent not only on board but also during the compensatory free time on shore.

In 1982 Francesc Larrauri and Jesús Carbajosa, psychologists and merchant navy officers, carried out a study of leisure on 42 Spanish vessels. The three questions below were passed, with the following results being obtained:

A) Question: What do you do in your free time?
Reply:
At sea, 86% devoted their free time to getting together with their friends and drinking, 12% to reading and 2% to studying.
In port, 86.7% spent their free time going out for entertainment, while 13.3% went on cultural trips.

B) Question: What would you like to be able to do?
Reply:
At sea, 72% would like to be able to engage in cultural activities, 14.7% in sports and recreational games, while 13.3% did not reply.
In port, 53.3% would have liked to undertake cultural activities, 26.7% amusements, while 20% did not reply.

C) Question: Why don’t you do that?
Reply:
At sea, 70.6% alleged lack of resources (material and human), 16.1% lack of willpower and 13.3% did not reply.
In port, 63.3% alleged lack of resources (material and human), 13.3% lack of willpower and 23.3% did not reply.

Although it would have been instructive to know the type of vessels, routes and distribution of those surveyed by professional grade, if we undertake a little analysis of these results we can draw a few conclusions.

The vast majority spent their free time in the way that came easiest to them: chatting and drinking at sea and having fun with no great mental effort in port. A large majority, though not so great this time, stated that they would have liked to do something with rather more content, more along cultural lines, while the reason they gave for this mismatch between what they did and what they would have liked to do was lack of resources.

When a vessel is to spend two or three days in port, some are keen to find out what there is of interest there, and they spend their free time rather as tourists might. If the crew member in question has already visited that port many times he might devote the time to strolling about and experiencing the atmosphere of the city for a few hours. Others under the same circumstances confine their interest to the first group of bars they find near the port.

A lower-rank crew member who may speak no language other than his own will have more difficulties making himself understand than will an officer who can get by in English and has had an education which makes access to many of the cultural activities referred to easier. Many officers nonetheless also take the line of least resistance. But this tendency not to make suitable use of free time has another important explanation: lack of stimuli.

Culture has to be cultivated, in a process in which one develops an appetite for assimilating new knowledge, while at the same time one appraises things in a new way. Life at sea is poor in stimulus. Day after day one speaks with a small group of people, and the news that reaches the crew comes over the radio and normally in only brief form. Free time has to be organized with what there is on board.

A person leaving work on land can find concert halls, sports centres, cultural centres, theatres, cinemas, or can simply go round to a friend's house. Society on land is broadly diversified so that a person who works at a keyboard all day in an office can on leaving the office find a more or less wide range of possibilities for filling the free time. At sea all this has to be organized oneself. Crew members can, of course, organize domino, draughts or chess championships, or several music enthusiasts can get together and form a small band. But this has been organized oneself and therefore calls for special initiative. But when one is tired of sea and more sea, and may be in a low mood and with thoughts set on how long is left to get back home, it is not so very easy to create those situations in which the leisure activities we would like to enjoy are indeed those we engage in.

Ships these days normally have video, and more and more crew has own laptops. So, it happened that after working time, many people shut in itself in their cabin, without scarcely relating to the companions.

On the contrary, games of cards, or other games or common activities, become truly festive occasions. If people come together with enthusiasm, have their spirits lifted by an atmosphere of enjoyment and friendship, and then the occasion can be really marvelous. Teams are sometimes formed to compete against each other, so that the games session is anticipated with delight throughout the entire day.

For pleasant co-existence on board ship, it is important that crew members take part in shared leisure activities. If during free time each one shuts himself away in his cabin, the weight of solitude and lack of communication gradually become greater and crew members lose any feeling of belonging to a common family.

Something similar happens in port. It is important to go on cultural visits, but also that they be shared. If a seamen devotes his time to walking around a city's streets alone he will see things which may be new, but he will remain as alone or more alone than at sea. That is why seamen's welfare centres like "Stella Maris", "Flying Angel",a.s.o. are important, offering sports, games and excursions, but as a group.

The problem of leisure time at sea is aggravated when crews are small. One has only to imagine the case of a crew of twelve, of whom four are on watch, four are sleeping prior to taking over the watch themselves and, of the remaining four, two have no desire to do anything and the other two will thus not be very highly motivated to organise anything.

Physical exercise is also important. Some ships have a gymnasium, though even here a certain amount of willpower is required, or they have organised games to encourage people to participate. Easier to take up are ping pong or swimming, especially on large supertankers with routes through warm zones.

Dr Gareth Evans wrote in June 2009, in “www.ship-technology.com” an article regarding the importance of leisure.

He said:

Other aspects of crew life have also seen major changes over the years and a number of those whose careers span the transition testify to a particular transformation in their leisure time. Most particularly, as technology has yielded faster loading and discharging speeds, the corollary has been a gradual reduction of the available time for excursions ashore.

Although the opportunity is still there for junior officers and crew, more senior personnel may often find their chance to escape the confines of the ship somewhat curtailed, often adding to the feeling of pressure already generated by tight schedules among ships’ Masters and higher ranks.

For off-duty time away from port, however, today’s ship-board facilities offer significant advances, which in some ways go towards offsetting these changes even though individual crew members often may be virtually alone when using them. It is a pattern that seems to have been repeated in other aspects of crew leisure too, as traditional card or board games increasingly give way to more solitary electronic pursuits. While the technological innovation of the video game may have successfully circumvented the need for the simultaneous physical presence of two or more players – a boon amid a shrinking muster – it has done little to improve the growing isolationism of ship life.

4. LEISURE AND HEALTH

The International Committee on Seafarers’ Welfare, aware of the importance of lifestyle aspect in the health of seafarers, launches a project FIT ONBOARD as one of the topics in the Seafarers’ Health Information Programme, sponsored by the ITF Seafarers' Trust.

SHIP encourages seafarers to take responsibility for their health within their living and working environment.

Although SHIP addresses individual seafarers on lifestyle related issues, SHIP is also an instrument for health promotion in the workplace.

The ship, where seafarers not only work but spend all their time during a voyage, is seen as the best place for health intervention.

Onboard ship, the modern way of life is a sedentary one and opportunities for sport and fitness are limited. Even modern ships cannot always meet the needs of today’s seafarers: to do sport and fitness activities.

Sports activities on ships have to take into account the general safety measures on board. Ships do not always have sufficient or suitable accommodation or facilities for sport. The strict organisation of work and tasks on board does not leave a lot of time for physical activity.

Sport contributes to a general sense of physical, psychological and social well-being. Sport not only improves health but, through social interaction, it also encourages team-building.

5. LEISURE ACTIVITIES AND CHANGE OF ROL

The various actions performed in a society are for the most part classified, with such classification depending on them having some objective sense, and this in turn requiring linguistic objectification.

People who enact different roles over a short period of time sometimes have the feeling that they are actors changing costume from act to act in order to play another part. In fact each role that a person acts out throughout his or her life amounts to a different role in the theatre of life.

General speaking, we can say that on ships the identification of individuals with their roles is greater than it is on land, since a person goes on being a captain, or a greaser, galley boy or whatever, all the time he is aboard ship. Indeed there will probably even be a little sign on his cabin door stating his position.

He will have his meals in whichever mess room is appointed for his professional rank. On many ships there is one mess room for the officers (sometimes even one for the bridge and another for the engine department), another for the petty officers and another for the crewmen in general.

Leisure time becomes an opportunity to change the role. The change of role is very important for any person and for his mental equilibrium. When playing cards or organizing some leisure activity, the seafarer has the opportunity to feel that his not only a crew member, but a person enjoying his free time.

Ronald Hope shows the importance of such activities. He tells how on board a tanker darts and cards championships were organised, along with games of cricket on deck. The captain himself took part and was eliminated in the first round of darts by an oiler.

So, during this activity there was no captain, no oiler, just to people playing darts.

Hope also explains in his paper the important role of the captain in life aboard ship. He does not think that the captain has to be the organiser of things, but he does have to lend encouragement.

Hope is critical of the mentality of many captains, concerned only about the working efficiency of their crew and not the quality of their leisure. This, in Hope’s view, is a serious mistake, for seamen who do not have an enriching, amusing and pleasant leisure time are more likely to succumb to drink, drugs and dozing away time, and such persons will not then be in the best condition for efficient work.

6. THE VOICE OF ILO: MLC 2006

The new Maritime Labour Convention 2006 consolidates and updates more than 65 international labour standards related to seafarers adopted over the last 80 years. The Convention sets out seafarers' rights to decent conditions of work, included recreational facilities for the crews.

We reproduce here now the Guideline B 3.1.11 of this Convention, regarding recreational facilities, mail and ship visit arrangements:

1. Recreational facilities and services should be reviewed frequently to ensure that they are appropriate in the light of changes in the needs of seafarers resulting from technical, operational and other developments in the shipping industry.

2. Furnishings for recreational facilities should as a minimum include a bookcase and facilities for reading, writing and, where practicable, games.

3. In connection with the planning of recreation facilities, the competent authority should give consideration to the provision of a canteen.

4. Consideration should also be given to including the following facilities at no cost to the seafarer, where practicable:

(a) a smoking room;

(b) television viewing and the reception of radio broadcasts;

(c) showing of films, the stock of which should be adequate for the duration of the voyage and, where necessary, changed at reasonable intervals;

(d) sports equipment including exercise equipment, table games and deck games;

(e) where possible, facilities for swimming;

(f) a library containing vocational and other books, the stock of which should be adequate for the duration of the voyage and changed at reasonable intervals;

(g) facilities for recreational handicrafts;

(h) electronic equipment such as a radio, television, video recorders, DVD/CD player, personal computer and software and cassette recorder/player;

(i) where appropriate, the provision of bars on board for seafarers unless these are contrary to national, religious or social customs; and

(j) reasonable access to ship-to-shore telephone communications, and email and Internet facilities, where available, with any charges for the use of these services being reasonable in amount.

5. Every effort should be given to ensuring that the forwarding of seafarers' mail is as reliable and expeditious as possible. Efforts should also be considered for avoiding seafarers being required to pay additional postage when mail has to be readdressed owing to circumstances beyond their control.

6. Measures should be considered to ensure, subject to any applicable national or international laws or regulations, that whenever possible and reasonable seafarers are expeditiously granted permission to have their partners, relatives and friends as visitors on board their ship when in port. Such measures should meet any concerns for security clearances.

7. Consideration should be given to the possibility of allowing seafarers to be accompanied by their partners on occasional voyages where this is practicable and reasonable. Such partners should carry adequate insurance cover against accident and illness; the shipowners should give every assistance to the seafarer to effect such insurance.

7. CONCLUSIONS

It is very difficult to establish how important a proper leisure time for safety on board a vessel is. However, there are enough arguments to take it in account. Slogans like “a happy crew is a safe crew” or “a fit crew is a safe crew” are eloquent. We also can approach this question taking in account the impact of stress and mental fatigue has in maritime safety. The next step will be to consider the importance of an enjoyable leisure time to combat stress and mental fatigue. Leisure is necessary for a mental equilibrium.

The problem is that it is neither on board nor at port easy to find the time and the resurces for a satisfactory leisure.

The crew’s reduction allows hardly sharing leisure activities with other crew members. On short trips, if we take in account working hours and manoeuvres time, there is no time less for leisure.

Only few ship owners spend some money for leisure activities like books, games, videos, etc. Only few ships dispose of a gym or a swimming pool.

When in port, very often the short turnaround offers few possibilities to go a shore. Ships come also more and more alongside in peers which lie far from the city and very often there is no transport available.

The already mentioned MLC 2006 is very explicit about what ship owners should provide for crew’s welfare and leisure and we just refer to it.

This new convention offers a promising horizon for seafarers’ wellbeing.

REFERENCES

[1]. Hope, R. Spare time at sea. The Nautical Institute on Command. London. 1955 (Article).

[2]. ICSW: http://www.seafarershealth.org/fit_on_board.html

[3].) Larrauri, F; Carbajosa, J. **El ocio en la mar.** Barcelona, 1982.

[4]. McDaniels, Carl ***The Role of Leisure in Career Development*** . Journal of Career Development 1984 11: SAGE Publications. 2455 Teller Road. Newbury Park, CA 91320

[5]. Maritime Labour Convention, 2006. ILO. Geneva. Session of the Conference:94. Date of adoption:07:02:2006

(http://www.ilo.org/ilolex/cgi-lex/convde.pl?C186)

[6]. Pearson, Quinn M ***Role overload, job satisfaction, leisure satisfaction, and psychological health among employed women.(Report)*** Journal of Counseling and Development. January 1, 2008. The Pennsylvania State University. 327 CEDAR Building. University Park, PA 16802-3110

[7]. Rodriguez-Martos, R. ***The Merchant vessel a sociological analysis*.** Edicions UPC. Barcelona, Sept, 2009

[8]. Saarni H, Pentti J. ***Free-time activities among seafarers on board Finnish cargo ships***. Turku Regional Institute of Occupational Health, Finland. (http://www.ncbi.nlm.nih.gov/pubmed/9101050)

[9]. Super , Donald E. *Leisure:* ***What It Is and Might Be*** . Journal of Career Development 1984 11: 71-80

SAGE Publications. 2455 Teller Road. Newbury Park, CA

[10]. Trenberth, L. and . P. Dewe (2002) '***The importance of leisure as a means of coping with work related stress: an exploratory study'***, Counselling Psychology Quarterly 15(1): 59-72. Routledge, Taylor & Francis Group London UK

MODELLING PRESSURE WAVES IN FUEL INJECTION PIPES

[1]SABAU ADRIAN, [1]BARHALESCU MIHAELA

[1]Constanta Maritime University, Constanta, Romania

Fuel injection pipes pressure are measured and computed to study the injection system characteristics at partial load in a direct injection Diesel engine whit a distributor-type injection pump. The fuel injection simulation is based on a linear model. The governing equations are solved by the finite difference method.

Keywords: injection, nozzle, finite difference method, fuel pipe

1. INTRODUCTION

Diesel engine is one of the power generation devices which convert chemical energy to mechanical energy. Due to its high thermal efficiency, diesel engines have been applied more and more to the vehicles and power plant. Due to the pollution of the environment and the shortage of energy sources, many diesel engine researches are carried on to improve the performance and to reduce the toxic emissions such as NOx and Particulates [12]. Many of these researches are focused on the optimization of the fuel injection system. This is because the diesel combustion processes are characterized by non-homogeneous diffusion flame and auto-ignition. The fuel injection system affects the diesel engine combustion process through the control of injection time, injection quantity and injection rate [6]. Many simulations of the diesel engine fuel injection system are carried out to understand the fuel injection system characteristics[8].The method of characteristics and the finite difference method have been used to solve the governing equations. Recent studies show that finite difference method is more advantageous than the method of characteristics concerning computation time and nonlinearity [7]. A simple linear model solved by the finite difference method is developed in this study which is programmed in Matlab language. An one-zone heat release calculation [5] is carried out using the measured cylinder pressure to analyze the combustion process.

2. SIMULATION

Fuel injection system modeling

The task of the fuel injection system is to meter the appropriate quantity of fuel for given engine speed and load, and to inject that fuel at an appropriate time. A fuel injection system is divided into pump, pipe and nozzle component to model the entire system. Following assumptions are made to develop a model [8] The variation of fuel bulk modulus and density is negligible.

The flow in the fuel injection pipe is one dimensional laminar flow. The convective term in the momentum equation can be neglected. The steady flow friction coefficient is used for the transient flow friction coefficient. The discharge coefficient is constant everywhere in the fuel injection system. As a result of above assumptions, a linear equation of state for the pressure can be formulated as Eqs. (1) and (2).

$$P = \beta_0 S \quad (1)$$

$$S = \frac{\rho - \rho_0}{\rho_0} \quad (2)$$

Fuel injection pump

The volume of the pump component can be divided into 2 control volumes such as plunger chamber, delivery chamber, and spill port as shown in Fig. 1. The continuity of flow in 3 control volumes and the equilibrium of forces on the delivery valve give three governing equations.

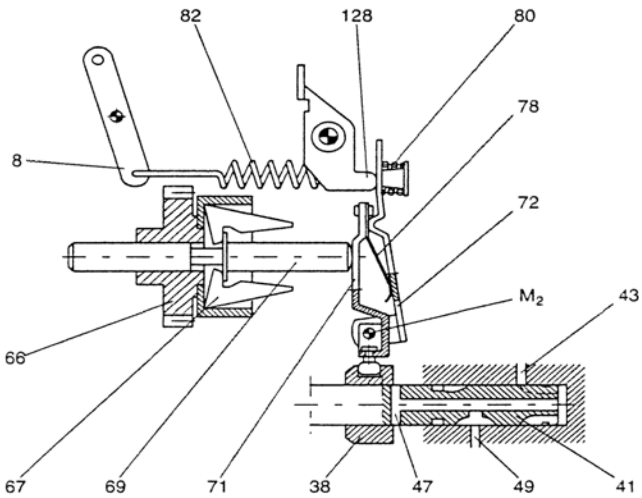

8 Control lever
38 Control collar
41 Distributor-pump plunger
43 Inlet port
47 Spill port
49 Outlet port
66 Flyweight assembly
67 Flyweights
69 Sliding sleeve
71 Starting lever
72 Tensioning lever
78 Starting spring
80 Intermediate spring
82 Governor spring
128 Stop lever

Fig 1 Schematic diagram of a fuel pump modeling

An orifice model is used as a flow model for the interfacing control volume.

$$A_p \frac{dX_p}{dt} = \frac{V_p}{\beta_0} \frac{dP_p}{dt} + A_v \frac{dX_d}{dt} + Q_{pd} + Q_{ps} \quad (3)$$

$$A_v \frac{dX_d}{dt} + Q_{pd} = \frac{V_p}{\beta_0} \frac{dP_p}{dt} + \frac{dW_1}{dt} \quad (4)$$

$$M_d \frac{d^2 X_p}{dt^2} + k_d X_d = A_v (P_p - P_d) - f_d \tag{5}$$

Fuel injection pipe

The continuity equation, momentum equation and the equation of state (Eq. (1)) are taken into account to calculate the flow and the pressure in the fuel injection pipe. The momentum equation can be expressed by Eq. (6) in the form of a cumulative flow equation.

$$\frac{d^2 W}{dt^2} = -\frac{A_{pipe}}{\rho_0} \frac{\partial P}{\partial x} - \frac{32\nu}{D^2} \frac{\partial W}{\partial t} \tag{6}$$

Fuel injection nozzle

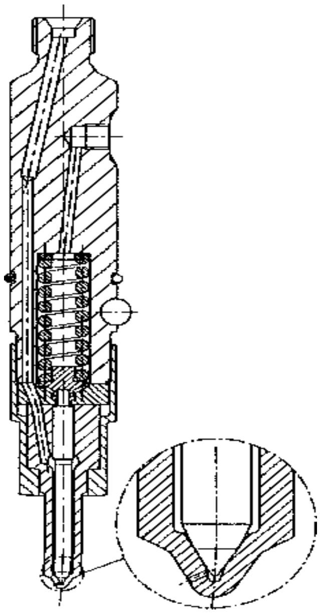

Fig. 2 Schematic diagram of a nozzle

The fuel injection nozzle volume can be separated into two control volumes, i. e. nozzle chamber volume and sac volume as in Fig. 2. It is assumed in the process of constructing governing equations that the injection rate into the combustion chamber is the same as the fuel flow rate from the nozzle chamber to the sac volume. By considering of the continuity equation and the equilibrium of force on the needle valve, Eqs. (7) and (8) can be obtained.

$$\frac{dW_L}{dt} = \frac{V_n}{\beta_0} \frac{dp_n}{dt} + A_n \frac{dX_n}{dt} + C_d \frac{A_{hole} A_{no}}{\sqrt{A_{hole}^2 + A_{no}^2}} \sqrt{\frac{2(P_n - P_c)}{\rho}} \tag{7}$$

$$M_d \frac{d^2 X_n}{dt^2} + k_n X_n = P_n (A_n - A_{sc}) + P_s A_{sc} - f_n \tag{8}$$

Boundary conditions

Fuel is delivered into the cylinder through the injection pump, the injection pipe, and the injection nozzle. Fuel is compressed by the plunger lift in the pump and injected into the cylinder. For that reason, the plunger lift and the cylinder pressure are used as the boundary condition. The plunger lift is calculated from the cam profile and roller's diameter in the in-line pump. The cylinder pressure is measured by the pressure transducer mounted in the cylinder head. As mentioned above, the entire fuel injection system is modeled as a three-component model i. e. pump, pipe, and nozzle. In order to calculate the whole system, it is assumed that the delivery chamber pressure is identical to the first node pressure of the injection pipe. Similar assumption is also applied to another boundary section where the last node of the fuel pipe meets the nozzle chamber.

Calculation method

When Eqs. (3), (4), and (7) are discretized by the finite difference method, they are nonlinear equations. To find solutions for these nonlinear simultaneous equations, Newton Raphson method is employed. The fuel injection pipe governing equations are turned into a finite difference form by the Leap-Frog scheme. This explicit scheme converges when Eq. (9) is satisfied. [1]

$$\frac{\Delta X}{\Delta t} \geq C_0 = \sqrt{\frac{\beta_0}{\rho_0}} \tag{9}$$

3. EXPERIMENT AND ANALYSIS

The experiment is carried out to measure the fuel injection pipe pressure four tow characteristic speed and tree partial load.

The test bench was also set up and applied for experimental simulations of transient system operation under control. During the steady operations, pressure time-histories were acquired cycle-by-cycle in the pumping chamber and at the extremities of the delivery-pipe. Injector needle-lift and injection-rate distributions versus the pump-shaft crank angle were also measured in the stationary operating conditions.

Pressures were measured with piezoresistive transducers, the needle lift data were acquired by means of an inductive transducer and the injection rate was determined using a modified Bosch indicator. Based on previous experience [11] and on the average deviations of repeated measurement sets, by cumulating the effects of the different uncertainty sources, it was prudential to assign a maximum overall uncertainty of ±12% to the experimental data, in general. However, this did not influence the result involvements and conclusions.

The experimental set-up includes a 4 stroke cycle 4 cylinder diesel engine T684, a dynamometer, data acquisition system, pressure transducers, and etc. Table 1 shows the specifications of the injection system of engine.

Tabel 1 Specification of fuel injection system

Plunger diameter	10.5 mm
Plunger stroke	3.2 mm
Fuel pipe diameter	2 mm
Nozzle type	Hole type
Nozzle hole number	4
Nozzle hole diameter mm	0.24
Nozzle hole angle	90

Figures 3 show the measured and simulated fuel pipe pressures for the engine speeds of 2400 rpm and 1440 rpm at full load. The maximum fuel pipe pressure of the simulation is similar to that of the measurement with slight

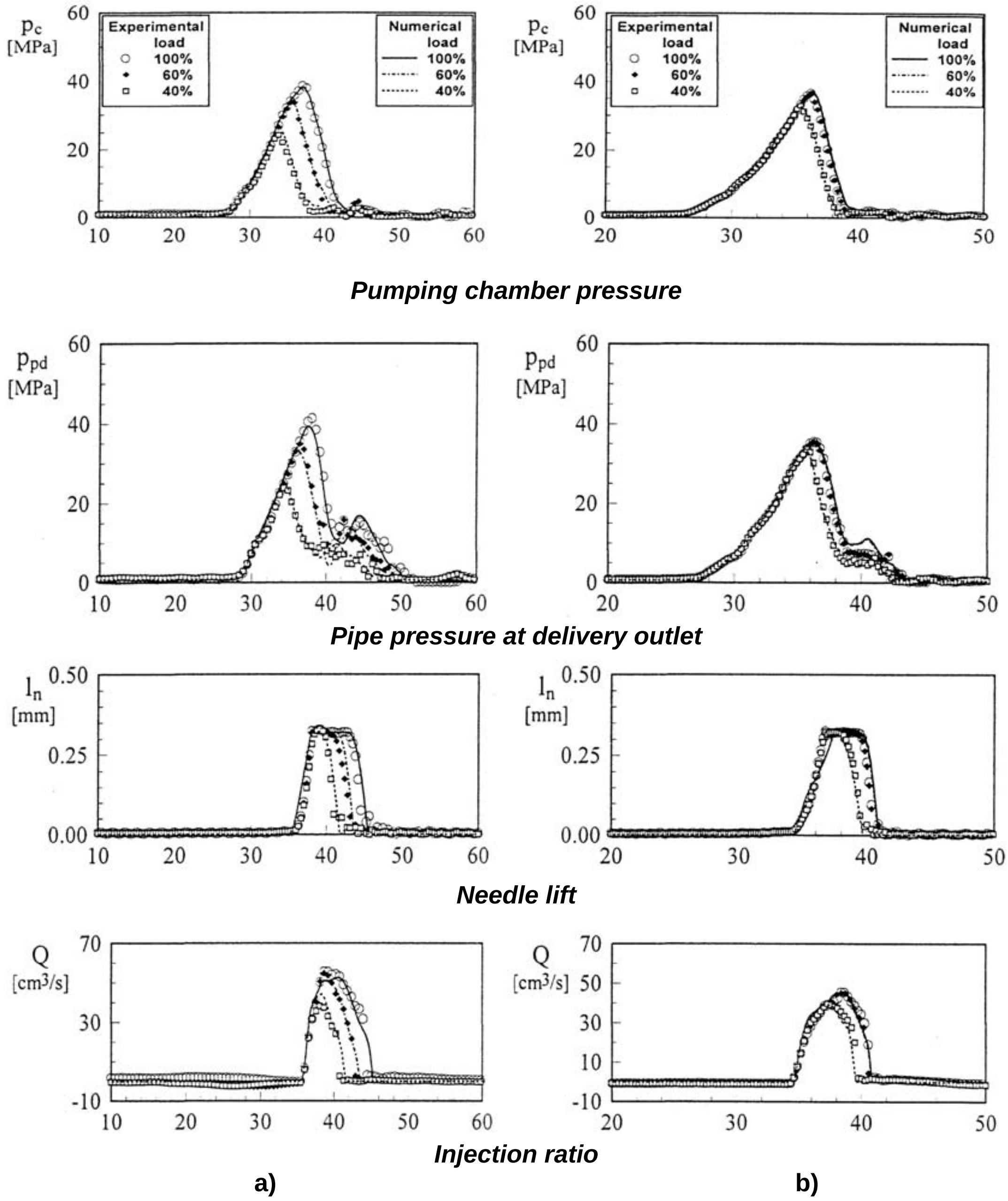

Fig. 3 Fuel pipe pressure a) 2400 rpm and b) 1440 rpm speed

4. SUMMARY AND CONCLUSION

Unsteady flow phenomena were numerically simulated and experimentally investigated in an automotive diesel injection equipment with a distributor-type pump, at several loads and pump speeds, over a wide range of steady operating conditions.

The program, with a modular structure given by a library containing a variety of system component models, is based on a robust and efficient second-order accurate numerical algorithm of the implicit type. This resolves all of the system component equations at the same time, ensuring an essential fluid-dynamic coupling between them. The code takes the dependence of fuel properties on pressure and temperature, friction and minor losses, as well as the nozzle-hole flow-coefficient unsteadiness, into account. Besides, it is capable of simulating cavitation occurrence and propagation.

Pressure time-histories were measured and computed in the pumping chamber and at the extremities of the delivery pipe. Injector needle-lift and fuel injection-rate distributions versus the pump-shaft crank angle were also analyzed in the stationary operating conditions.

The consistency of theoretical and experimental results substantiated the validity of the program at the engine part-loads. The code presented good predictive capabilities even for idling engine operation at the lowest pump speed, where the nozzle-hole discharge flow-coefficient was shown to be critical for the fuel injection-rate simulation.

The numerical system-model application to predict the test actuated part-load phases confirmed the code capability of accurately predicting more critical dynamics conditions requiring a cycle-by-cycle simulation of intensely cavitating pipe-flow, mainly at low loads, after the nozzle closure. A virtually negligible residual void-fraction effect was apparent in subsequent cycles during the pump compression stroke. This and the small sensitivity of the pipe residual pressure to significant load variations, allowed by the reflux valve, were the main reason for the injection system to adapt to steady operation in a few cycles, soon after the effective pump-plunger stroke had come into its full-load position.

REFERENCES

[1]. Anderson, D A., Tannehill, J. C. and Pletcher, R. H., 1984, ***Computational Fluid, Mechanics and Heat Transfer***, Hemisphere Publishing Corporation, pp. 87--178.

[2]. Arcoumanis, C. and Fairbrother, R. J., 1992, ***Computer Simulation of Fuel Injection Systems for DI Diesel Engines***, SAE Paper 922223.

[3]. Cheng, Wai and Gentry, Richard, 1986, ***Effects on Charge Non-Uniformity on Diesel Heat Release Analysis***, SAE Paper 861568

[4]. Cheung, Hon M. and Heywood, John B., 1993, ***Evaluation of One-zone Burn-Rate Analysis Procedure Using Production SI Engine Pressure Data***, SAE Paper 932749.

[5]. Chun, Kwang Min and Heywood, John B., 1987, ***Estimating Heat-Release and Mass-of -Mixture burned from Spark-Ignition Engine Pressure Data***, Combust. Sci. and Tech. Vol. 54, pp. 133-- 143.

[6]. Heywood, John B., 1988, ***Internal Combustion Engine Fundamentals***, McGraw-Hill, pp. 491 562.

[7]. Kumar, K., Gaur, R. R., Garg, R. D. and Babu, M. K. Gajendra, 1983, ***A Finite Difference Scheme for the Simulation of a Fuel Injection System***, SAE Paper 831337.

[8]. Lee, Hang-kyung, 1994, ***Effects of Injection Pressure and Nozzle Geometry on D. I. Diesel Emissions and Performance***, SAE Paper 950604.

[8]. Shin, Bum-sik, Lee, Suk-Young and Chun Kwang Min, 1996, ***An One-zone Heat Release Analysis of a 6 Cylinder Compression—Ignition Engine***, KSAE 96370013 Transaction Vol. 4, No. 1.

[9]. Sabau, A., Buzbuchi, N., Şoloiu, V.A.: ***Combustion Numerical Modelling in Diesel Engines***. In Volumul "A XI-a Conferință Națională de Termotehnică", 8 pag., Galați, 2001.

[10]. Sabau, A. (2007). ***Studies regarding the combustion process in marine diesel engines in order to reduce the pollutant emissions***, PhD Thesis, 'Transilvania' University of Brasov

[11]. Sugiyama, G., Ryu, H. and Kobayashi, S., 1994, ***Computational Simulation of Diesel Combustion with High Pressure Fuel Injection***, COMODIA 94, pp. 391--396.

SPECIAL SYNCHRONOUS MICRO GENERATORS USED IN HYDROELECTRIC ENERGY CONVERSIONS

[1]SAMOILESCU GHEORGHE, [2]SERGIU NICOLAE, [2]DORIAN MARIN, [3]SERGHEI RADU, [1]LAURA CIZER

[1]*Naval Academy "Mircea cel Batran", Constanta, Romania,* [2]*National Institute for Research and Development in Electric Engineering, Constanta, Romania,* [3]*Zodiac Company, Constanta, Romania*

In order to meet the energetic needs in isolated areas by means of wind or hydro technical potential, conversion micro units can be used. This paper reveals the extensive investigation into the use of synchronous AC micro generators operating on water energy, performed by INCDIE ICPE-CA, "Mircea cel Batran" Naval Academy and U.P.B. Our research includes: normal model of a generator, reversed model in accordance with its functional purpose: out of water (in atmosphere) or in immersion.

Keywords*:* hydroelectric conversion, micro generator, permanent magnets

1. TECHNICAL SOLUTIONS FOR USING SMALL STREAMS OF WATER AS ENERGY RESOURCES

The main technical solutions taken into consideration are as follows [Cazacu, 2005], [Cazacu, 2002], [Gordon, 2003]:
- intubated model with vertical or horizontal axis, axial turbine and external electric generators, figure 2;
- model with vertical axis, flow of water in cavity regime and external generator, figure 3;

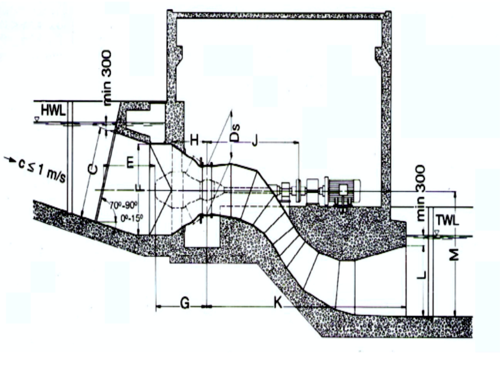

Fig. 1. Intubated model with horizontal axis

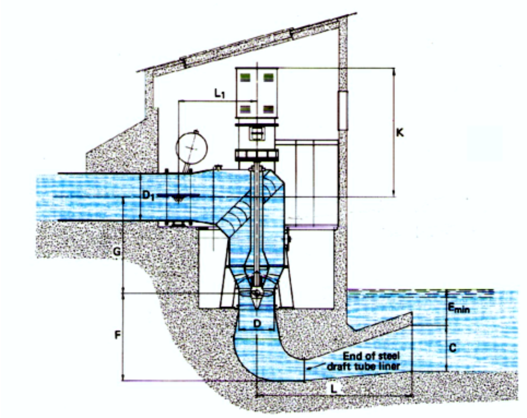

Fig. 2. Intubated model with vertical axis

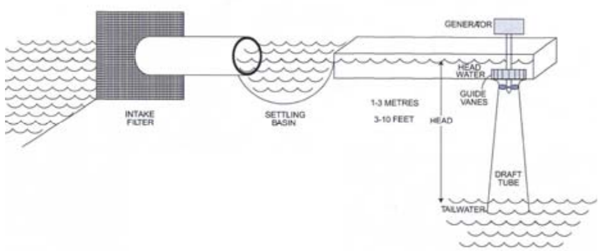

Fig. 3. Model with vertical axis, flow of water in cavity regime

The alternative voltage between its terminals is brought to a normal state again and applied to the terminals of a series of storage batteries which also plays the role of a buffer in stabilizing the voltage. The receivers are connected in parallel and can use: the direct current (DC), the nominal voltage of a battery or the alternating current (AC), complying with the industrial requirements by means of an adequated built-in electric power inverter.

The following solution has been resorted to in order to ensure the highest electromechanical parameters at optimal dimensions: the excitation by means of high energy permanent magnets that have earth metals as their basis and have been synthesized from NdFeB. The basic magnetic parameters are as follows: the remnant induction of 1.14 T, the coercive field of 740 KA/m and the maximum energetic product of 240 KJ/m^3.

2. SYNCHRONOUS GENERATOR, NORMAL MODEL FOR OPERATING IN THE AIR

A three-phase synchronous electrical model has been built and designed to be compatible with a maximum power of 1500 W at a range of 300-500 rpm, fig. 4 [4,5,6,7,8,9].

The excitation is applied by using high energy permanent magnets made from earth metals and synthesized from NdFeB; the number of pairs of magnetic poles is relatively large (p=6), corroborated with the low number of revolutions and the usual working frequencies for the passive magnetic materials that have been used so far.

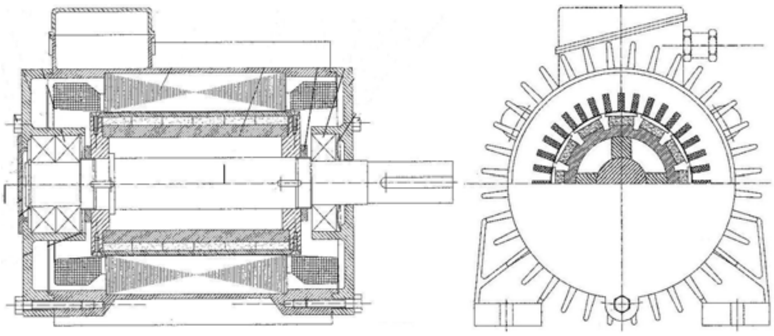

Fig. 4. Synchronous generator, normal model

The shape and dimensions of the inductor are subject to an existent sheet plate that can be obtained as follows (a package of sheet plates from an asynchronous engine of 7,5/1,500 rpm equipped with an aluminum frame, IMEP). The inductor is massive and has sides to allow permanent magnets to be glued on.

It is a closed model, and several measures have been taken to prevent rain water from coming through (buried shields, differenty sized axes, double insulated bearings).

The bearings are equipped with radial and axial double ball bearing situated at the opposite end of the traction and double and axially secured with the shield and on the shaft for a safe functioning when axially strained, there is also a normal radial medium heavy bearing, on the traction side.

The rotor is an empty cylinder (with a view to a better mass), the magnetic yoke is radially dimensioned due to magnetic saturations and is consolidated on the shaft by side bearings. The rotor polar pieces are lopsided in order to keep the start coupling within safe values. Its geometry is compact to allow advantageous dimension minimization.

The number of both pole and phase slots is q=1. The total number of slots is Z=36. The winding pitch is diametric. There is a two-layer winding. The total number of coils is 36 (Z=36, two-layer winding). The number of phase coils is 12. The number of phase spires is $W_1 = 156$. The dimension of the entrefer is δ=1mm. The outer diameter of the rotor is D_r = 131 mm. The average magnetic induction within the entrefer is B_δ =0,79 T. The actual phase voltage when idle is U_0=55 V at 300 rpm. The average nominal phase current is I_{fN} =11 A.

Tests have outlined a good behavior in the case of the generator when idle and loaded that presents the following features: [Samoilescu, 2006], [Nicolae,et.alii,2003]:

- the rigid external characteristic of the voltage at terminals in accordance with the current that is delivered on the load, figure 5 (representation for the factual average values of the three phase voltages and current), at constant rotation values;

- the high values of the efficiency in accordance with the duty delivered to the load, figure 6, at constant rotation values.

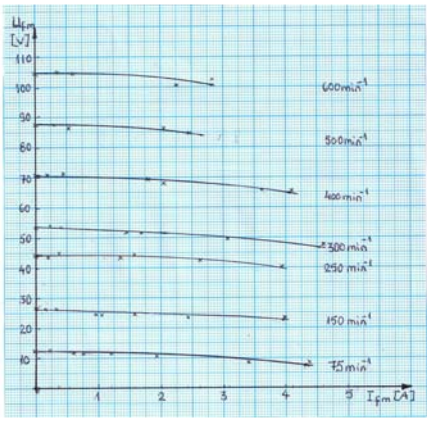

Fig. 5. Rigid external characteristic

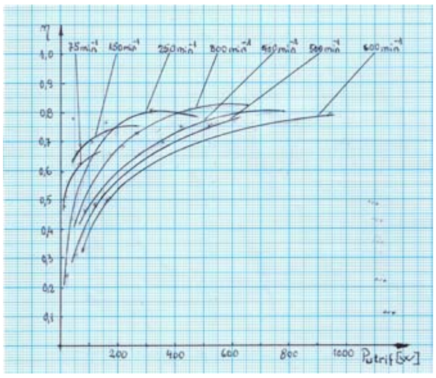

Fig.6. High value of the efficiency

3. SYNCHRONOUS REVERSED BUILT-UP MICRO GENERATOR DESIGNED TO OPERATE IN IMMERSION

Figure 7 displays the building solution adopted in the case of this micro generator [Nicolae,et.alii, 2003], [Mihaescu,et.alii,2004], [Kappel,et.alii,2004].

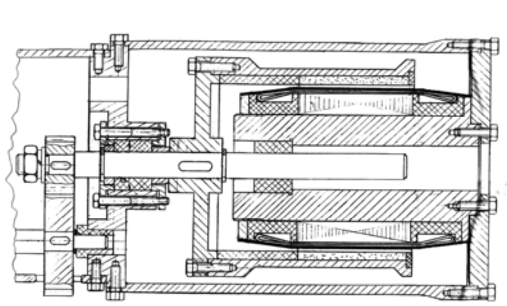

Fig. 7. Synchronous reversed built-up micro generator

The electric generator is of synchronous, single phase, reversed built-up type and has its inner stator equipped with windings while its outer rotor (pot shaped) is equipped with permanent magnets on the inner side.

The inner stator is centrally fixed in the support on the right shield of the generator. It includes a central hub against which the package of FeSi plates and the insulating coil heads are pressed. The winding is accomplished by means of flat coils located on the package of no slot plates. The insulation of the entire construction is accomplished by means of an outer thermo contracted located over the windings as well as over the insulating bolsters and metal flange at the end.

The outer rotor backed by the shaft is pot shaped (cylinder – magnetic yoke plus end flange), and is equipped with permanent magnets located inside in horizontal rows for each pole. The magnets are of Nd-Fe-B type and synthesized, and also present high magnetic parameters. The environmental protection is accomplished through a cylindrical foil on the active surface and through end elements made up of synthetic materials; the components are glued and the gaps are bridged by using a synthetic resin mixture compatible with the used materials.

The shaft crosses the left side shield of the generator by sliding and it is backed up (outside the shield) by the cogwheel of the rotation multiplier (it is thus moved by the hydraulic rotor). The second sliding of the (sliding) shaft takes place inside the stator hub.

The transversal marks of the construction (shields, flanges) are provided with holes to allow water to freely circulate within the entrefer.

4. SYNCHRONOUS, NORMAL BUILT-UP GENERATOR EQUIPPED WITH CLAW SHAPED POLES AND DESIGNED TO OPERATE IN IMMERSION

This type of generator represents a variant of electric hydro generator that is directly operated from the hydraulic rotor. It is synchronous, normal built-up and three phased. It has been designed to be close and insulated, and provided with inner sliding and passing of the shaft and with ferrules. The inductor is the stator and the rotor is the inductor with cylindrical permanent and Nd-Fe-B synthesized magnets, and with claw shaped magnets.

Figure 8 presents a crosscut. This construction includes three subunits made up of a 36 slot alternator stator with intermediary distance spaces and wound together (the windings cross the three stators), which are aligned inside the armature, there are also three more claw-shaped pole subunits supported by the common shaft. Several cylindrical permanent magnets (Φ70/ Φ45) with axial anisotropy interwine the pieces with claw shaped poles (number of pole pairs p=6).

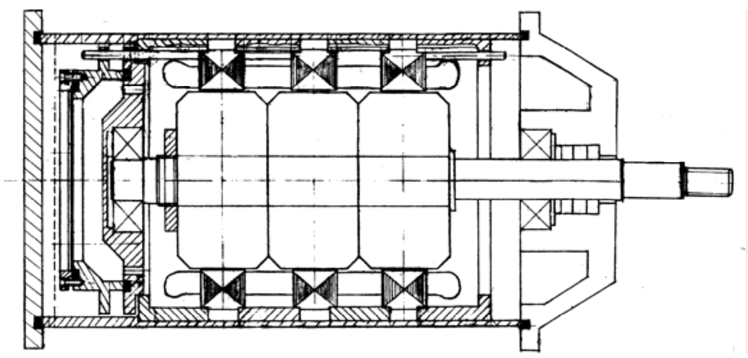

Fig. 8. Crosscut of synchronous generator equipped with claw shaped poles

The entrefer between the claw shaped poles and the stator teeth is relatively small; its value: 0,5 mm. On the front surface (towards the entrefer) of the claw shaped poles of 312,5 mm^2, the actual entrefer of 0,5 mm and the dispersal between the claws over an air corrugated wiring, (25+25)x6 mm long, 4 mm wide, about 5 mm high, there is an average entrefer induction of 0,85T, and at a rotation of 150 rpm, with induced winding of 216 phase spires there was a terminal voltage of about 10 V per phase, an efficient value (experimentally confirmed). For a winding conductor of a 0,6 mm diameter inductor the estimated maximal apparent power is 40 VA (at 150 rpm).

5. CONCLUSIONS

In order to choose the optimal solution for the submersible, electric generator, there have been proposals for technical solutions compatible with complex experiments, intended to get the whole picture of both the hydraulic – mechanical – electric system and its component subunits by gathering quality and quantity data. These results have allowed us to identify the optimal elements of designing and experimenting the final solution. In order to avoid super sized dimensions, exaggerated inertia momentum for the elements of the electric generator (due to low values of rotation and voltage), research will be undertaken to introduce a rotation multiplying mechanical element between the hydraulic rotor and the electric generator. The inductor (rotor) field is accomplished by means of permanent magnets and the inductor (stator) is equipped with monophase windings mounted on a cylindrical yoke made up of tiles. The rotor-stator subunits are independently insulated, allowing water to circulate through the space between the armatures and the bearings.

REFERENCES

[1]. Cazacu M.D. – ***Cresterea eficentei tehnico-economice a hidroagregatelor de mica putere***, A V-a Conferinta Nationala multidisciplinara “Profesorul Dorin Pavel – fondatorul hidroenergeticii romanesti” 3-4 Iunie 2005, Sebes, Editura AGIR, Bucuresti 2005, Vol. 7, 195-200
[2]. Cazacu M.D.; Nicolae S. – ***Micro-hydro turbine for run-of-river power station,*** A II-a Conferinta a Hidroenergeticienilor din Romania, 24-25 Mai 2002, Univ. Politehnica, Bucuresti, Vol. II, 443-448
[3]. Gordon J.L. – ***Turbine selection for low-head hydro developments*****,** Conference: Innovative small hydro technologies, organised by Natural resources Canada at Water-power Cancada, New York, USA, 2003
[4]. Kappel W.; et.alii – ***Magneti permanenti pe baza de NdFeB pentru hidrogeneratoare de mica putere,*** Conferinta Nationala de surse noi si regenerabile, CNSNRE, Targoviste, 2004
[5]. Mihaescu Gh.M., Kappel W., et.alii – ***Hidrogeneratoare de mica putere. Atelierul. Actualitati si perspective in domeniul masinilor electrice,*** ICPE-ME-SA, 2004
[6]. Nicolae S.; et.alii – ***Instalatie de conversie neconventionala de mica putere bazata pe integrarea unor material avansate si solutii tehnologice noi,*** proiect RELANSIN /2003
[7]. Nicolae S.; et.alii – ***Baliza fluvial autonoma din punct de vedere energetic cu semnalizare luminoasa, utilizata pe Dunare,*** proiect AMTRANS /2003
[8]. Samoilescu Gh.; et.alii – ***Sistem cu autonomie energetic destinat supravegherii paselor de trecere pe Dunare,*** A VI-a Conferinta Nationala “Profesorul Dorin Pavel – fondatorul hidroenergeticii romanesti”, 2-3 Iunie 2006, Sebes
[9]. Samoilescu Gh.; et.alii – ***The analysis of the buoys used on the river for making a non conventional energetic system,*** ICATE 2006 - 8th International Conference on Applied and Theoretical Electricity, 26-28 Octombrie 2006, Baile Herculane

APPLIED RESEARCH REGARDING THE PROJECTION OF A SUBMERSIBLE ELECTRIC GENERATOR

[1]SAMOILESCU GHEORGHE, [2]NICOLAE SERGIU, [2]MARIN DORIAN, [3]SAMOILESCU ADELINA, [1]KAITER EDITH

[1]*Naval Academy "Mircea cel Batran", Constanta, Romania,* [2]*National Institute for Research and Development in Electric Engineering, Constanta, Romania,* [3]*Politechnic University of Bucharest, Romania*

The paper presents a new model of a perfect watertight submersible electric generator, tightness which is due to a pair of simerings directly connected to the generator's shaft, in which the impulse is carried out by means of permanent magnets from rare grounds mounted on the electrical machine's rotor with the help of epoxy resins. Due to the total tightness of the generator, the rolling bearings (ball bearings) were used, increasing in this way the mechanical yields on shaft. The encased joint stator winding is not movable and it can be both single and three phased. The inductive field (rotor) is made up of permanent magnets and the induced (stator) is equipped with single phased winding situated on the surface of cylindrical yoke laminations. The subsystems rotor and stator are independently sealed; water can flow into the space between the fittings and in the camps.

Keywords: electric generator, electrotechnical materials, coercive field, residual induction

1. CONSTRUCTIVE SOLUTIONS PROPOSED FOR THE ELECTRIC GENERATOR

The constructive solution proposed for the electric generator is characterized by a highly unconventional nature, highlighted mainly by the following elements [Cazacu, 2003], [Gordon, 2004], [Samoilescu, 2006]:

a) it is a synchronous electric generator, single phased, with an excitation by means of permanent magnets, having the rotor inductor and induced (equipped with winding) stator.

b) the inductor is similar to a cylindrical shaped pot (being at the same time an iron yake while closing the magnetic circuit), within which permanent magnet poles are fixed, having a radial direction of magnetization and circumferential heteropolar arrangement.

Fixing permanent magnets in the slots of the pot is made with epoxy resins. In the interior part, they are protected by a sheet of insulating material and, in the interstices between them, a casting mass, based also on resins, is inserted. This provides fluid sealing magnets towards the environment (river water).

The pot magnetic-yoke fuses with the shaft drive through a lateral flange (clamping the console) with bushing

c) the induced stator, having the magnetic yoke laminations and single-phase winding without any notches located on the outside part, is mounted helped by the permanent magnets inside the rotor pot, the interruption in the magnetic circuit being determined by the space occupied after radial direction, by conductors, by the insulating structures, and by protection (sealing), and outside the stator by the clearance distance (in water) towards the inside of the rotor.

The ends of the coil are protected in the recess that exists in the lateral cylindrical isolated parts, located at both ends of the yoke laminations.

The isolated structures from conductors and yoke are made up of mechanical sheet strength and of appropriate insulation class.

The components of the rotor are enhanced by a bush steel plant (having one threaded lateral flange). A casting mass of resins is inserted in all interstices. Sealing and strengthening on the external level is achieved by insulation heat tube over the conductors, the coil sides, insulation lateral parts and lateral flanges.

The electrical conductor-cable connection is removed through the lateral flange of the central bushing with metal socket bearing and heat-absorbing exterior tube.

The unit stator is fixed, to the supporting structure, relatively elastic with screws and rubber pad in between.

The truth and correct position to the rotor pot is achieved while crossing the rotor drive shaft through the stator central bushing, and suspension towards this one with two sliding bearings (graphite bearings) – radial.

Figure 1 presents a variant of submersible electric generator in unconventional architecture.

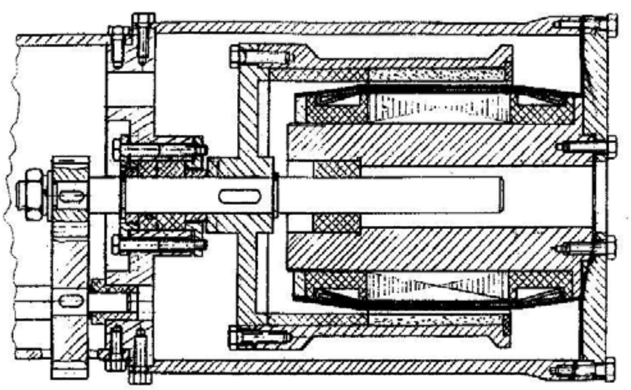

Fig. 1. Submersible electric generator

2. PRELIMINARY CALCULATIONS FOR THE ELECTRIC GENERATOR

The assessment of the power and energy quantities required for the sizing and calculation of the electric generator was based on two considerations: the energy consumption in all functional utilities of consumers and the energy consumption for battery charging operating under buffer (it endures reserve power when the electrical parameters of the generator are falling, and it also stabilizes the output voltage towards utilities, within certain limits).

The energy consumption of utilities is 20 W. Considering an average voltage of 12 V (on the direct current side), current debt is about 17 A. Regarding the buffer battery charge, a voltage of 14.4 V at a normal loading current of 7 A is taken into account [Samoilescu, 2006], [Mihailescu, 2004].

Cumulating these considerations, the results is – in an initial assessment – that at the exit from the block recovery and protection, under maximal load, values of the electrical quantities within the direct current can coexist as follows:

- continuous voltage on nominal load (average): $\mathrm{U_{dN}} = 14{,}4\mathrm{V}$
- nominal direct current (average value): $I_{dN} = 8{,}7A$

For the experimental model phase, it was chosen the solution with one phase synchronous electric generator and bridge rectifier.

Under these conditions, the electric quantities values on the alternative current (AC) side are as follows:

- RMS value of AC voltage at idle (entrance of the charger, in case the load voltage output versus electric as the scheme with buffer accumulator battery):

$$U_{s0} \cong 0{,}71 \times 1{,}1 \times U_{dN} = 0{,}71 \times 1{,}1 \times 14{,}4 = 11{,}25V \qquad (1)$$

- RMS value of AC on the conductor's level at the rectifier's entrance:

$$I_l \cong 1{,}11 \times I_{dN} = 1{,}11 \times 8{,}7 = 9{,}66A \qquad (2)$$

- Rated apparent nominal power of the electric generator

$$P_G \cong 1{,}23 \times 1{,}1 \times U_{dN} \times I_{dN} \cong 169{,}5VA \qquad (3)$$

3. MATERIAL CHARACTERISTICS AND CALCULATING ELEMENETS FOR THE ELECTRIC GENERATOR

Materials used in construction of electric generators parts and subassemblies are subject to the following conditioning, specific to the application:

- operating in total immersion in water;
- relatively small overall dimensions;
- high power efficiency;

Therefore, the development work is considering:

- metallic materials in contact with water for marks of support and movement transfer, stainless or with suitable protective coatings;
- insulating materials resistant to the aquatic environment, insulating class being not a priority due to good cooling conditions and low voltage functioning;
- waterproof sealing synthetic materials;
- conductors for stator winding with as low as possible resistivity, made up of copper;
- Fe-Si laminations for the stator ferromagnetic yoke with specific losses as less;
- permanent magnets with high parameters.

As the dimensions and the efficiency of the generator primarily depend on the ecitation inductive system, in the case of permanent magnets it was chosen the synthesized variant with rare earths NdFeB with the following magnetic parameters [Mihailescu, 2004], [Kappel, 2006]:

- Minimum retained induction: $\mathrm{B}_r = 10{,}500$ Gauss
- Minimum coercive field: B_{Hc} = 9000 Oe
- Energetic value: $(BH)_{\max.} \cong 22{,}5 MGsOe$

For these magnetic materials, the relative differential permeability in the normal working area on the demagnetization features has actually the value 1.

As shown so far, the main dimensions of the electrical machine are in close connection with the inner power.

For AC machines this is expressed as follows:

$$S_i = \left(\frac{\pi\, k_w}{2\sqrt{2}} \times \alpha_i\right) \times (\pi D)^2 \times l \times n \times A \times B_\sigma \tag{4}$$

S_i - inner power (VA) which in this case is practically assimilated with P_G.

k_w - winding factor, which in this case can be approximated k_w=0,9 and so:

$$\frac{\pi\, k_w}{2\sqrt{2}} \cong 1$$

α_i - ideal polar coverage factor, considering at this stage a sinusoidal distribution of magnetic induction in the interruption within the magnetic circuit $\alpha_i = \frac{2}{\pi}$ (in this situation B_σ stands for the apmplitude of magnetic induction in the interruption within the magnetic circuit)

D – average diameter at the interruption within the magnetic circuit, the location of the windings

n – speed (rev/sec); n = 550 rev/min = 9,17 rot/sec

A – the current layer, which taking into account the polar step, the number of poles and good cooling conditions can be approximated by $A \cong 1{,}5 \times 10^4\, A/m$

Considering some availability in the sintered NdFeB permanent magnets, as well as the experience within magnetic circuit construction achieved with them, the following version was chosen for the ME stage:

- tangential directional magnet width: $b_m = 19 \times 10^{-3}\, m$
- number of poles pairs: p = 8
- magnet height: $h_m \cong 5 \times 10^{-3}\, m$
- inner diameter of the magnets location: $120 \times 10^{-3}\, m$

Current in the stator winding conductors is equal to the one situated at the entrance of the charger (winding with a single current path) and taking into account the admitted value of current density $\mathrm{J} = 7\mathrm{A}/\mathrm{mm}^2$, the diameter of the conductor apperars:

$$d_c = \sqrt{\frac{I_l}{j}} \times \sqrt{\frac{4}{\pi}} \cong 1{,}32 mm \tag{5}$$

(electrical resistance: 0,01259 Σ/m).

For a two-layer winding, disposed on the surface of lamination stator yoke, with intermediate insulating layer and outer sealing coat of heat-absorbing tube, adopting an internal space rotor also – outer the stator of approx. 1mm/radius – a total value of the interruption within the magnetic circuit (between the magnet area and the yoke of sheets) is of δ = 5 mm.

Accordingly, in a first approximation, the value of the induction at the interruption within the magnetic circuit is:

$$\mathrm{B}_{\sigma} = \frac{\mathrm{B}_{\Omega}}{k_n \times \frac{\sigma}{h_m} + \sigma} \cong 0{,}4T \quad (6)$$

($k_n \cong 1{,}1$ - increase coefficient of the magneto-motor tension due to parasite intensities; $\sigma \cong 1{,}2$ - magnetic dispersion coefficient, $\mathrm{B}_r \cong 1T$)

Average diameter at the level of the interruption within the magnetic circuit and of the winding location has the following result: $\mathrm{D} = 112 \times 10^{-3}\,\mathrm{m}$

Having these values known, the minimum active length (at the level of magnetic circuit) of the electric machine after the axial direction becomes:

$$l = \frac{P_G}{\alpha_i \times \pi^2 \times D^2 \times n \times A \times \mathrm{B}_{\delta}} \cong 39 \times 10^{-3} m \quad (7)$$

Taking into account the new dimensions of permanent magnets and willing to concentrate coils on poles in the absence of notches (conductors are located on the surface of the stator yoke) the value Aprons was adopted:

$$l = 57 \times 10^{-3} m \quad (8)$$

Basic geometry dimensions of the machine being in this way determined and taking into account the magnetic requests at the level of the interruption within the magnetic circuit, one can determine the number of turns (spires) of one phased stator winding:

$$w = \frac{E}{\pi\sqrt{2} \times f \times k_w \times \Phi} \quad (9)$$

E – electric voltage (effective) which is practically identified with U_{S0}

$f = \frac{p \times n}{60} = 73{,}33 Hz$ - frequency in the stator winding.

$\Phi = \frac{\pi \times D}{2p} \times l \times \mathrm{B}_{\delta} = 501{,}4 \times 10^{-6} W_b$ – magnetic flux per pole at the level of the winding.

$$w = 76{,}5\text{spire}$$

$$w \cong 80\text{spire}$$

The total number of conductors at the level of the interruption within the magnetic circuit, towards the margins of the stator yoke is 2w = 160 conductors, which returns to 10 conductors per pole, with two layer disposal.

Having this dimensional data, characteristic of magnetic and electrical circuit, and with the specifications on material, the mechanical project was elaborated in accordance with the technical solution described above.

4. CONCLUSIONS

The energetic hydraulic-electric conversion is performed with electric turbine groups-electric generator in two phases. In the first stage it is performed at the hydraulic-mechanic level at the joint shaft turbine-generator and in the second, mechanical-electrical at the generator terminals.

Uploading the generator at different loads for different speeds of the shaft, one can determine the thermocouple and the power provided by the axial turbine, depending on the electrical characteristics of the electri generator.

REFERENCES

[1]. Cazacu M.D.; Nicolaie S. – ***Micro-hydroturbine for run-of-riwer power station,*** A II-a Conferinta a Hidroenergeticienilor din Romania, 24-25 Mai 2002, Univ.Politehnica, Bucuresti, Vol. II 443-448;
[2]. Gordon J.L. – ***Turbine selection for low-head hydro developments,*** Conference: Inovative small hydro technologies, organized by Natural resources Canda at Water-power Canada, New York, USA 2003;
[5]. Kappel W.; et.al. – ***Magnet permanenti pe baza de NdFeB pentru hidrogeneratoare de mica putere,*** Conferinta Nationala de surse noi si regenerabile, CNSNRE, Targoviste, 2004.
[4]. Mihailescu Gh.M; et.al. – ***Hidrogeneratoare de mica putere, Atelierul: Actualitati si perspective in domeniul masinilor electrice,*** ICPE-ME-SA, 2004;
[3]. Samoilescu Gh; et.al. – ***The analysis of the bouys used on the river for making a non-conventional energetic system,*** ICATE 2006 - 8th International Conference on Applied and Theoretical Electricity, 26-28 Octombrie 2006, Baile Herculane;

KINETIC ACTIVITY OF SOME TRANSITION METALS COORDINATION COMPLEXES IN SEA WATER

ZAGAN SABINA

Constanta Maritime University, Constanta, Romania

Sea water has an important role not only in coordination process due to the presence of micro-organisms exist in marine plankton, but also in the decomposition process at a moderate value of pH.
All the coordination reactions products remain in the sea water surface and their decrease or increase of concentration could be correlated and predicted by determining the kinetic activity. The kinetic rate has been determined in sea water using a pH of 7,5 and 8,5 at 20 and 25^{o}C temperature and 1 atmosphere pressure for Ni (II) and Au (III) coordination complexes.

Keywords: metal ions in sea water, kinetic activity and reaction rates on sea water media

1. INTRODUCTION

In sea water, marine micro-organisms have transport systems capable of accumulating essential trace metals present at low oceanic concentrations. The nutrients of sea water contains different kinds of mono or bidentate donor-ligands which forms a lots of coordination compounds using for coordination the N, O or S atoms. In these conditions, the metal ions which form complexes are soft acids, as Ni (II), Cu (II) or Au (III), even if their concentration in sea water is in traces.

The characteristics of coordination for metal ions

The group of d8 transition elements (Ni, Pd, Pt) principally occur with oxidation number II. In sea water the heavier metals ions of Pd^{II} and Pt^{II} exist dominantly as tetrachloroplatinate, $PdCl_4^{2-}$ and tetrachloropalladate, $PtCl_4^{2-}$ having square – planar structures due to their steric requirements.

Also it is well known that Ni (II) forms a square – planar complex with cyanide ion, whereas ammonia and water form six- coordinated octahedral species and chloride, bromide or iodide form tetrahedral complexes. According to Pearson's classification [2], Ni (II) is acting as a borderline acid and form square-planar complexes with N,O - bidentate ligands.

As regarding nickel, sea water contains approximately 0.5 - 2 ppb of nickel, rivers contain approximately 0.3 ppb and phytoplankton contains 1-10 ppm nickel (dry mass), resulting in a 10^3-10^4 bio-concentration factor compared to sea water [1].

Elementary nickel is insoluble in water in normal conditions of pressure and temperature, but the most of the nickel compounds are soluble in water. Ni ions exist as free hydrated Ni^{2+}.forming coordination complexes. Nickel chloride and carbonate are soluble in water, but other nickel compounds, such as nickel oxide, nickel sulphide and nickel tetra carbonyl are insoluble in water.

The group of d9 transition elements (Cu, Ag, Au) are normally presented as Cu (I), Ag (I) and Au (I), but in sea water the oxidation numbers for this group of elements is irregularly.

Ag solely exists as Ag (I), Cu occurs dominantly as Cu (II) in oxygenated sea water and oxidation number III is important for Au. All the metal ions are strongly coordinated with Cl^- as chloro-complexes and hydrolysed and Cu (II) easily forms carbonate coordination complexes.

The gold (III) complexes are diamagnetic with a low – spin $5d^8$ electron configuration and the majority of these compounds have four coordinated square planar stereochemistry. Example include complex ions $[AuCl_4]^-$ and $[Au(NH_3)_4]^{3+}$, but the simple aqua ion $\{Au(OH_2)_4]^{3+}$ is never formed even on dissolution of gold (III) hydroxide in nitric acid or sulphuric acid. The complexes of Au(III) with bidentate ligands show square planar configurations. For square planar gold (III) complexes, Valence Bond Theory predicts that gold (III) will have a $5d^8$ configuration and σ bonds will be formed using four hybrid orbitals: $5d_{x^2-y^2}$, $6s$, $6p_x$, $6p_y$ [4].

In sea water the concentration of gold in about 0.00011 ppm The presence of dissolved gold in sea water was detected by the reduction to metallic gold using sodium polysulphide and on adsorption of gold in various media, including polymers containing thiol groups, which coordinate strongly to gold. Due to the low concentration, it is not possible to determine directly the nature of the gold species present in sea water, but calculation based on redox potentials of gold compounds and the composition of sea water suggest that gold complexes are chloro-, iodo-, bromo- coordination compounds and Au (III) speciation in sea water appears to be dominated by mixed-ligand chlorohydroxy complexes.

The characteristics of coordination for oxamic acid as ligand

Oxamic acid, $C_2H_3NO_3$, ($H_2NCOCOOH$)

The principal chemical characteristics for oxamic acide are the decomposition temperature at 483 K[3], and its solubility in water and DMSO. The conductivity of oxamic acid in water (11,3 mmol acid oxamic in 10 cm^3 of water) is $1,890 \cdot 10^{-3}$ S/cm and the conductivity in DMSO decrease to the $2,96 \cdot 10^{-6}$ S/cm at the room temperature.

The chemical structure for this ligand is presented in Fig 1.

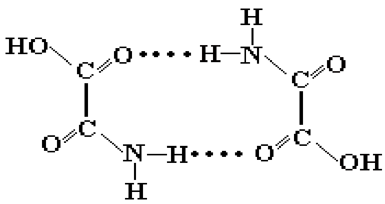

Figure 1. The structure of oxalic acid monoamide

Oxamic acid is acting as a bidentate O, N – donor ligand [5] and coordinate to metal ions as $(H_2NCOCOO)^-$ through both oxygen atoms or one nitrogen and one oxygen atom. The proton on the N-atom can be removed and deprotonated $(HNCOCOO)^{2-}$ - complexes could be prepared in these cases oxalic acid monoamide is acting as a bidentate O, N – donor ligand.

2. EXPERIMENTAL

The coordination complexes used for the kinetic activity study in sea water are:

- Au(III) complex with oxamic acid: $K[Au(NHCOCOO)(OH)_2].H_2O$
- Ni(II) complex with oxamic acid: $K_2[Ni(NHCOCOO)_2].2H_2O$

The complex $K[Au(NHCOCOO)(OH)_2].H_2O$ is soluble in DMSO, DMFA and water and insoluble in ethanol, acetone and ethylic ether.

The aqueous solution of the complex is alkaline (*p*H=9-10) and the molar electrical conductivity (Λm) is 0.080μS/cm

The complex $K_2[Ni(NHCOCOO)_2].2H_2O$ is soluble in water, DMSO and DMFA and insoluble in ethanol, acetone and ethilic ether. The molar electrical conductivity (Λm) is 232 Scm^2mol^{-1} meaning that the complex is 2:1 electrolite.

The complexes have square- planar structures as represented in Fig 2 and Fig 3.

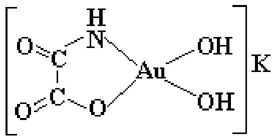

Fig. 2 The structure of $K[Au(C_2O_3NH)(OH)_2]$

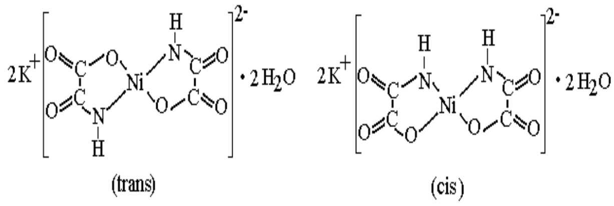

Fig. 3 The structure of $K_2[Ni(NHCOCOO)_2] . 2H_2O$

The complexes have been hydrolysed in sea water at two values for pH (7,5 and 8,5) and at two values for temperature (293 and 298 K) and during hydrolyse reactions the OH^- ion act as a nucleophile agent which modifies the kinetic rate of reactions.

The kinetic rate has been determined by spectrophotometric method recording the absorbance of the complexes in time at the characteristic wavelength for each complex. The electronic spectra have been recorded with a Jasco V -570 UV/VIS/NIR spectrophotometer using MgO as reference, on 190 - 2300 nm domain using the special programme for kinetic data.

3. Results and discussions

The kinetic rate in sea water media of the coordinated complexes has been studied. The results are presented in table 1.

Table 1 Kinetic rate for hydrolyse reactions in sea water for the complexes:

Coordination compounds	pH of seawater	T (K)	λ (nm)	k (s^{-1})
$K[Au(NHCOCOO)(OH)_2].H_2O$	7,5	293	275	0,2403
$K_2[Ni(NHCOCOO)_2].2H_2O$	7,5	293	322	0,0004
$K[Au(NHCOCOO)(OH)_2].H_2O$	7,5	298	275	1,9561
$K_2[Ni(NHCOCOO)_2].2H_2O$	7,5	298	322	0,0011
$K[Au(NHCOCOO)(OH)_2].H_2O$	8,5	293	275	$1,0785 .10^2$
$K_2[Ni(NHCOCOO)_2].2H_2O$	8,5	293	322	0,0291
$K[Au(NHCOCOO)(OH)_2].H_2O$	8,5	298	275	$4,2447.10^2$
$K_2[Ni(NHCOCOO)_2].2H_2O$	8,5	298	322	0,1773

The experimental data shows that the influence of sea water acting as an alkaline media on the kinetic rate of the complexes depend on:

- the reaction conditions: the kinetic rate increase with the increases of pH and temperature values
- the elimination process of anionic ligand from coordination complexes: the process is happened faster if the positive metal ions is bigger
- the mechanism of elimination: in this case the elimination process is an associative mechanism consisting in the obtaining of an intermediate coordination complex characterise by a short lifetime
- the alkaline media determine the appearance of some secondary reactions as disproportion, decomposition racemisation and isomerisation of the complexes.

4. CONCLUSIONS

In sea water, the heavy metals coordination complexes containing Au(III) and Ni(II) ions present hydrolyse reactions. By analysing the kinetics of these reactions it could be predicted the properties for the hydrolyse products taking into account the types of nutrients exist in sea water. The kinetic rate could gives information about the life time of new products which are useful in determining the ecosystem structure.

REFFERENCES

[1]. Greenwood N.N., Earnshaw A., ***Chemistry of the Elements***. Second Edition. Oxford, Butterworth-Heinemann. 2002
[2]. Huheey J. E. ***Inorganic Chemistry: -Principles of Structure and Reactivity -*** Third Edition, Ed. Harper and Row, New York, 1983
[3]. Keuleers R., Janssens J.F., Desseyn H.O. ***Thermal analysis of oxamates, thiooxamates and their complexes*** Thermochimica Acta, vol. 311, p. 152–162, 1998
[4]. Shriver D.F., Atkins P.W., Langford C.H. ***Chimie anorganica.*** Editura Tehnica, Bucuresti, 1998
[5]. Slootmaekers B., Keuleers R., Janssens J.F., Desseyn H.O. ***Influence of hydrogen bonding on some physical constants of oxamides and thiooxamides*** Thermochimica Acta vol. 311, p. 141 – 147, 1998.

For Authors

Are edited scientific papers in topics, written in English. Papers are selected after a peer review. Each participant is allowed to send maximum 2 papers as first author. Authors should make sure that the manuscripts submitted are ready for refereeing. The papers that are to be published must bring scientific contributions to the journal. The papers also have to contain the results of some of your work. It is strongly recommended an even number of pages, no longer than 6-10 pages. The papers that do not respect the publishing conditions and which are not integrated in the thematic of this journal will be rejected from the start by the Editorial Board. Authors submitting an article affirm that the same manuscript is not concurrently submitted to another publication. The authors are entirely responsible for the content of their papers.

PUBLISHED SINCE 2008
ISSN:1844-6116
ON LINE SINCE: 2008
PUBLISHED BY: Editura Nautica/ Constanta Maritime University